3-2022

Spatial and Temporal Analysis of Big Dataset on PM2.5 Air Pollution in Beijing, China, 2014 to 2018

Hutong Fan
fanh01@mail.buffalostate.edu

Advisor
Tao Tang
First Reader
Tao Tang
Second Reader
Stephen J. Vermette
Third Reader
Qiang Sun

Spatial and Temporal Analysis of Big Dataset on $PM_{2.5}$ Air Pollution in Beijing, China, 2014 to 2018

by

Hutong Fan

An Abstract of a Thesis
in
Great Lake Environmental Science

Submitted in Partial Fulfillment
of the Requirements for the Degree of
Master of Arts
May 2022

State University of New York
College at Buffalo
Great Lake Center

ABSTRACT OF THESIS

Air particulate matter ($PM_{2.5}$) pollution is a critical environment problem worldwide and also in Beijing, China. We gathered five-year $PM_{2.5}$ contaminate concentrations from 2014 to 2018, from the Beijing Municipal Environmental Monitoring Center and China Air Quality Real-time Distribution Platform. This is a big dataset, and we collected with crawler technology from Python programming. After examining the quality of the recorded data, we determined to conduct the temporal and spatial analysis using 27 observation stations located in both urban and suburb area in the municipality of Beijing. The big dataset of five-year hourly $PM_{2.5}$ concentrations was sorted to actionable datasets (Selected Datasets and Seasonal Average Selected Datasets) with the help of Python programming. Linear Regression based Fundamental Data Analysis was conducted as the first part of temporal analysis in R studio to gather the temporal patterns of five-year seasonal $PM_{2.5}$ contaminant concentrations on each observation sites. As the second part of temporal analysis, the Principal Component Analysis (PCA) was conducted in MATLAB to gather the patterns of variations of entire five-year $PM_{2.5}$ contaminant concentration on each of the sites. Geographic Information System (GIS) was utilized to study the spatial pattern of air pollution distribution from the selected 27 observation sites during selected time periods. The results of this research are, 1) $PM_{2.5}$ pollutions in winter are the most severe or the highest in each of the natural years. 2) $PM_{2.5}$ pollution concentrations in Beijing were gradually decrease during 2014 to 2018. 3) In terms of a five-year time perspective, the improvements of air quality and reduction of $PM_{2.5}$ contaminant appeared in all the seasons based on Fundamental Data Analysis. 4) $PM_{2.5}$ contaminant concentrations in summer are

significantly less than other seasons. 5) The least $PM_{2.5}$ pollutant influenced area is north and northwest regions in Beijing, and the most $PM_{2.5}$ pollutant influenced area is south and southeast areas in Beijing. 6) Vehicle concentration and traffic congestion is not the significant impact factor of $PM_{2.5}$ pollutions in Beijing. 7) Heating supply of buildings and houses generated great contributions to the $PM_{2.5}$ contaminant concentration in Beijing. While, in the background of rigorous emission reduction policy and management operations by the municipal government, contribution of heating supplies is gradually decreasing. 8) Human activities have limited contributions to the $PM_{2.5}$ contaminants in Beijing. Meanwhile, type and quantity of fossil fuel energy consumptions might contribute large amount of air pollutions.

_____

Your Signature

_____

Date

State University of New York
College at Buffalo
Great Lake Center

Spatial and Temporal Analysis of Big Dataset on $PM_{2.5}$ Air Pollution in Beijing, China, 2014 to 2018

A Thesis in
Great Lake Environmental Science

by

Hutong Fan

Submitted in Partial Fulfillment
of the Requirements
for the Degree of

Master of Arts
May 2022

Approved by:

Tao Tang, Ph.D.
Professor of Geography
Chairperson of the Committee/Thesis Adviser

Stephen Vermette, Ph.D.
Professor of Geography

Bruce Swan, Ph.D.
Professor of Mathematics

Dates of Approval:

03/03/2022

Tao Tang, Ph.D.
Professor of Geography
Chairperson of the Committee/Thesis Adviser

3/3/2022

Stephen Vermette, Ph.D.
Professor of Geography

03/03/2022

Bruce Swan

Bruce Swan, Ph.D.
Professor of Mathematics

Table of Content

ILLUSTRATIONS

TABLES

1. Introduction

Air particulate matter ($PM_{2.5}$) pollution is a critical environment problem worldwide and in China. $PM_{2.5}$ is a kind of tiny air particulate pollution which diameter is usually 2.5 microns or less, as contrasted with gaseous pollutants (ozone, carbon monoxide, etc.) (EPA Particulate Matter, 2016). Those particles are able to go through the nose and throat into the lungs. Different particles may have many types of components, such as bacteria, pollen, heavy metals, dust, sulfates, and nitrates. Those different combinations mean $PM_{2.5}$ will provide complex effects on the body (EPA. Integrated Science Assessment for Particulate Matter (Final Report), 2009). Moreover, $PM_{2.5}$ also causes more health burden worldwide. The life expectancy decrease is positively correlated with the average $PM_{2.5}$ concentrations. In 2016 worldwide statistics, the expected average life was reduced about 1 year globally in average to the people exposed to $PM_{2.5}$ pollution at birth and about 1.2-1.9 years in the heavily polluted countries (Joshua et al., 2018). Based on some researches, the primary pollutant type of air pollution that causes lung cancer was ambient $PM_{2.5}$ air pollution. In addition, the exposure in $PM_{2.5}$ is more harmful to male and elderly group (Wu et al., 2021). With the metagenomic methods, several inhalable respiratory microbial allergens and pathogens were determined in the $PM_{2.5}$ contaminant of severe haze disaster in January 2014 (Chen et al., 2014).

Reducing and mitigate air pollutions is also the key emphasis in the focus of Chinese government. In Dr. Tang's previous research, field work was conducted with handheld laser particle counters (Tang et al., 2010). To obtain the proper interpolation map, the researchers had to measure at different observation sites in Beijing at different times during a day. This process caused the field measuring of $PM_{2.5}$ to be less reliable for purposes of spatial analysis. The objective of this research is to analyze the officially published daily $PM_{2.5}$ data from 2014 to

2018 by the Bureau of Environmental Protections, City of Beijing, that was measured at its air pollution monitoring stations in finding the temporal and spatial distribution and variation patterns. This research also analyzes the major sources and impacting factors of $PM_{2.5}$ in the city. The original dataset covers a total of 35 field measuring stations with hourly measurements taken daily for a total of five years. Analyzing this big data of $PM_{2.5}$ pollution can yield results with higher precision, accuracy, and consistency comparison to the previous study. The variations of $PM_{2.5}$ pollutant temporal pattern can be used to analyze the trend and evaluate the effects of the air pollution control policies of the government. The variations of spatial pattern of $PM_{2.5}$ contaminant concentrations can be also used to identify the highly polluted areas, to visualize the variation trend in different regions, and to trace the major source of pollutant in different times during a day and in different seasons in a year.

The hypothesis of this research is, first, that the $PM_{2.5}$ pollution in Beijing becomes gradually reduced and mitigated chronologically with the "Air Pollution Prevention and Control Action Plan". The "Air Pollution Prevention and Control Action Plan", introduced in 2013, is the most rigorous emission reduction policy enacted by the Chinese government in Chinese history (Zhao et al., 2018). Secondly, the major concentrations of $PM_{2.5}$ pollutant might come from different sources at different time periods. During the building heat supply time-period (the winter season of each year), the major source of $PM_{2.5}$ pollutant is from building heat supply using coal or natural gas. During other seasons, the major contributor to the $PM_{2.5}$ pollutant in Beijing is mainly from vehicle traffic emissions.

2. Literature Review

2.1. Social-Economic and Natural Factors Analysis

2.1.1. Studies of Social-Economic Indicators

From the perspective of socio-economic indicators, air pollutions are the indicators that reflect all social phenomena and are related to human industrial production activities. Frank (et al., 2001), looking at the impact of economic growth on air pollution (taking the actual per capita GDP as an economic index in Hebei Province, China), found that the energy consumption generated in industrial activities is the main factor producing air pollution. Du (2016) analyzed the changing trend of industrial waste gasses. The research found that industrial sulfur dioxide and industrial dust emissions are correlated with the economic index. Dinda (2004) proved that the relationship between air pollution and the growth of secondary sector followed the inverted 'U' environmental Kuznets curve (EKC). That is to say, the air pollution will be aggravated at the initial stage of the development of the secondary industry. The air pollution will be slowed down when the secondary industry and people income develop which caused people seek for the better air quality. Wang and Shen (2017) selected the per capita GDP, the proportion of added industrial value, the proportion of coal consumption, the building area, and the number of civilian automobiles to study the influence of automobile exhaust and dust on air pollution. Hui, Mao and Dai (2018) comprehensively analyzed the influencing factors of air pollution in Hebei Province, China. Among them, the output values of indicators on secondary sector and urbanization level have positive effects on haze pollution. In the meantime, they pointed out actual per capita GDP, foreign direct investment, population density, and highway mileage have different effects on haze pollution. Li (et al., 2013) studied the air pollution of 237 cities in finding the impact variables. There is a significant positive correlation between the factors of urban secondary industry and the size of built-up area and the concentration of major pollutants in urban air. Jiang (et al., 2017) explored the influencing factors of air pollution from the

perspective of exponential decay effect, and considered that SO_2 emission, per capita GDP and $PM_{2.5}$ concentration were the main influencing factors of air pollution.

2.1.2. Studies of Natural Factors

From the perspective of natural factors, natural factors mainly refer to geographical factors and meteorological factors. Zhou (et al., 2010) studied the influence on the air quality of cities in middle Liaoning province of two sandstorm events in March 31st and May 7th, 2007. The conclusion showed that the average PM_{10} concentration increased 20% to 260% and 150% to 380% respectively than the daily average PM_{10} mass during those two events. PM_{10} was also the major factor which influenced the air quality during the sandstorm events. Chen and Zhan (2018) considered that the particle of sand and dust made major impact to the concentration of PM_{10} and secondary impact to the concentration of $PM_{2.5}$ based on the sandstorm event in Jilin province, May 5th, 2017. Spiroska, Rahman and Pal (2011) found that the concentration of pollutants in the air was the lowest in windy seasons and open terrain. Zhou and Liang (2013) took Shanghai as an example - the long-term relationship between air quality, wind speed and direction was studied, and it was found that the concentration of PM_{10} decreased with the increase of wind speed. Based on meteorological factors such as air pressure, air temperature, relative humidity, wind speed and direction, sunshine, and geographical indicators such as vegetation coverage, altitude, and topographic relief, Liu et al. (2018) studied comprehensively influencing factors of air pollution in urban agglomeration of Beijing-Tianjin-Hebei. Zhou (et al., 2014) incorporated a precipitation index into influencing factors, studied the future changes of meteorological factors, and estimated their impact on air quality in Beijing-Tianjin-Hebei region. Zhang (et al., 2015) studied the temporal and spatial distribution pattern of fine particulate pollution in China. The

results indicated that the overall pollution degree of $PM_{2.5}$ was intensive and shows seasonal effect. The concentration of air pollutants in winter and autumn was higher than that in spring and summer, and the concentration of air pollutants in summer was the lowest.

2.2. Classical Modeling in Air Pollution Analysis

Air quality is related to people's health and has always been one of the focuses of scientists. Accurately evaluating and quantifying the relationship between $PM_{2.5}$ and pollution sources (including traffic emissions) is the premise of effectively guiding pollution prevention and mitigation. Related research methods can be divided into the following two categories: physical methods and statistical methods.

2.2.1. Physical Methods

Physical methods were based on the physical and chemical reactions in the atmosphere, and the modeling of pollutant emission process. Physical methods are mainly referring to the source analysis method of atmospheric particulate matter, including source emission inventory method, source model method and receptor model method.

2.2.1.1. Source Emission Inventory Method

The emission inventory method is to make statistical analysis on the activity status and emission level of various emission sources in a certain region or a certain country, to determine the emissions of pollutants from various emission sources, and then to obtain the pollution emissions of different pollution sources to the atmospheric environment (Zhu, Lian and Liu, 2017). This

method has simple and clear objectives and has been widely used up to this date. Some scientific research institutions in China had established emission source inventories for some typical cities in China, such as China Multi-scale Emission Inventory (MEIC), established by Tsinghua University (Shen, Yao and Zhang, 2015, and Zheng, Tong and Li, 2018).

2.2.1.2. Source Model Method

Source model method, also called diffusion model method, simulates different meteorological conditions and emission sources through numerical simulation process, and further estimates the contribution of different pollution sources to pollutant concentration (Burr and Zhang, 2011, and Koo, Wilson and Morris, 2009). The most widely used source model methods include multi-scale motor Vehicle and equipment Emission System (MOVES) (Koupal et al., 2003), Computer Program to Calculate Emissions from Road Transport (COPERT) (Nikoleris et al., 2011) and International Vehicle Emission (IVE) (Zhang et al., 2008). The U.S. Environmental Protection Agency developed the MOVES model to estimate the emissions from road and off-road mobile pollution sources (Koupal et al., 2003). COPERT is a commonly used emission model in Europe. The model utilizes a large amount of experimental data to determine the emission parameters of road traffic and obtain the emission list (Nikoleris et al., 2011). IVE model uses the information of vehicle emission rate and vehicle driving characteristics to obtain the predicted emissions, and establishes the pollutant emission list (Zhang et al., 2008). The source model can obtain the spatial distribution of emission sources and analyze the sharing rate of different regions.

2.2.1.3. Receptor Model Method

The receptor model method starts from the receptor sampling points and backtracks the contribution ratio of each pollution source through the physical and chemical information of the sampling points (Henry et al., 1984). The receptor model method is mainly divided into two types, namely physical method and chemical method. Physical method mainly refers to the use of optical microscope, scanning electron microscope and other experimental tools to analyze the physical characteristics of many particles (Ogulei et al., 2007). Chemical method uses chemical tracing with indicating ability in atmospheric particulate matters and statistical analysis method to obtain the source of particulate matter (Zhao et al., 2007).

2.2.2. Statistical Methods

The statistical method is to study the correlation of air quality from the perspective of air quality data and use the existing urban spatio-temporal multi-source data to conduct statistical modeling and analysis of air quality. With the wide development of air quality monitoring technology, a large number of data from air quality monitoring networks are generated and collected at an unprecedented level (Zheng et al., 2014). These spatio-temporal data, generally, can more effectively capture the local fine-grained grids closely related to the air quality of a certain place, thus obtaining better inference results than physical methods. In statistical methods, related work can be further divided into pollutant concentration prediction, correlation analysis and spatio-temporal emission modeling.

2.2.2.1. Prediction of Pollutant Concentration

Pollutant concentration prediction is based on a data-driven method, which uses the historical data of air pollutant concentration and other related data, such as human activity data and meteorological data, to predict the future changes of pollutant concentration, and then realize the effect of air quality for prediction or early warning (Lin et al., 2011). A great deal of research is focused on using urban spatio-temporal data and capturing the characteristic information closely related to air quality, then a better air pollution model than the physical method can be obtained. In recent years, more researchers have used machine learning methods, such as Support Vector Regression (SVR), Hidden Markov Model (HMM), to achieve air quality prediction and improve the accuracy of predictions (Welling, 2004; Awad and Khanna, 2015; Zhang et al., 2012).

2.2.2.2. Correlation Analysis

The correlation between transportation traffic and air quality can be analyzed. Many studies have used Pearson/Spearman correlation coefficient to analyze the correlation between road traffic related data and air quality data, and then evaluated the impact of road traffic on air quality (Guo et al., 2019 and Ni et al., 2017). However, due to the dynamic and complex process from pollutant emission, emission source to air pollution, it is difficult to effectively capture the complex nonlinear relationship between transportation traffic characteristics and air quality by correlation analysis. Deep learning is a subfield of machine learning that involves algorithms inspired by the structure and function of the brain (Najafabadi et al., 2015). Because of the ability of deep learning to fit complex relationships, many people considered using deep learning methods to analyze the relevance. For example, Qi (et al., 2018) proposed research to embed feature selection methods into deep learning models, reveal the internal mechanism of the

deep-layer network model, and explore the relationship between air pollution prediction and input features. However, although feature selection methods can select the most relevant input information in training, but at the same time, it will also reduce prediction accuracy. Recently, more and more researchers think that it can be a powerful tool to explain the model by paying attention to important input features (Vaswani et al., 2017).

2.2.2.3. Modeling of Spatio-Temporal Emissions

Spatio-temporal emission modeling is to reconstruct the spatio-temporal pattern of traffic volume by using big data mining technology, and then calculate the pollution emissions by using the emission model and match the calculation results to the actual road network to obtain the spatio-temporal emission pattern of urban traffic. This is the most common method to analyze transportation traffic emission at current time (Liu et al., 2019). However, many studies used taxi GPS track data to infer urban traffic volume, and then use emission models to calculate pollution emissions, thus obtaining the spatio-temporal emission patterns of urban traffic (Liu et al., 2019, Jamshidnejad et al., 2017 and Shang et al., 2014). However, taxi GPS data can only represent part of traffic volume in the reality (Liu et al., 2019 and Shang et al., 2014).

2.3. Application of Big Data and GIS in Air Quality Research

In the view of complexity of air pollution, it is necessary to continuously explore effective methods and technologies to simulate the pollution diffusion process (Yuan, 2016). Based on the existing environmental data, the simulation of pollution diffusion and the prediction of the total amount of pollutants discharged provided auxiliary decision support for the industries of pollutant emissions to mitigate the total amount of air pollution and manage effectively. GIS

(Geographic Information System), as a multidisciplinary science, has powerful spatial data analysis and processing functions. In the study of air pollution, according to the requirements of ease of use, high efficiency, safety and reliability, the air pollution diffusion model is integrated with GIS. The advantages of GIS in data integration, spatial data processing and analysis, spatial data visualization are fully utilized to study the influencing factors among various pollution elements (Ma, 2015). The air pollution diffusion simulation and prediction management system were established by using GIS related technology combined with commonly used diffusion models and prediction methods, which provides comprehensive and efficient functions such as air environment information inquiry, pollution diffusion simulation and pollution prediction, and auxiliary decision-making. It can directly reveal the spatial characteristics of air pollution related information and visualize pollution information based on GIS. The system can provide air pollution analysis and visualizations for meteorological departments, environmental protection departments and transportation departments. It has great application values.

In the 1970s and 1980s, the study of the atmospheric environmental information system begun. In some western countries, with the improvement of environmental awareness, people began to conduct research on atmospheric environmental pollution (Holmes, 2006). At the same time, environmental protection organizations and software R&D companies began to research and develop application models and applications related to air pollution. For example, CALPUFF model and Atmospheric Dispersion Module (AERMOD) of U.S. Environmental Protection Agency (EPA), Atmospheric Dispersion Modelling System (ADMS), atmospheric diffusion model system of Cambridge environmental research company (CERC) (Holmes, 2006). Some countries have successively established geographic information application systems for air pollution management, and it is an important trend in international research on environmental

pollution management to use GIS technology to analyze data. The U.S. Environmental Protection Agency made spatial analysis and visual expression of the numerical simulation results of various air quality models by means of GIS and put forward an integrated system model. GIS enabled prediction model provides an effective method for users to carry out spatial analysis. The concentration distribution simulation research by Tchepel (et al., 1993) based on GIS technology combined with atmospheric model shows that GIS is outstanding in data processing. Marquez (et al., 1999) proposed a framework for integrating land use, transportation, and air diffusion models to assess the impact of urban morphology on air quality. The framework defined the relationships among the various components, such as GIS database, land use-traffic-environment module and atmospheric model. The frame structure and robustness were discussed, and the results of recent air quality survey were introduced. Combining the ADMS model of Carruthers with commercial GIS software, the ADMS-Urban application system was established, which enhanced the spatial visualization and spatial analysis ability in air pollution prediction results of the model (Carruthers et al., 1997). The results could be applied to environmental monitoring and governance by government.

Although the research on air pollution control, pollution diffusion simulation and pollution impact analysis based on GIS technology is relatively late in China, some achievements have been made after years of development (Zhao, 2007). In the 1980s, China established the State Key Laboratory of Resources and Environmental Information System. The laboratory devotes itself to the research of the basic theory and practical methods of geographic information, builds a professional scientific system integrating data and application, and promotes data integration and sharing in the industries. Some domestic higher education institutions, experts and scholars have done a great deal of scientific research in the integrated application of atmospheric

diffusion simulation and GIS. Jing (et al., 2006) used the spatial analysis and geostatistical analysis functions of GIS, based on the research on the diffusion characteristics of ozone pollution in Changchun urban area in summer, combined with relevant data such as air quality grades, and assessed the air quality status in the research area by regions. Using ArcGIS, the analysis results are spatially superimposed, measured, analyzed; and the dynamic change classification model of the research area is constructed, and the spatial distribution characteristics and change laws of air pollution in this area are deeply studied. Based on GIS and Remote Sensing (RS) techniques, some factors are mapped affecting Beijing urban airborne particulates pollutions, the ground surface pattern for example. With the one-year particular pollution observation data from 76 air sampling stations in Beijing, Tang et al. conducted the interpolation with the universal kriging model in GIS to analyze the spatial distribution of contaminants within different diameters (Zhao et al. 2009; Tang et al., 2010). Population distribution at the community level is also used in this research to ascertain the community exposure issues to the high air particle pollution. In the subsequent research (Tang et al., 2009; Xiong et al., 2015), the records of residents' disease of the respiratory system were used to ascertain the spatial relationship with the concentration of airborne particulate matter pollution in 2008 using a geographically weighted regression model in GIS. The studies indicated that PM diameter between 0.5 to 3 micrometers had severe affection to the occurrences of respiratory diseases in Beijing. Zhao (et al., 2008) realized the air pollution diffusion model by using VB programming environment and built the air pollution diffusion application program based on GIS by using Map Objects and Surfer 8.0 components. The simulation of different types of pollution diffusion and the visualization of the results are realized, which provides a scientific auxiliary decision for the relevant government departments to effectively manage and solve the urban air environment

problems. Li (2012) compared and analyzed various spatial interpolation methods, finally chose Kriging interpolation method, and designed and developed an air pollution diffusion simulation system based on IDL language. The spatial visualization of the model simulation results was presented, and Beijing was selected as the research area for practical research and analysis. The research results can be used to show the spatial distribution characteristics and forecast for air pollutant diffusion. An (et al., 2012) used GIS spatial analysis and interpolation function to study the spatial distribution of air pollution in Lanzhou in winter. Using Surfer to draw isolines, the research shows that GIS spatial analysis function can effectively simulate the air pollution diffusion in the research area, intuitively display the spatial distribution of pollutants, and provide a feasible method for studying the spatial distribution and spatial diffusion of air pollution in cities with similar geographical environment. Zhang and Zhao (2008) combined air pollution diffusion model with GIS, displayed simulation results of air pollution diffusion based on GIS spatial visualization function, and summarized the theoretical method and implementation process in combining GIS with Gaussian diffusion model.

It clear that, GIS has made great contribution and wide application in the air pollution studies worldwide. With the gradual deterioration of human living environment and the destruction of ecological balance, GIS can play a greater role in the field of environmental comprehensive management, especially in the prevention and management of air pollution. The exploration of air pollution reduction and elimination based on GIS technology will also make great progress in practice.

2.4. The Applications of Machine Learning and Deep Learning in The Research of Air Pollution

At present, the main air quality prediction methods using machine learning are based on neural network, gray model and support vector machine (Zhang et al., 2017). The prediction method based on gray model has the advantage of convenient calculation, but it cannot adapt to the nonlinear and time-varying characteristics of air quality. The prediction method based on support vector machine has the ability to quickly obtain the global optimal solution, but its processes of setting parameters are difficult. The reasonable selection of parameters directly affects the accuracy of the prediction results (Zhang, 2014). The artificial neural network technology has good adaptability to uncertain, multi-input and complex nonlinear problems (Yan et al., 2015), and shows excellent ability in the field of prediction. Therefore, the prediction method based on neural network was selected by Yan et al. (2015). The exploration of neural network began in the 1940s (Li et al., 2015). Based on biological neurology, it imitated the transmission of brain neurons and abstracts a way of information processing. In the progress of scientific research, neural network is constantly enriched, from the simple linear approach to be able to simulate the complex network structure now, in order to solve more complex problems. According to the characteristics of neurons and learning rules, at present, it has formed dozens of kinds, such as BP neural network and Boltzmann machine (Asja and Christian, 2014), Hopfield neural network, radial basis function neural network (Schilling et al., 2001), self-organizing competitive neural network, convolution neural network, and deep neural network (Szegedy et al., 2014) and cyclic neural network developed on the basis of convolution neural network. According to the topological structure, it can be divided into feedforward neural network and back fed neural

network. Artificial neural network has strong noise tolerance and nonlinear processing ability, so it has a place in the research of air quality prediction.

As a branch of machine learning method, deep learning technology has the ability to fit any continuous function (Chang, 2015), and can better mine the characteristic information closely related to air quality in urban spatiotemporal data, so as to achieve good prediction accuracy (Cai et al., 2019). A hybrid artificial neural network model combining air quality trajectory analysis and wavelet transform was adopted by (Liu, 2003), and predicted the change of $PM_{2.5}$ average concentration in the next two days. Using the memory function of Recurrent Neural Network (RNN) in time series, a special RNN, Long Short-Term Memory network (LSTM) was used to replace the fully connected neural network for time series prediction (Mehmed, 2003). The Deep Air team at UC Berkeley also used machine learning to predict air pollution. The LSTM based air pollution sequence prediction model was studied, which can accurately predict the air pollution in the next ten hours. Tan (2013) constructed a real-time air quality prediction system, using data-driven models to predict fine-grained air quality in the next 48 hours. Zhao (2017) and Zhu (2017) proposed to use two-stage attention model (DA_RNN) to achieve time series prediction task and multi-level attention based RNN time series prediction model (GEO_MAN) to achieve air quality prediction. However, the existing models can improve the accuracy of the models by using the latest network structures, such as Long-Short-Term Memory network (LSTM), Gating Cycle Unit (GRU), while the dynamic process modeling of air pollution is not considered. For example, the generation process of $PM_{2.5}$ is hierarchical, including direct emission and secondary generation. Although the effective air pollution concentration prediction and early warning can provide guidance for people's travel safety, the existing methods only

realize the prediction of $PM_{2.5}$ concentration, which cannot provide effective help to solve the pollution problem fundamentally.

2.5. Air Pollution Studies in China

There are various methods for Chinese researchers to analyze the influencing factors of air pollution. Wang (et al., 2020) used the grey correlation analysis model to analyze the impact of industry, resident population, agriculture, and automobile ownership on air quality based on the air pollution data of cities Tianjin and Xingtai. Gray correlation analysis was proposed by Deng (1990) from the gray system approach. It is a methodology for quantitative analysis of dynamic processes using similarity of trends and patterns between reference and comparison series. Wang (et al., 2019) used the grey correlation analysis method to study the correlation degree of industrial added value, energy consumption and vehicle ownership on air pollution components in Handan City, Hebei Province, China during 2014 to 2018. Huang (2016) used the grey correlation analysis method to calculate the correlation degree between the total population, the proportion of the secondary industry and the concentration of air pollutants, so as to measure the degree of air quality affected by various indicators. He (et al., 2016) used the principal component analysis method to analyze the influencing factors of air pollution in Beijing – Tianjin – Hebei region from the aspects of regional environment, economic development level and resource consumption.

Chen and Jin (2019) analyzed the impact of $PM_{2.5}$ concentration on housing prices in 286 Chinese cities and indicated that the housing prices in cities with high air pollution were lower. The housing prices were also affected by population density, average wage, industrial structure, public service level and other factors to a large extent according to the study. Jia (et al., 2020)

analyzed the $PM_{2.5}$ data and showed that the areas with poor air quality were mainly concentrated in the vicinity of urban construction and urban main traffic network areas. Zheng et al. (2015) conducted the model-assisted analysis on major chemical compositions of $PM_{2.5}$ pollutant in Beijing based on the hourly observation data. Their conclusions are: (1) The severe haze incidents happened in Beijing were driven by stable weather conditions in Northeast China. (2) The major component of $PM_{2.5}$ during 2012 to 2013 were secondary species or made by human activities, including organics, sulfate, nitrate, and ammonium. (3) The aerosol concentration accumulation process that happened in southeast part of Beijing was persistent. The instantly increased $PM_{2.5}$ concentration represented the imported contaminant accumulations in Beijing, rather than locally produced pollutants. Research suggested regional migration of pollutants plays an important role in those severe haze events in Beijing (Zheng et al. 2015). Zheng et al. (2005) also found the seasonal trend of Beijing $PM_{2.5}$ contaminant. The major contents of Beijing $PM_{2.5}$ mass are dust (20%), sulfate (17%) is the second largest, and nitrate (10%) is the third. But during the building heating time period in winter, coal combustion and biomass aerosol contributed more to the $PM_{2.5}$ concentrations. Dust storms also made major impact on $PM_{2.5}$ concentrations. During the dust storm event in April 2004, 36% of $PM_{2.5}$ mass was contributed by dust alone. According to Li's (2016) study, the distribution of $PM_{2.5}$ in Beijing area is obviously affected by the surrounding regions. The process of $PM_{2.5}$ pollutant diffusion was greatly influenced by the landscape and weather conditions in Beijing. The results showed the importance of controlling the transport of pollutants in the southern and western regions in winter (Li, 2016). Taking Wuhan as the research area, Xu and Chen (2020) elaborated the impact of urban development structure on air quality and found that air pollution decreased

from the center of the city to the periphery. It is suggested that the urban development method with high capacity and low density could reduce urban air pollution.

In Fan and Shan's research (2017), based on the air quality monitoring data and relevant meteorological data of 17 cities in Shandong Province, using the methods of spatial autocorrelation analysis and spatial interpolation, they studied the temporal and spatial characteristics of $PM_{2.5}$ and the influence of meteorological factors. Sun (2019) analyzed and compared the air pollution status of Beijing – Tianjin – Hebei – region from aspects of natural factors and social economy and constructed a spatial econometric model. The results showed that the influence directions of $PM_{2.5}$ concentration and six indicators such as temperature, relative humidity, wind speed, regional GDP, the proportion of primary and tertiary industries were the same, the influence directions of population density, urban green coverage rate and precipitation were opposite.

Ye (2016) and others found that the bad situation of Hebei environment had a negative role in promoting economic growth and would inhibit economic growth in the long term. Based on the semi parametric panel data model, Lu (2018) and others found that there is an inverted 'U' curve relationship between economic growth and environmental pollution emissions in Jiangsu Province. When exploring the relationship between economic growth and air pollution, Wu (2018) found that there was a shock curve relationship between air pollution and economic growth, but it was not completely consistent with the traditional inverted 'U' curve and compared the ordinary parameter model and semi parameter space model, and the results showed that the semi parametric spatial model was more accurate than the ordinary parameter model. Chen and Qiao (2017) studied the semi parametric spatial error model. Based on small sample

data, the model fitting effect was better, and the model accuracy increased with the increase of sample size.

Yang and Chen (2018) analyzed the precision and real-time performance of ARIMA and LSTM, the results showed that LSTM model had obvious advantages in real-time online prediction. Li and Yang (2018) fully used the LSTM model to process the time series, which could consider the characteristics of the correlation information before and after the data and used it to predict the silicon content. Based on LSTM, Bai and Shen (2019) used air pollutants as predictive indicators to build a $PM_{2.5}$ prediction model. Shi and Jiang (2019) conducted multiple comparative experiments with the models established by SVM, BP neural network and multiple linear regression, which showed that the LSTM prediction model had better prediction effect. Zheng, Bai and Hou (2019) constructed a LSTM model based on Keras deep learning framework to predict the AQI in Taiyuan. Zhang and Wei (2019) built a prediction model based on LSTM to predict water saturation distribution. Zhang and Chen (2019) put forward the method of space-time adjustment to eliminate meteorological interference and evaluated the air quality in Beijing. Deng and Wu (2020) constructed a $PM_{2.5}$ hourly concentration prediction model combining Stack Sparse Auto-Encoder (SSAE) and LSTM to analyze the air quality data of Beijing Tianjin Hebei region.

2.6. Air Pollution Studies in The United States and Other Countries

From the 1960s to the 1980s, most of the air pollution studies have taken American cities as empirical cases. Ridker and Henning (1967) pointed out earlier that the market value of a house was determined by a series of attributes. Their study, taking the metropolitan area of St. Louis as an example, proposed that with some improvements in air quality, the value of real estate can be

greatly improved. Rosen (1974) developed a classical hedonic price model, which interpreted housing characteristics as independent variables, and applied air pollution as implicit price to housing value evaluation. Harrison and Rubinfeld (1978) used hedonic price models to investigate consumers' willingness to pursue clean air in the Boston area housing market. Nelson (1978) used a two-stage model to estimate people's demand for urban air quality from the value of housing in Washington, D.C. Since 2000, Researchers have also begun to pay more attention to the impact of air quality in developing countries. Azmi (et al., 2012) took Bangkok as an example to study the relationship between air quality and the real estate market through the air quality index (AQI).

In addition, environmental justice research provided a lot of evidence that ethnic minorities and low-income people were more vulnerable to the negative impact of air pollution. Brulle and Pellow (2006) proposed that environmental inequality is the result of social processes. Hajat (et al., 2015) collected 37 environmental justice studies around the world, to examine trends in the impact of air pollution on ethnicity and socio-economic status. Their research showed that in North America, people with lower socioeconomic status were more likely to suffer from more severe air pollution. Although air pollution was decreasing over time, it was important to assess whether certain environmental policies had an impact on the unequal distribution of air pollution. The research of Miranda (et al., 2011) made use of the ethnic distribution of the population, age and income level to test the impact of air pollution on different groups of people, especially the non-Hispanic and African American population in the United States. The study found that this group was always exposed to the worst urban air. Brochu (et al., 2011) studied the impact of $PM_{2.5}$ on urban population in northern America. It was found that people with lower socioeconomic status were at higher risk of air pollution. Mathieu Carrier (et al., 2014) also

studied the relationship between urban population income, minority groups and air pollution, and found that low-income minority groups tend to live near major roads with higher air pollution levels.

Felix (et al., 2000) introduced forgetting gate, that is, LSTM pattern, on the basis of RNN to solve the problem of step elimination. Thomas and Christopher (2017) constructed the LSTM neural network prediction model in deep learning to predict the environmental quality, which has a good prediction effect. Suleiman (et al., 2018) based on AQI and CO, NO_2, O_3, PM_{10} and SO_2 in Romania, constructed a machine learning model to predict the air pollutants ($PM_{2.5}$, PM10), and the final result achieved good prediction accuracy. Wang (et al.,2017) combined the two-phase decomposition technology and improved extreme learning to construct the AQI prediction model and achieved good prediction results. Ji and Xie (2018) combined FCM and BP neural network to construct AQI prediction model. The predicted value is close to the true value, and the prediction accuracy of the model is very high. Esposito (et al., 2016) built a dynamic neural network volume prediction model which can be used for random calibration in the field based on the air quality sensing system with good cost performance. Alimissis, Philippopoulos and Tzanis (2018) used the BP neural network pre-model to predict the air pollution index, and achieved good prediction results.

Johnson, Bartosz and Constantine (2018) studied the universality of air quality sensor in dense heterogeneous urban agglomeration. Tang and Ji (2018) made full use of WRF-Chem model to predict pollution, weather and chemical composition as input features, and designed a comprehensive evaluation framework to improve the prediction performance. Belavadi (et al., 2020) used two neural network models, LSTM and RNN, to predict air quality. Navares and Aznarte (2021) studied a method to predict the concentration of CO, NO_2, O_3, PM_{10}, SO_2 and

pollen. This method introduced different topologies of LSTM. Compared with the traditional two forecasting methods, the LSTM model has higher accuracy.

2.7. $PM_{2.5}$ National Standard Differentiation

The global average annual concentration of $PM_{2.5}$ ranges from less than 10 μg/m^3 to more than 100 μg/m3. Based on World Health organization guideline values, the annual mean particulate matter is 10 μg/m^3, the 24-hour mean is 25 μg/m^3 (Ambient (outdoor) air pollution, 2018). Based on the National Ambient Air Quality Standards (NAQQS), in the United States, 12.0 μg/m^3 is the primary annual mean standard and 15.0 μg/m^3 is the secondary annual mean standard. In NAQQS, primary standard provides public health protection, and secondary standard provides public welfare protection. The 24-hour standard based on the NAQQS Table is 35 μg/m^3 (NAQQS Table, 2021). In China, based on the Ambient Air Quality Standards (GB3095-2012), 15 μg/m^3 is the primary annual mean standard and 35 μg/m^3 is the secondary annual mean standard. 35 μg/m^3 is the primary 24-hour mean standard and 75 μg/m^3 is the secondary 24-hour mean standard. In Chinese Ambient Air Quality Standards, primary standard is used in nature reserve, tourist attractions, and other areas need special protections. Secondary standard is used in residential, commercial traffic mixed area, cultural area, industrial parks and rural areas Ambient Air Quality Standard (Ministry of Ecology and Environment Protection of the People's Republic of China, 2012). In addition, the breakpoints for the Air Quality Index (AQI) in the U.S. and China are different. AQI is a non-linear dimensionless index that quantitatively describes the air quality condition. The larger the value and higher the level, the more serious the air pollution condition is and the greater the health risk to humans (Monteiro et al., 2017). According to Table 1 below, the major differentiates are in the 0 to 200 AQI section. It's clearly

showed that, in good, moderate and unhealthy for sensitive groups categories, Chinese breakpoints have a wider range to the 24-hour $PM_{2.5}$ concentrations.

Category	**AQI**	**$PM_{2.5}$ (μg/m3)** **24-hour America**	**$PM_{2.5}$ (μg/m3)** **24-hour China**
Good	0-50	0.0-12.0	0-35
Moderate	51-100	12.1-35.4	35-75
Unhealthy for Sensitive Groups	101-150	35.5-55.4	75-115
Unhealthy	151-200	55.5-150.4	115-150
Very Unhealthy	201-300	150.5-250.4	150-250
Hazardous	301-400	250.5-350.4	250-350
	401-500	350.5-500.4	350-500

Table 1: Comparation between Chinese and American Breakpoints for the AQI

3. Method

3.1. The Study Area

Beijing is in the northern part of North China Plain, 39.9042°N and 116.4074°E. The city area is surrounded by the Yan Mountain located to Beijing's north, northwest, and west sides (Figure 1). The climate in Beijing is a monsoon-influenced humid continental climate (Dwa: Köppen Climate Classification) which is characterized by relatively high humidity and high temperature in the summer times; relatively dry and low temperature in the winter times (Beck et al., 2020).

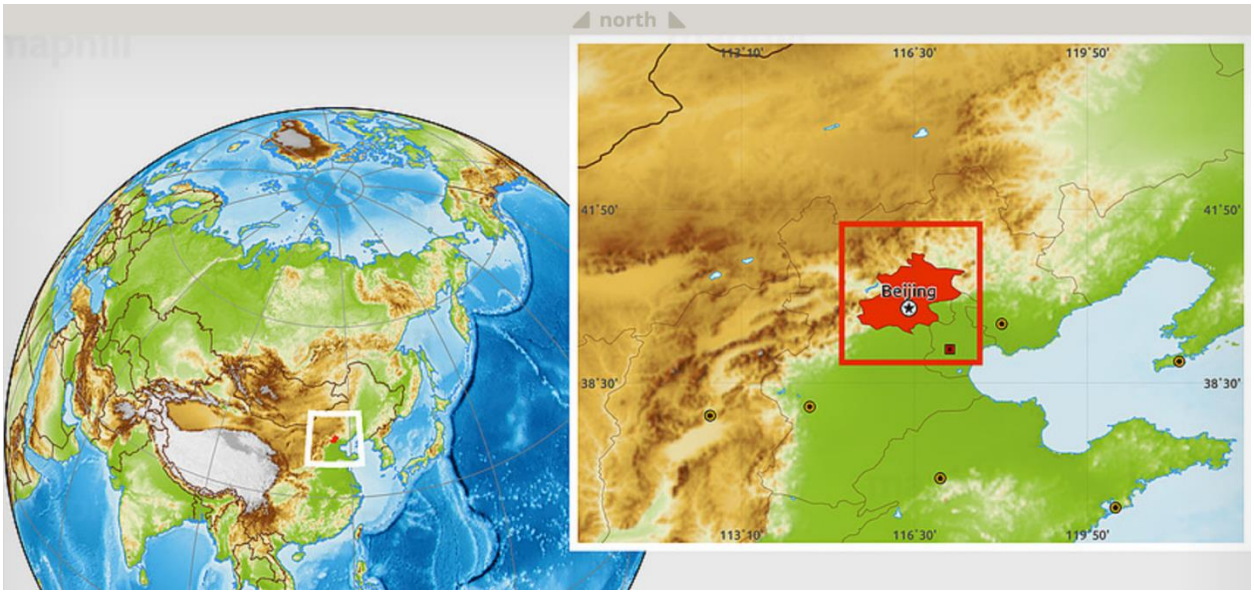

Figure 1: The Location of Beijing in the North China Plain.

(Maphill, 2011)

With the fast urbanization and industrialization process, Beijing has observed a sharp increase in the frequency of severe air pollution incidents in the past few decades. During the wintertime in 2012 and 2013, the severe haze incident affected Beijing repeatedly, causing serious environmental and health problems. Zheng et al. (2015) conducted the model-assisted analysis on major chemical compositions of $PM_{2.5}$ pollutant in Beijing based on the hourly observation data. Their conclusions are, (1) The severe haze incidents happened in Beijing were driven by stable weather conditions in Northeast China. (2) The major component of $PM_{2.5}$ during 2012 to 2013 were secondary species or made by human activities, including organics, sulfate, nitrate, and ammonium. (3) The aerosol concentration accumulation process happened in southeast part of Beijing was persistent.

3.2. Data Acquisition and Processing

3.2.1. Siting Criteria of Official Beijing Municipal $PM_{2.5}$ Datasets

The $PM_{2.5}$ air pollution were monitored and published by the Beijing Municipal Environmental Monitoring Center. The siting criteria was according to the *Technical Specifications for Installation and Acceptance of Ambient Air Quality Continuous Automated Monitoring System for PM_{10} and $PM_{2.5}$* (HJ 655-2013) (Ministry of Ecology and Environment Protection of the People's Republic of China, 2013). All the monitoring sites should be on the ground when intermittent monitoring method is used. Around the monitoring site, there should not be new construction site, or tall buildings, trees or other obstacles to hinder the air circulations. The height of sample collection ports from the ground should be within 3 to 15 meters. The air flow within the space of 270 degrees around the sample collection port should not be affected by other environmental factors. For the road traffic pollution monitoring sites, the height of sampling ports from the ground should be within 2 to 5 meters. The distance between the sampling ports and the upholder surface such as building walls, roof should be more than 1 meter. If there are physical fences around the upholder surface, the sampling ports should be higher than solid fences at least 0.5 meters. When the multiple sampling sites are set up, to prevent interference of other particulate sample collection, particulate matter sampling ports should be kept greater than 1-meter in horizontal distance with other sampling ports. If the reference sampler flow rate ⩽ 200L/min during the comparative monitoring, the linear distance between each sampling port of the sampler and the monitor should be about 1 meter. If the reference sampler flow rate >200L/min, the linear distance between each sampling port of the sampler and the monitor should be 2 ~ 4 meters. If high vacuum and large flow sampling devices are used for comparative monitoring, the linear distance between them should be 3 ~ 4 meters.

Beijing Municipal Environmental Monitoring Center manages a total of 35 environmental air monitoring stations, which are located in different districts and counties in both urban and suburb areas in Beijing. The particle matter sampling site located at Longevity West Palace is one of the selected daily $PM_{2.5}$ data source stations in Beijing which is used in this study (Figure 2)

Figure 2: The Particle Matters Sampling Site and Equipment Setup in Longevity West Palace

3.2.2. Research Data Collection

Hourly values of $PM_{2.5}$ air pollution were monitored and published by the Beijing Municipal Environmental Monitoring Center (http://www.bjmemc.com.cn/). The five-year period datasets

of this research were downloaded with the help of Professor Zhao and his graduate students at the Capital Normal University, Beijing, China. The $PM_{2.5}$ concentration data was collected from the websites of Beijing Municipal Environmental Monitoring Center (http://www.bjmemc.com.cn/) and China Air Quality Real-time Distribution Platform (http://106.37.208.233:20035/) with crawler technology using a Python program. Web crawler is a program or script that automatically captures information on the World Wide Web according to certain rules. Crawler technology is an efficient downloading software that can transfer massive amounts of web data to the local storage space in a continuously manner, where it forms a mirror backup of Internet pages (Meng et al., 2006).

After the $PM_{2.5}$ source data was collected, we conducted manual examinations and data quality evaluations. Eight (8) monitoring stations were removed owing to large quantity of "null" values in the database. We think the reason to cause this situation is the instability of the data collecting computer. This research used the datasets of remaining 27 environmental air monitoring stations located in both urban area and suburb area (Figure 3) across Beijing.

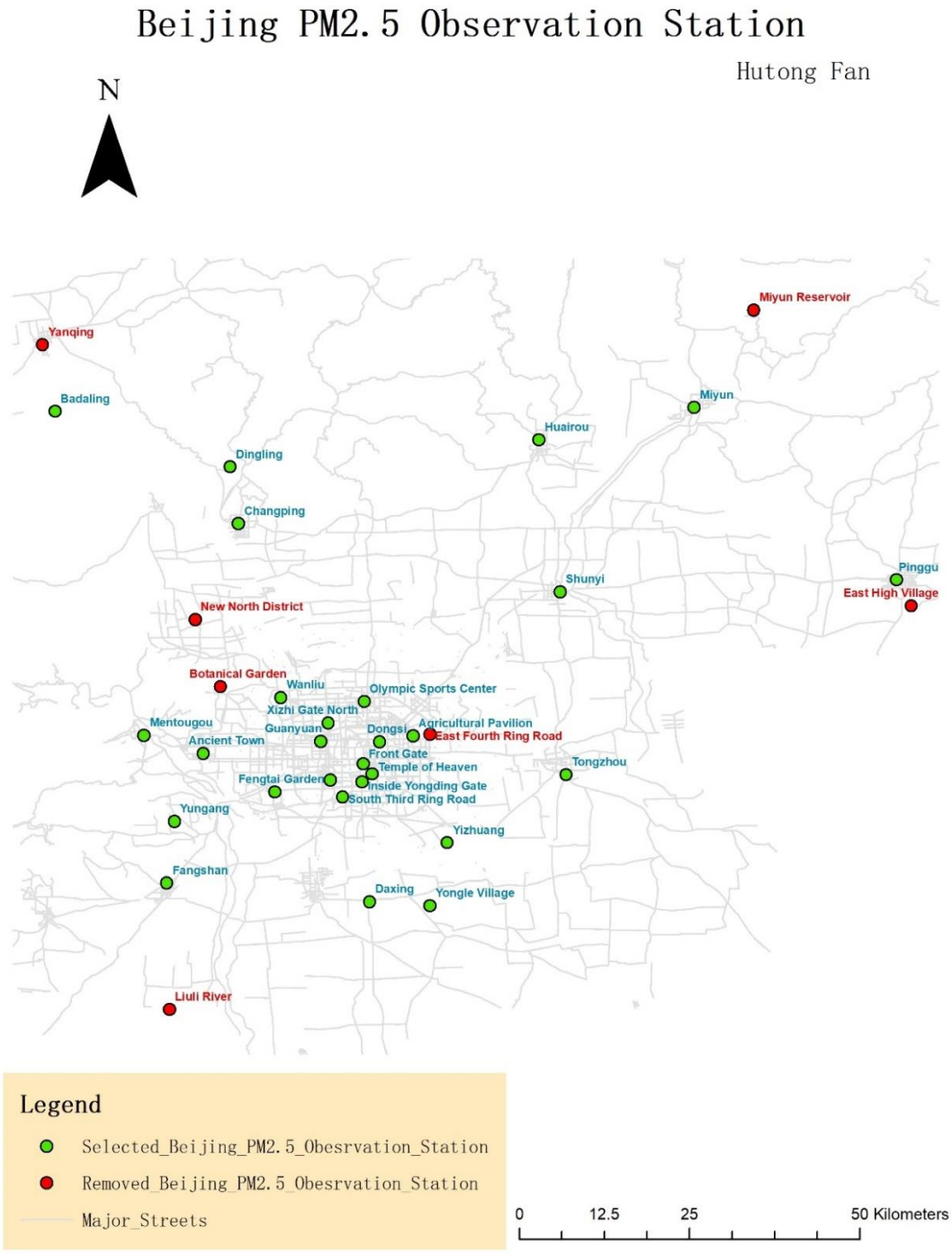

Figure 3: Map of Total $PM_{2.5}$ Observation Sites and the Sites Used in This Research in Beijing Municipality

3.2.3. Research Time Selection and Data Processing

Fan et al. (2015) studied emission characteristics of vehicle exhaust based on actual traffic flow information in Beijing. The research analyzed the spatial and temporal distribution patterns of vehicle volume and pollutant emission quantities. The research indicated there was a positive correlation between pollutant emission intensities and traffic volume. The emission intensity was generally higher during the daytime and high traffic hours than the evening hours. Based on the results of this research, we hypothesized the possible high and low pollution time periods during a 24-hour day. A total of five (5) sample time periods were classified for each of the monitoring days during the five-year period. These are: morning peak traffic time period (MPT, an average $PM_{2.5}$ concentration data from 06:00am and 08:00am); morning low traffic time period (MLT, an average $PM_{2.5}$ concentration data from 9:00am and 11:00am); afternoon low traffic time period (ALT, an average $PM_{2.5}$ concentration data from 01:00pm and 03:00pm); afternoon peak traffic time period (APT, an average $PM_{2.5}$ concentration data from 04:00pm and 06:00pm); and midnight time period (MIDN, an average $PM_{2.5}$ concentration data from 01:00am and 03:00am). MPT and APT are the commuting peak time in Beijing which have the maximum traffic flow. MLT and ALT are the major working time periods during a day. We would like to find the contribution of human activities on the $PM_{2.5}$ pollutions in Beijing. To discover the potential contributions of $PM_{2.5}$ concentration from heating supply to buildings and houses in Beijing, we also selected a mid-night sample period.

Data of sampling time periods were extracted using MATLAB software and stored in Excel. Python programming was applied to integrate those Excel charts into yearly different and site different Excel sheets (Appendix A, several notes and result output language in Chinese). One

example of Python program was inserted into the appendix. A total of 27 programs were made for the 27 environmental air pollution observation sites. In each dataset, our selected time periods are in the order of MIDN, MPT, MLT, ALT, APT. (Figure 4)

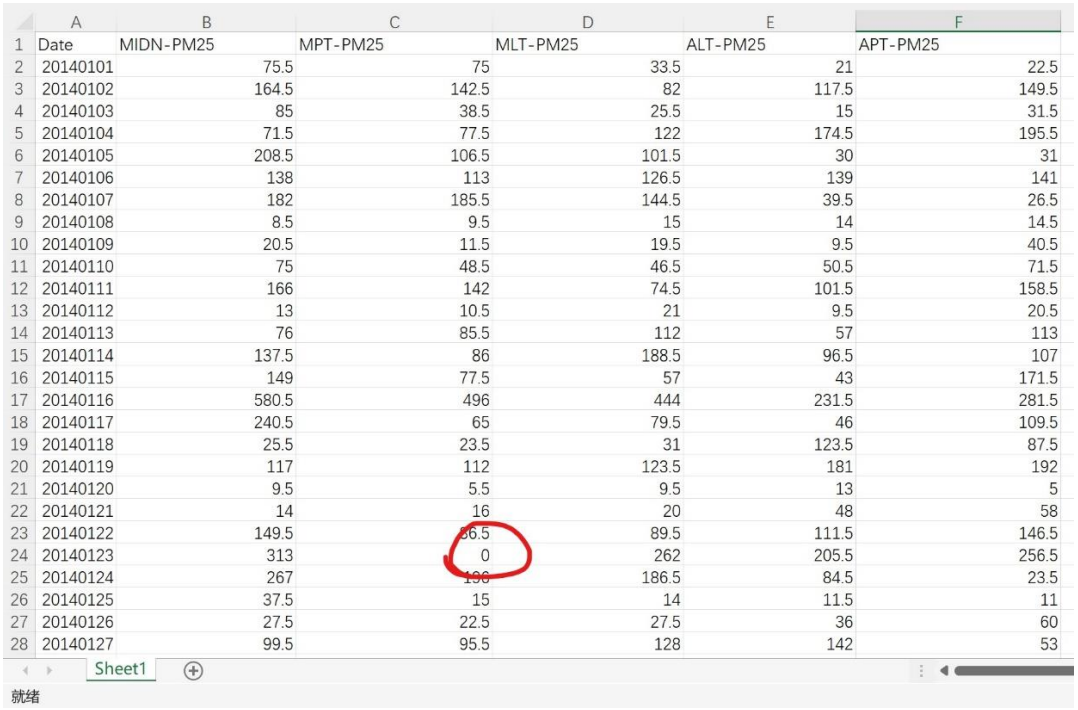

	A	B	C	D	E	F
1	Date	MIDN-PM25	MPT-PM25	MLT-PM25	ALT-PM25	APT-PM25
2	20140101	75.5	75	33.5	21	22.5
3	20140102	164.5	142.5	82	117.5	149.5
4	20140103	85	38.5	25.5	15	31.5
5	20140104	71.5	77.5	122	174.5	195.5
6	20140105	208.5	106.5	101.5	30	31
7	20140106	138	113	126.5	139	141
8	20140107	182	185.5	144.5	39.5	26.5
9	20140108	8.5	9.5	15	14	14.5
10	20140109	20.5	11.5	19.5	9.5	40.5
11	20140110	75	48.5	46.5	50.5	71.5
12	20140111	166	142	74.5	101.5	158.5
13	20140112	13	10.5	21	9.5	20.5
14	20140113	76	85.5	112	57	113
15	20140114	137.5	86	188.5	96.5	107
16	20140115	149	77.5	57	43	171.5
17	20140116	580.5	496	444	231.5	281.5
18	20140117	240.5	65	79.5	46	109.5
19	20140118	25.5	23.5	31	123.5	87.5
20	20140119	117	112	123.5	181	192
21	20140120	9.5	5.5	9.5	13	5
22	20140121	14	16	20	48	58
23	20140122	149.5	86.5	89.5	111.5	146.5
24	20140123	313	0	262	205.5	256.5
25	20140124	267	196	186.5	84.5	23.5
26	20140125	37.5	15	14	11.5	11
27	20140126	27.5	22.5	27.5	36	60
28	20140127	99.5	95.5	128	142	53

Sheet1

就绪

Figure 4: Example of Integrated Dataset, Agriculture Pavilion Site, 2014

After reorganizing the hourly $PM_{2.5}$ air pollution observation datasets during five years, each site has 5 Selected Datasets for each sampling year, and there are 135 Selected Datasets in total for the 27 air pollution monitoring stations.

In order to capture the seasonal distribution and changes of the $PM_{2.5}$ air pollutions, one of the major approaches in this study is to divide the season in each year and calculate the mean value. Using a typical meteorological breakdown of seasons, we decided to use March, April, May in each year as months of spring season; June, July, August in each year as months of summer

season; September, October, November in each year as months of autumn season; December, January, February in each year as months of winter season. Then we calculated the seasonal average of $PM_{2.5}$ concentrations in each of the observation sites in each year and saved them into new datasets (Seasonal Average Selected Datasets). (Figure 5) These operations were completed with Excel. We obtained 5 Seasonal Average Selected Datasets for each sampling year which include all the observation sites.

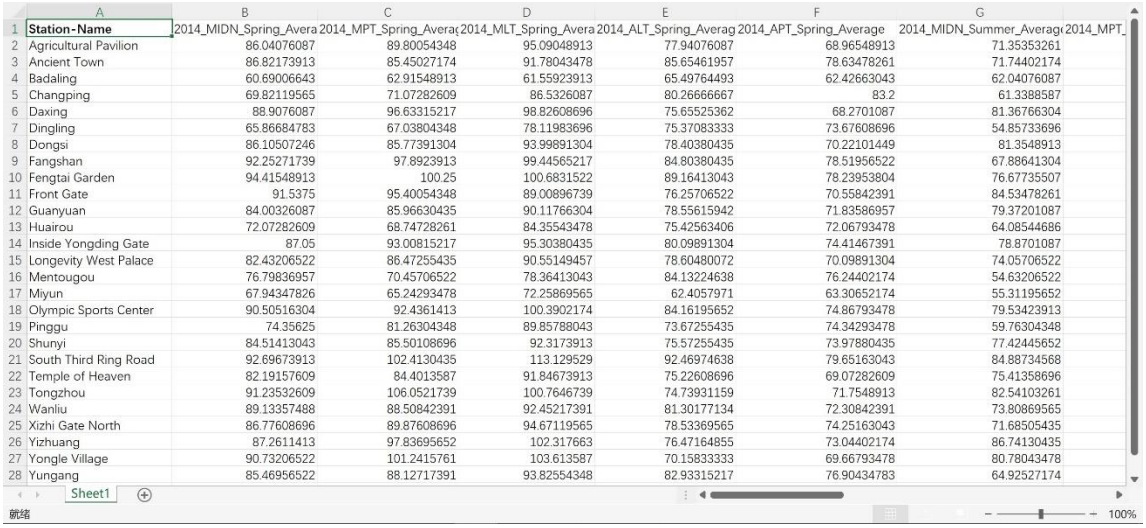

	A	B	C	D	E	F	G	
1	Station-Name	2014_MIDN_Spring_Avera	2014_MPT_Spring_Avera	2014_MLT_Spring_Avera	2014_ALT_Spring_Averag	2014_APT_Spring_Average	2014_MIDN_Summer_Averag	2014_MPT_
2	Agricultural Pavilion	86.04076087	89.80054348	95.09048913	77.94076087	68.96548913	71.35353261	
3	Ancient Town	86.82173913	85.45027174	91.78043478	85.65461957	78.63478261	71.74402174	
4	Badaling	60.69006643	62.91548913	61.55923913	65.49764493	62.42663043	62.04076087	
5	Changping	69.82119565	71.07282609	86.5326087	80.26666667	83.2	61.3388587	
6	Daxing	88.9076087	96.63315217	98.82608696	75.65525362	68.2701087	81.36766304	
7	Dingling	65.86684783	67.03804348	78.11983696	75.37083333	73.67608696	54.85733696	
8	Dongsi	86.10507246	85.77391304	93.99891304	78.40380435	70.22101449	81.3548913	
9	Fangshan	92.25271739	97.8923913	99.44565217	84.80380435	78.51956522	67.88641304	
10	Fengtai Garden	94.41548913	100.25	100.6831522	89.16413043	78.23953804	76.67735507	
11	Front Gate	91.5375	95.40054348	89.00896739	76.25706522	70.55842391	84.53478261	
12	Guanyuan	84.00326087	85.96630435	90.11766304	78.55615942	71.83586957	79.37201087	
13	Huairou	72.07282609	68.74728261	84.35543478	75.42563406	72.06793478	64.08544686	
14	Inside Yongding Gate	87.05	93.00815217	95.30380435	80.09891304	74.41467391	78.8701087	
15	Longevity West Palace	82.43206522	86.47255435	90.55149457	78.60480072	70.09891304	74.05706522	
16	Mentougou	76.79836957	70.45706522	78.36413043	84.13224638	76.24402174	54.63206522	
17	Miyun	67.94347826	65.24293478	72.25869565	62.4057971	63.30652174	55.31195652	
18	Olympic Sports Center	90.50516304	92.4361413	100.3902174	84.16195652	74.86793478	79.53423913	
19	Pinggu	74.35625	81.26304348	89.85788043	73.67255435	74.34293478	59.76304348	
20	Shunyi	84.51413043	85.50108696	92.3173913	75.57255435	73.97880435	77.42445652	
21	South Third Ring Road	92.69673913	102.4130435	113.129529	92.46974638	79.65163043	84.88734568	
22	Temple of Heaven	82.19157609	84.4013587	91.84673913	75.22608696	69.07282609	75.41358696	
23	Tongzhou	91.23532609	106.0521739	100.7646739	74.73931159	71.7548913	82.54103261	
24	Wanliu	89.13357488	88.50842391	92.45217391	81.30177134	72.30842391	73.80869565	
25	Xizhi Gate North	86.77608696	89.87608696	94.67119565	78.53369565	74.25163043	71.68505435	
26	Yizhuang	87.2611413	97.83695652	102.317663	76.47164855	73.04402174	86.74130435	
27	Yongle Village	90.73206522	101.2415761	103.613587	70.15833333	69.66793478	80.78043478	
28	Yungang	85.46956522	88.12717391	93.82554348	82.93315217	76.90434783	64.92527174	

Sheet1

就绪

100%

Figure 5: Example of Seasonal Average Selected Datasets, 2014

3.3. Methods and Approaches of Temporal Distributions and Change of Air Pollution

3.3.1. Fundamental Data Analysis – Linear Regression Model Regression Trend Lines

In big data analysis, regression analysis is a predictive modeling technique that studies the relationship between dependent variables (targets) and independent variables (predictors). This technique is often used in predictive analysis. In statistics, regression analysis refers to a statistical analysis method that determines the quantitative relationship between two or more variables that are depended on each other. We conducted basic analysis of simple seasonal

temporal pattern with the linear regression model of daily average $PM_{2.5}$ concentration data in R studio (Appendix C). Linear regression model is one of the most well-known modeling techniques. Linear regression model is a statistical analysis method that uses regression analysis in mathematical statistics to determine the interdependent quantitative relationship between two or more variables. Linear regression uses the best fitting line (regression line) to establish a relationship between the dependent variable (Y) and one or more independent variables (X). In our study, daily variation or temporal change patterns were specified as the dependent variable and $PM_{2.5}$ concentrations as independent variable. The objective of this analysis is to demonstrate the general trend of slopes on decreasing or increasing of seasonal $PM_{2.5}$ concentrations with regression trend lines of linear regression model in the 5-year period. This simple temporal pattern can show the general trends of seasonal variation on $PM_{2.5}$ pollutants in Beijing.

To show the significance of time trend in these sites, we conducted Mann-Kendall statistical test in the R studio (Appendix C). The Mann-Kendall nonparametric statistical method recommended by the World Meteorological Organization and is widely used. The method can effectively distinguish whether a natural process is in natural fluctuation or has a monotonic trend (Cao et al., 2008). Mann-Kendall nonparametric rank test is useful in trend detection of data. Its advantage are as follows, first, the series is allowed to have missing values. Secondly, there is no need to conduct specific distribution test for data series, and trend test can also be performed for extreme values. Thirdly, the analysis is mainly about the relative order of magnitude rather than the number itself, which enables the analysis of trace values or values below the detection range (Karmeshu, 2012).

With the help of R studio, we generated 5-year seasonal datasets in the program and conducted analyses of two observation sites by two observation sites, all the codes we used are in the Appendix C.

3.3.2. Principal Component Analysis – PCA

Principal Component Analysis (PCA), is a multivariate statistical method to examine the correlation among multiple variables. PCA studies how to reveal the internal structure among multiple variables through a few principal components, deriving a few principal components from the original variables so that they retain as much information as possible about the original variables. The objective of using PCA in this research is to look for the major impact pollution pattern among the five different sampling times during a day in five-year period in temporal scale for the entire five years.

We analyzed aggregative temporal patterns of the dataset with the principal component analysis (PCA) in MATLAB platform. The detail program code of this analysis is listed in Appendix D. The first step in PCA procedure is Data Arrangement. We converted the data from Excel worksheets into a MATLAB data file, which organized by location and year. In order to standardize the data, we subtracted the mean and dividing by the standard deviation for each value of the variables. The purpose of this step is to standardize the range of continuous initial variables so that each of them contributes equally to the analysis. The next step is the Covariance Matrix Computation. The purpose of this step is to understand how the variables in the input data set vary relative to each other's means, in order to determine the relationships between variables. Then we computed the eigenvectors and eigenvalues of the covariance matrix to identify the principal components. The principal component with the highest variance is termed the “first principal

component." To avoid protentional negative values in the process, which are meaninglessness in $PM_{2.5}$ concentration values, we only used the result of "first principal component". In the end, we recasted the data along the axes of principal components. The purpose is to redirect the data from the original axes to the axes represented by the principal components using the eigenvectors formed by the eigenvectors of the covariance matrix.

Based on tutorial textbook of Shlens (2014), the central idea of principal component analysis is to reduce the dimensionality of a data set composed of many related variables while preserving the variation existed in the data set as much as possible. This is achieved by converting input variables to a new set of variables, known as principal components (PCS), which are unrelated and ordered so that the first few retain most of the changes that occurred in all the original variables. The principal component represents the direction of the data that explains the largest amount of variance or changes over time period, that means the line that captures most of the information in the dataset. In this study, our objective is to find the principal component that represents the temporal variations of the entire time during this 5-year on the hourly basis, which is a measurement or survey in this large database.

3.4. Methods and Approaches of Spatial Distributions of Air Pollution

3.4.1. Recent Development of Spatial Interpolation Methods – A General Review

Spatial interpolation is the process of estimating the values of the variables to be studied at unsampled locations with data of known observation points in the same region. Statistical interpolation methods were applied to air pollutant modeling to estimate the spatial distribution of air pollutions based on data provided by air quality monitoring sites (Lozano et al, 2009; Deligiorgi et al, 2011). In general, there are two major categories of interpolation techniques:

deterministic and geostatistical. Proximity interpolation, global polynomial interpolation (GPI), local polynomial interpolation (LPI), inverse distance weighted (IDW), and radial basis functions (RBF) belong to the category of deterministic methods. Geostatistical interpolation techniques include surface trend and Kriging. Deterministic interpolation methods create prediction value surfaces with measured points based on degree of similarity or smoothness (Gimond, 2021). Geostatistical methods quantify the spatial autocorrelation between measurement points and account the spatial configuration of sampling points around the predicted location. Based on statistical data, these approaches are able to generate not only prediction value surface, but also error surface or uncertainty surface to indicate the ideal degree of prediction results (Gimond, 2021). In addition, based on different application scenarios, several spatial analysis models were developed. Triangular Irregular Network (TIN) is for elevation, slope and aspect modelling. Neighborhood Analysis is for spatial analysis of categorical data. Data with natural neighborhood points should be mapped to discrete regions where the value assigned to each point is constant, such as soil type and land use.

3.4.2. Methods of Inverse Distance Weighted Spatial Interpolation

The Inverse Distance Weighted (IDW) technique uses values from nearby weighted positions to calculate the average of unsampled positions. IDW interpolation explicitly assumes that things are close to one another are more alike than those that are further apart. It is expected that we will have more accurate result from IDW interpolation for those physically generated features or events. Based on Gimond's guidance article (2021), the weight is proportional to the proximity of the sampling point to the unsampled position and can be specified by the IDW power

coefficient. The bigger the power coefficient, the stronger the weight of nearby points as can be gleaned from the following equation that estimates the value *z* at an unsampled location *j:*

$$\hat{Z}_j = \frac{\sum_i Z_i / d_{ij}^n}{\sum_i 1 / d_{ij}^n}$$

The carat ^ above the variable *z* points out that the value at *j* is being estimated. The parameter *n* is the weight parameter that is applied as an exponent to the distance thus amplifying the irrelevance of a point at location *i* as distance to *j* increases.

IDW algorithm is actually a moving average interpolator that is typically applied to highly variable data. For some specific data types, it is possible to return to the collection site and record a new value within the overall trend for the region. Examples of such data include soil chemistry results, and environmental monitoring data. To predict a value for any unmeasured location, IDW uses the measured values surrounding the prediction location. In this study, we used the average data that was calculated from observation stations to predict spatial distributions of $PM_{2.5}$ air pollutions. In addition, IDW assumes that the local effect of each of the measurement points decreases with increasing distance, which better reflects the geographic distribution pattern of the $PM_{2.5}$ in the city. In our study, we will make $PM_{2.5}$ concentration spatial interpolation maps in annual average and in seasonal average by five different sample time periods for each of the 27 air pollution monitoring stations applying ArcGIS Desktop.

3.5. Integration of Spatial and Temporal Analyses with Large Air Pollution Dataset

Reading the result atlas of spatial interpolations, we decided to perform standardization procedures to separate and standardize the legend in our annual average spatial interpolation

atlas (Annual Average Atlas) of $PM_{2.5}$ concentrations and seasonal average spatial interpolation atlas (Seasonal Average Atlas) for different daily sample time periods of $PM_{2.5}$ concentrations. For the annual average spatial interpolation atlas of $PM_{2.5}$ concentrations, we selected 5 ug/m^3 as the legend group unit. All the maps in the annual average spatial interpolation atlas of $PM_{2.5}$ concentrations began at 50 ~ 55 ug/m^3 group and end at 95 ~ 100 ug/m^3 group. There are a 10 concentration groups in total.

In the spatial interpolation atlas for seasonal average of $PM_{2.5}$ concentrations at different daily sample time periods, we found 27 ug/m^3 is the lowest $PM_{2.5}$ concentration, which is from APT time in the summer of 2018. The highest $PM_{2.5}$ concentration is 200 ug/m^3 and is from MIDN time in the winter of 2015. To guarantee the distinguishability of each map, we defined 18 concentration groups in total. For the Seasonal Average Atlas, we selected 10 ug/m^3 as the legend group unit. All the maps of seasonal spatial interpolation atlas of $PM_{2.5}$ concentrations in the different daily sample time periods began at 20 ~ 30 ug/m^3 group and end at 190 ~ 200 ug/m^3 group.

Owing to majority of maps in the Seasonal Average Atlas have completely different $PM_{2.5}$ concentration range, we need to use ArcGIS Desktop to create a “hypothetical” standard $PM_{2.5}$ concentration map (Figure 6) based on the adjusted $PM_{2.5}$ concentration dataset to generate the standardized legend for the Seasonal Average Atlas. This “hypothetical” $PM_{2.5}$ concentration map includes the lowest and highest $PM_{2.5}$ pollutant values. Then, we used the function “convert a map element into a graphic” to convert the legend to a graphic, which means disconnect to the “hypothetical” map document and is able to copy to all the maps in the Seasonal Average Atlas.

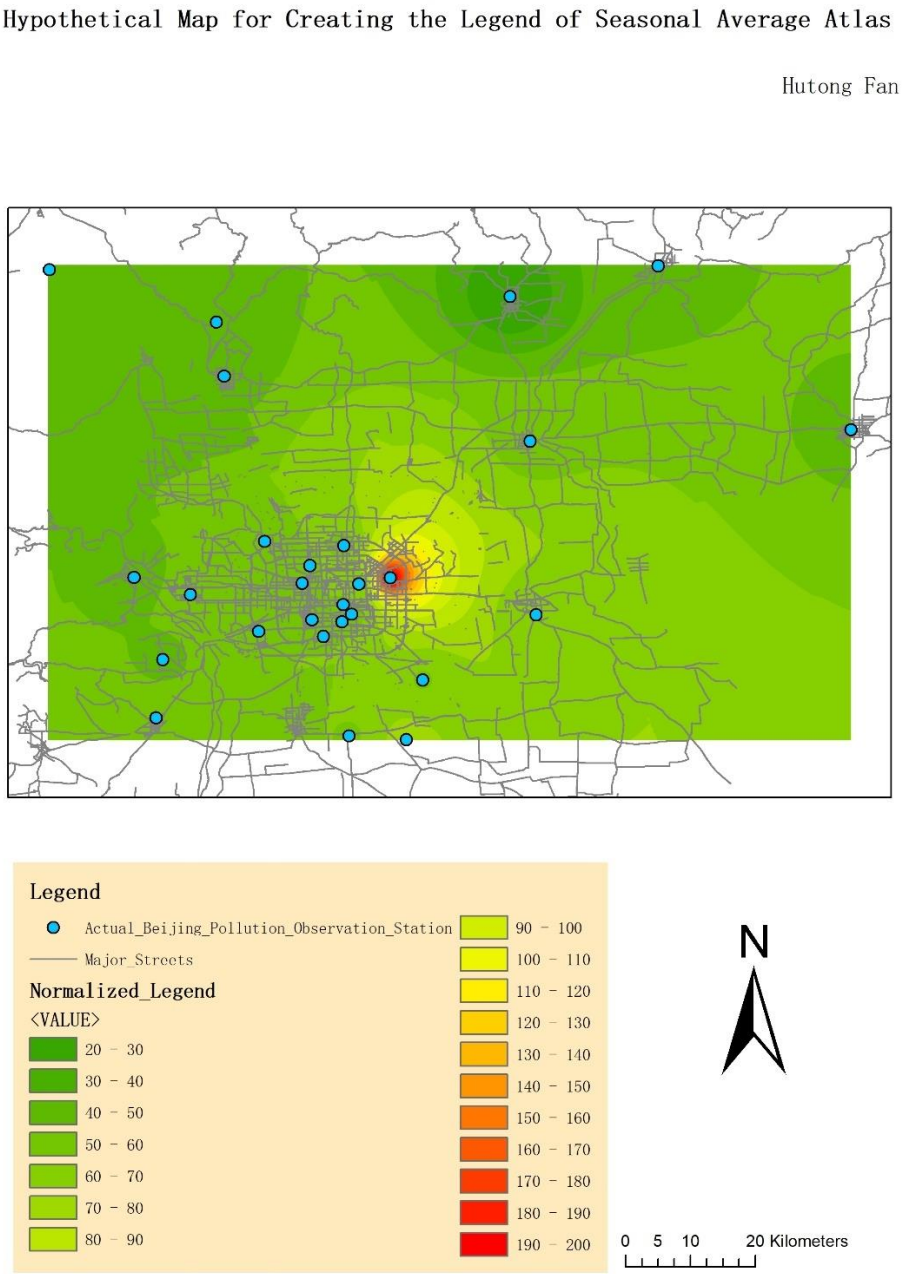

Figure 6: Hypothetical Map for Creating the Legend of Seasonal Average Atlas (ug/m^3)

4. Results

4.1. Results of Temporal Analysis of Air Pollution

4.1.1. Results of Mann-Kendall Trend Analysis

We analyzed the slope of trend lines and p-values and organized several charts in the R studio program (Appendix C). In our Basic Data Analysis, the null hypothesis is that there is no obvious up or down trend within the five-year period for different seasons. If p-value < 0.01, the description of the result is a stronger determination in rejecting the null hypothesis. If p-value is between 0.01 and 0.05, the description of the result is a weaker determination in rejecting the null hypothesis. If p-value > 0.05, it indicates that the results are more inclined to accept the null hypothesis.

Table 2 summarizes the result of slope and p-value of spring season trend line during the five-year period. Table 2 is sorted by the slope rate from lowest to highest. From Table 2, we can find p-values of several sites are between 0.01 and 0.05 (green section) or higher than 0.05 (orange section). Meanwhile, 11 of 27 $PM_{2.5}$ observation sites show that there are significant descending trends in the spring season during the five-year period of $PM_{2.5}$ contaminant concentrations. 11 of 27 $PM_{2.5}$ observation sites show there are weak descending trends in the spring season during the five-year period of $PM_{2.5}$ contaminant concentrations. 5 of 27 $PM_{2.5}$ observation sites show that there are no obvious up or down trends of $PM_{2.5}$ contaminant concentration in the spring season during the five-year period. Figure 7 shows the example result of 3 diagrams with different trend conclusions. The detailed diagrams can be found in Appendix E. From Figure 7, we can clearly identify the differences of the slope of trend lines. Although the variance of p-value results exists, majority of $PM_{2.5}$ observations (22 of 27) show descending trend (significant or weak trend) during the spring season of five years. Comparing different locations of the $PM_{2.5}$

observation sites in the spring (Table 2), all 5 sites with no obvious variation trends are located in the suburban areas in Beijing.

Station-Name	Spring Slope	P-value
Fangshan	-0.0842	<0.01
South Third Ring Road	-0.07639	<0.01
Yungang	-0.07217	<0.01
Yizhuang	-0.07102	<0.01
Daxing	-0.0642	<0.01
Fengtai Garden	-0.06266	<0.01
Inside Yongding Gate	-0.06159	<0.01
Agricultural Pavilion	-0.05878	<0.01
Tongzhou	-0.05798	<0.01
Wanliu	-0.05735	<0.01
Olympic Sports Center	-0.05692	<0.01
Front Gate	-0.05393	0.01019
Temple of Heaven	-0.05079	0.01083
Shunyi	-0.04966	0.02043
Yongle Village	-0.04934	0.01412
Huairou	-0.04844	0.01377
Longevity West Palace	-0.04674	0.02326
Pinggu	-0.04505	0.02396
Guanyuan	-0.0436	0.03119
Dongsi	-0.04342	0.04226
Changping	-0.04183	0.03521
Xizhi Gate North	-0.04166	0.04641
Ancient Town	-0.04018	>0.05
Dingling	-0.03518	>0.05
Mentougou	-0.03273	>0.05
Miyun	-0.01769	>0.05
Badaling	0.000885	>0.05

Table 2: Results of Slope rate and P-value from Five-year Spring Sampling Trend Line

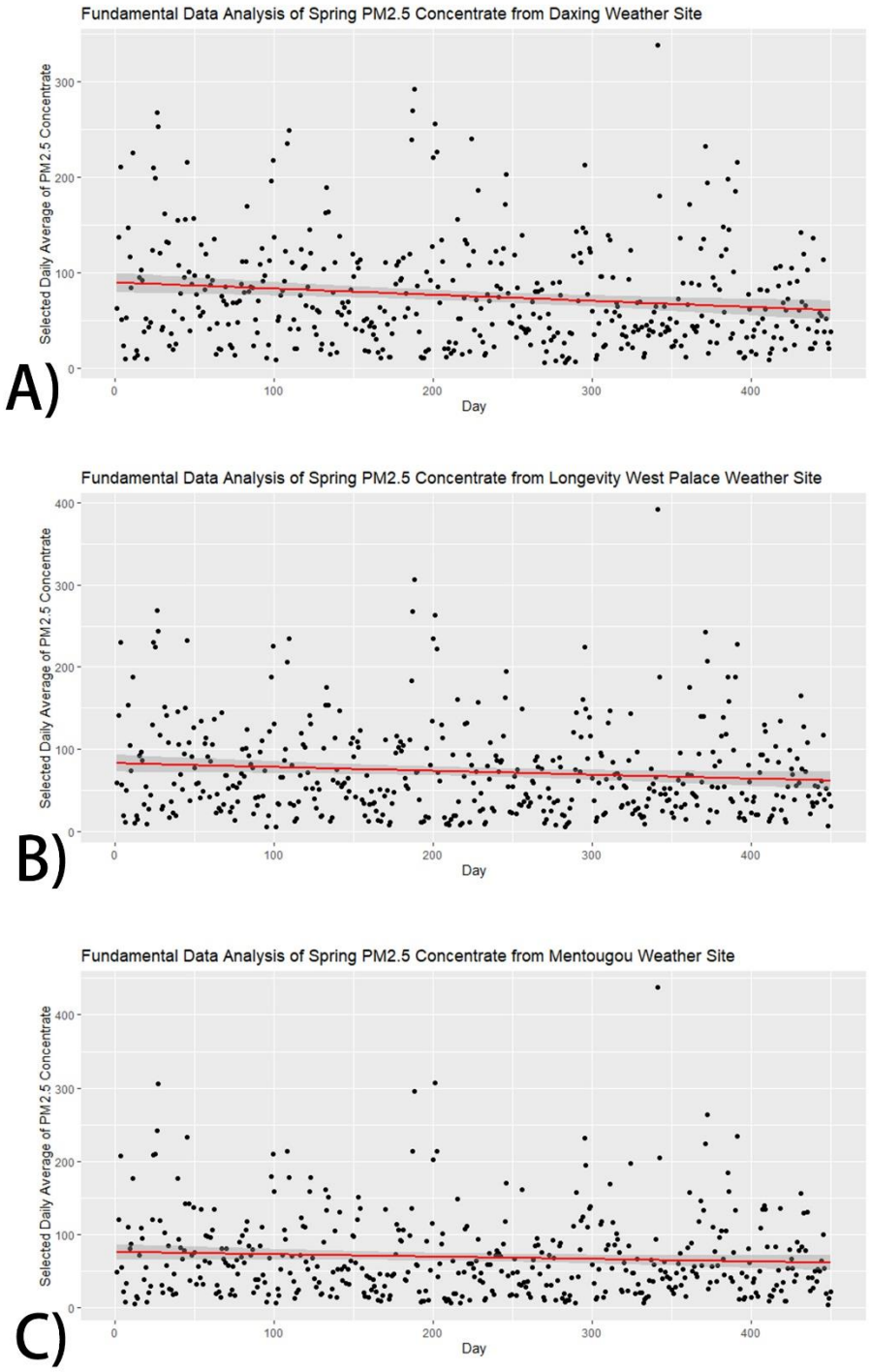

Figure 7: Examples of Different Trend Conclusions in Spring

A) Daxing ($p < 0.01$), B) Longevity West Palace ($0.01 < p < 0.05$), C) Mentougou ($p > 0.05$)

Table 3 presents the result of slopes and p-values of trend lines for the summer during the five-year period, sorted by slope rate from lowest to highest. The detailed graphs can be found in Appendix E. All the p-values of $PM_{2.5}$ observation sites are less than 0.01. Comparing with negative slope rates, all the $PM_{2.5}$ observation stations show there are significant decreasing trends of $PM_{2.5}$ contaminant concentration during the summer of five-year period.

Station-Name	Summer Slope	P-value
South Third Ring Road	-0.11223	<0.01
Yizhuang	-0.1022	<0.01
Daxing	-0.1004	<0.01
Guanyuan	-0.08778	<0.01
Tongzhou	-0.08653	<0.01
Olympic Sports Center	-0.08599	<0.01
Temple of Heaven	-0.08449	<0.01
Dongsi	-0.08321	<0.01
Front Gate	-0.08149	<0.01
Yungang	-0.08036	<0.01
Shunyi	-0.07902	<0.01
Pinggu	-0.07718	<0.01
Fangshan	-0.07604	<0.01
Wanliu	-0.07571	<0.01
Huairou	-0.07538	<0.01
Inside Yongding Gate	-0.07533	<0.01
Fengtai Garden	-0.07304	<0.01
Yongle Village	-0.07204	<0.01
Longevity West Palace	-0.06851	<0.01
Ancient Town	-0.06802	<0.01
Agricultural Pavilion	-0.06619	<0.01
Changping	-0.06546	<0.01
Dingling	-0.05571	<0.01
Mentougou	-0.04885	<0.01
Xizhi Gate North	-0.04631	<0.01
Badaling	-0.04514	<0.01
Miyun	-0.04451	<0.01

Table 3: Results of Slope rate and P-value from Five-year Summer Sampling Trend Line

Table 4 shows the result of slopes and p-values of autumn season during the five-year period, sorted by slope rate from lowest to highest. All the p-values of $PM_{2.5}$ observation sites are less than 0.01. Comping with negative slope rates, all the $PM_{2.5}$ observation sites show the trends of significant decrease of $PM_{2.5}$ contaminant concentration during the autumn of five-year period.

Station-Name	Autumn Slope	P-value
Yizhuang	-0.1553	<0.01
Daxing	-0.14174	<0.01
Front Gate	-0.12925	<0.01
South Third Ring Road	-0.12858	<0.01
Inside Yongding Gate	-0.12808	<0.01
Agricultural Pavilion	-0.12265	<0.01
Xizhi Gate North	-0.12028	<0.01
Fangshan	-0.11945	<0.01
Fengtai Garden	-0.11504	<0.01
Tongzhou	-0.11134	<0.01
Wanliu	-0.10973	<0.01
Yungang	-0.1071	<0.01
Yongle Village	-0.10435	<0.01
Olympic Sports Center	-0.1021	<0.01
Longevity West Palace	-0.09932	<0.01
Temple of Heaven	-0.09929	<0.01
Guanyuan	-0.09921	<0.01
Ancient Town	-0.09762	<0.01
Dingling	-0.09262	<0.01
Changping	-0.0917	<0.01
Dongsi	-0.08727	<0.01
Shunyi	-0.0828	<0.01
Huairou	-0.0809	<0.01
Mentougou	-0.07568	<0.01
Pinggu	-0.07493	<0.01
Miyun	-0.07254	<0.01
Badaling	-0.06505	<0.01

Table 4: Results of Slope rate and P-value from Five-year Autumn Sampling Trend Line

Table 5 indicates the result of slopes and p-values for winter during the five-year period, sorted by slope rate from lowest to highest. All the p-values of $PM_{2.5}$ observation sites are less than 0.01. Comparing the negative slope rates, all the $PM_{2.5}$ observation sites show there are significant decreasing trends of $PM_{2.5}$ contaminant concentrations in winter of the five-year period.

Station-Name	Winter Slope	P-value
Daxing	-0.24024	<0.01
Fangshan	-0.22595	<0.01
Tongzhou	-0.22527	<0.01
Yizhuang	-0.221	<0.01
Yongle Village	-0.20937	<0.01
Fengtai Garden	-0.19942	<0.01
South Third Ring Road	-0.19311	<0.01
Yungang	-0.18349	<0.01
Olympic Sports Center	-0.1822	<0.01
Front Gate	-0.17994	<0.01
Longevity West Palace	-0.17907	<0.01
Wanliu	-0.17718	<0.01
Agricultural Pavilion	-0.17653	<0.01
Inside Yongding Gate	-0.16561	<0.01
Pinggu	-0.165	<0.01
Dongsi	-0.15862	<0.01
Changping	-0.15601	<0.01
Ancient Town	-0.1541	<0.01
Guanyuan	-0.15385	<0.01
Temple of Heaven	-0.15187	<0.01
Huairou	-0.15095	<0.01
Dingling	-0.15053	<0.01
Xizhi Gate North	-0.14904	<0.01
Shunyi	-0.1459	<0.01
Miyun	-0.13578	<0.01
Mentougou	-0.13316	<0.01
Badaling	-0.09116	<0.01

Table 5: Results of Slope rate and P-value from Five-year Winter Sampling Trend Line

According to these four tables of slope rates during four seasons, almost all the p-values show that $PM_{2.5}$ concentrations were declining during the five-year period (103 of 108 p-value results). Results of both tables and diagrams demonstrate $PM_{2.5}$ air pollutions are decreasing in Beijing for all seasons during the survey period. Figure 8 is the result of different seasons during the five-year period at the Daxing observation station. The slope rates from Daxing observation site in spring, summer, autumn, winter are -0.0642, -0.1004, -0.14174, -0.24024.

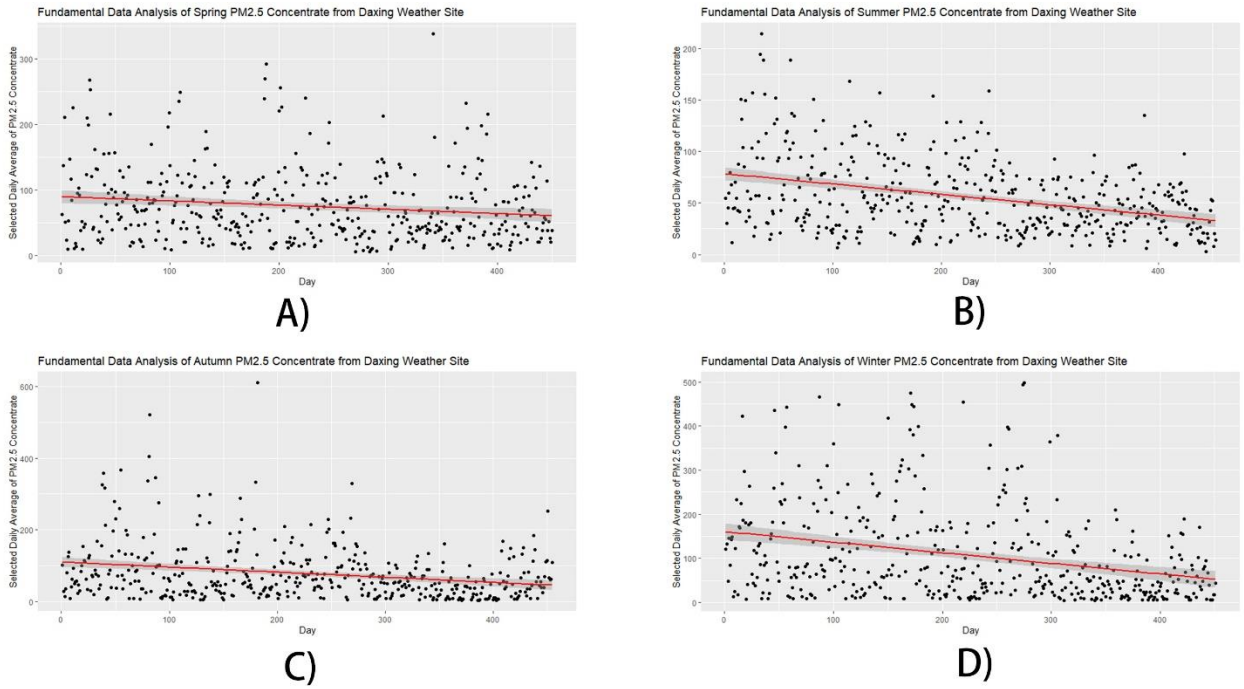

Figure 8: Example: Five-year Different Seasons of $PM_{2.5}$ Contaminant Result

A) Spring, B) Summer, C) Autumn, D) Winter in Daxing Station

4.1.2. Results of Principal Component Analysis

Principal component analysis (PCA) was conducted in the MATLAB environment. All the charts with five eigenvalues and corresponding weight percentage were outputted. Due to the limitation of space, we listed the table of five eigenvalues and corresponding weighting percentage in the Appendix E. To avoid protentional negative values in the process, which are meaninglessness in

$PM_{2.5}$ concentration variable, we only used the result of "first principal component". There are a total of five eigenvalues in the chart. The result of this chart shows that the lowest weight percentage of fifth eigenvalues is 77.62% and the highest weight percentage of fifth eigenvalues is 82.50%. All of the weight percentage of fifth eigenvalues are around 80%. These results of analysis suggest that the fifth eigenvalues are the "first principal component" in our research.

In the meantime, we also outputted the result figures of PCA with the "first principal component". These diagrams are attached in the Appendix F. It is important to point out that the unit in these diagrams are the same as unit of the $PM_{2.5}$ contaminant Datasets (ug/m3). Examples of PCA results of several $PM_{2.5}$ contaminant observation sites, showing Beijing urban and suburban areas similar to Figure 3, are in Figure 9. Sites of Inside Yongding Gate and Xizhi Gate North are located in the urban area in Beijing. Badaling site is located in the north suburb in Beijing and Yongle Village site is located in the south suburb in Beijing.

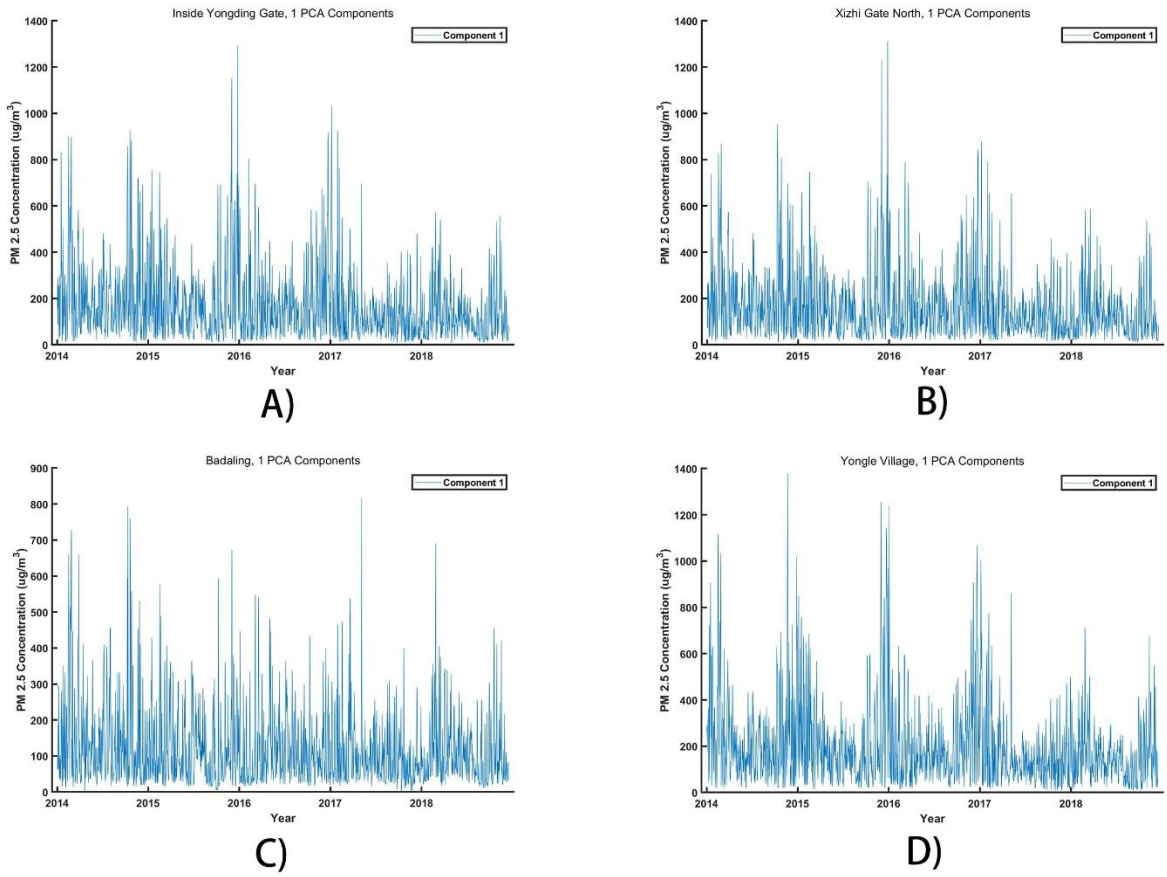

Figure 9: PCA Results of Selected $PM_{2.5}$ Contaminant Observation Sites

A) Inside Yongding Gate, B) Xizhi Gate North, C) Badaling, D) Yongle Village

According to principles of the PCA analysis, PCA is designed for identifying the most significant aspects or characteristics of the dataset. In order to identify the significant temporal distribution patterns of large dataset, the analysis replaces the original data with the most significant aspects of the data. Therefore, PCA analysis is a suitable method to combine $PM_{2.5}$ contaminant temporal variations in the five selected time periods using a single change (time series) curve. The results of PCA time series pattern reflect the daily variations of $PM_{2.5}$ contaminant concentration for the entire 5-year period (Figure 9).

According to all the result figures from PCA analysis in MATLAB (Appendix F), the general trends of $PM_{2.5}$ contaminant concentrations in Beijing at different observation stations are fluctuation downwards. The $PM_{2.5}$ air pollution concentration values are relative higher in the winter each year. This also means the $PM_{2.5}$ contaminate concentration values in winter reach the highest volumes in each year while the year-to-year trend is decreasing. Temporal pattern projected in PCA analysis shows the $PM_{2.5}$ contaminate concentration values in the middle of each year, such as late spring and summer tend to be the lowest. In summary, the results of this research suggest that the $PM_{2.5}$ contaminate concentration is relatively low in summer and relatively high in winter in Beijing. In addition, the Y-axis of $PM_{2.5}$ concentrations in each of result figures shows the magnitudes of $PM_{2.5}$ contaminant concentrations day by day during the five-year period. It is very straightforward to pinpoint when and where the most severe pollution situation occurred during the 5 years. In the urban area in Beijing (Figure 9 A), and B)), the most severe of $PM_{2.5}$ contaminant concentration is around 1300 ug/m3. In the north suburb of Beijing (Figure 9 C)) the most severe of $PM_{2.5}$ contaminant concentration is around 800 ug/m3. In the south suburb of Beijing (Figure 9 D)) the most severe of $PM_{2.5}$ contaminant concentration is around 1300 ug/m3. The $PM_{2.5}$ contaminant concentration in the south suburban region is on the same magnitude as which in the urban areas. This observation result suggests that the downtown urban area is not the highest region of $PM_{2.5}$ pollution distribution. Secondly, this result also suggests that major sources of $PM_{2.5}$ air pollution might at the south part of the urban area and south suburban regions.

4.2. Results of Spatial Distribution Analysis of Air Pollution

4.2.1. Result of Annual Average Spatial Distribution Patterns

Figure 10 shows the annual average spatial distribution patterns of five years from 2014 to 2018. The legend of these maps was standardized and the color presentations of the $PM_{2.5}$ air pollutions are comparable across all the five maps. ArcGIS Desktop was used to conduct IDW interpolations and construct these maps. Among these 5 maps that represent five consecutive years, the highest annual average $PM_{2.5}$ concentrate value range is 95 ~ 100 ug/m3, and the lowest annual average $PM_{2.5}$ concentrate value range is 50 ~ 55 ug/m3. These map results show that the area that suffered the most severe $PM_{2.5}$ air pollutions is in the south and southeast part of Beijing. The area affected least by $PM_{2.5}$ air pollutions is in the north and northwest section in Beijing. It is important to point out that the area with highest $PM_{2.5}$ air pollution concentrations is located in the southern suburban region, it is not in the urban area in Beijing. This suggests the core urban region in Beijing is not the area most impacted by $PM_{2.5}$ air pollutions. During the five-year study period, the severity of $PM_{2.5}$ contaminant concentrations in Beijing is reduced and the air quality becomes better. The annual average value of $PM_{2.5}$ contaminant concentrations become lower as time goes on.

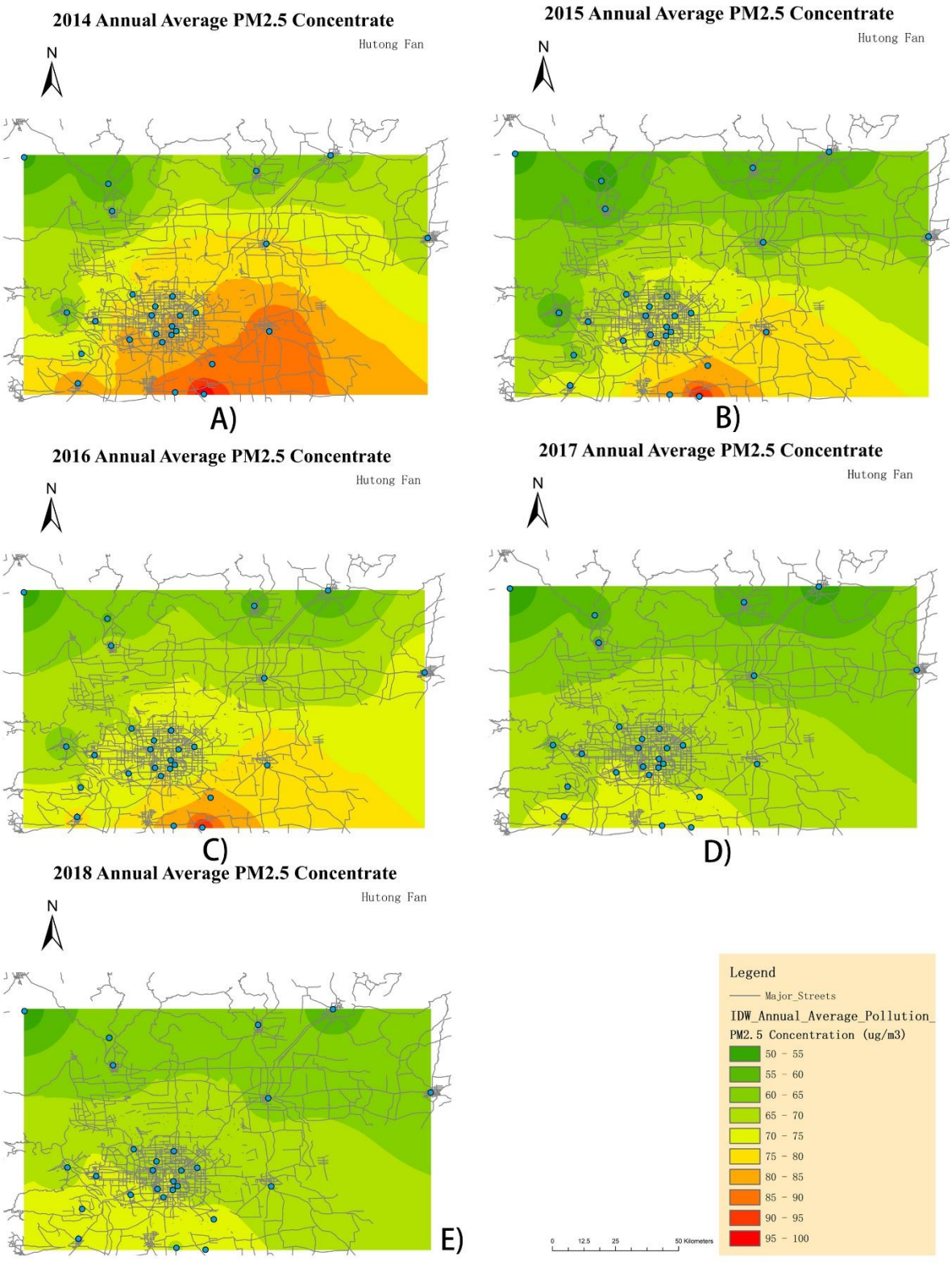

Figure 10: Results of Annual Average Spatial Distribution Patterns (ug/m^3)

A) 2014, B) 2015, C) 2018, D) 2017, E) 2018

4.2.2. Results of Seasonal Average Distribution Patterns for Different Daily Sample Time Periods

Example of seasonal average distribution patterns of the different daily sample time periods is shown in Figure 11. A total of 20 $PM_{2.5}$ air pollution maps are in the Appendix G, which are sorted by the time order. In the meantime, all the legends on these maps were standardized for the purpose of better visualization and comparisons. In this atlas of $PM_{2.5}$ air pollution maps, the highest average $PM_{2.5}$ concentration value range is 190 ~ 200 ug/m3, and the lowest average $PM_{2.5}$ concentration value range is 20 ~ 30 ug/m3. Comparing the seasonal changes with different daily monitoring time periods, we found that spatial distribution pattern of the $PM_{2.5}$ contaminant concentration also changes. In the majority of time periods in spring, autumn and winter, the area of least $PM_{2.5}$ pollutions is still in the north and northwest part in Beijing, while the area with most $PM_{2.5}$ pollutions is still in the south and southeast region of Beijing (Figure 11, A)). However, the $PM_{2.5}$ air pollution pattern in the summertime shows evenly distributed concentrations in Beijing. In the summer season, the area most affected by $PM_{2.5}$ air pollutions is in the central urban area in Beijing, as well as the south and southeast region of Beijing (Figure 11, B)).

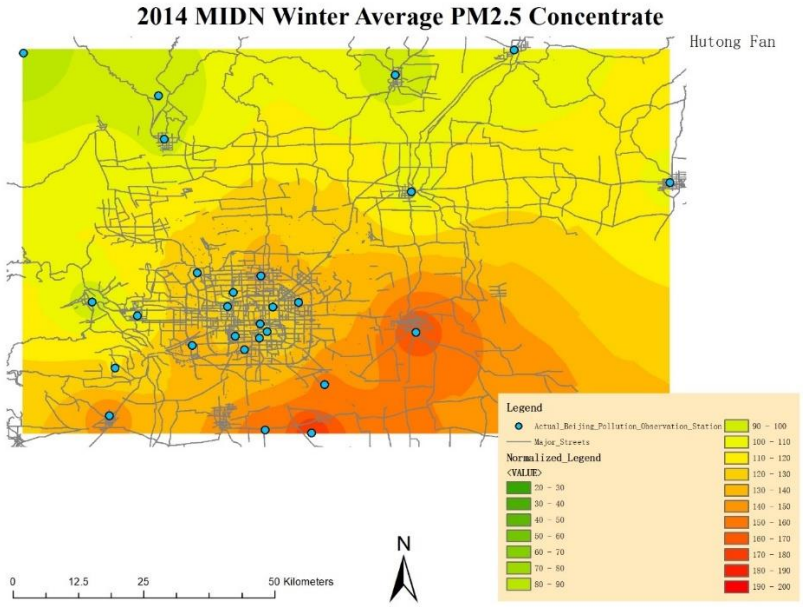

A)

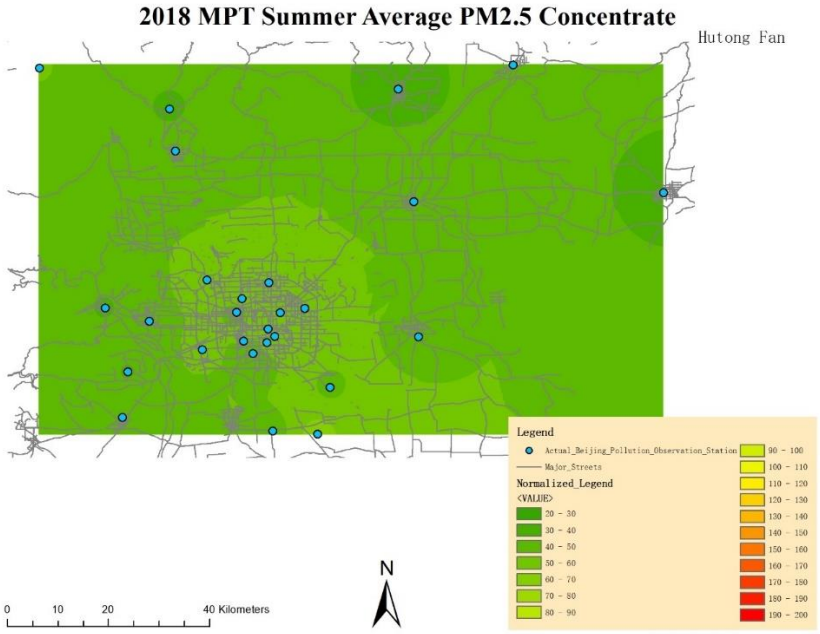

B)

Figure 11: $PM_{2.5}$ Contaminant Spatial Distribution Variation (ug/m^3)

A) 2014 MIDN Winter Average $PM_{2.5}$ Concentrate Map, B) 2018 MPT Summer Average $PM_{2.5}$ Concentrate Map

Figure 12 shows the selected results of spatial interpolations of different daily time periods by seasons. we found that severe $PM_{2.5}$ air pollutions often happened during the wintertime with building heat energy supply (The Government of Beijing Municipality, 2020). During winter, midnight periods (MIDN) present the heaviest $PM_{2.5}$ air pollutions. This evidence strongly suggests that heating supply to buildings and houses is a major $PM_{2.5}$ air pollution source. While the lowest temperature always occurs during midnight (MIDN) time period. Therefore, the heat supply facilities for buildings and houses need to consume more coals or fuels and ramp up power to maintain the indoor temperature higher than 16℃ (The Government of Beijing Municipality, 2020). This process in turn produced more $PM_{2.5}$ air pollutions.

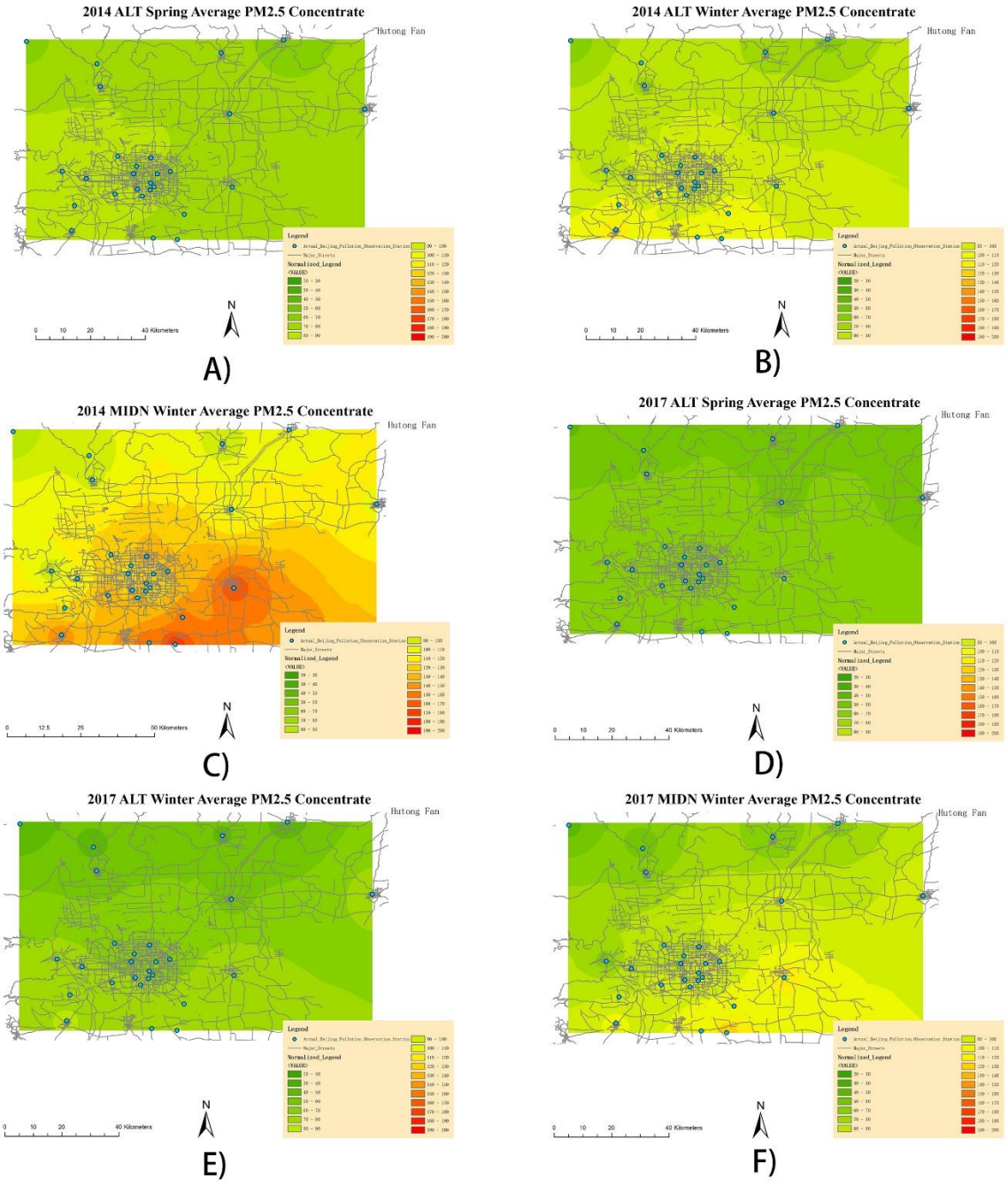

Figure 12: Severe $PM_{2.5}$ Contaminant Situation in Winter Time (ug/m^3)

A) 2014 Spring ALT Average $PM_{2.5}$ Concentrate Map, B) 2014 ALT Winter Average $PM_{2.5}$ Concentrate Map, C) 2014 MIDN Winter Average $PM_{2.5}$ Concentrate Map, D) 2017 Spring ALT Average $PM_{2.5}$ Concentrate Map, E) 2017 ALT Winter Average $PM_{2.5}$ Concentrate Map, F) 2017 MIDN Winter Average $PM_{2.5}$ Concentrate Map

This research also found that the $PM_{2.5}$ air pollutions were decreasing during the study time period across different daily sampling times and at the different seasons year by year. According to Figure 13, even in the time period of most severe $PM_{2.5}$ air pollutions – midnight (MIDN) in winter each year, the concentrations of $PM_{2.5}$ pollution show the declining trend. Assuming the heat energy supply to buildings and houses in winter kept the same, the decreasing of $PM_{2.5}$ air pollution concentrations should attribute to the government policy of converting coal combustion to natural gas combustion, to electricity heating, as well as clean coal technology replacement (Xie et al., 2019).

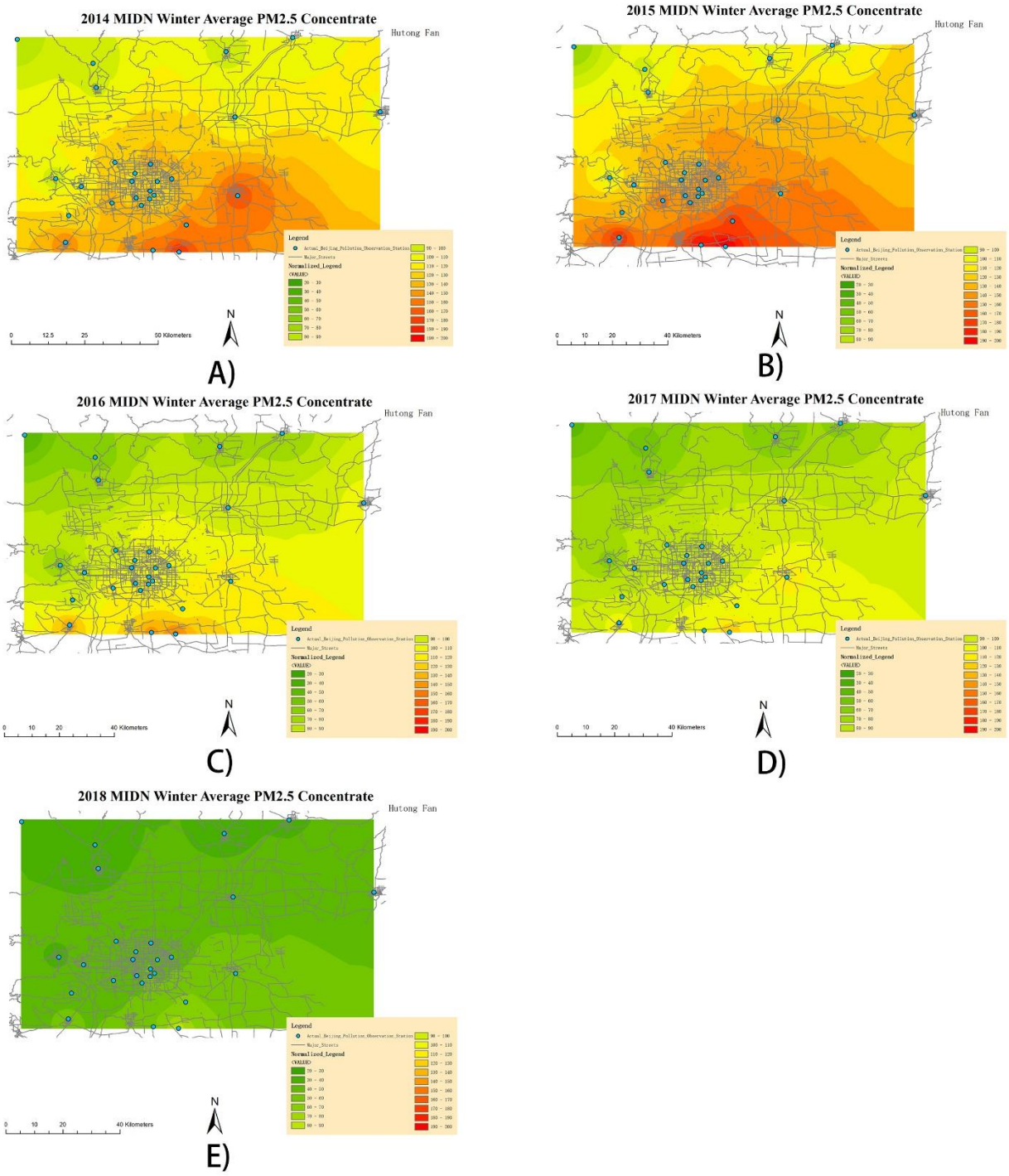

Figure 13: The Decreasing Trend of $PM_{2.5}$ Pollutant within MIDN Winter Sample Time (ug/m^3)

A) 2014 MIDN Winter Average $PM_{2.5}$ Concentrate Map, B) 2015 MIDN Winter Average $PM_{2.5}$ Concentrate Map, C) 2016 MIDN Winter Average $PM_{2.5}$ Concentrate Map, D) 2017 MIDN Winter Average $PM_{2.5}$ Concentrate Map, E) 2018 MIDN Winter Average $PM_{2.5}$ Concentrate Map

In addition, Figure 14 indicates the gradients of declining of $PM_{2.5}$ concentrations in the study area is decreasing as well during the five-year period. Comparing the APT sampling time period in winter with that in the summer in 2018, the gradient is much lower than that during 2014. The decreasing of $PM_{2.5}$ air pollution gradients through the years in the study area shows the strong reduction of $PM_{2.5}$ pollutants and represents the success of government policy and improvement of air quality in Beijing.

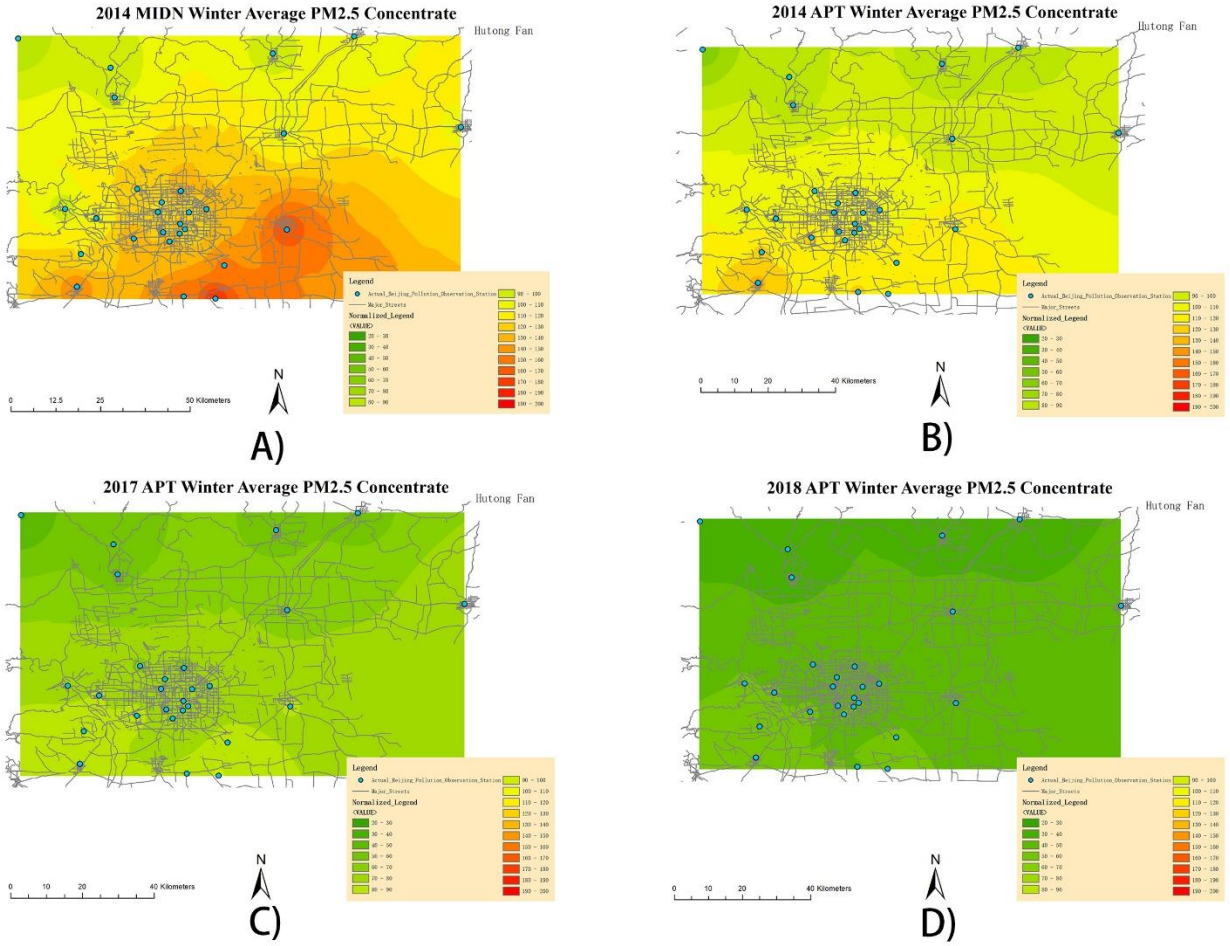

Figure 14: The Descending of $PM_{2.5}$ Contaminant Concentration Gradients (ug/m^3)

A) 2014 MIDN Winter Average $PM_{2.5}$ Concentrate Map, B) 2014 APT Winter Average $PM_{2.5}$ Concentrate Map, C) 2017 APT Winter Average $PM_{2.5}$ Concentrate Map, D) 2018 APT Winter Average $PM_{2.5}$ Concentrate Map

4.3. Summaries of Major Discoveries of Spatial and Temporal Distributions of Air Pollution in the Study Region

First, winter is the most severe period of $PM_{2.5}$ air pollution in each meteorological year. PCA results (Appendix F and Figure 9) indicates that the $PM_{2.5}$ air pollution peaks in each PCA result graph are during the winter season in each year. The results of Seasonal Average Distribution Patterns (Appendix G) show that most of the high $PM_{2.5}$ air pollution concentration ranges occur during the winter season, especially within the midnight (MIDN) sample time period (Figure 13). Secondly, the $PM_{2.5}$ air pollution concentrations in Beijing were gradually decreasing from 2014 to 2018. The evidence to support this conclusion are from PCA results (Appendix F and Figure 9) and Results of Annual Average Spatial Distribution Patterns (Figure 10). All the PCA results show the fluctuation decline of the air pollution from 2014 to 2018 (Appendix F and Figure 9). Standardized Result Atlas of Annual Average Spatial Distribution Patterns (Figure 10) show the improvement of the air quality during the study period.

Thirdly, in terms of a five-year time perspective, Mann-Kendall Trend Analysis shows the reductions of $PM_{2.5}$ air pollutions in summer, autumn, and winter seasons (Table 3, Table 4, Table 5). Although there are a few observation sites (5 of 27) support there are no obvious up or down trends among spring samplings of $PM_{2.5}$ air pollution concentrations during the five-year period (Table 2), most of observation sites (22 of 27) support that there is descending trend (significant or weak trend) in the spring seasons during the five-year period. The most rigorous emission reduction policy in Chinese history, “Air Pollution Prevention and Control Action Plan” that was enacted by the Chinese government in 2013 and the actions to comply with this policy may cause the overall improvement of air quality and declining trend of $PM_{2.5}$ air pollution in Beijing (Zhao et al., 2018).

Fourthly, the $PM_{2.5}$ air pollution concentrations in summer are significantly lower than other seasons. According to the results of PCA analysis (Appendix F and Figure 9), the values of $PM_{2.5}$ air pollution concentration are the lowest during the summer comparing to other seasons. Meanwhile, based on the Result Atlas of Seasonal Average Distribution Patterns (Appendix G), even in the most polluted years, the highest $PM_{2.5}$ pollution concentration range is lower than 80 ~ 90 ug/m3 level (Figure 15) in summers.

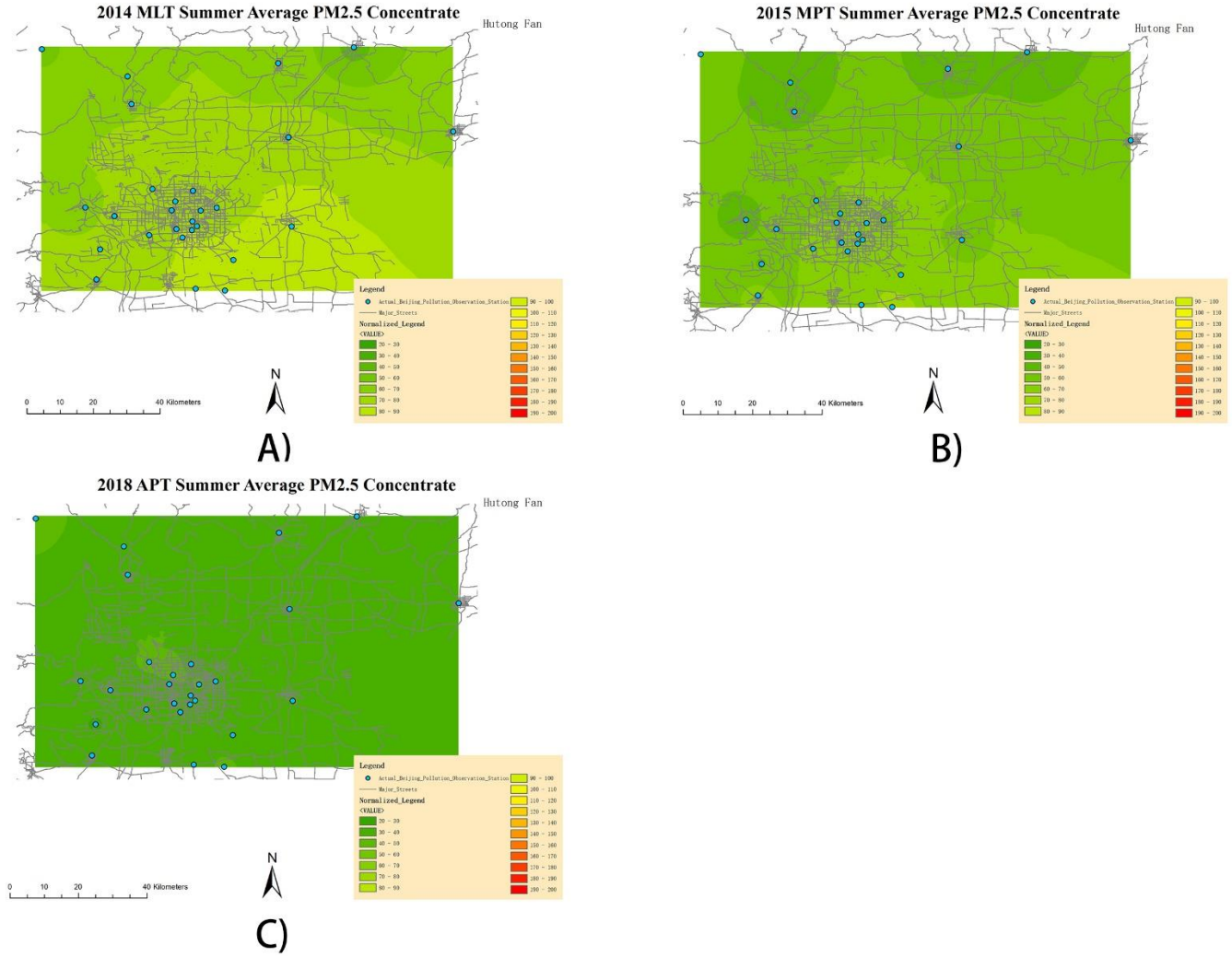

Figure 15: Better $PM_{2.5}$ Contaminant Situation in Summer Time (ug/m^3)

A) 2014 MLT Summer Average $PM_{2.5}$ Concentrate Map, B) 2015 MPT Summer Average $PM_{2.5}$ Concentrate Map, C) 2018 APT Summer Average $PM_{2.5}$ Concentrate Map

Fifthly, spatial distribution patterns show the area of lowest $PM_{2.5}$ pollutions in Beijing is north and northwest region (Appendix G). The highest concentrations of $PM_{2.5}$ air pollution in the northwest part in Beijing occurred during midnight (MIDN) in 2014 winter (Figure 16). The $PM_{2.5}$ air pollution concentration record at Badaling Observation Site reached to the 80 ~ 90 ug/m3 level. Also, the most polluted area is in the south and southeast part of Beijing. The core urban area in Beijing is not the most polluted regions according to both Annual Average Concentrate Atlas (Figure 10) and Result Atlas of Seasonal Average Distribution Patterns (Figure 12, 13, 14, 15, 16, Appendix G).

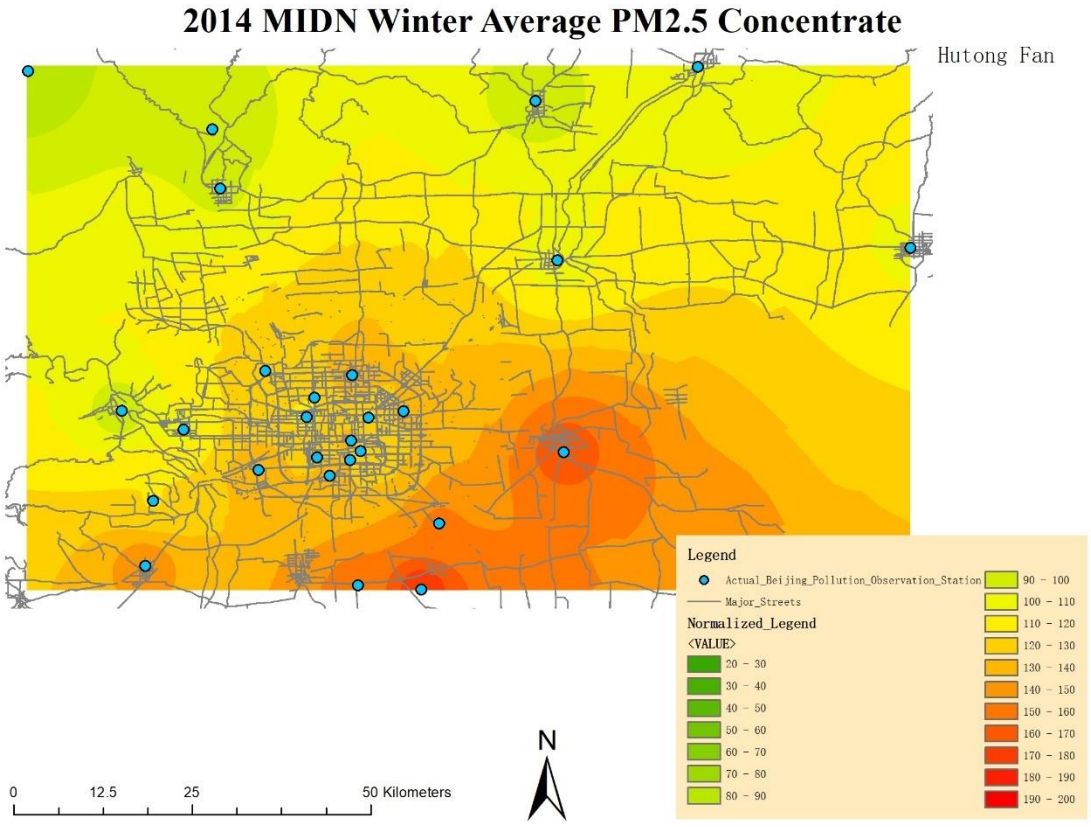

Figure 16: 2014 MIDN Winter Average $PM_{2.5}$ Concentrate Map (ug/m^3)

Sixthly, the results of this research suggest that vehicle traffic volume may not be the major influential factor of $PM_{2.5}$ air pollution in Beijing. The Result Atlas of Seasonal Average Distribution Patterns (Figure 17, Appendix G) does not show significant high level of $PM_{2.5}$ air pollution concentrations during the peak traffic time periods, nor does it show high values in the dense road network area in the study region. However, the interpolation patterns might be impacted by the locations and density of air pollution monitoring stations. Further studies are needed.

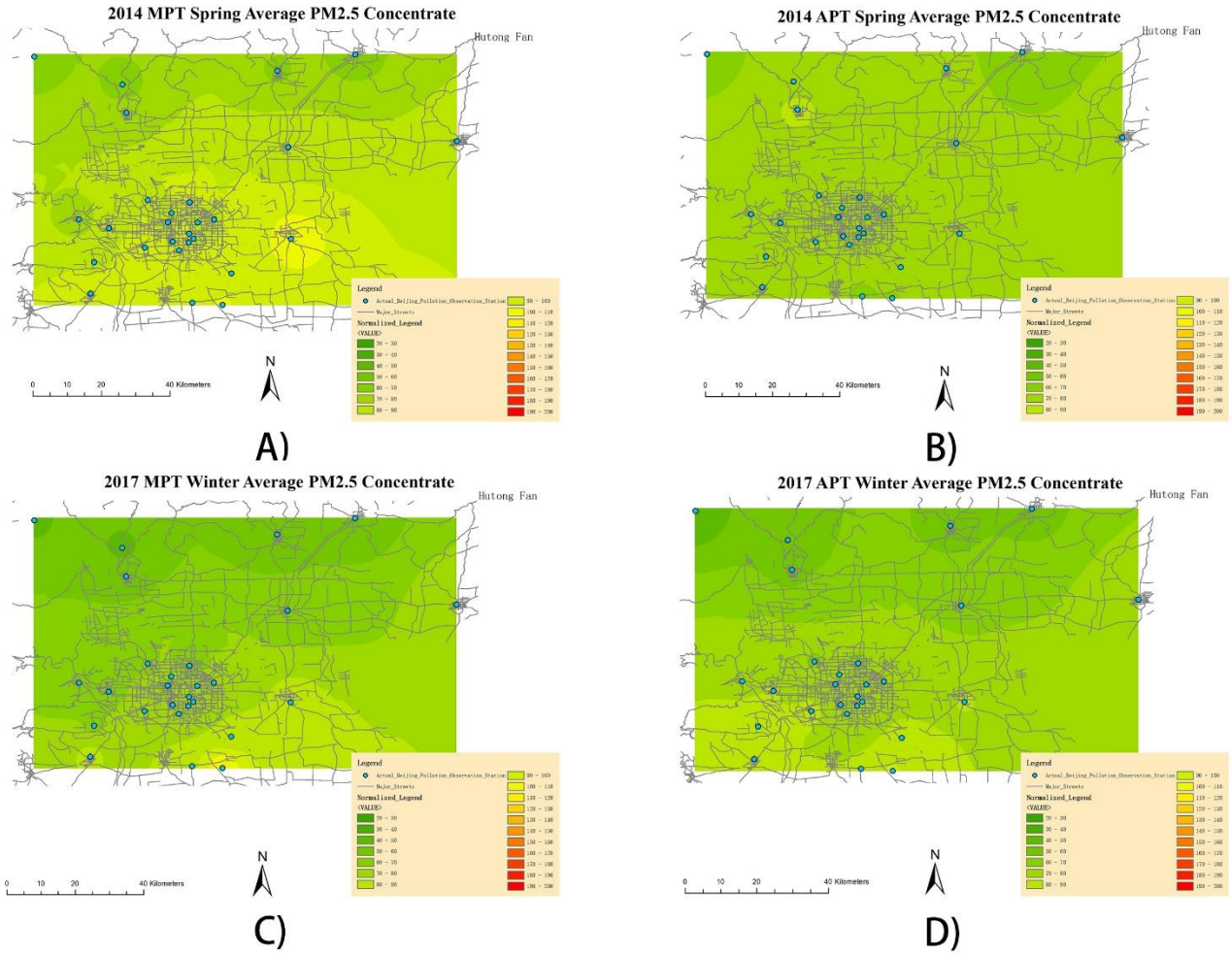

Figure 17: Selected Part of the MPT and APT Sample Time Periods' Map (ug/m^3)

A) 2014 MPT Spring Average $PM_{2.5}$ Concentrate Map, B) 2014 APT Spring Average $PM_{2.5}$ Concentrate Map, C) 2017 MPT Winter Average $PM_{2.5}$ Concentrate Map, D) 2017 APT Winter Average $PM_{2.5}$ Concentrate Map

Seventhly, winter season heat energy supply to buildings and houses generated great impacts to the $PM_{2.5}$ air pollution concentrations in Beijing. According to the Result Atlas of Average Distribution Patterns (Figure 12, Appendix G), the $PM_{2.5}$ concentrations in winter are the highest in each meteorological year.

5. Discussions and Conclusion

The selection of time period of winter season in this research coincides with building and house heating supply time period in Beijing (The Government of Beijing Municipality, 2020). The analytical results of this research indicate building and house heating in winter contributed a great amount of $PM_{2.5}$ air pollution during the season. It makes the winter season as the highest air pollution season. While, implementing the rigorous emission reduction policy "Air Pollution Prevention and Control Action Plan" enacted in 2013 (Zhao et al., 2018), the $PM_{2.5}$ pollution was gradually reduced in the winter. Figure 13 clearly indicates the improvement of air quality and reduction of $PM_{2.5}$ pollution in winter seasons, in particular for midnight (MIDN) time periods. Thanks to the policy actions of converting coal combustion to electricity or natural gas combustion, or clean coal technology replacement (Xie et al., 2019), the proportion of fossil fuel consumptions in heat supply activities gradually declined year by year. According to the Northern Region Winter Clean Heating Plan (2017-2021) (Chinese Central Leading Group on Finance and Economics, 2016), the percentage of clean energy heating supply in the northern region in China should reach 50% by the end of 2019, and 74 million tons of CO_2 should be reduced from the coal consumptions and from inefficient small furnace shutdowns. With the help of multiple government policies and macro-management, the pollution from winter heat supply decreased during this research time (2014 ~ 2018).

This research demonstrates the preliminary step to analyze temporal and spatial patterns using a five-year hourly monitored large $PM_{2.5}$ air pollution dataset. The focus of this research is the data processing and analysis for the big $PM_{2.5}$ air pollution dataset itself. In the future, we can combine the population distribution data to analyze the impacts to the $PM_{2.5}$ pollutions by

population density. We can also combine the temperature variations and weather condition data to gain better understanding to the winter heating supply factor on $PM_{2.5}$ air pollutions. According to Li's (2016) study, the distribution of $PM_{2.5}$ in Beijing area is obviously affected by the surrounding areas. The process of $PM_{2.5}$ pollutant diffusion was greatly influenced by the landscape and weather conditions in Beijing. Therefore, exploring the diffusion process of $PM_{2.5}$ pollutants with the terrain around Beijing and big datasets will also be significant in the future studies. In addition, we can also improve the accuracy of our spatial pattern analysis. For example, the standardized legend of Average Distribution Patterns (Appendix G) could have higher contrast ratio and more precise $PM_{2.5}$ pollution concentration categories.

6. Bibliography

Ai Hongfu, & Shi Ying. (2015). Research on Haze Weather Forecast Based on BP Artificial Neural Network. Computer Simulation, 32(1), 402-405.

Alimissis, A., Philippopoulos, K., Tzanis, C. G., & Deligiorgi, D. (2018). Spatial estimation of urban air pollution with the use of artificial neural network models. Atmospheric environment, 191, 205-213.

Azmi, A. S. M., Azhar, R. F., & Nawawi, A. H. (2012). The Relationship between air quality and property Price. Procedia-Social and Behavioral Sciences, 50, 839-854.

Awad, M., & Khanna, R. (2015). Support vector regression. In Efficient learning machines (pp. 67-80). Apress, Berkeley, CA.

Bai Shengnan, & Shen Xiaoliu. (2019). $PM_{2.5}$ prediction based on LsTM recurrent neural network. Computer Applications and Software, 36(1), 67r70-104.

Beck, H. E., Zimmermann, N. E., McVicar, T. R., Vergopolan, N., Berg, A., & Wood, E. F. (2020). Publisher Correction: Present and future Köppen-Geiger climate classification maps at 1-km resolution. Scientific Data, 7(1), 1-2.

Belavadi, S. V., Rajagopal, S., Ranjani, R., & Mohan, R. (2020). Air quality forecasting using LSTM RNN and wireless sensor networks. Procedia Computer Science, 170, 241-248.

Brulle, R. J., & Pellow, D. N. (2006). Environmental justice: human health and environmental inequalities. Annu. Rev. Public Health, 27, 103-124.

Burr, M. J., & Zhang, Y. (2011). Source apportionment of fine particulate matter over the Eastern US Part I: source sensitivity simulations using CMAQ with the Brute Force method. Atmospheric Pollution Research, 2(3), 300-317.

Cao, J.B., Chi, D.C., Wu, L.Q., Liu, L., Li, S.Y., Yu, M. (2008). Study on the application of Mann-kendall test method in the analysis of precipitation trends. Agricultural Technology and Equipment. (5),4.

Carrier, M., Apparicio, P., Séguin, A. M., & Crouse, D. (2014). Ambient air pollution concentration in Montreal and environmental equity: Are children at risk at school? Case Studies on Transport Policy, 2(2), 61-69.

Chaloulakou, A., Kassomenos, P., Spyrellis, N., Demokritou, P., & Koutrakis, P. (2003). Measurements of PM10 and PM2. 5 particle concentrations in Athens, Greece. Atmospheric Environment, 37(5), 649-660.

Chattopadhyay, A., Hassanzadeh, P., & Pasha, S. (2018). A test case for application of convolutional neural networks to spatio-temporal climate data: Re-identifying clustered weather patterns. arXiv preprint arXiv:1811.04817.

Chen, C., Wen, J.J., Wang, B.Y., Fang, J.H., Lang, J.D., Tian, G., Jiang, J.K., Zhu, T.F. (2014) Inhalable Microorganisms in Beijing's PM2.5 and PM10 Pollutants during a Severe Smog Event. Environmental Science & Technology, 48(3), 1499-1507. DOI: 10.1021/es4048472

Chen Jianbao, & Qiao Ningning. (2017). Estimation of semiparametric variable coefficient spatial error regression model. Quantitative Economics and Technical Economics Research, 34(4), 129-146.

Chen, L., Zhan, Z.M. (2017). Analysis of PM_{10} and $PM_{2.5}$ characteristics during a sandstorm in Jilin province. Agriculture and Technology, 19, 139-141.

Chen, S., Jin, H. (2019). Pricing for the clean air: Evidence from Chinese housing market. Journal of Cleaner Production, 206, 297-306.

Chinese Central Leading Group on Finance and Economics. (2016). Northern Region Winter Clean Heating Plan (2017-2021).

Dao, M. S., & Zettsu, K. (2018, December). Complex event analysis of urban environmental data based on deep CNN of spatiotemporal raster images. In 2018 IEEE International Conference on Big Data (Big Data) (pp. 2160-2169). IEEE.

De Leeuw, F. A., Moussiopoulos, N., Sahm, P., & Bartonova, A. (2001). Urban air quality in larger conurbations in the European Union. Environmental Modelling & Software, 16(4), 399-414.

Degang, J., Ao, X., & Xiaoxian, X. (2018). Prediction and Analysis of Air Quality Based on FCM and BP Neural Network. Meteorological & Environmental Research, 9(3).

Deligiorgi, D. and Philippopoulos, K. (2011). Spatial Interpolation Methodologies in Urban Air Pollution Modeling: Application for the Greater Area of Metropolitan Athens, Greece, Advanced Air Pollution, Dr. Farhad Nejadkoorki (Ed.), InTech, DOI: 10.5772/17734.

Deng, J. L. (1990). Grey system theory course. Huazhong University of Science and Technology Press, Wuhan.

Dinda, S. (2004). Environmental Kuznets curve hypothesis: a survey. Ecological economics, 49(4), 431-455.

Du Ying. (2016). Research on the relationship between economic growth and air pollution in Hebei Province (Doctoral dissertation, Beijing: China University of Geosciences (Beijing)).

Esposito, E., De Vito, S., Salvato, M., Bright, V., Jones, R. L., & Popoola, O. (2016). Dynamic neural network architectures for on field stochastic calibration of indicative low-cost air quality sensing systems. Sensors and Actuators B: Chemical, 231, 701-713.

EPA Particulate Matter (2021) NAQQS Table. Retrieved from: https://www.epa.gov/criteria-air-pollutants/naaqs-table Last accessed: 24 Aug 2021.

EPA Particulate Matter (2016) Particulate Matter (PM) Pollution. Retrieved from: https://www3.epa.gov/pm/https://www3.epa.gov/pm/ Last accessed: 13 May 2021.

Fan Junxiang, Li Qi, Zhu Yajie, Hou Junxiong, & Feng Xiao. (2017). Research on air pollution spatiotemporal forecast model based on RNN. Science of Surveying and Mapping, 42(7), 76-83.

Fan Kaikai, & Shan Baoyan. (2017). Analysis of the temporal and spatial variation of $PM_{2.5}$ concentration in Shandong Province and its influencing factors. Journal of Shandong Jianzhu University, 32(1), 39-46.

Fan, S.B., Tian, L.D., Zhang, D.X., Qu, S. (2015) Emission Characteristics of Vehicle Exhaust in Beijing Based on Actual Traffic Flow Information. Environmental Science, 36(8): 2750-2757.

Fischer, T., & Krauss, C. (2018). Deep learning with long short-term memory networks for financial market predictions. European Journal of Operational Research, 270(2), 654-669.

Gers, F. A., Schmidhuber, J., & Cummins, F. (2000). Learning to forget: Continual prediction with LSTM. Neural computation, 12(10), 2451-2471.

Gimond, M. (2021). Intro to GIS and Spatial Analysis. Retrieved November 29, 2021, from https://mgimond.github.io/Spatial/index.html

Guo Lijin, Jing Haiming, Nan Yaxiang, & Xiu Chunbo. (2017). Air quality index prediction based on Kalman filter fusion algorithm. Environmental Pollution and Prevention, 39(4), 388-391.

Guo, H., Gu, X., Ma, G., Shi, S., Wang, W., Zuo, X., & Zhang, X. (2019). Spatial and temporal variations of air quality and six air pollutants in China during 2015–2017. Scientific reports, 9(1), 1-11.

Hajat, A., Hsia, C., & O'Neill, M. S. (2015). Socioeconomic disparities and air pollution exposure: a global review. Current environmental health reports, 2(4), 440-450.

Hao, Y., & Liu, Y. M. (2016). The influential factors of urban PM2. 5 concentrations in China: a spatial econometric analysis. Journal of Cleaner Production, 112, 1443-1453.

Harrison Jr, D., & Rubinfeld, D. L. (1978). Hedonic housing prices and the demand for clean air. Journal of environmental economics and management, 5(1), 81-102.

Henry, R.C., Lewis, C.W., Hopke, P.K., & Williamson, H.J. (1984). Review of receptor model fundamentals. Atmospheric Environment, 18, 1507-1515.

Holmes, N. S., & Morawska, L. (2006). A review of dispersion modelling and its application to the dispersion of particles: an overview of different dispersion models available. Atmospheric environment, 40(30), 5902-5928.

Huang Yusheng. (2016). Based on Beijing and Shanghai megacities environmental pollution economic loss accounting and analysis of its influencing factors (Doctoral dissertation, Lanzhou: Lanzhou University).

Hui Ying, Mao Pei, & Dai Hongwei. (2018). An empirical analysis of the spatial distribution of haze pollution and its influencing factors in Hebei Province. Economics and Management, 32(3), 65-71.

Jia, B., Liu, S., & Ng, M. (2021). Air Quality and Key Variables in High-Density Housing. Sustainability, 13(8), 4281. https://doi.org/10.3390/su13084281

Jiang Lei, Zhou Haifeng, Bai Ling, & Chen Zhongsheng. (2018). Analysis of the Socio-economic Influencing Factors of Air Quality Index (AQI)——Based on the Perspective of Exponential Decay Effect. Journal of Environmental Sciences, 38(1), 390-398.

Johnson, N. E., Bonczak, B., & Kontokosta, C. E. (2018). Using a gradient boosting model to improve the performance of low-cost aerosol monitors in a dense, heterogeneous urban environment. Atmospheric environment, 184, 9-16.

Joshua, S.A., Michael, B., Aaron J.C., Majid E., C, Arden, P. (2018). Ambient PM2.5 Reduces Global and Regional Life Expectancy. Environmental Science & Technology Letters, 5(9), 546-551.

Karatzoglou, A., Schnell, N., & Beigl, M. (2018, October). A convolutional neural network approach for modeling semantic trajectories and predicting future locations. In International Conference on Artificial Neural Networks (pp. 61-72). Springer, Cham.

Karmeshu, N. (2012). Trend Detection in Annual Temperature & Precipitation using the Mann Kendall Test – A Case Study to Assess Climate Change on Select States in the Northeastern United States.

Kim, T., Yue, Y., Taylor, S., & Matthews, I. (2015, August). A decision tree framework for spatiotemporal sequence prediction. In Proceedings of the 21th ACM SIGKDD international conference on knowledge discovery and data mining (pp. 577-586).

Koo, B., Wilson, G. M., Morris, R. E., Dunker, A. M., & Yarwood, G. (2009). Comparison of source apportionment and sensitivity analysis in a particulate matter air quality model. Environmental science & technology, 43(17), 6669-6675.

Li, L. (2016). The Spatial Distribution Patterns of $PM_{2.5}$ as Observed before, During and after APEC Period in Beijing. 2016 24^{th} International Conference On Geoinformatics (Geoinformatics).

Li Qian, Song Jinping, Zhang Jianhui, Yu Wei, & Hu Hao. (2013). Research on the evolutionary law of the impact of China's urbanization on ambient air quality.

Lin, K. P., Pai, P. F., & Yang, S. L. (2011). Forecasting concentrations of air pollutants by logarithm support vector regression with immune algorithms. Applied Mathematics and Computation, 217(12), 5318-5327.

Liu Dameng, Huang Jie, Gao Shaopeng, Ma Yongsheng, & An Xianghua. (2006). The pollution level of atmospheric particulate matter from traffic sources in Beijing urban area and its influencing factors in spring. The Frontier of Earth Science, 13(2), 228-233.

Liu Jiaojiao, Yu Suping, Wu Bo, Jiang Hua, He Fengxing, & Li Fengrong. (2016). Time-space sequence prediction method based on hidden Markov model. Microcomputers and Applications, 35(1), 74-76.

Londhe, A. N., & Atulkar, M. (2021). Semantic segmentation of ECG waves using hybrid channel-mix convolutional and bidirectional LSTM. Biomedical Signal Processing and Control, 63, 102-162.

Lozano, A., Usero, J., Vanderlinden, E., Raez, J., Contreras, J., Navarrete, B., Bakouri, H.E. (2009). Design of air quality monitoring networks and its application to 2 and O3 in Cordova, Spain. Microchemical Journal, 93 No. 2, (November 2009), 211 219, 0002-6265X

Meng, T., Wang, J.M., Yan, H.F. (2006). Web evolution and incremental crawling. Journal of Software, 17(5): 1051−1067. http://www.jos.org.cn/1000-9825/17/1051.htm

Ministry of Ecology and Environment of the People's Republic of China; General Administration of Quality Supervision, Inspection and Quarantine of the People's Republic of China. (2012). Ambient Air Quality Standards

Ministry of Ecology and Environment of the People's Republic of China. (2013). Technical Specifications for Installation and Acceptance of Ambient Air Quality Continuous Automated Monitoring System for PM10 and PM2.5 (HJ 655-2013)

Miranda, M. L., Edwards, S. E., Keating, M. H., & Paul, C. J. (2011). Making the environmental justice grade: the relative burden of air pollution exposure in the United States. International journal of environmental research and public health, 8(6), 1755-1771.

Monteiro, A., Vieira, M., Gama, C., & Miranda, A. I. (2017). Towards an improved air quality index. Air Quality, Atmosphere & Health, 10(4), 447-455.

Najafabadi, M. M., Villanustre, F., Khoshgoftaar, T. M., Seliya, N., Wald, R., & Muharemagic, E. (2015). Deep learning applications and challenges in big data analytics. Journal of big data, 2(1), 1-21.

Nanni, M., Kuijpers, B., Körner, C., May, M., & Pedreschi, D. (2008). Spatiotemporal data mining. In Mobility, data mining and privacy (pp. 267-296). Springer, Berlin, Heidelberg.

Navares, R., & Aznarte, J. L. (2020). Predicting air quality with deep learning LSTM: Towards comprehensive models. Ecological Informatics, 55, 101019.

Nelson, J. P. (1978). Residential choice, hedonic prices, and the demand for urban air quality. Journal of urban Economics, 5(3), 357-369.

Ni, X. Y., Huang, H., & Du, W. P. (2017). Relevance analysis and short-term prediction of PM2. 5 concentrations in Beijing based on multi-source data. Atmospheric environment, 150, 146-161.

Nikoleris, T., Gupta, G., & Kistler, M. (2011). Detailed estimation of fuel consumption and emissions during aircraft taxi operations at Dallas/Fort Worth International Airport. Transportation Research Part D: Transport and Environment, 16(4), 302-308.

Ogulei, D., Hopke, P. K., Ferro, A. R., Jaques, P. A. (2007). Factor analysis of submicron particle size distributions near a major United States–Canada trade bridge. Journal of the Air & Waste Management Association, 57(2), 190-203.

Pan, C., Tan, J., Feng, D., & Li, Y. (2019, December). Very short-term solar generation forecasting based on LSTM with temporal attention mechanism. In 2019 IEEE 5th International Conference on Computer and Communications (ICCC) (pp. 267-271). IEEE.

Ridker, R. G., & Henning, J. A. (1967). The determinants of residential property values with special reference to air pollution. The review of Economics and Statistics, 246-257.

Rosen, S. (1974). Hedonic prices and implicit markets: product differentiation in pure competition. Journal of political economy, 82(1), 34-55.

Shlens, J. (2014). A tutorial on principal component analysis. arXiv preprint arXiv:1404.1100.

Shen, X., Yao, Z., Zhang, Q., Wagner, D. V., Huo, H., Zhang, Y., ... & He, K. (2015). Development of database of real-world diesel vehicle emission factors for China. Journal of Environmental Sciences, 31, 209-220.

Song, X., Huang, J., & Song, D. (2019, May). Air quality prediction based on LSTM-Kalman model. In 2019 IEEE 8th Joint International Information Technology and Artificial Intelligence Conference (ITAIC) (pp. 695-699). IEEE.

Spiroska, J., Rahman, M. A., & Pal, S. (2011). Air pollution in Kolkata: An analysis of current status and interrelation between different factors. SEEU Review, 8(1), 182-214.

Tang, M., & Ji, D. (2018). Fuzzy Comprehensive Evaluation and Prediction of Air Quality in Baoding City. Agricultural Biotechnology (2164-4993), 7(3).

Tang T., W. Zhao, H. Gong, X. Li, K. Zang, W. H. Zhao, Bernosky J. D., and S. Li, (2010). GIS spatial analysis of population exposure to fine particulate air pollution in Beijing, China. Environmental GeoSciences. Vol. 17 No. 01: 1-16

Tang, T., W. H. Zhao, W. Zhao, H. Gong, and L. Cai, (2009). GIS analysis of spatial and temporal changes of air particulate concentrations and their impacts on respiratory diseases in Beijing, China. Middle States Geographe, Volume 42, 73-82

The People's Government of Beijing Municipality. (2020, June 29). Beijing Heating Tips. The People's Government of Beijing Municipality. Retrieved from http://english.beijing.gov.cn/livinginbeijing/housing/202005/t20200513_1895777.html.

U.S. Environmental Protection Agency, Washington, DC. EPA/600/R-08/139F, (2009). U.S. EPA. Integrated Science Assessment for Particulate Matter (Final Report). Available at http://cfpub.epa.gov/ncea/cfm/recordisplay.cfm?deid=216546.

Wang Yichen, & Shen Yingchun. (2017). Spatial correlation characteristics of Beijing-Tianjin-Hebei smog and its influencing factors spillover effect analysis. China Population, Resources and Environment, 27(S1), 41-44.

Wang, D., Wei, S., Luo, H., Yue, C., & Grunder, O. (2017). A novel hybrid model for air quality index forecasting based on two-phase decomposition technique and modified extreme learning machine. Science of The Total Environment, 580, 719-733.

Wang, S., Zhang, X., Li, F., Philip, S. Y., & Huang, Z. (2018). Efficient traffic estimation with multi-sourced data by parallel coupled hidden markov model. IEEE Transactions on Intelligent Transportation Systems, 20(8), 3010-3023.

Welling, M. (2004). Support vector regression. Department of Computer Science, University of Toronto, Toronto (Kanada).

World Health Organization. (2018) Ambient (outdoor) air pollution. Retrieved from: https://www.who.int/news-room/fact-sheets/detail/ambient-(outdoor)-air-quality-and-health Last accessed: 24 Aug 2021.

Wu Xueping, Gao Ming, & Zeng Lanting. (2018). Re-examination of the relationship between air pollution and economic growth based on a semi-parametric spatial model. Statistical Research, 35(8), 82-93.

Wu, X., Zhu, B., Zhou, J., Bi, Y., Xu, S., & Zhou, B. (2021). The epidemiological trends in the burden of lung cancer attributable to PM2.5 exposure in China. BMC Public Health, 21(1), 1-8.

Xie L.Y., Chang Y.X., Lan Y. (2019). The Effectiveness and Cost-Benefit Analysis of Clean Heating Program in Beijing. Chinese Journal of Environmental Management, 11(3): 87-93.

Xiong, Q.L., W.J. Zhao, Z.N. Gong, W.H. Zhao, and T. Tang. (2015). Fine Particulate Matter Pollution and Hospital Admissions for Respiratory Diseases during Heating Period in Beijing,China . International Journal of Environmental Research and Public Health, 12(9), 11880-11892; doi: 10.3390/ijerph120911880.

Xu, H., Zhu, J., & Wang, Z. (2019). Exploring the spatial pattern of urban block development based on POI analysis: A case study in Wuhan, China. Sustainability, 11(24), 6961.

Yang Mian, & Wang Yin. (2017). Research on the Temporal and Spatial Characteristics and Influencing Factors of $PM_{2.5}$ in the Yangtze River Economic Belt. China Population Resources and Environment, (1), 91-100.

Yang Qi, Chen Shuizhong, Shen Shumei, & Zhu Zhenhua. (2018). Adaptability analysis of LSTM network and ARMA model to random error prediction of inertial devices. Electro-Optics and Control, 25(3), 68-72.

Ye Azhong, & Zheng Wanji. (2016). Research on the Spatiotemporal Conduction Effect of Economic Growth, FDI and Environmental Pollution——Based on the Analysis of Semi-parametric Spatial Panel VAR Model. Soft Science, 30(1), 17-21.

Ye, N., Zhang, Y., Wang, R., & Malekian, R. (2016). Vehicle trajectory prediction based on Hidden Markov Model.

Zhang, H., Zhang, W., Palazoglu, A., & Sun, W. (2012). Prediction of ozone levels using a Hidden Markov Model (HMM) with Gamma distribution. Atmospheric environment, 62, 64-73.

Zhang Shuyi, Chen Songqi, Guo Bin, Wang Hengfang, & Lin Wei. (2020). Regional air quality assessment under meteorological adjustment. Science in China: Mathematics.

Zhang Yinjun, Chen Xi, Xie Gaodi, Zhang Jianhui, Zhang Changshun, Shi Yu, & Wang Shuai. (2015). China's fine particulate matter ($PM_{2.5}$) pollution status and spatial distribution. Resource Science, 37(7), 1339-1346.

Zhang, Q., Chang, J., Meng, G., Xiang, S., & Pan, C. (2020, April). Spatio-temporal graph structure learning for traffic forecasting. In Proceedings of the AAAI Conference on Artificial Intelligence (Vol. 34, No. 01, pp. 1177-1185).

Zhang, Q., Wei, C., Wang, Y., Du, S., Zhou, Y., & Song, H. (2019). Potential for prediction of water saturation distribution in reservoirs utilizing machine learning methods. Energies, 12(19), 3597.

Zhang, Q., Xu, J., Wang, G., Tian, W., & Jiang, H. (2008). Vehicle emission inventories projection based on dynamic emission factors: a case study of Hangzhou, China. Atmospheric Environment, 42(20), 4989-5002.

Zheng, G.J., Duan, F.K., Su, H., Ma, Y.L., Cheng,Y., Zheng, B., Zhang, Q., Huang, T., Kimoto, T., Chang, D., Pöschl, U., Cheng, Y.F., He, K.B. (2015). Exploring the severe winter haze in Beijing: the impact of synoptic weather, regional transport and heterogeneous reactions. Atmos. Chem. Phys. 15, 2969-2983, https://doi.org/10.5194/acp-15-2969-2015.

Zhao Mingzhu, Wang Dan, Fang Jie, Li Yan, & Mao Jun. (2020). Metro station temperature prediction based on LSTM neural network. Journal of Beijing Jiaotong University, 44(04), 94.

Zhao, W.H., Gong, H.L., Zhao, W.J., Zhu, L., Tang, T. (2009). Temporal and Spatial Variation of Urban Airborne Inhalable Particle and It's Influence Factor Analysis using GIS & RS. Temporal and Spatial Variation of Urban Airborne Inhalable Particle and It's Influence Factor Analysis Using GIS & RS, 369–374.

Zhao, W.X., Hopke, Philip., Zhou, L.M., (2007). Spatial distribution of source locations for particulate nitrate and sulfate in the upper-midwestern United States. Atmospheric Environment, 41, 1831-1847. 10.1016/j.atmosenv.2006.10.060.

Zheng Yangyang, Bai Yanping, & Hou Yuchao. (2019). Application of Keras-based LSTM model in air quality index prediction. Mathematical Practice and Understanding, (7), 138-143.

Zheng, B., Tong, D., Li, M., Liu, F., Hong, C., Geng, G., Zhang, Q. (2018). Trends in China's anthropogenic emissions since 2010 as the consequence of clean air actions. Atmospheric Chemistry and Physics, 18(19), 14095-14111.

Zheng, Y., Capra, L., Wolfson, O., & Yang, H. (2014). Urban computing: concepts, methodologies, and applications. ACM Transactions on Intelligent Systems and Technology (TIST), 5(3), 1-55.

Zhou, D.P., Wang, Y.F., Hong, Y., Liu, N.W. (2010). Influence of Dust Storm on Air Quality of Cities in Middle Liaoning Province in Spring of 2007. Journal of Desert Research, 30(4), 976-982.

Zhou Weidong., Liang Ping. (2013). The possible impact of wind and climate change on air quality in autumn in Shanghai. Resources Science, 35(5), 1044-1050.

Zhou Zhaoyuan., Zhang Shihuang., Gao Qingxian., Li Wenjie., Zhao Lingmei., Feng Yongheng., Shi Leilei. (2014). The impact of meteorological elements on air quality in the Beijing-Tianjin-Hebei region and analysis of future trends. Resource Science, 36(1), 191-199.

Zhu, S., Lian, X., Liu, H., Hu, J., Wang, Y., Che, J. (2017). Daily air quality index forecasting with hybrid models: A case in China. Environmental pollution, 231, 1232-1244.

Appendix A

Codes of Import and Integrate Beijing $PM_{2.5}$ Data Based on Python

```
import datetime
import xlrd, openpyxl
from openpyxl.workbook import Workbook
from openpyxl.writer.excel import ExcelWriter
def main():
    begin = datetime.date(2018,1,1)
    end = datetime.date(2018,12,31)
    for i in range((end - begin).days+1):
        day = begin + datetime.timedelta(days=i)
        day1 = day.strftime("%y%m%d")
        path = "beijing_PM25_20180101-20181231/Beijing_PM25_20" + (str(day1)) + ".xlsx"
        print("Open"+path)

        data = xlrd.open_workbook(path)
        table = data.sheets()[0]
        time1 = int(table.cell_value(rowx=1, colx=0))
        MIDValue = table.cell_value(colx=8, rowx=5)
        OtherValue = table.col_values(colx=8, start_rowx=1, end_rowx=5)
        print(f"Date is：{time1},Data from OtherValue is：{MIDValue}{OtherValue}")

        resultdata = openpyxl.load_workbook(' /PM25_2018_Agricultural Pavilion.xlsx')
        resultsheet = resultdata['Sheet1']
        OtherValue.insert(0, MIDValue)
        OtherValue.insert(0, time1)
        resultsheet.append(OtherValue)
        resultdata.save('2015/PM25_2018_Agricultural Pavilion.xlsx')
```

```
        print("Finished " + path)
if __name__ == '__main__':
        main()
```

Appendix B

Codes of Compute Beijing $PM_{2.5}$ Data Based on Python

```
import os
import openpyxl
import xlrd, openpyxl
from openpyxl.workbook import Workbook
from openpyxl.writer.excel import ExcelWriter

def getFileNames(path):
    filenames = os.listdir(path) #os.listdir
    for i, filename in enumerate(filenames): #enumerate



        iSpecialFile = i + 1
        print('==================%s
 ========================' % (iSpecialFile))
        print('name：  %s' % (filename))
        #getSheetNames(path, filename)
        filepath = path+"/"+filename
        replace_zero(filepath)
        print('\n')
        print('==================
 ========================' % (iSpecialFile))
        print('\n')

def replace_zero(path):

    data = xlrd.open_workbook(path)
```

```
    table = data.sheets()[0]
    nrows = table.nrows
    ncols = table.ncols
    alist = []
    dlist = []
    clist = []
    blist = []

    print(f"：  {nrows}")
    print(f"：  {ncols}")
    for rownum in range(0, nrows):
        for colnum in range(0, ncols):
            if table.cell_value(colx=colnum, rowx=rownum) == 0:
                #print (f" {rownum+1} {colnum+1}")
                alist.append((rownum,colnum))
                if colnum == 1
                    if (table.cell_value(colx=colnum+1, rowx=rownum) == 0) and
(table.cell_value(colx=colnum+2, rowx=rownum) != 0):
                        print(f" {rownum+1}{colnum+1}，  {colnum+2}")
                        clist.append((rownum, colnum))
                    elif (table.cell_value(colx=colnum + 1, rowx=rownum) == 0) and
(table.cell_value(colx=colnum + 2, rowx=rownum) == 0) and (table.cell_value(colx=colnum+3,
rowx=rownum) != 0):
                        print(f" {rownum+1}{colnum+1}，  {colnum+2}，  {colnum+3}")
                        blist.append((rownum, colnum))
                    elif table.cell_value(colx=colnum + 1, rowx=rownum) != 0 :
                        print(f"{rownum+1} {colnum+1}")
                        dlist.append((rownum, colnum))
```

```
        elif colnum == 2:
            if (table.cell_value(colx=colnum + 1, rowx=rownum) == 0) and
(table.cell_value(colx=colnum + 2, rowx=rownum) != 0) and (table.cell_value(colx=colnum - 1,
rowx=rownum) != 0) :
                print(f" {rownum+1}{colnum+1},  {colnum+2}")
                clist.append((rownum, colnum))
            elif (table.cell_value(colx=colnum + 1, rowx=rownum) == 0) and
(table.cell_value(colx=colnum + 2, rowx=rownum) == 0) and (table.cell_value(colx=colnum+3,
rowx=rownum) != 0) and (table.cell_value(colx=colnum-1, rowx=rownum) != 0):
                print(f"{rownum+1}{colnum+1},  {colnum+2}{colnum+3}")
                blist.append((rownum, colnum))
            elif (table.cell_value(colx=colnum + 1, rowx=rownum) != 0) and
(table.cell_value(colx=colnum - 1, rowx=rownum) != 0):
                print(f"{rownum+1}{colnum+1}")
                dlist.append((rownum, colnum))
        elif colnum == 3:
            if (table.cell_value(colx=colnum + 1, rowx=rownum) == 0) and
(table.cell_value(colx=colnum + 2, rowx=rownum) != 0) and (table.cell_value(colx=colnum - 1,
rowx=rownum) != 0) :
                print(f"{rownum+1}{colnum+1},  {colnum+2}")
                clist.append((rownum, colnum))
            elif (table.cell_value(colx=colnum + 1, rowx=rownum) == 0) and
(table.cell_value(colx=colnum + 2, rowx=rownum) == 0) and (table.cell_value(colx=colnum-1,
rowx=rownum) != 0):
                print(f" {rownum+1}{colnum+1},  {colnum+2},  {colnum+3}")
                blist.append((rownum, colnum))
            elif (table.cell_value(colx=colnum + 1, rowx=rownum) != 0) and
(table.cell_value(colx=colnum - 1, rowx=rownum) != 0):
                print(f"{rownum+1}{colnum+1}")
                dlist.append((rownum, colnum))
        elif colnum == 4:
```

```
                if (table.cell_value(colx=colnum + 1, rowx=rownum) == 0)  and
(table.cell_value(colx=colnum - 1, rowx=rownum) != 0) :
                    print(f"0：  {rownum+1}{colnum+1}，  {colnum+2}")
                    clist.append((rownum, colnum))
                elif (table.cell_value(colx=colnum + 1, rowx=rownum) != 0) and
(table.cell_value(colx=colnum - 1, rowx=rownum) != 0):
                    print(f"{rownum+1}{colnum+1}")
                    dlist.append((rownum, colnum))
            elif colnum == 5:
                if (table.cell_value(colx=colnum - 1, rowx=rownum) != 0):
                    print(f"：  {rownum+1} {colnum+1}")
                    dlist.append((rownum, colnum))



    #print (clist)
    #print (blist)
    print (f" 0{len(alist)}")



    workbase = openpyxl.load_workbook(path)
    print (workbase.sheetnames)
    sheet=workbase.sheetnames[0]
    table = workbase[sheet]
    for blistn in range(0, len(blist)):
        if (blist[blistn][0]!=0):
            x = blist[blistn][0] + 1
            y = blist[blistn][1] + 1
            #print(x)
            #print(y)
```

```
        a0 = table.cell(row=x - 1, column=y).value
        b0 = table.cell(row=x + 1, column=y).value
        a1 = table.cell(row=x - 1, column=y+1).value
        b1 = table.cell(row=x + 1, column=y+1).value
        a2 = table.cell(row=x - 1, column=y+2).value
        b2 = table.cell(row=x + 1, column=y+2).value
        #print(a0)
        table.cell(row=x, column=y, value=(a0 + b0) / 2)
        table.cell(row=x, column=y + 1, value=(a1 + b1) / 2)
        table.cell(row=x, column=y + 2, value=(a2 + b2) / 2)
        print(f"{x} {y}{y+1}，{y+2}")


for clistn in range(0, len(clist)):
    if (clist[clistn][0]!=0):
        x = clist[clistn][0] + 1
        y = clist[clistn][1] + 1
        #print(x,y)
        if y == 2: #
            a0 = table.cell(row=x - 1, column=4).value
            b0 = table.cell(row=x - 1, column=5).value
            c0 = table.cell(row=x - 1, column=6).value
            table.cell(row=x, column=y, value=(a0 + b0 + c0) / 3)
        elif y == 3:
            a0 = table.cell(row=x - 1, column=5).value
            b0 = table.cell(row=x - 1, column=6).value
            c0 = table.cell(row=x , column=2).value
            table.cell(row=x, column=y, value=(a0 + b0 + c0) / 3)
        elif y == 4:
```

```
            a0 = table.cell(row=x - 1, column=6).value
            b0 = table.cell(row=x , column=2).value
            c0 = table.cell(row=x , column=3).value
            table.cell(row=x, column=y, value=(a0 + b0 + c0) / 3)
        else :
            a0 = table.cell(row=x , column=y-3).value
            b0 = table.cell(row=x , column=y-2).value
            c0 = table.cell(row=x , column=y-1).value
            table.cell(row=x, column=y, value=(a0 + b0 + c0) / 3)
        print(f" {x}{y} ")


for clistn in range(0, len(clist)):#
    if (clist[clistn][0]!=0):
        x = clist[clistn][0] + 1
        y = clist[clistn][1] + 1
        if y == 2:
            a0 = table.cell(row=x - 1, column=6).value
            b0 = table.cell(row=x , column=y + 1).value
            table.cell(row=x, column=y+1, value=(a0 + b0) / 2)
        elif 2< y < 6 :
            a0 = table.cell(row=x, column=y-1).value
            b0 = table.cell(row=x, column=y+1).value
            table.cell(row=x, column=y+1, value=(a0 + b0) / 2)
        elif y == 6:
            a0 = table.cell(row=x, column=y - 1).value
            b0 = table.cell(row=x + 1, column=2).value
            table.cell(row=x, column=y+1, value=(a0 + b0 ) / 2)
        print(f" {x} {y} ")
```

```
    for dlistn in range(0, len(dlist)):
        if (dlist[dlistn][0]!=0):
            x = dlist[dlistn][0] + 1
            y = dlist[dlistn][1] + 1
            if y == 2:
                a0 = table.cell(row=x - 1, column=6).value
                b0 = table.cell(row=x , column=y + 1).value
                table.cell(row=x, column=y, value=(a0 + b0) / 2)
            elif 2< y < 6 :
                a0 = table.cell(row=x, column=y-1).value
                b0 = table.cell(row=x, column=y+1).value
                table.cell(row=x, column=y, value=(a0 + b0) / 2)
            elif y == 6:
                a0 = table.cell(row=x, column=y - 1).value
                b0 = table.cell(row=x + 1, column=2).value
                table.cell(row=x, column=y, value=(a0 + b0 ) / 2)
            print(f" {x} {y} ")



    save_path=path+"_new.xlsx"
    workbase.save(save_path)



if __name__ == '__main__':
    path = r'D:\MrVans Document\Buffalo Fourth Semester\Thesis\Thesis
Program\Beijing_PM25_Rebuilt_Result_03\Miyun'
    getFileNames(path)
```

```
#resultdata = openpyxl.load_workbook('2015 /PM25_2018_Fengtai Garden.xlsx')
#resultsheet = resultdata['Sheet1']
#OtherValue.insert(0, MIDValue)
#OtherValue.insert(0, time1)
#resultsheet.append(OtherValue)
#resultdata.save('2015 /PM25_2018_Fengtai Garden.xlsx')
#print("Finished " + path)
```

Appendix C

Codes of Mann-Kendall Trend Analysis Based on R-studio

```
library(trend)

library(ggplot2)


csv_1 <- read.csv("D:/MrVans Document/Buffalo Fourth Semester/Thesis/R Program/5 Years PM25 data/.csv File/PM25_five_years_Yungang.csv")

csv_2 <- read.csv("D:/MrVans Document/Buffalo Fourth Semester/Thesis/R Program/5 Years PM25 data/.csv File/PM25_five_years_Yongle Village.csv")


#Spring

Spring_csv_1 <- subset(csv_1, Season == "Spring")

Spring_csv_2 <- subset(csv_2, Season == "Spring")


Spring_csv_1$New_Day<-order(Spring_csv_1[,8])

Spring_csv_2$New_Day<-order(Spring_csv_2[,8])


lm_Spring_csv_1 <- lm(Daily_Average ~ New_Day, data = Spring_csv_1)

lm_Spring_csv_2 <- lm(Daily_Average ~ New_Day, data = Spring_csv_2)



summary(lm_Spring_csv_1)

mk.test(Spring_csv_1$Daily_Average, continuity = TRUE)


summary(lm_Spring_csv_2)

mk.test(Spring_csv_2$Daily_Average, continuity = TRUE)



ggplot(Spring_csv_1, aes(New_Day, Daily_Average)) +
```

```
  geom_point() +
  geom_smooth(method = "lm", colour = "Red") +
  labs(x = "Day",
       y = "Selected Daily Average of PM2.5 Concentrate",
       title = "Fundamental Data Analysis of Spring PM2.5 Concentrate from Yungang Weather Site")


ggplot(Spring_csv_2, aes(New_Day, Daily_Average)) +
  geom_point() +
  geom_smooth(method = "lm", colour = "Red") +
  labs(x = "Day",
       y = "Selected Daily Average of PM2.5 Concentrate",
       title = "Fundamental Data Analysis of Spring PM2.5 Concentrate from Yongle Village Weather Site")


#Summer
Summer_csv_1 <- subset(csv_1, Season == "Summer")
Summer_csv_2 <- subset(csv_2, Season == "Summer")


Summer_csv_1$New_Day<-order(Summer_csv_1[,8])
Summer_csv_2$New_Day<-order(Summer_csv_2[,8])


lm_Summer_csv_1 <- lm(Daily_Average ~ New_Day, data = Summer_csv_1)
lm_Summer_csv_2 <- lm(Daily_Average ~ New_Day, data = Summer_csv_2)



summary(lm_Summer_csv_1)
mk.test(Summer_csv_1$Daily_Average, continuity = TRUE)
```

```
summary(lm_Summer_csv_2)
mk.test(Summer_csv_2$Daily_Average, continuity = TRUE)



ggplot(Summer_csv_1, aes(New_Day, Daily_Average)) +
  geom_point() +
  geom_smooth(method = "lm", colour = "Red") +
  labs(x = "Day",
       y = "Selected Daily Average of PM2.5 Concentrate",
       title = "Fundamental Data Analysis of Summer PM2.5 Concentrate from Yizhuang Weather Site")


ggplot(Summer_csv_2, aes(New_Day, Daily_Average)) +
  geom_point() +
  geom_smooth(method = "lm", colour = "Red") +
  labs(x = "Day",
       y = "Selected Daily Average of PM2.5 Concentrate",
       title = "Fundamental Data Analysis of Summer PM2.5 Concentrate from Xizhi Gate North Weather Site")


#Autumn


Autumn_csv_1 <- subset(csv_1, Season == "Autumn")
Autumn_csv_2 <- subset(csv_2, Season == "Autumn")


Autumn_csv_1$New_Day<-order(Autumn_csv_1[,8])
Autumn_csv_2$New_Day<-order(Autumn_csv_2[,8])


lm_Autumn_csv_1 <- lm(Daily_Average ~ New_Day, data = Autumn_csv_1)
```

```
lm_Autumn_csv_2 <- lm(Daily_Average ~ New_Day, data = Autumn_csv_2)



summary(lm_Autumn_csv_1)
mk.test(Autumn_csv_1$Daily_Average, continuity = TRUE)

summary(lm_Autumn_csv_2)
mk.test(Autumn_csv_2$Daily_Average, continuity = TRUE)



ggplot(Autumn_csv_1, aes(New_Day, Daily_Average)) +
  geom_point() +
  geom_smooth(method = "lm", colour = "Red") +
  labs(x = "Day",
       y = "Selected Daily Average of PM2.5 Concentrate",
       title = "Fundamental Data Analysis of Autumn PM2.5 Concentrate from Yizhuang Site")



ggplot(Autumn_csv_2, aes(New_Day, Daily_Average)) +
  geom_point() +
  geom_smooth(method = "lm", colour = "Red") +
  labs(x = "Day",
       y = "Selected Daily Average of PM2.5 Concentrate",
       title = "Fundamental Data Analysis of Autumn PM2.5 Concentrate from Xizhi Gate North
Weather Site")

#Winter
Winter_csv_1 <- subset(csv_1, Season == "Winter")
Winter_csv_2 <- subset(csv_2, Season == "Winter")
```

```
Winter_csv_1$New_Day<-order(Winter_csv_1[,8])
Winter_csv_2$New_Day<-order(Winter_csv_2[,8])

lm_Winter_csv_1 <- lm(Daily_Average ~ New_Day, data = Winter_csv_1)
lm_Winter_csv_2 <- lm(Daily_Average ~ New_Day, data = Winter_csv_2)

summary(lm_Winter_csv_1)
mk.test(Winter_csv_1$Daily_Average, continuity = TRUE)

summary(lm_Winter_csv_2)
mk.test(Winter_csv_2$Daily_Average, continuity = TRUE)

ggplot(Winter_csv_1, aes(New_Day, Daily_Average)) +
  geom_point() +
  geom_smooth(method = "lm", colour = "Red") +
  labs(x = "Day",
       y = "Selected Daily Average of PM2.5 Concentrate",
       title = "Fundamental Data Analysis of Winter PM2.5 Concentrate from Yizhuang Weather Site")

ggplot(Winter_csv_2, aes(New_Day, Daily_Average)) +
  geom_point() +
  geom_smooth(method = "lm", colour = "Red") +
  labs(x = "Day",
       y = "Selected Daily Average of PM2.5 Concentrate",
       title = "Fundamental Data Analysis of Winter PM2.5 Concentrate from Xizhi Gate North Weather Site")
```

Appendix D

PCA Codes Based on MATLAB

```
%This script turns the Excel worksheets into a MATLAB data file
%organized by location, then year e.g. to get the first year of
%the Ancient Town would be data(2).site{1,1}
clear, clc, close all
%E.g. for the 2018 Midnight data of Badaling, data(2).site{1,5}(:,1)

%%
%Get folder names
d = dir(pwd);
foldernames = {d.name};
foldernames = foldernames([d.isdir]); %Remove non-folders
foldernames = foldernames(~ismember(foldernames,{'.','..'})); %Remove extra folders
%Set up data structure
data = struct('name',foldernames,'site',cell(1,length(foldernames)));
for i = 1:length(foldernames) %Iterate through 27 locations
    %Get the names of the files in each folder
    dd = dir([foldernames{i} '\*.xlsx']);
    filenames = {dd.name};
    filenames = filenames(~contains(filenames,'~$')); %Remove extra filenames

    %Set up cell array for 5 years (5 Excel files)
    temp = cell(1,length(filenames));
    %Populate cell array with tables
    for j = 1:length(filenames)
        T = readtable([foldernames{i} '\' filenames{j}]);
        temp{j} = T;
```

```
    end
    data(i).site = temp;
end

%Save the variable 'data' in the file 'BPollution.mat'
save('BPollutionData.mat','data');



%This script uses PCA to reduce the five year data at each location to 2
%variables
clear, clc, close all

%Load .mat file
load('BPollutionData.mat');

for i = 1:length(data)
%for i = 27
    %Assemble column-normalized 5-year data
    fiveyeardata = [];
    for j = 2:6
        fiveyeardata(:,j-1) = table2array([data(i).site{1,1}(:,j); data(i).site{1,2}(:,j);...
            data(i).site{1,3}(:,j); data(i).site{1,4}(:,j); data(i).site{1,5}(:,j)]);
    end
    %norm_data = fiveyeardata - mean(fiveyeardata);

    %Get covariance matrix
    C = cov(fiveyeardata);
    %Get eigenvectors and eigenvalues
```

```
[V,D] = eig(C);

%Form new data from eigenvectors
newdata = fiveyeardata*V;

%Calculate variance from eigenvalues
variance = D / sum(D(:));
variance = sum(variance);

%Reduce to the only the biggest (two) columns of max variance
[~, ix1] = max(variance);
[~, ix2] = max(variance(~(variance == max(variance))));
if ix2 >= ix1
  ix2 = ix2 + 1;
end
newdata = newdata(:,[ix1])
%newdata = newdata(:,[ix1 ix2]);

A = diag(D)
A(5)/ sum(A)

%Plot
figure('Position',[80, 80, 900, 600])
hold on
for i = 1:size(newdata,2)
plot(newdata(:,i))
end
```

```
    %Plot formatting
    xticks(0:365:length(newdata))
    xlim([-20, length(newdata)+20])
    xlabel('Year')
    xticklabels(2014:2018)
    ylabel('PM 2.5 Concentration (ug/m^3)')
    title([data(i).name ', 1 PCA Components'])
    set(gca,'FontWeight','Bold','FontSize',12,'LineWidth',2)
    legend('Component 1', 'Component 2')
end
```

Appendix E

Tables of Five Eigenvalues and Corresponding Weighting Percentage

Station-Name	First Eigenvalues	Weighting (Percentage)	Second Eigenvalues	Weighting (Percentage)
Agricultural Pavilion	0.0275	0.97%	0.0408	1.44%
Ancient Town	0.0326	1.24%	0.0471	1.80%
Badaling	0.0176	1.22%	0.0306	2.12%
Changping	0.0301	1.44%	0.0418	2.00%
Daxing	0.0329	0.92%	0.0499	1.40%
Dingling	0.023	1.09%	0.0345	1.63%
Dongsi	0.0271	0.97%	0.042	1.50%
Fangshan	0.0316	0.99%	0.0486	1.52%
Fengtai Garden	0.0317	1.00%	0.0495	1.57%
Front Gate	0.0408	1.35%	0.0625	2.07%
Guanyuan	0.025	0.99%	0.0432	1.71%
Huairou	0.0192	0.97%	0.0288	1.45%
Inside Yongding Gate	0.0398	1.30%	0.0525	1.71%
Longevity West Palace	0.0327	1.16%	0.0502	1.78%
Mentougou	0.0279	1.28%	0.0415	1.91%
Miyun	0.0166	0.84%	0.0267	1.35%
Olympic Sports Center	0.026	0.97%	0.0418	1.55%
Pinggu	0.0306	1.28%	0.0374	1.56%
Shunyi	0.0263	1.04%	0.0389	1.54%
South Third Ring Road	0.0428	1.34%	0.0658	2.06%
Temple of Heaven	0.0311	1.22%	0.0463	1.81%
Tongzhou	0.0288	0.90%	0.053	1.66%
Wanliu	0.0272	1.09%	0.04	1.59%
Xizhi Gate North	0.0293	1.09%	0.0465	1.73%
Yizhuang	0.0386	1.17%	0.0559	1.70%
Yongle Village	0.0403	1.07%	0.0652	1.73%
Yungang	0.0262	1.00%	0.0371	1.41%

Station-Name	Third Eigenvalues	Weighting (Percentage)	Fourth Eigenvalues	Weighting (Percentage)
Agricultural Pavilion	0.1534	5.43%	0.3366	11.90%
Ancient Town	0.1216	4.63%	0.3	11.44%
Badaling	0.0646	4.48%	0.17	11.78%
Changping	0.1042	4.98%	0.2493	11.92%
Daxing	0.2123	5.97%	0.3514	9.89%
Dingling	0.0818	3.86%	0.2317	10.93%
Dongsi	0.1537	5.49%	0.3257	11.63%
Fangshan	0.1885	5.90%	0.362	11.34%
Fengtai Garden	0.1558	4.94%	0.3464	10.97%
Front Gate	0.1679	5.56%	0.4042	13.40%
Guanyuan	0.1201	4.76%	0.2903	11.51%
Huairou	0.0842	4.24%	0.2568	12.92%
Inside Yongding Gate	0.1654	5.40%	0.3702	12.09%
Longevity West Palace	0.1483	5.25%	0.3245	11.50%
Mentougou	0.0972	4.48%	0.3027	13.94%
Miyun	0.0769	3.90%	0.2841	14.41%
Olympic Sports Center	0.1486	5.53%	0.3345	12.45%
Pinggu	0.1029	4.30%	0.3367	14.08%
Shunyi	0.1323	5.22%	0.3652	14.43%
South Third Ring Road	0.1844	5.79%	0.3762	11.80%
Temple of Heaven	0.1396	5.45%	0.2987	11.66%
Tongzhou	0.1752	5.48%	0.3989	12.49%
Wanliu	0.1209	4.82%	0.2987	11.91%
Xizhi Gate North	0.1368	5.09%	0.3235	12.03%
Yizhuang	0.1757	5.34%	0.3697	11.23%
Yongle Village	0.17	4.51%	0.4908	13.01%
Yungang	0.1165	4.44%	0.293	11.17%

Station-Name	Fifth Eigenvalues	Weighting (Percentage)
Agricultural Pavilion	2.2697	80.26%
Ancient Town	2.1221	80.89%
Badaling	1.1609	80.41%
Changping	1.6661	79.66%
Daxing	2.908	81.82%
Dingling	1.7492	82.50%
Dongsi	2.2517	80.42%
Fangshan	2.5628	80.25%
Fengtai Garden	2.5742	81.52%
Front Gate	2.3422	77.62%
Guanyuan	2.0424	81.02%
Huairou	1.5981	80.43%
Inside Yongding Gate	2.4346	79.50%
Longevity West Palace	2.2665	80.31%
Mentougou	1.7022	78.39%
Miyun	1.5672	79.49%
Olympic Sports Center	2.1357	79.50%
Pinggu	1.8843	78.78%
Shunyi	1.9689	77.78%
South Third Ring Road	2.5177	79.00%
Temple of Heaven	2.0466	79.87%
Tongzhou	2.5387	79.47%
Wanliu	2.0215	80.59%
Xizhi Gate North	2.1528	80.06%
Yizhuang	2.6514	80.56%
Yongle Village	3.006	79.69%
Yungang	2.1508	81.98%

Appendix F

PCA Result Graphs of 27 Observation Sites

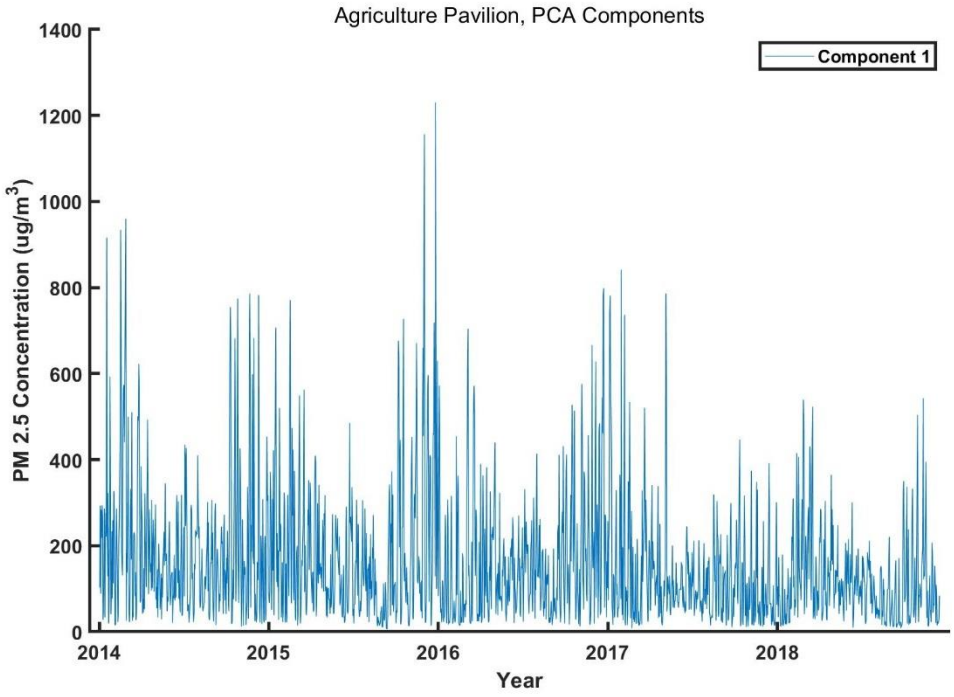

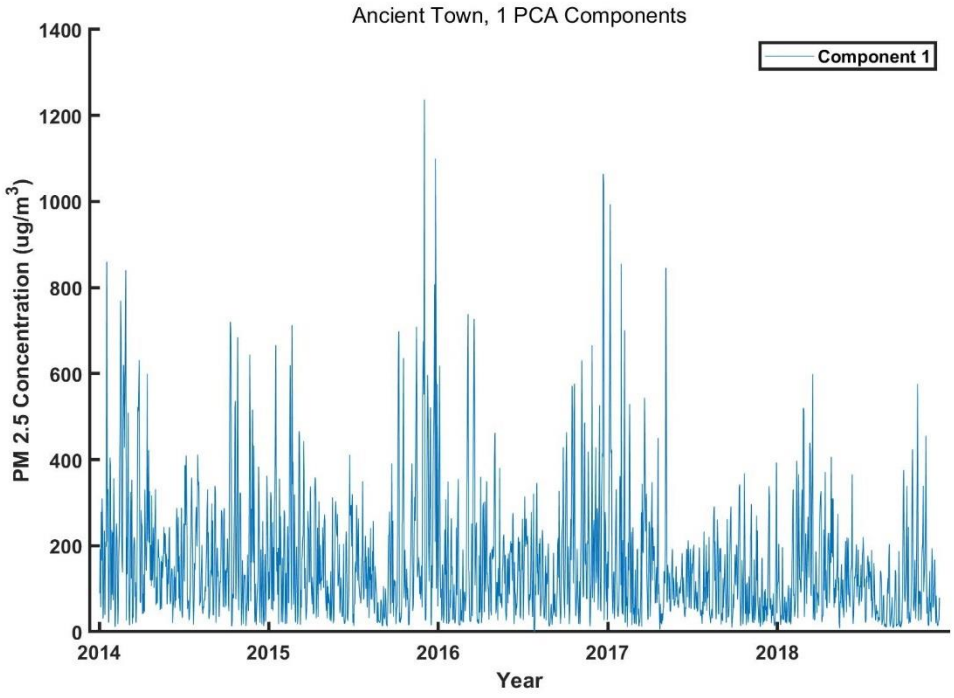

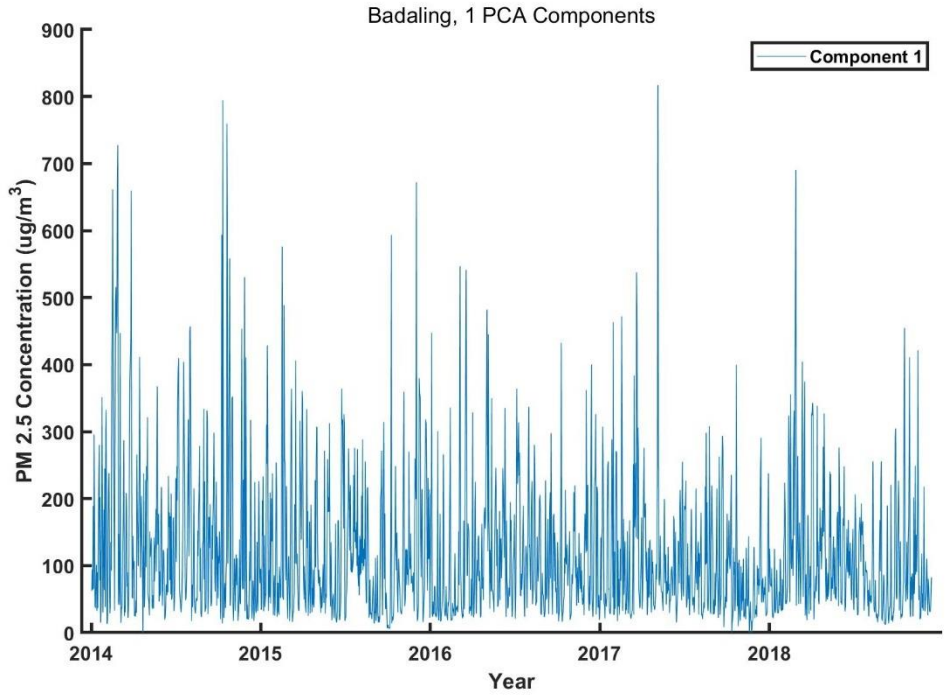
Badaling, 1 PCA Components
Component 1
PM 2.5 Concentration (ug/m3)
0
100
200
300
400
500
600
700
800
900
2014
2015
2016
2017
2018
Year

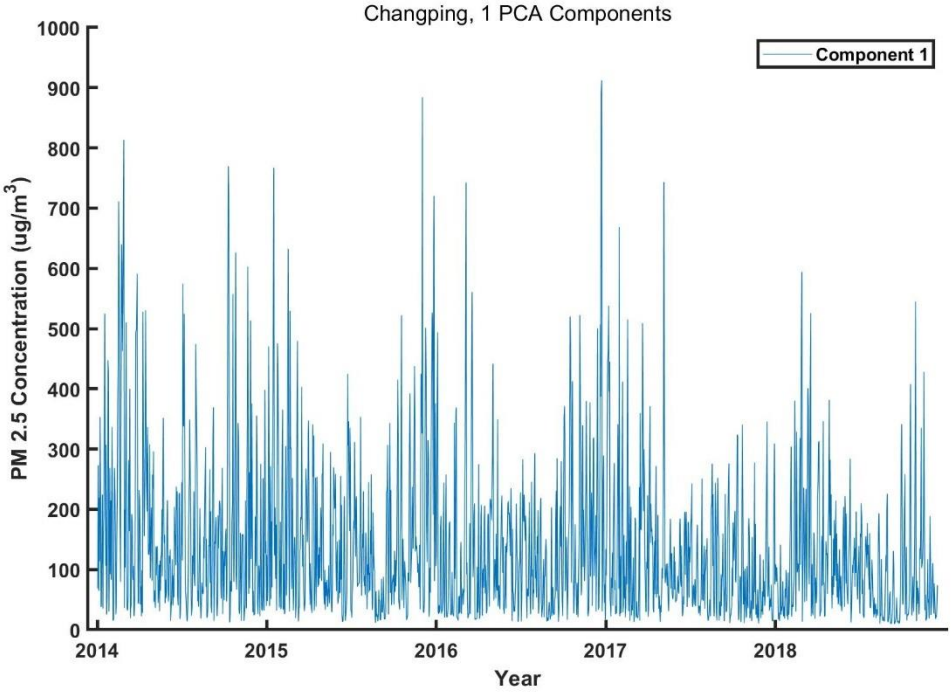
Changping, 1 PCA Components
Component 1
PM 2.5 Concentration (ug/m3)
0
100
200
300
400
500
600
700
800
900
1000
2014
2015
2016
2017
2018
Year

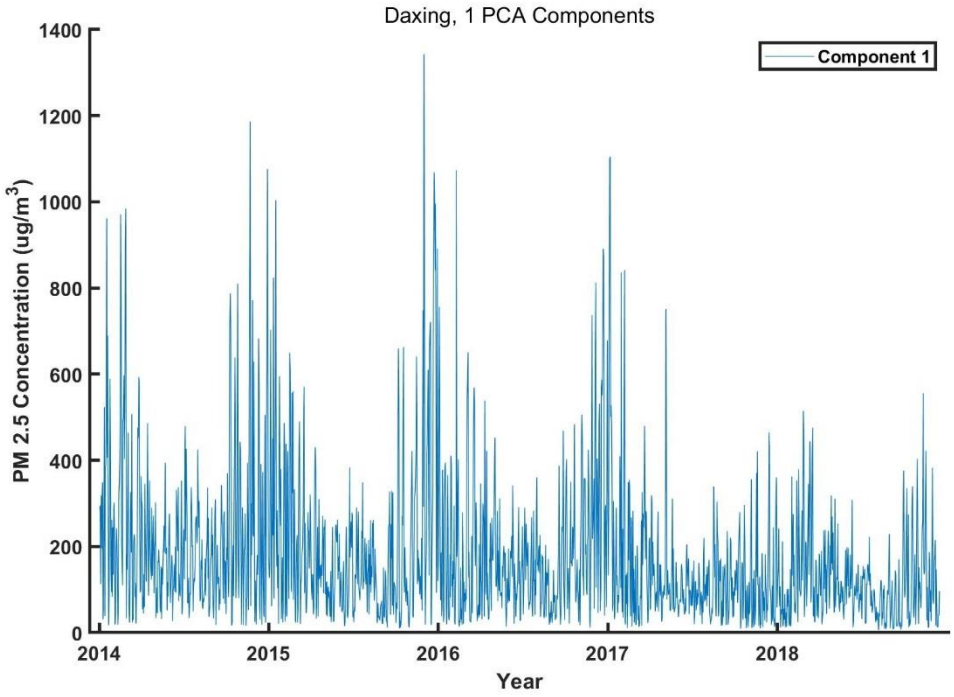
Daxing, 1 PCA Components
Component 1
PM 2.5 Concentration (ug/m3)
0
200
400
600
800
1000
1200
1400
2014
2015
2016
2017
2018
Year

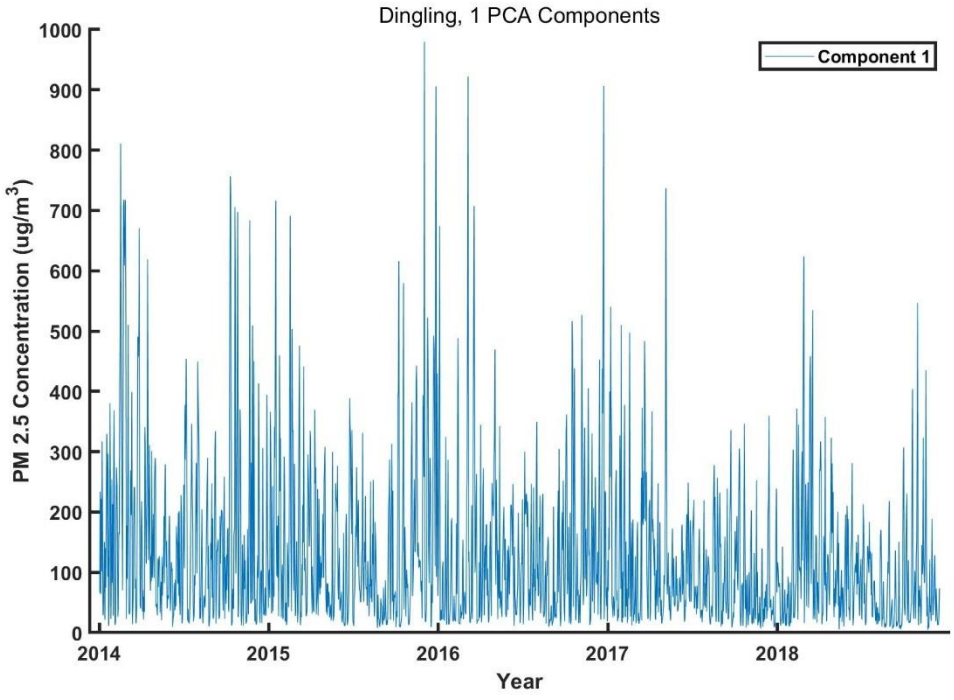
Dingling, 1 PCA Components
Component 1
PM 2.5 Concentration (ug/m3)
0
100
200
300
400
500
600
700
800
900
1000
2014
2015
2016
2017
2018
Year

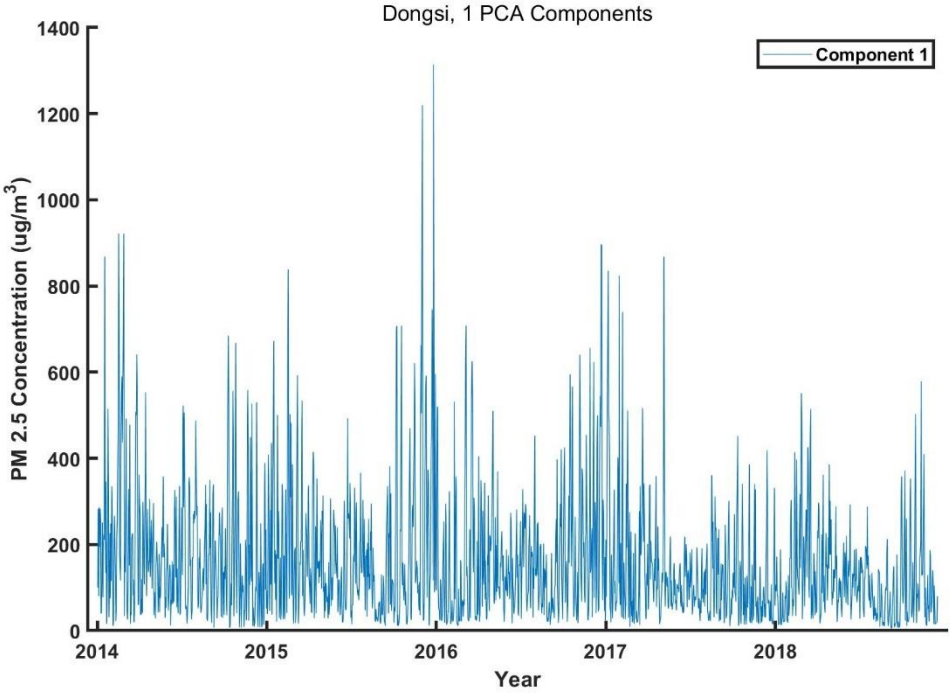
Dongsi, 1 PCA Components
Component 1
PM 2.5 Concentration (ug/m3)
1400
1200
1000
800
600
400
200
0
2014
2015
2016
2017
2018
Year

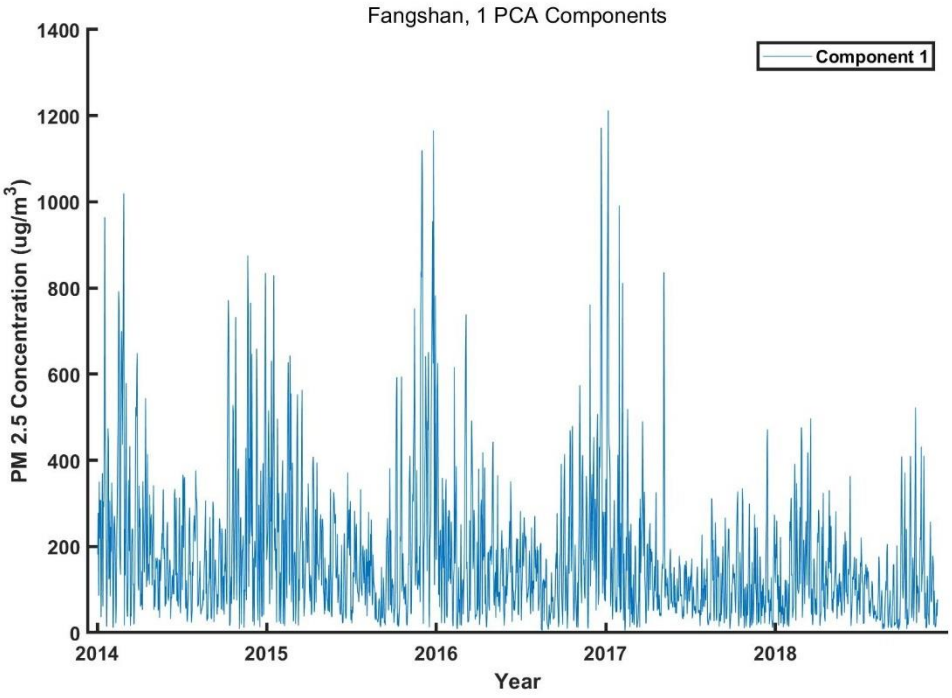
Fangshan, 1 PCA Components
Component 1
PM 2.5 Concentration (ug/m3)
1400
1200
1000
800
600
400
200
0
2014
2015
2016
2017
2018
Year

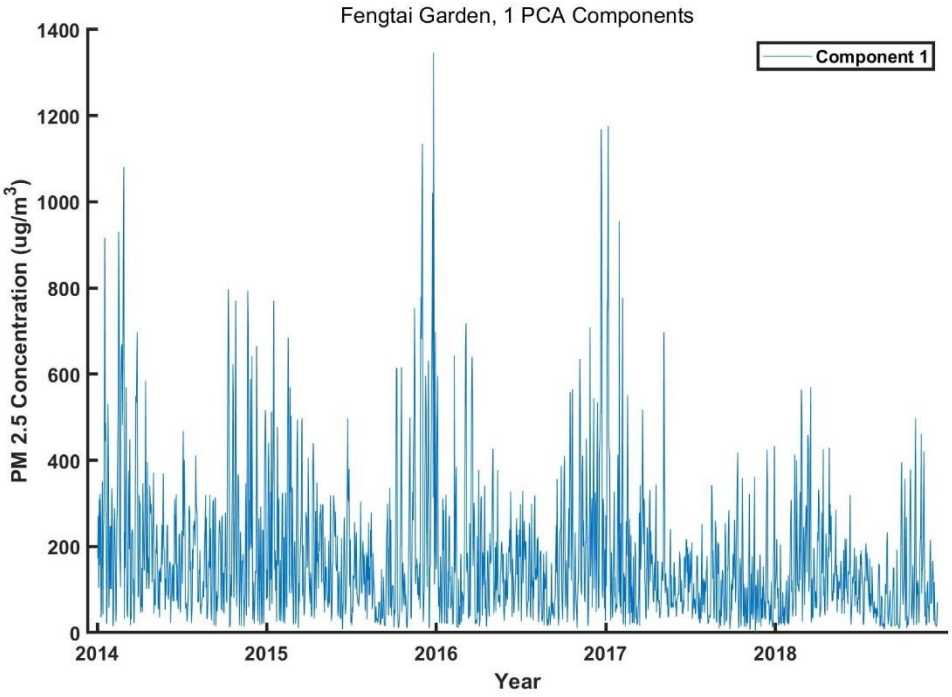
Fengtai Garden, 1 PCA Components
Component 1
PM 2.5 Concentration (ug/m3)
1400
1200
1000
800
600
400
200
0
2014
2015
2016
2017
2018
Year

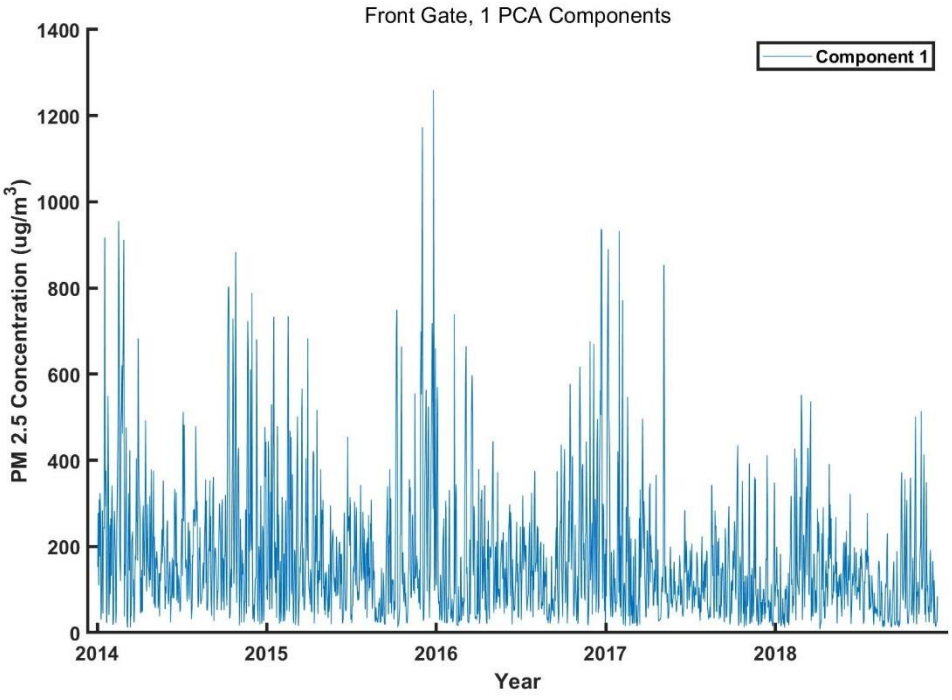
Front Gate, 1 PCA Components
Component 1
PM 2.5 Concentration (ug/m3)
1400
1200
1000
800
600
400
200
0
2014
2015
2016
2017
2018
Year

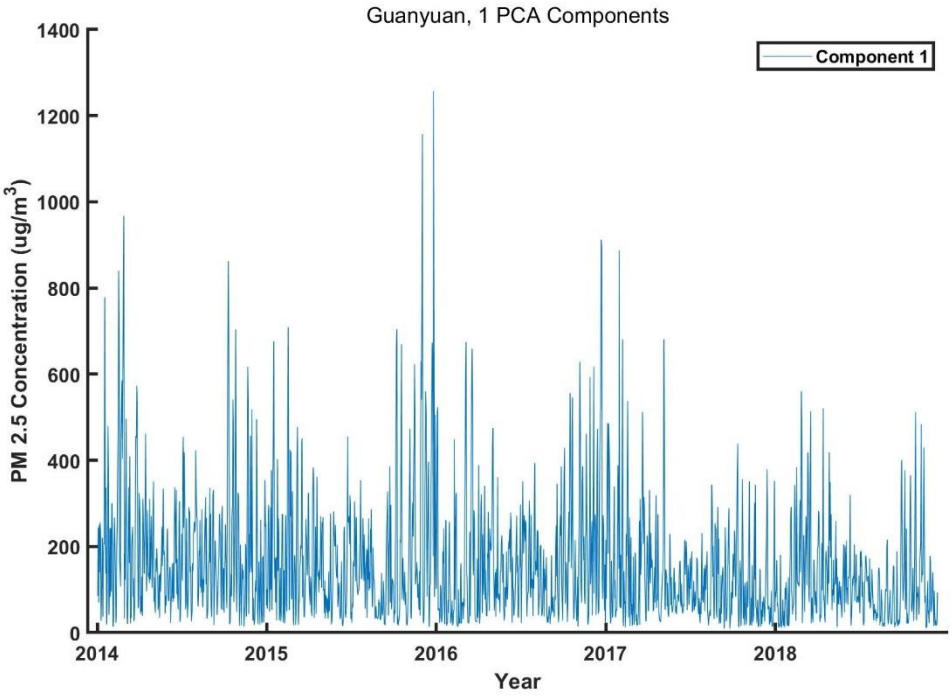
Guanyuan, 1 PCA Components
Component 1
PM 2.5 Concentration (ug/m3)
0
200
400
600
800
1000
1200
1400
2014
2015
2016
2017
2018
Year

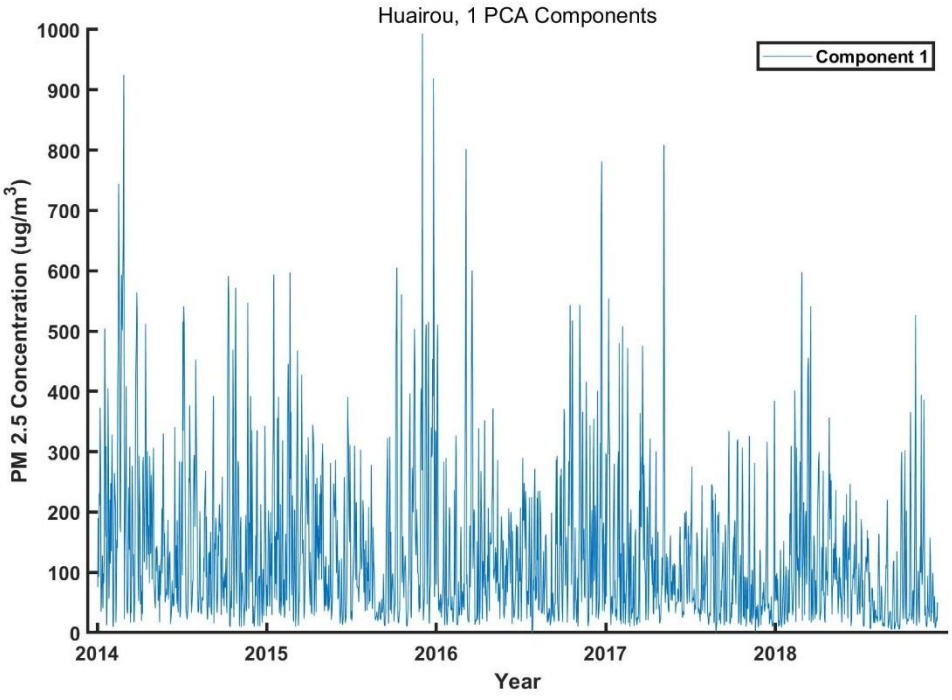
Huairou, 1 PCA Components
Component 1
PM 2.5 Concentration (ug/m3)
0
100
200
300
400
500
600
700
800
900
1000
2014
2015
2016
2017
2018
Year

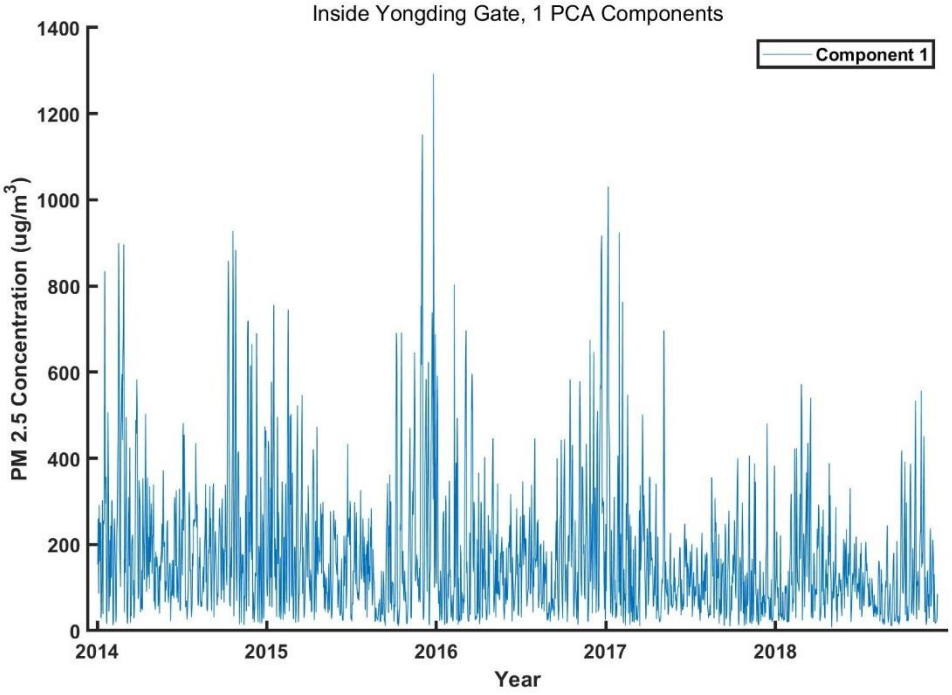
Inside Yongding Gate, 1 PCA Components
Component 1
PM 2.5 Concentration (ug/m3)
1400
1200
1000
800
600
400
200
0
2014
2015
2016
2017
2018
Year

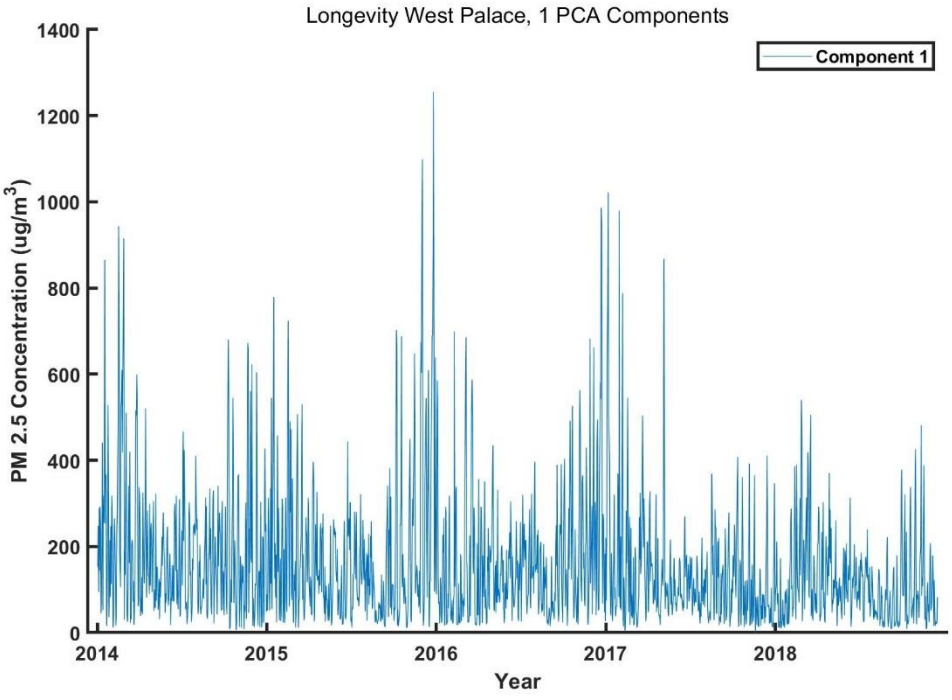
Longevity West Palace, 1 PCA Components
Component 1
PM 2.5 Concentration (ug/m3)
1400
1200
1000
800
600
400
200
0
2014
2015
2016
2017
2018
Year

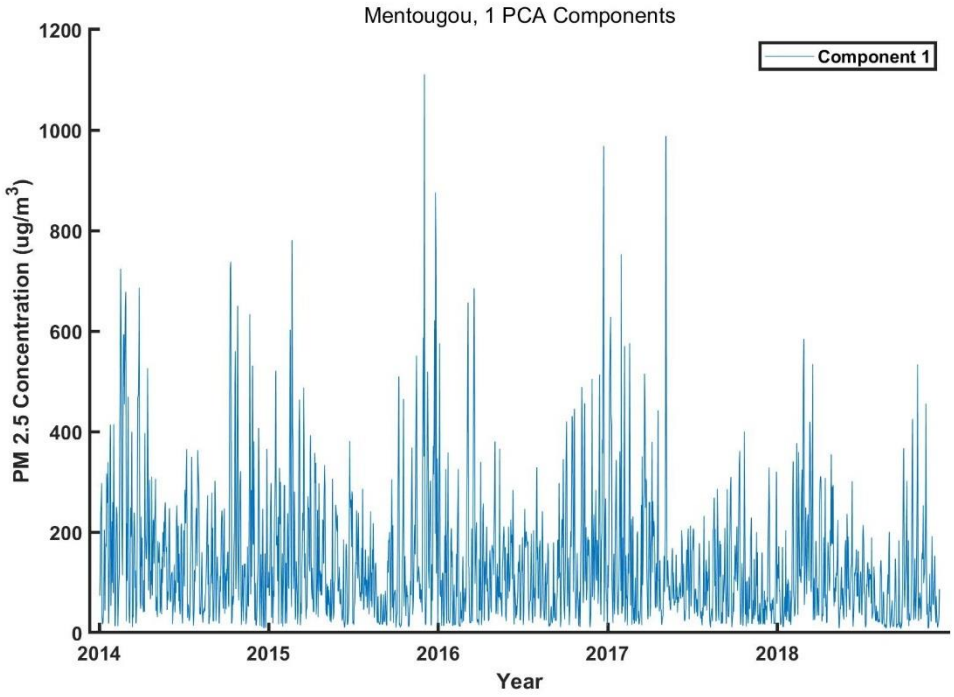
Mentougou, 1 PCA Components
Component 1
PM 2.5 Concentration (ug/m3)
0
200
400
600
800
1000
1200
2014
2015
2016
2017
2018
Year

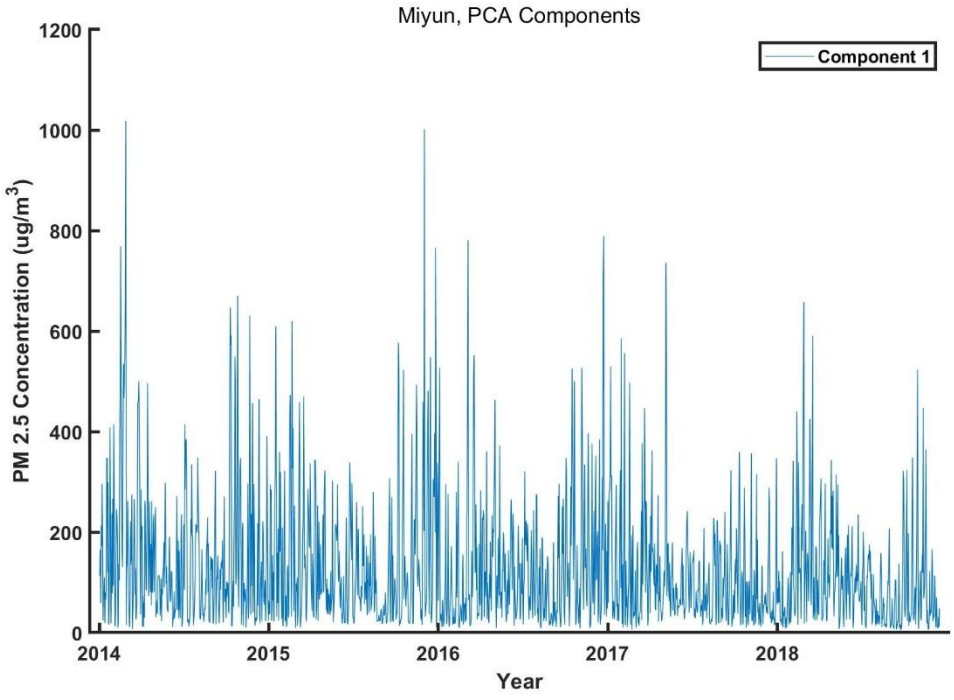
Miyun, PCA Components
Component 1
PM 2.5 Concentration (ug/m3)
0
200
400
600
800
1000
1200
2014
2015
2016
2017
2018
Year

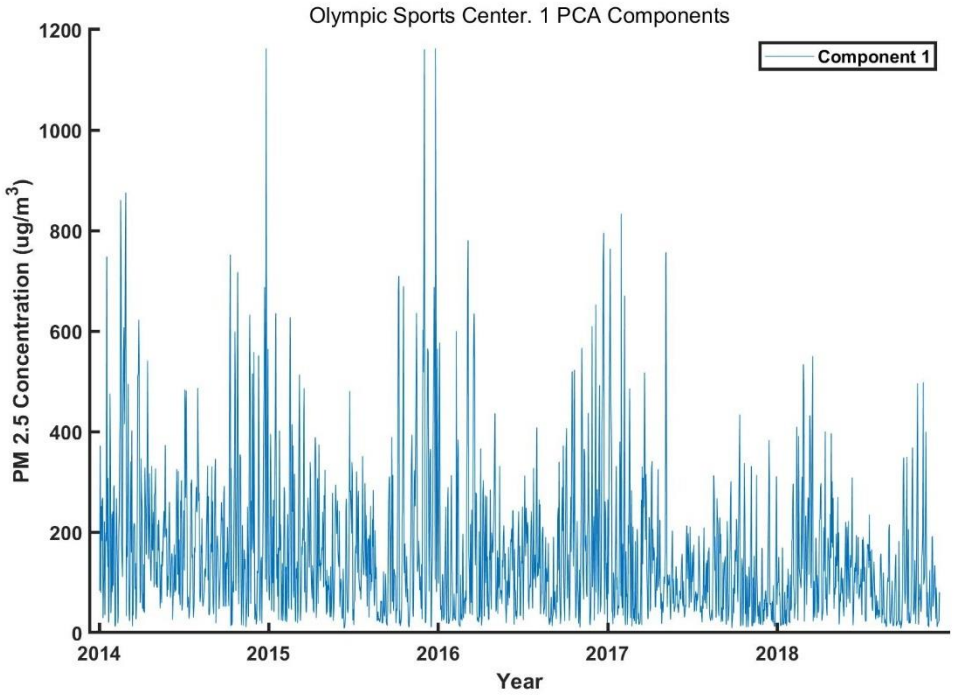
Olympic Sports Center. 1 PCA Components
Component 1
PM 2.5 Concentration (ug/m3)
1200
1000
800
600
400
200
0
2014
2015
2016
2017
2018
Year

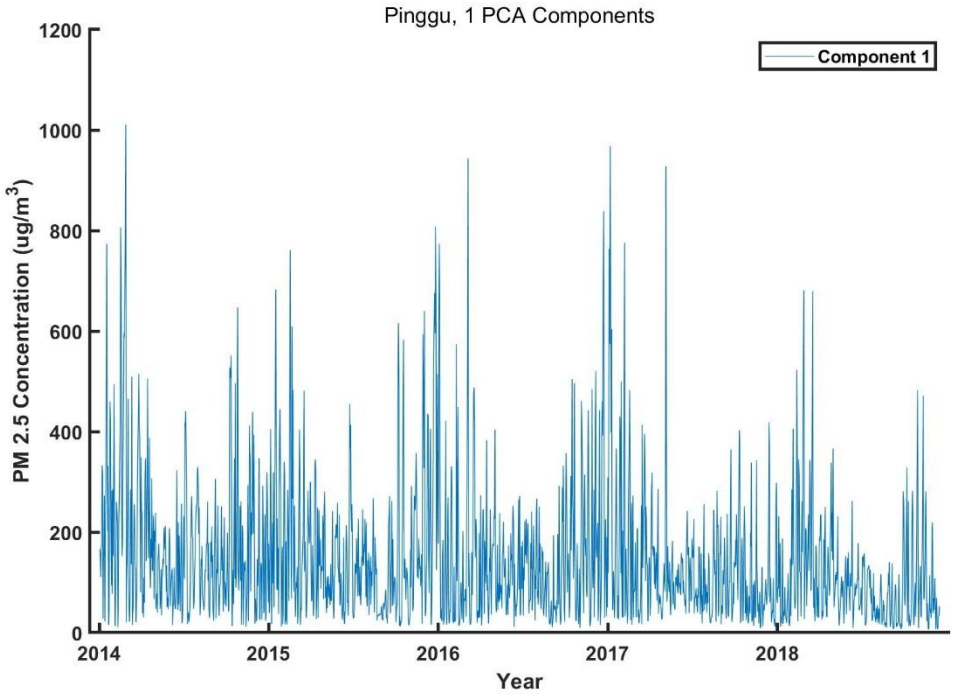
Pinggu, 1 PCA Components
Component 1
PM 2.5 Concentration (ug/m3)
1200
1000
800
600
400
200
0
2014
2015
2016
2017
2018
Year

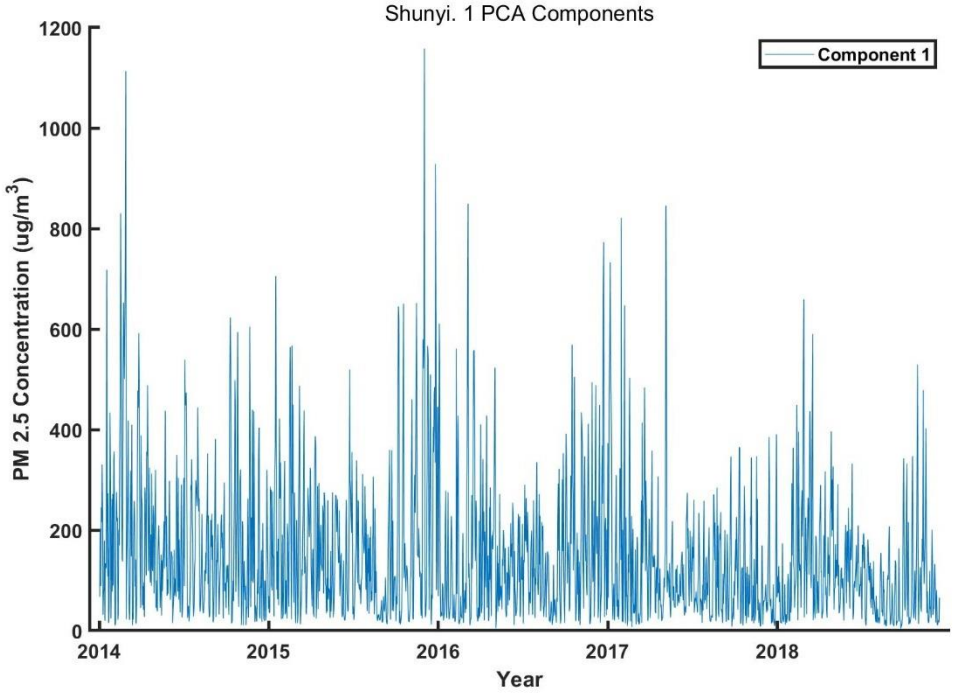
Shunyi. 1 PCA Components
Component 1
PM 2.5 Concentration (ug/m3)
Year
0
200
400
600
800
1000
1200
2014
2015
2016
2017
2018

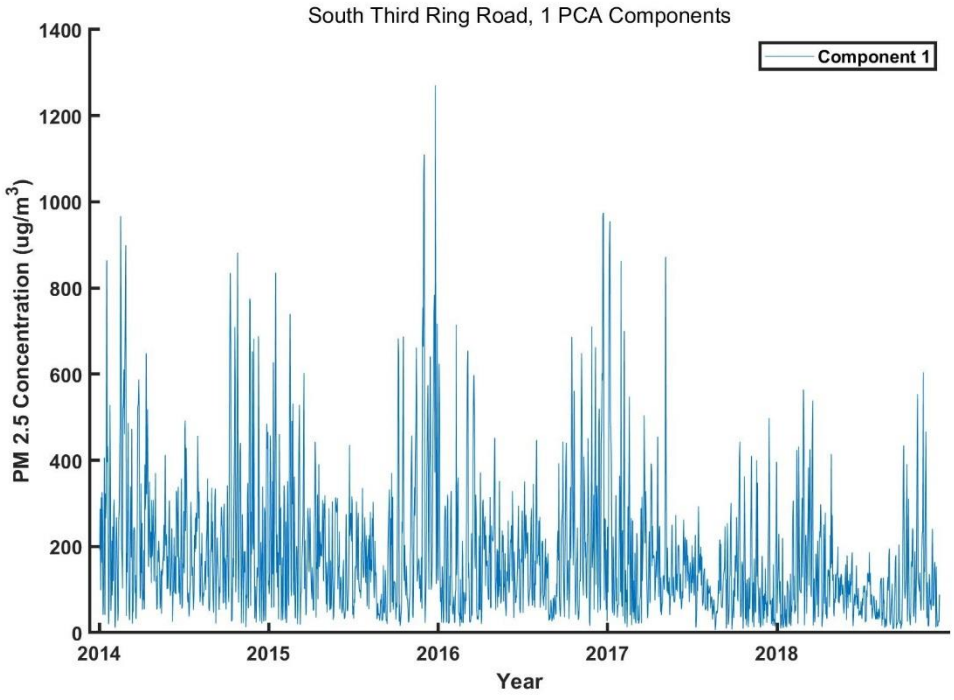
South Third Ring Road, 1 PCA Components
Component 1
PM 2.5 Concentration (ug/m3)
Year
0
200
400
600
800
1000
1200
1400
2014
2015
2016
2017
2018

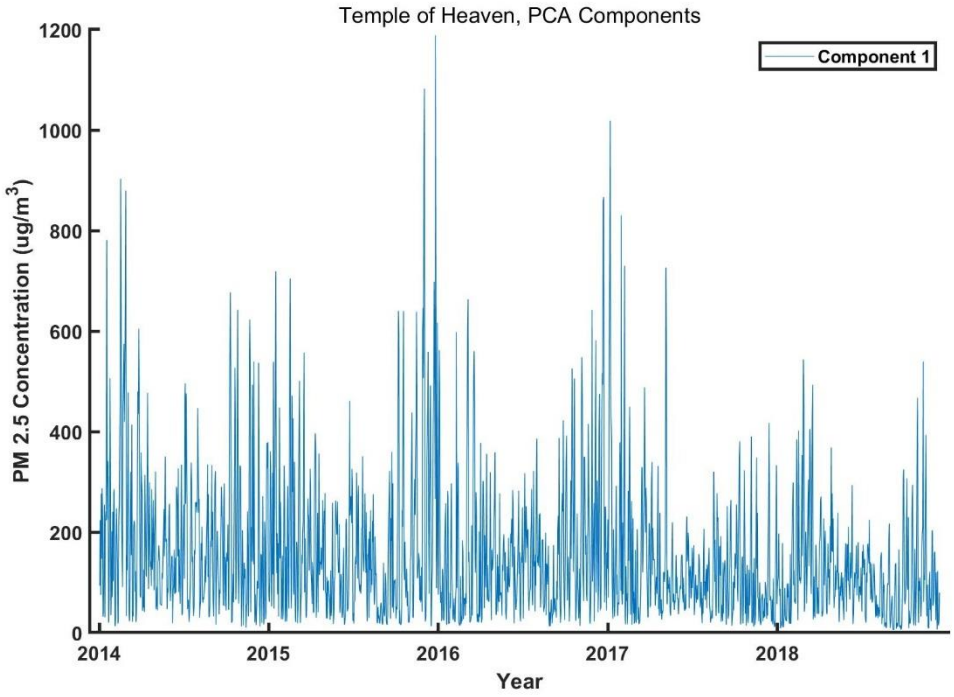
Temple of Heaven, PCA Components
Component 1
PM 2.5 Concentration (ug/m3)
1200
1000
800
600
400
200
0
2014
2015
2016
2017
2018
Year

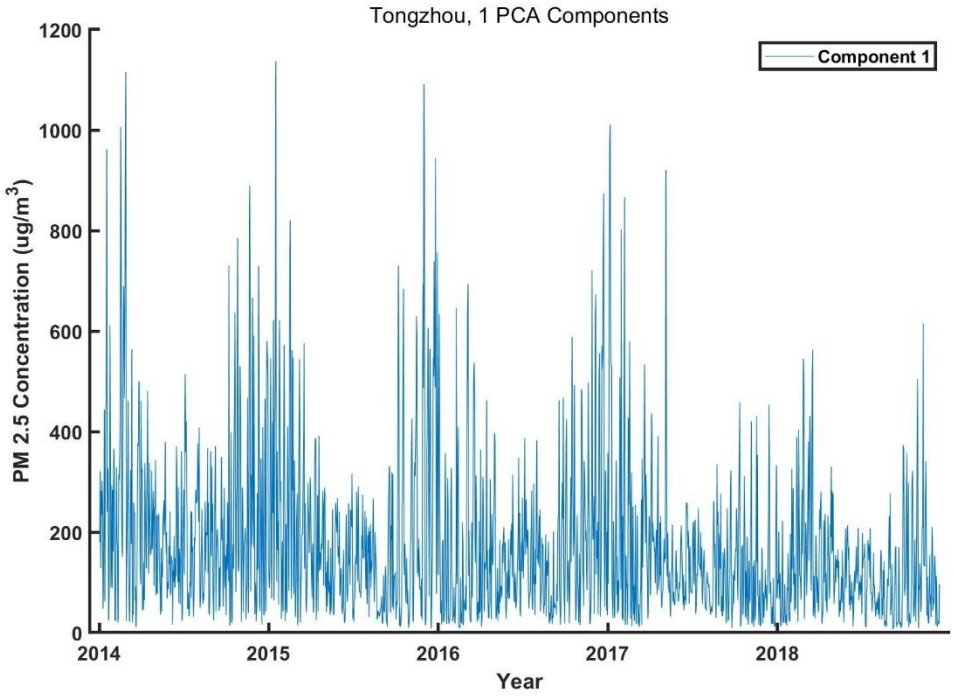
Tongzhou, 1 PCA Components
Component 1
PM 2.5 Concentration (ug/m3)
0
200
400
600
800
1000
1200
2014
2015
2016
2017
2018
Year

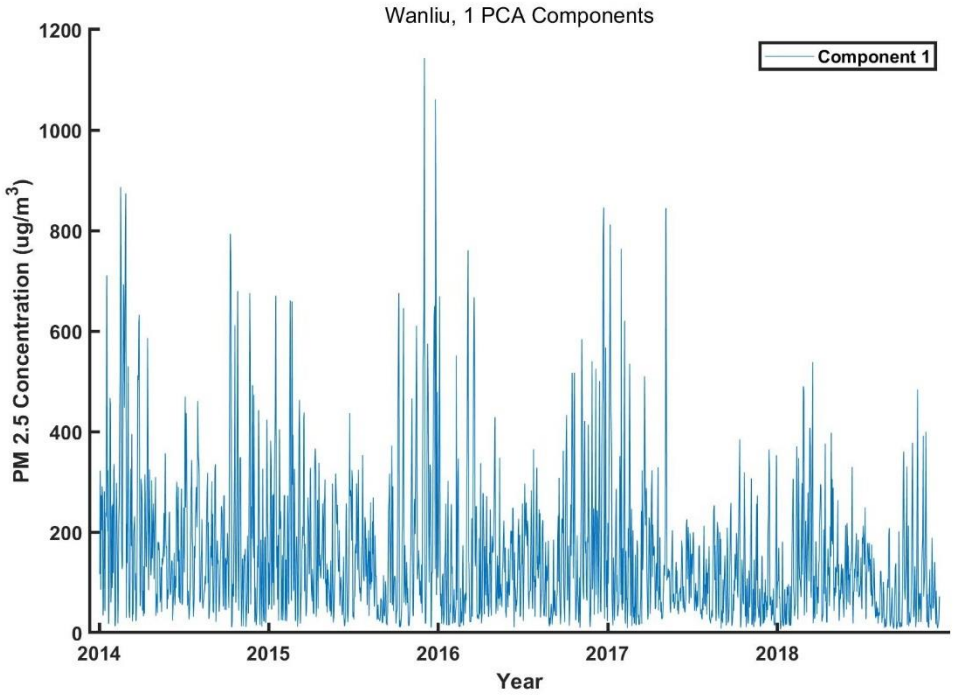
Wanliu, 1 PCA Components
Component 1
PM 2.5 Concentration (ug/m3)
0
200
400
600
800
1000
1200
2014
2015
2016
2017
2018
Year

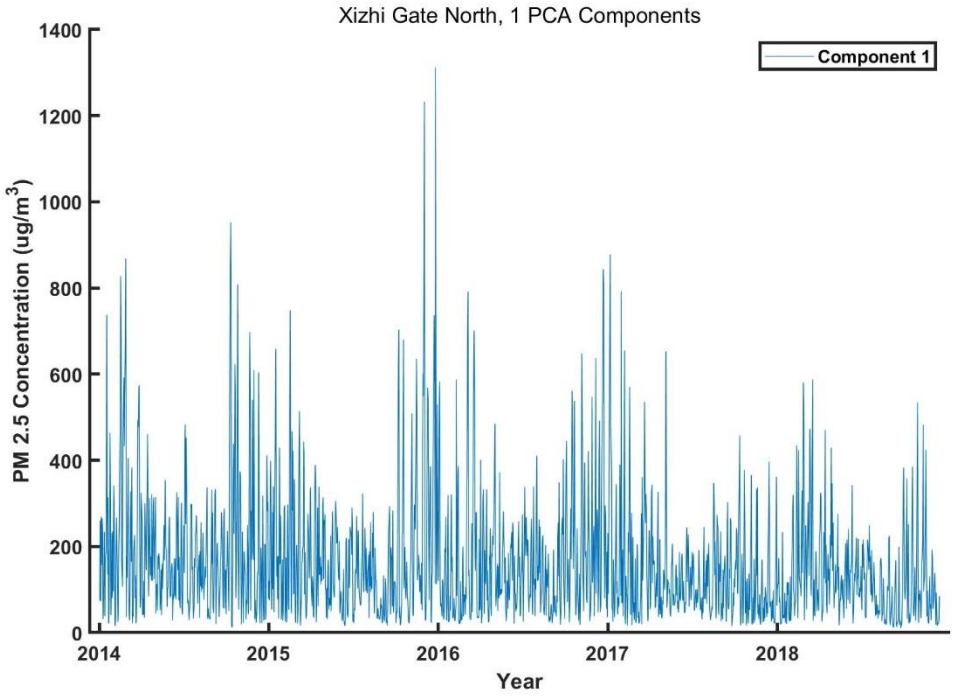
Xizhi Gate North, 1 PCA Components
Component 1
PM 2.5 Concentration (ug/m3)
1400
1200
1000
800
600
400
200
0
2014
2015
2016
2017
2018
Year

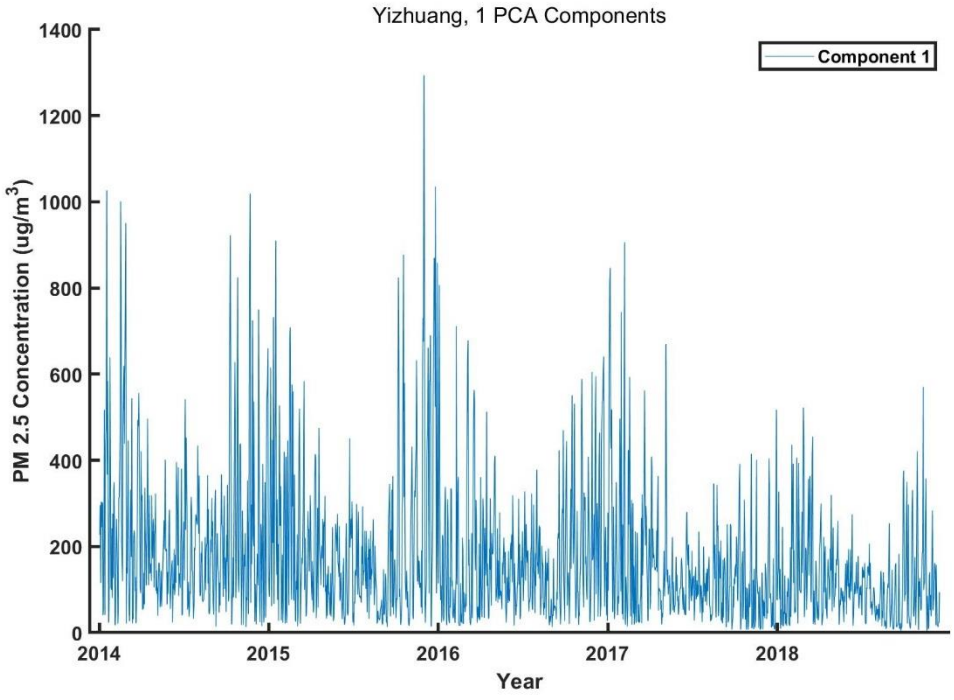
Yizhuang, 1 PCA Components
Component 1
PM 2.5 Concentration (ug/m3)
1400
1200
1000
800
600
400
200
0
2014
2015
2016
2017
2018
Year

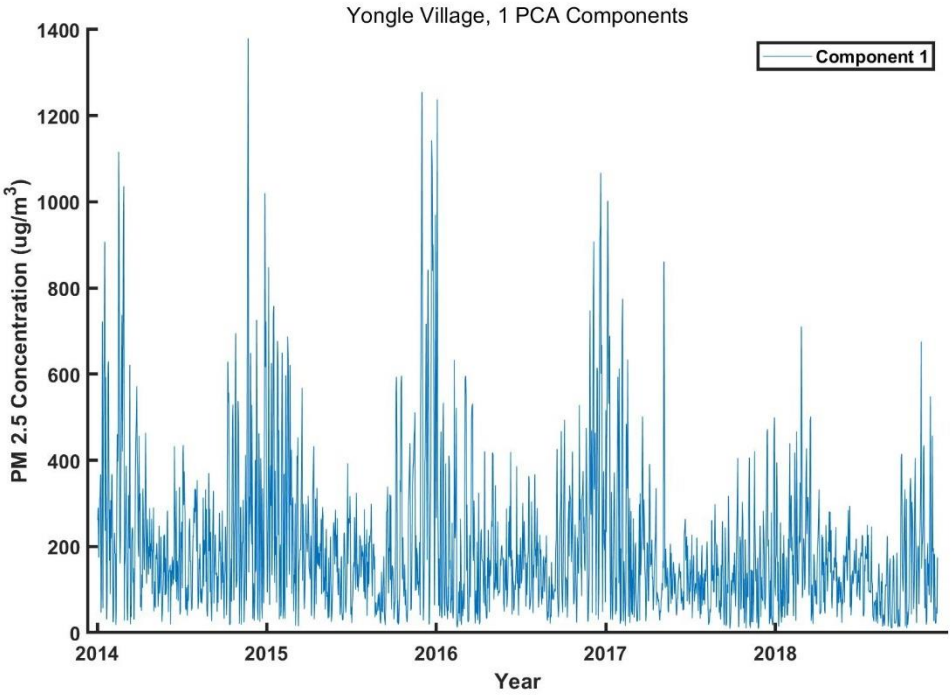
Yongle Village, 1 PCA Components
Component 1
PM 2.5 Concentration (ug/m3)
1400
1200
1000
800
600
400
200
0
2014
2015
2016
2017
2018
Year

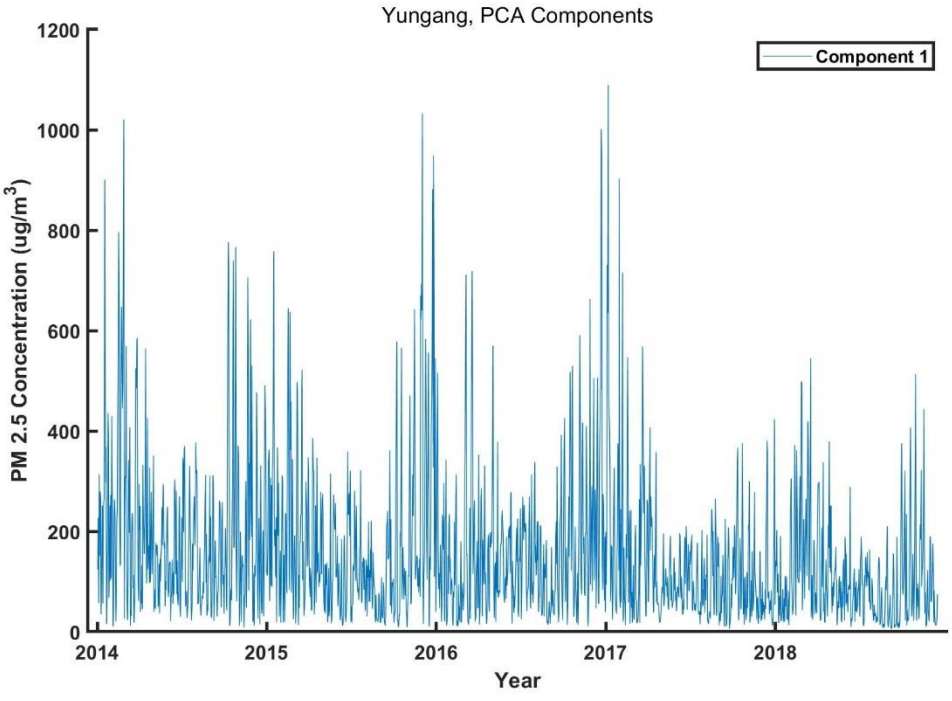
Yungang, PCA Components
Component 1
PM 2.5 Concentration (ug/m3)
1200
1000
800
600
400
200
0
2014
2015
2016
2017
2018
Year

Appendix G

Beijing $PM_{2.5}$ Air Pollution Maps

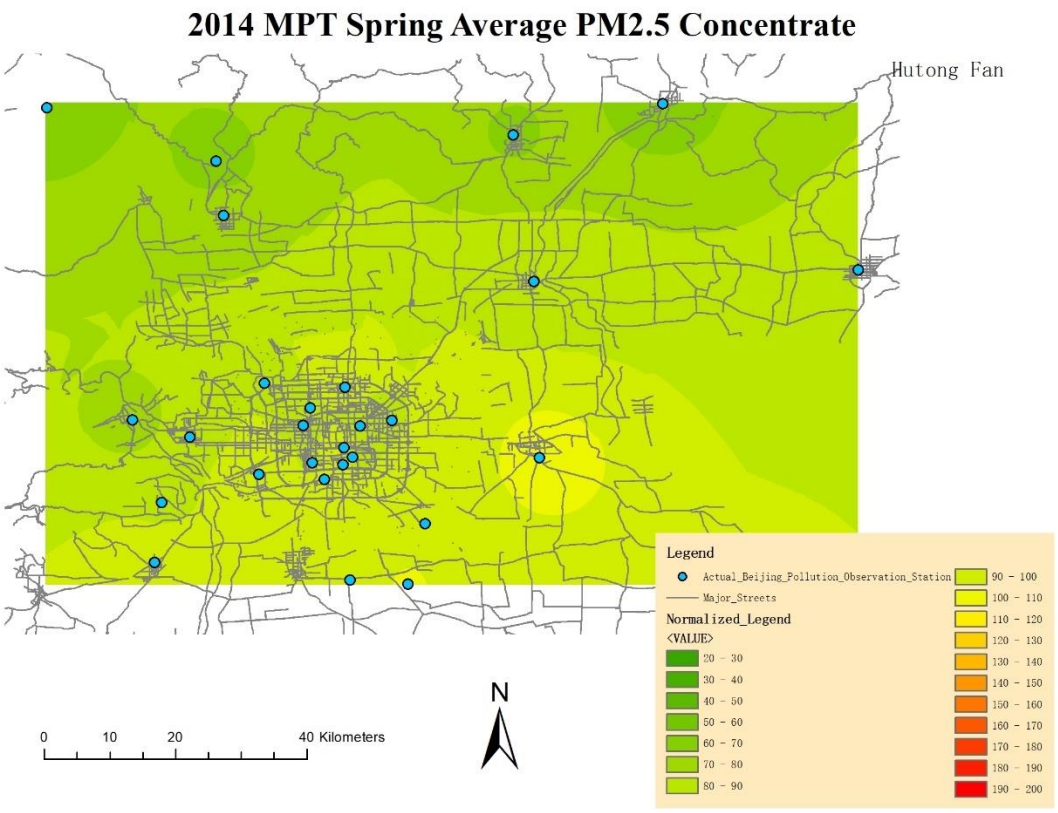

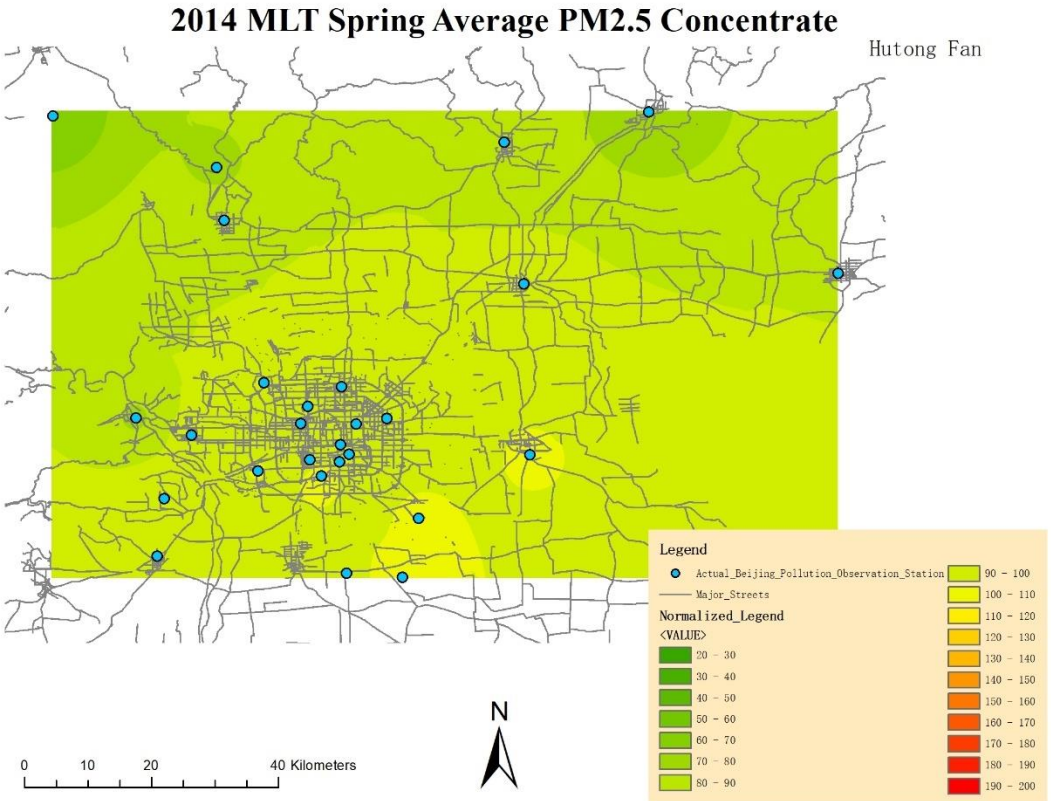
2014 MLT Spring Average PM2.5 Concentrate
Hutong Fan
Legend
Actual_Beijing_Pollution_Observation_Station
Major_Streets
Normalized_Legend
<VALUE>
20 - 30
30 - 40
40 - 50
50 - 60
60 - 70
70 - 80
80 - 90
90 - 100
100 - 110
110 - 120
120 - 130
130 - 140
140 - 150
150 - 160
160 - 170
170 - 180
180 - 190
190 - 200
N
0 10 20 40 Kilometers

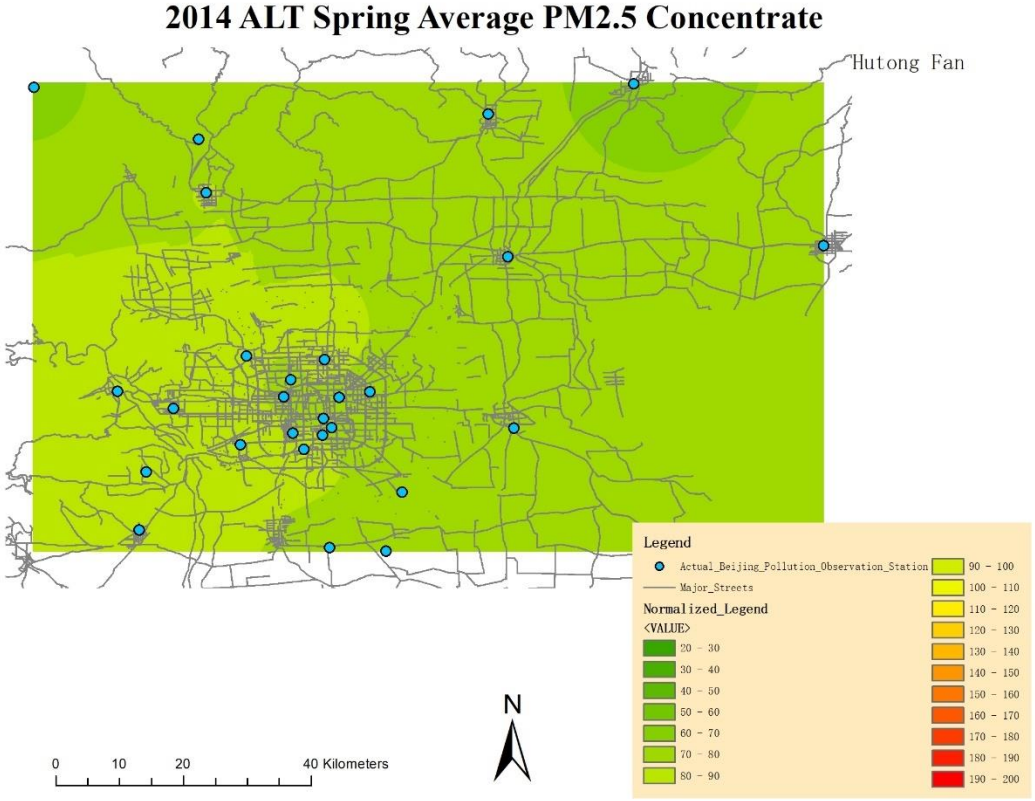
2014 ALT Spring Average PM2.5 Concentrate
Hutong Fan
Legend
Actual_Beijing_Pollution_Observation_Station
Major_Streets
Normalized_Legend
<VALUE>
20 - 30
30 - 40
40 - 50
50 - 60
60 - 70
70 - 80
80 - 90
90 - 100
100 - 110
110 - 120
120 - 130
130 - 140
140 - 150
150 - 160
160 - 170
170 - 180
180 - 190
190 - 200
N
0 10 20 40 Kilometers

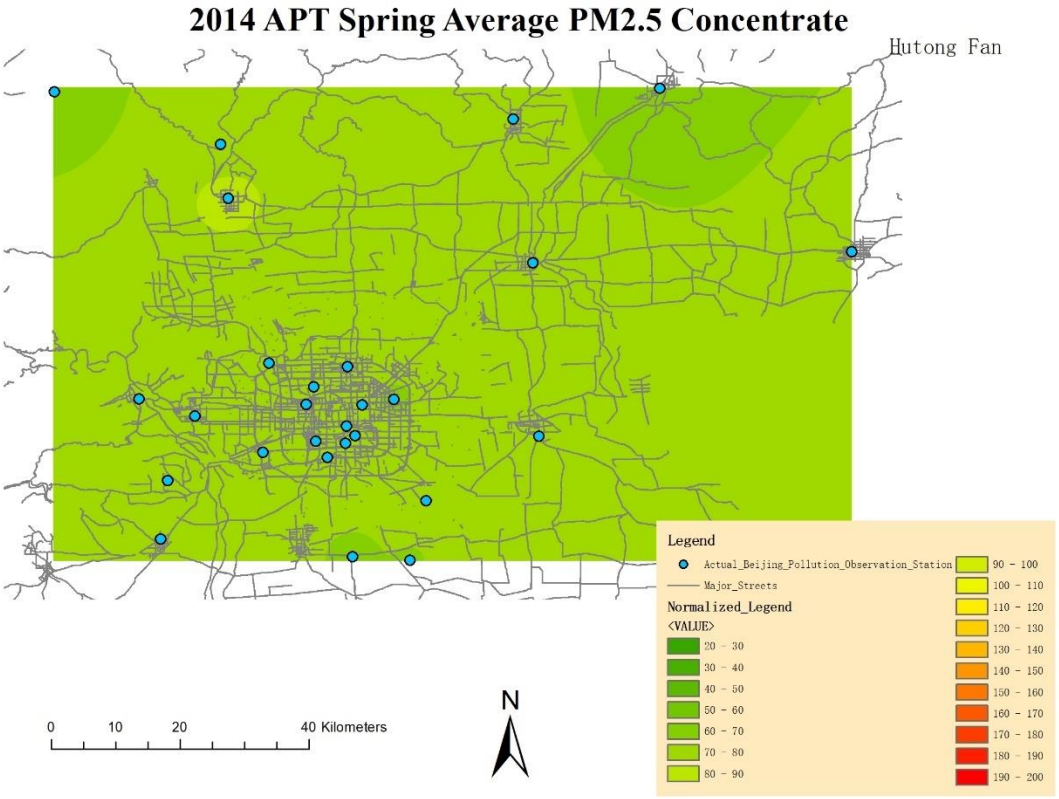
2014 APT Spring Average PM2.5 Concentrate
Hutong Fan
Legend
Actual_Beijing_Pollution_Observation_Station
Major_Streets
Normalized_Legend
<VALUE>
20 - 30
30 - 40
40 - 50
50 - 60
60 - 70
70 - 80
80 - 90
90 - 100
100 - 110
110 - 120
120 - 130
130 - 140
140 - 150
150 - 160
160 - 170
170 - 180
180 - 190
190 - 200
0 10 20 40 Kilometers
N

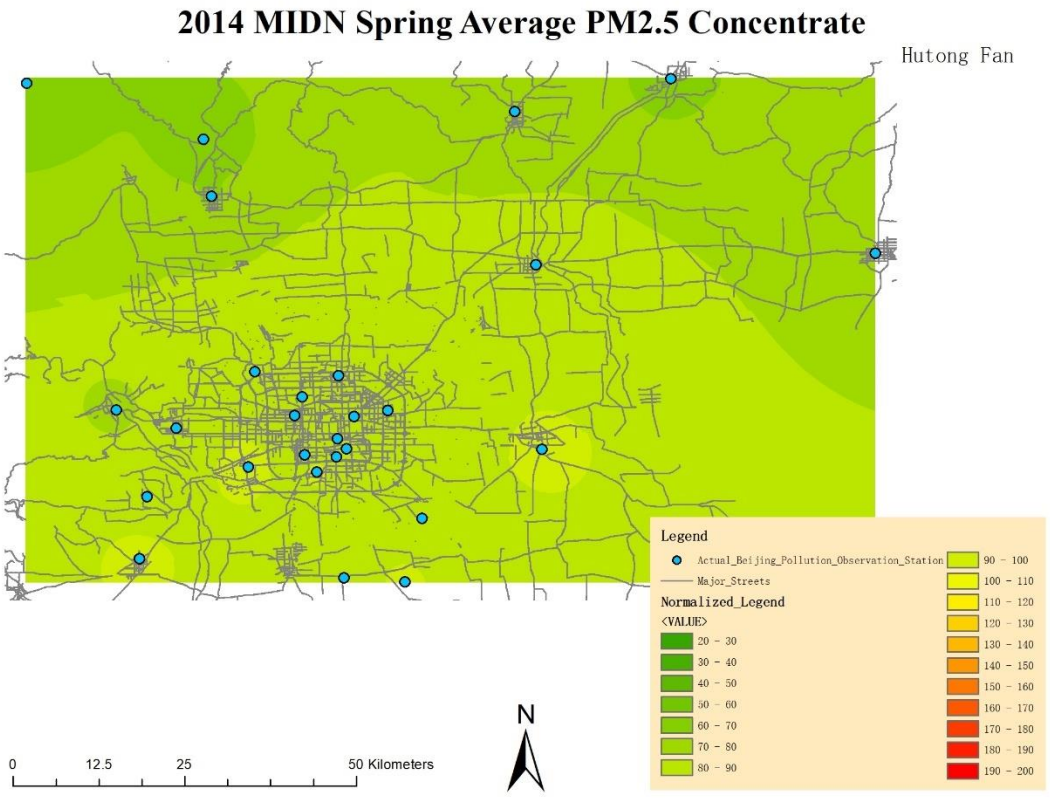
2014 MIDN Spring Average PM2.5 Concentrate
Hutong Fan
Legend
Actual_Beijing_Pollution_Observation_Station
Major_Streets
Normalized_Legend
<VALUE>
20 - 30
30 - 40
40 - 50
50 - 60
60 - 70
70 - 80
80 - 90
90 - 100
100 - 110
110 - 120
120 - 130
130 - 140
140 - 150
150 - 160
160 - 170
170 - 180
180 - 190
190 - 200
0 12.5 25 50 Kilometers
N

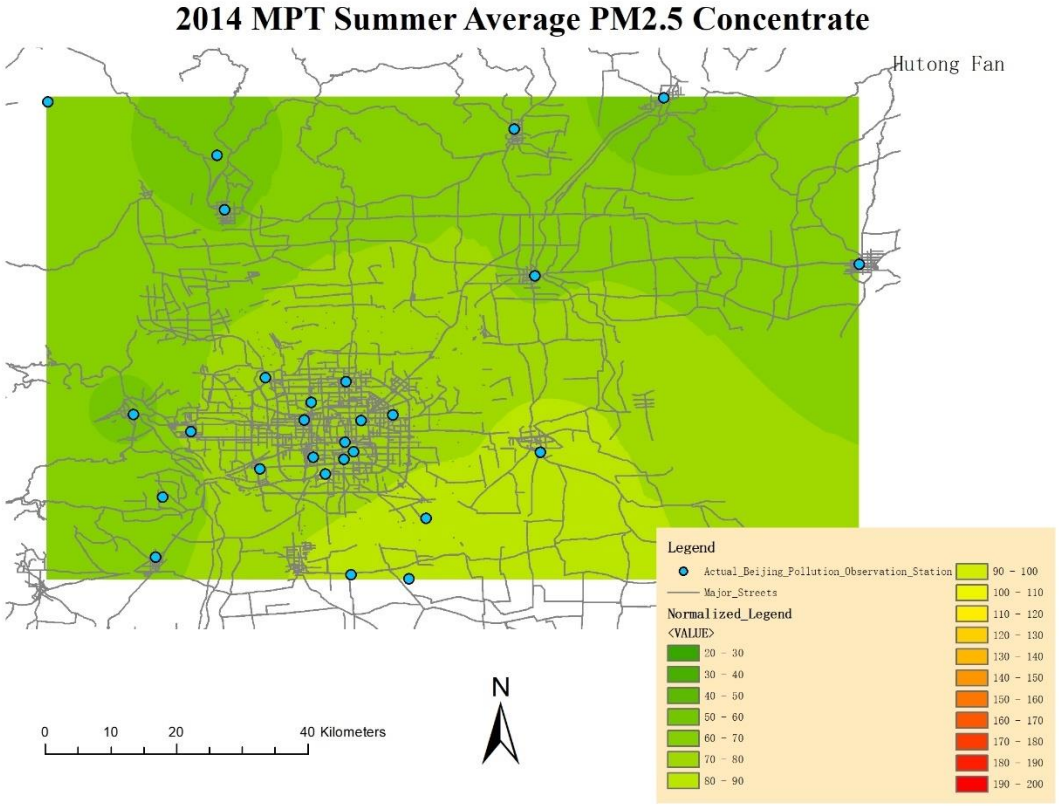
2014 MPT Summer Average PM2.5 Concentrate
Hutong Fan
Legend
Actual_Beijing_Pollution_Observation_Station
Major_Streets
Normalized_Legend
<VALUE>
20 - 30
30 - 40
40 - 50
50 - 60
60 - 70
70 - 80
80 - 90
90 - 100
100 - 110
110 - 120
120 - 130
130 - 140
140 - 150
150 - 160
160 - 170
170 - 180
180 - 190
190 - 200
N
0 10 20 40 Kilometers

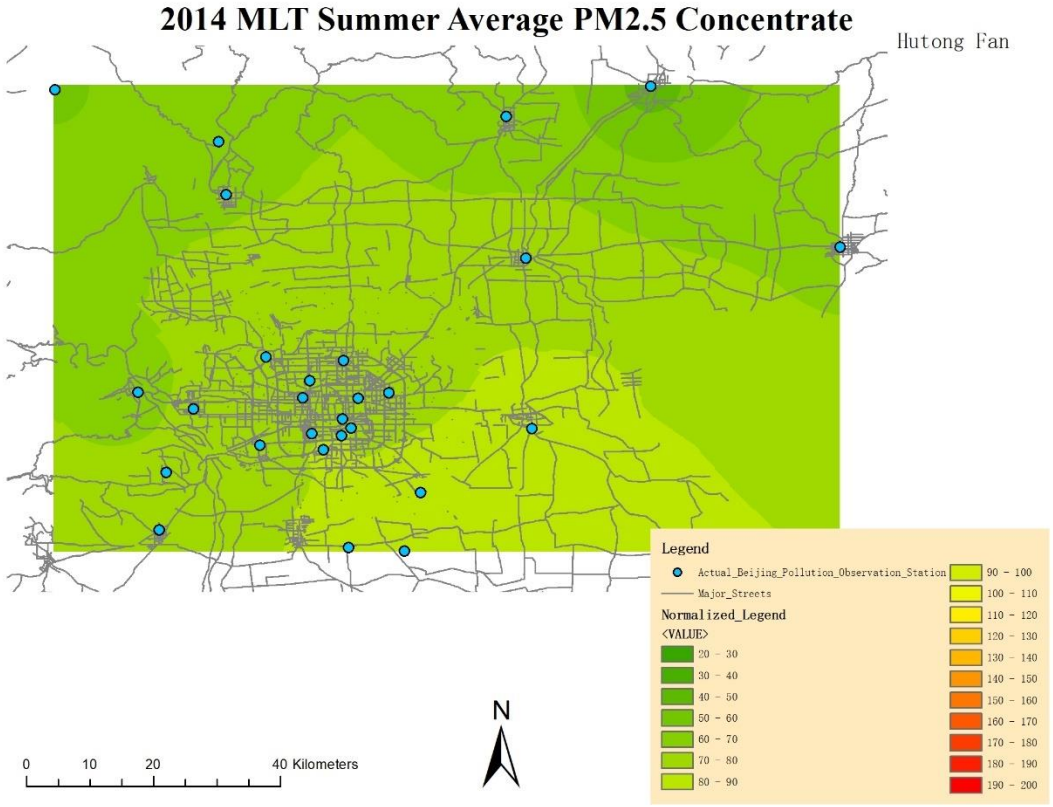
2014 MLT Summer Average PM2.5 Concentrate
Hutong Fan
Legend
Actual_Beijing_Pollution_Observation_Station
Major_Streets
Normalized_Legend
<VALUE>
20 - 30
30 - 40
40 - 50
50 - 60
60 - 70
70 - 80
80 - 90
90 - 100
100 - 110
110 - 120
120 - 130
130 - 140
140 - 150
150 - 160
160 - 170
170 - 180
180 - 190
190 - 200
N
0 10 20 40 Kilometers

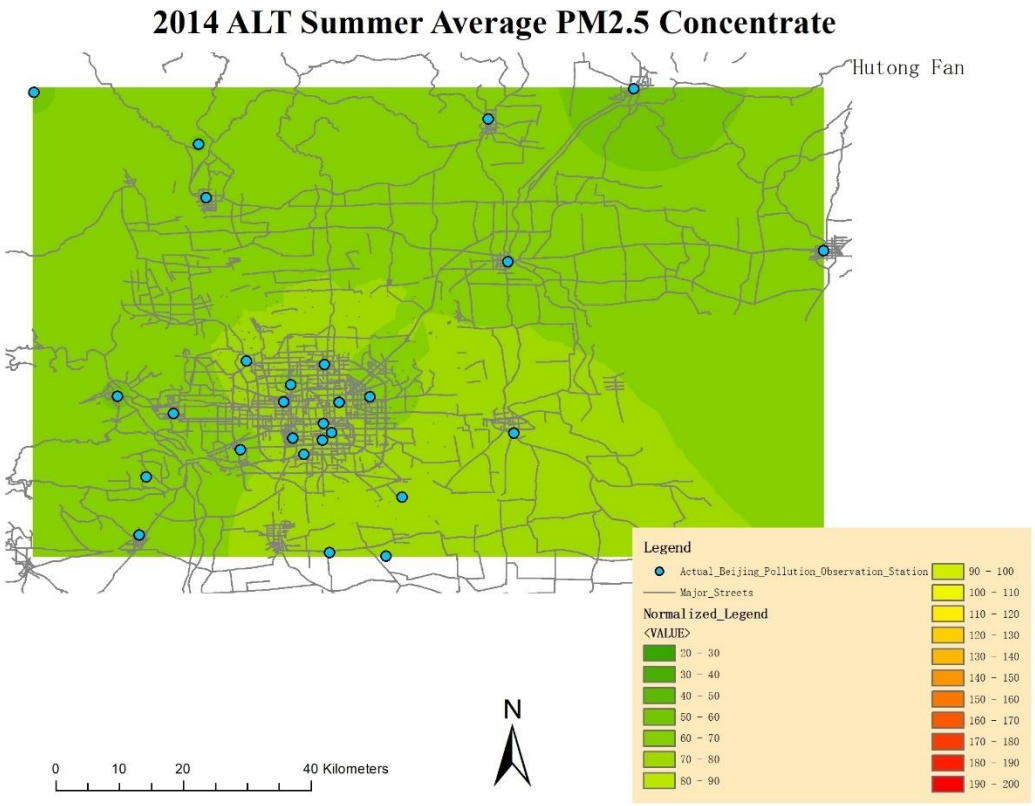
2014 ALT Summer Average PM2.5 Concentrate
Hutong Fan
Legend
Actual_Beijing_Pollution_Observation_Station
Major_Streets
Normalized_Legend
<VALUE>
20 - 30
30 - 40
40 - 50
50 - 60
60 - 70
70 - 80
80 - 90
90 - 100
100 - 110
110 - 120
120 - 130
130 - 140
140 - 150
150 - 160
160 - 170
170 - 180
180 - 190
190 - 200
N
0
10
20
40 Kilometers

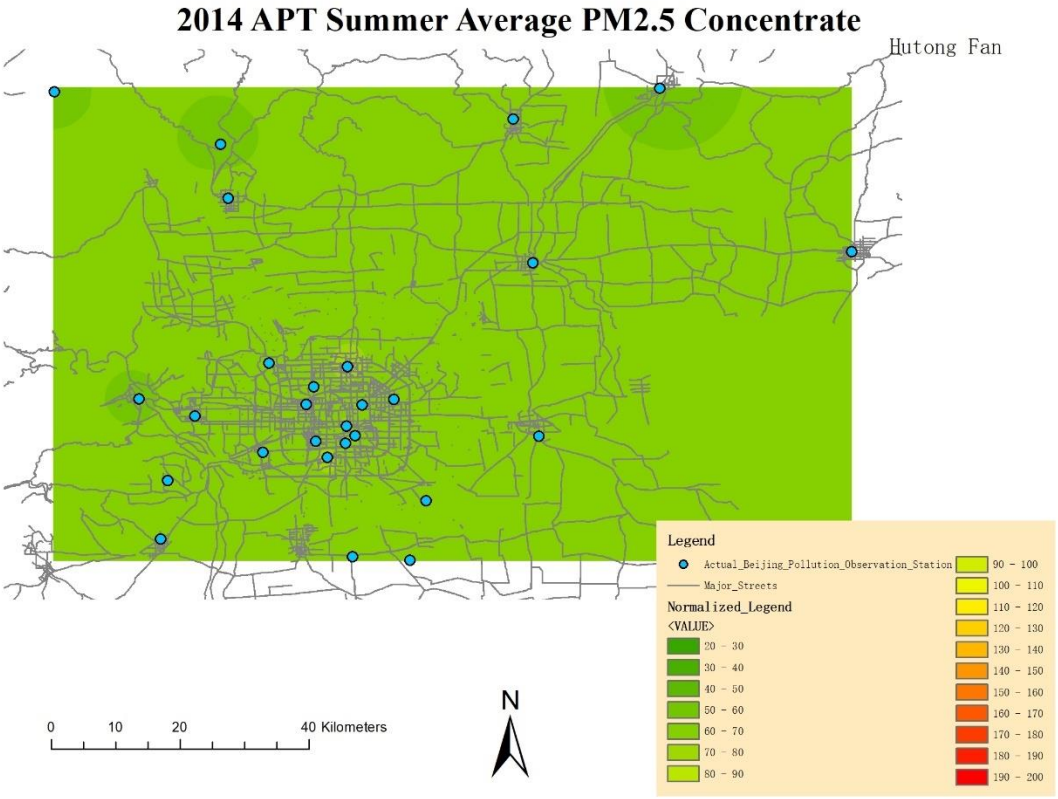
2014 APT Summer Average PM2.5 Concentrate
Hutong Fan
Legend
Actual_Beijing_Pollution_Observation_Station
Major_Streets
Normalized_Legend
<VALUE>
20 - 30
30 - 40
40 - 50
50 - 60
60 - 70
70 - 80
80 - 90
90 - 100
100 - 110
110 - 120
120 - 130
130 - 140
140 - 150
150 - 160
160 - 170
170 - 180
180 - 190
190 - 200
0
10
20
40 Kilometers
N

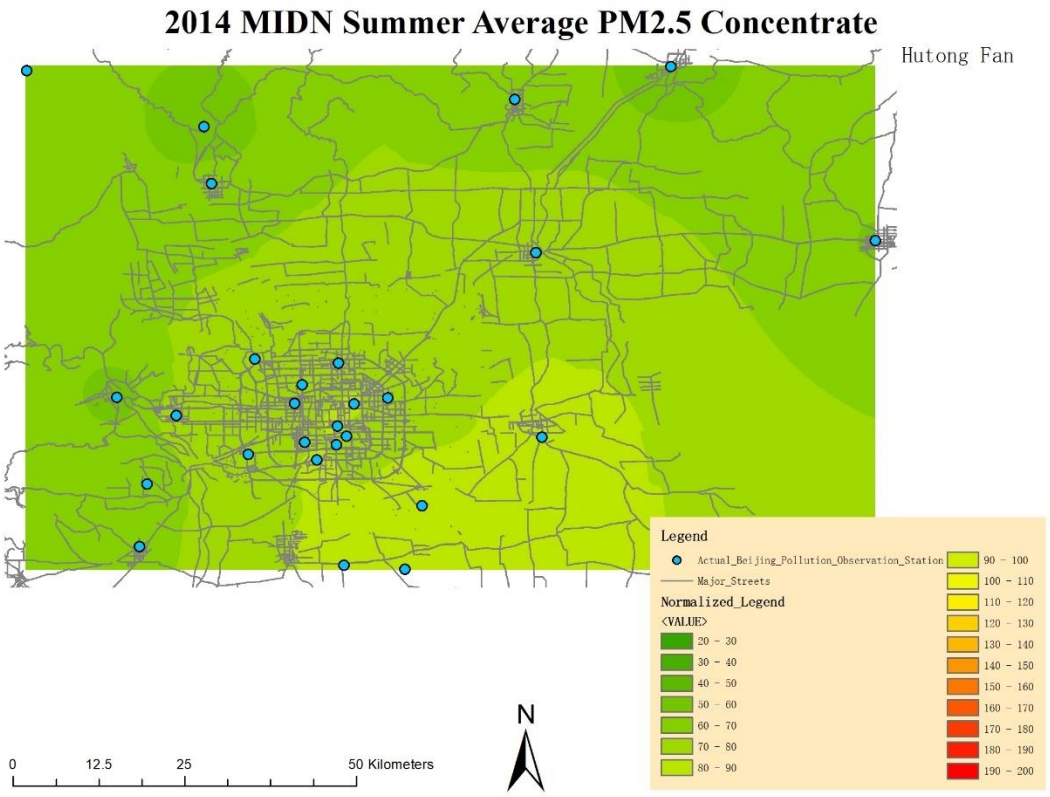
2014 MIDN Summer Average PM2.5 Concentrate
Hutong Fan
Legend
Actual_Beijing_Pollution_Observation_Station
Major_Streets
Normalized_Legend
<VALUE>
20 - 30
30 - 40
40 - 50
50 - 60
60 - 70
70 - 80
80 - 90
90 - 100
100 - 110
110 - 120
120 - 130
130 - 140
140 - 150
150 - 160
160 - 170
170 - 180
180 - 190
190 - 200
N
0
12.5
25
50 Kilometers

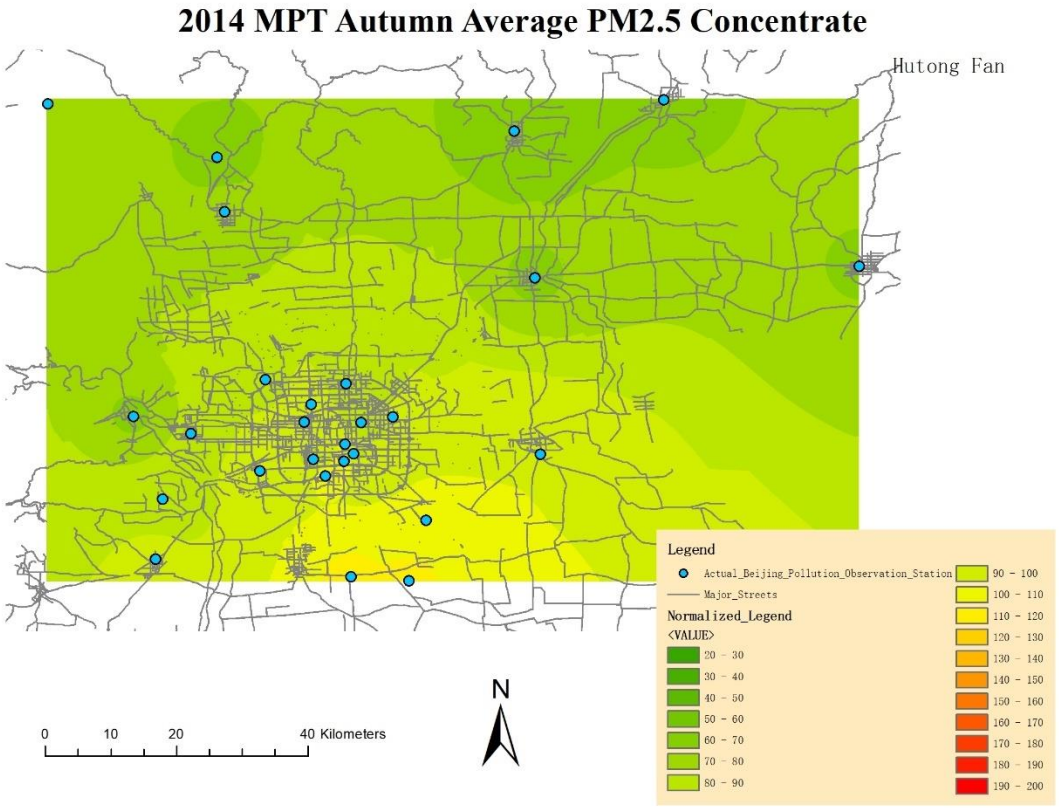
2014 MPT Autumn Average PM2.5 Concentrate
Hutong Fan
Legend
Actual_Beijing_Pollution_Observation_Station
Major_Streets
Normalized_Legend
<VALUE>
20 - 30
30 - 40
40 - 50
50 - 60
60 - 70
70 - 80
80 - 90
90 - 100
100 - 110
110 - 120
120 - 130
130 - 140
140 - 150
150 - 160
160 - 170
170 - 180
180 - 190
190 - 200
N
0
10
20
40 Kilometers

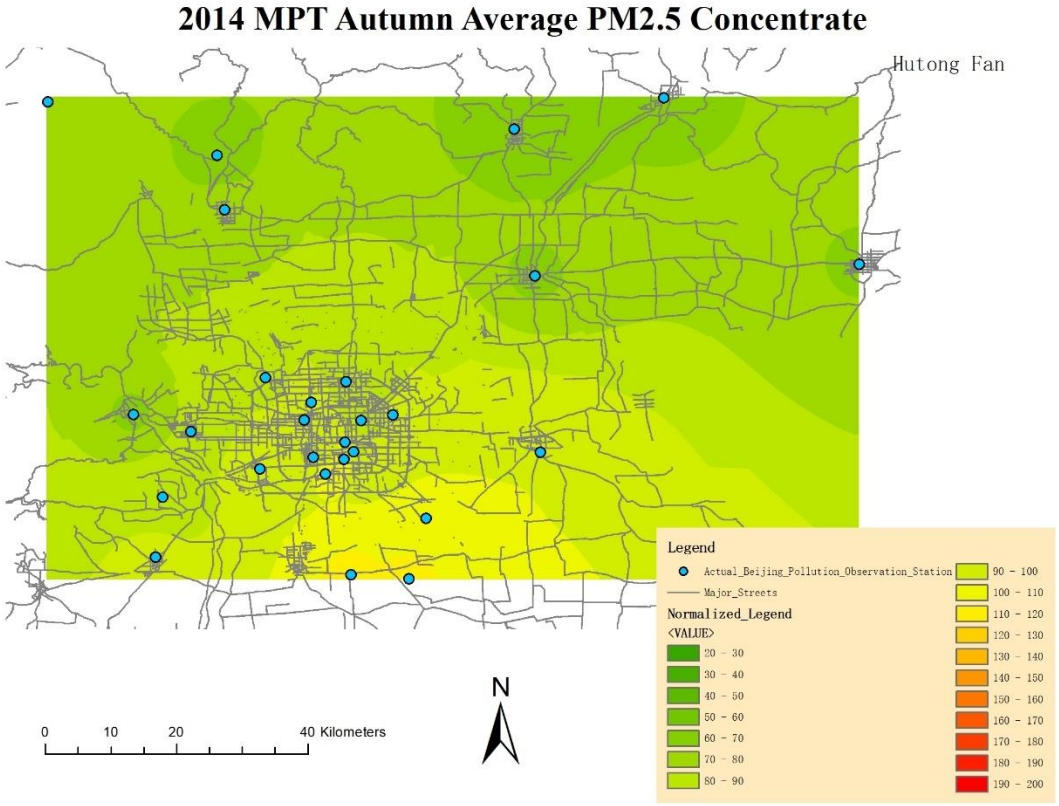
2014 MPT Autumn Average PM2.5 Concentrate
Hutong Fan
Legend
Actual_Beijing_Pollution_Observation_Station
Major_Streets
Normalized_Legend
<VALUE>
20 - 30
30 - 40
40 - 50
50 - 60
60 - 70
70 - 80
80 - 90
90 - 100
100 - 110
110 - 120
120 - 130
130 - 140
140 - 150
150 - 160
160 - 170
170 - 180
180 - 190
190 - 200
N
0
10
20
40 Kilometers

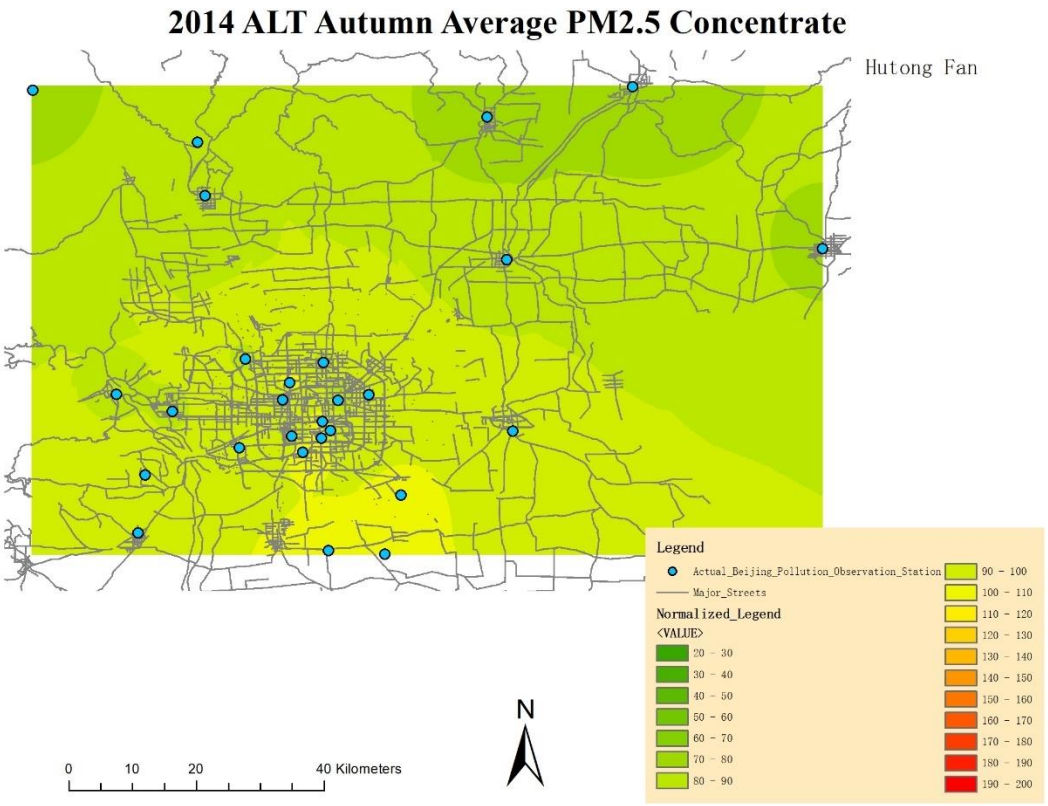
2014 ALT Autumn Average PM2.5 Concentrate
Hutong Fan
Legend
Actual_Beijing_Pollution_Observation_Station
Major_Streets
Normalized_Legend
<VALUE>
20 - 30
30 - 40
40 - 50
50 - 60
60 - 70
70 - 80
80 - 90
90 - 100
100 - 110
110 - 120
120 - 130
130 - 140
140 - 150
150 - 160
160 - 170
170 - 180
180 - 190
190 - 200
N
0
10
20
40 Kilometers

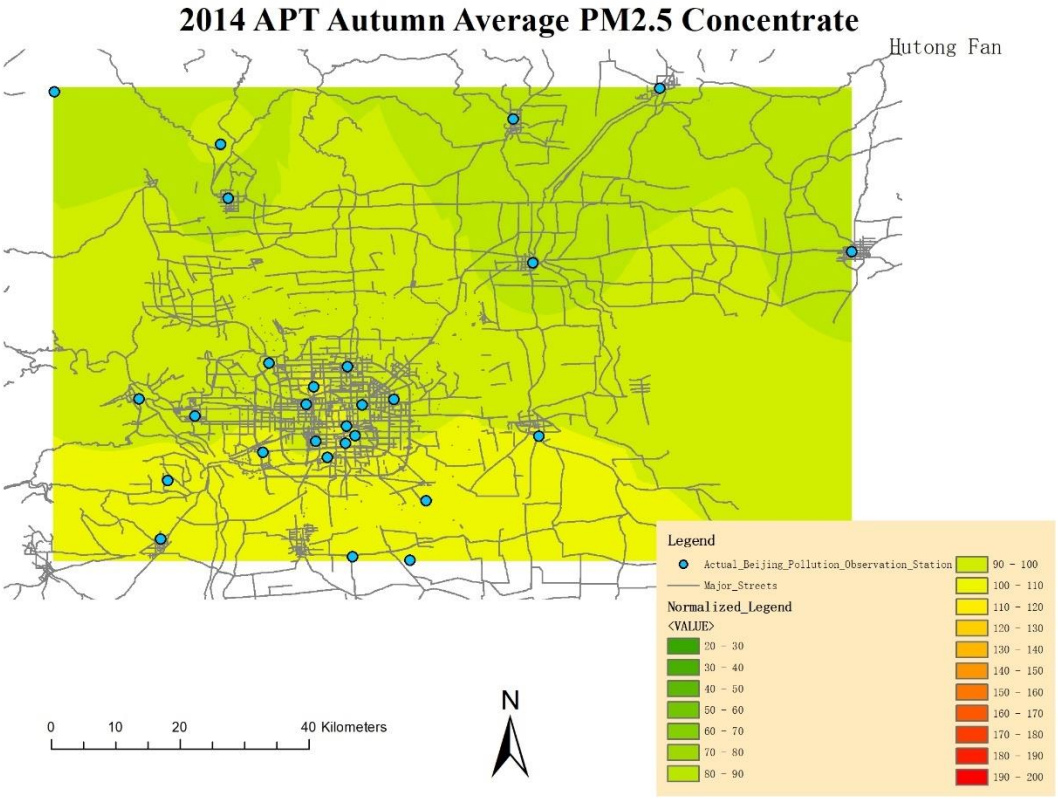
2014 APT Autumn Average PM2.5 Concentrate
Hutong Fan
Legend
Actual_Beijing_Pollution_Observation_Station
Major_Streets
Normalized_Legend
<VALUE>
20 - 30
30 - 40
40 - 50
50 - 60
60 - 70
70 - 80
80 - 90
90 - 100
100 - 110
110 - 120
120 - 130
130 - 140
140 - 150
150 - 160
160 - 170
170 - 180
180 - 190
190 - 200
0
10
20
40 Kilometers
N

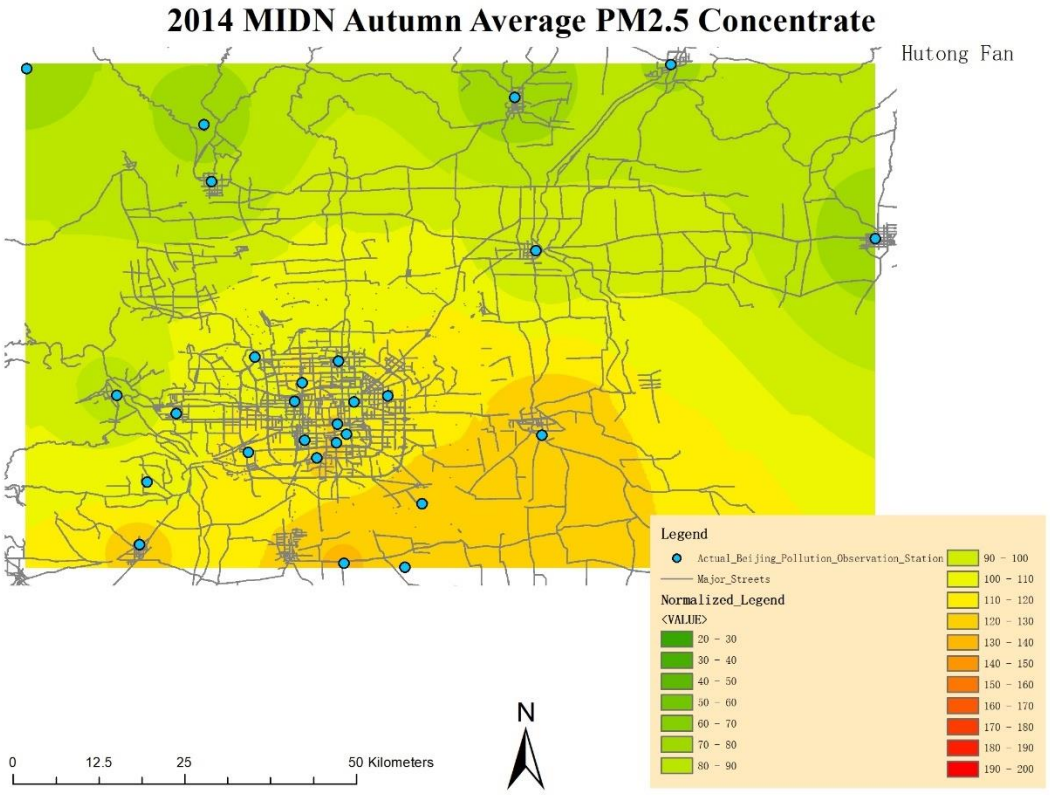
2014 MIDN Autumn Average PM2.5 Concentrate
Hutong Fan
Legend
Actual_Beijing_Pollution_Observation_Station
Major_Streets
Normalized_Legend
<VALUE>
20 - 30
30 - 40
40 - 50
50 - 60
60 - 70
70 - 80
80 - 90
90 - 100
100 - 110
110 - 120
120 - 130
130 - 140
140 - 150
150 - 160
160 - 170
170 - 180
180 - 190
190 - 200
N
0
12.5
25
50 Kilometers

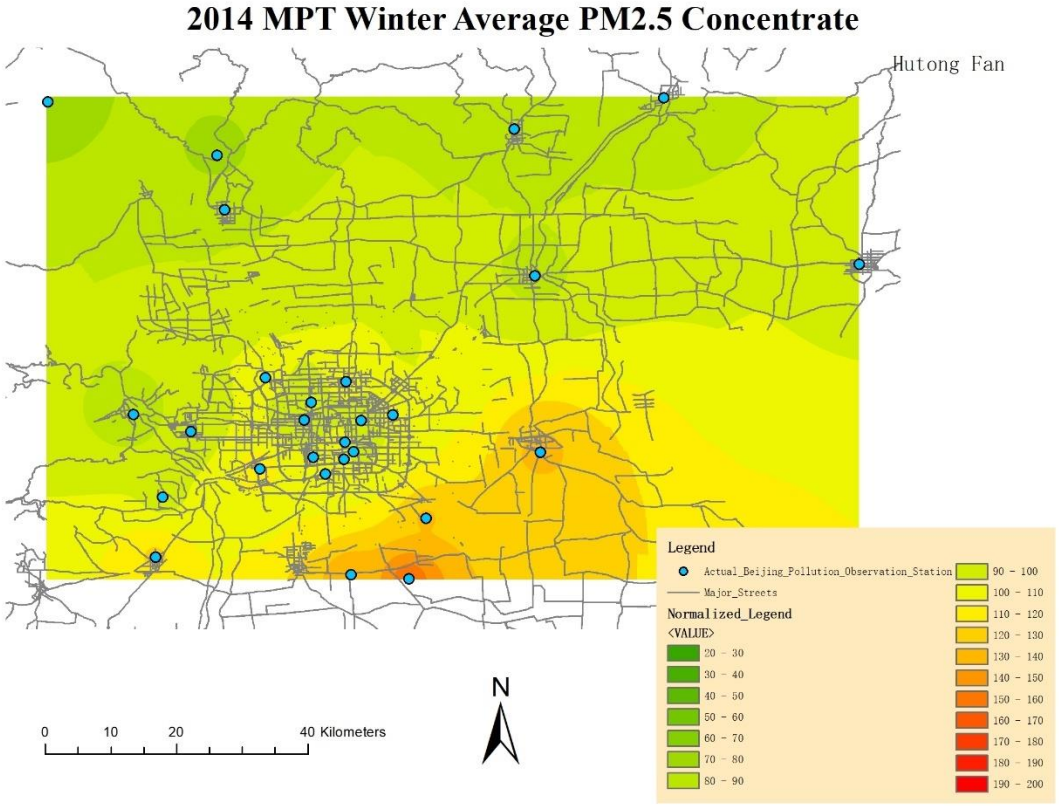
2014 MPT Winter Average PM2.5 Concentrate
Hutong Fan
Legend
Actual_Beijing_Pollution_Observation_Station
Major_Streets
Normalized_Legend
<VALUE>
20 - 30
30 - 40
40 - 50
50 - 60
60 - 70
70 - 80
80 - 90
90 - 100
100 - 110
110 - 120
120 - 130
130 - 140
140 - 150
150 - 160
160 - 170
170 - 180
180 - 190
190 - 200
N
0
10
20
40 Kilometers

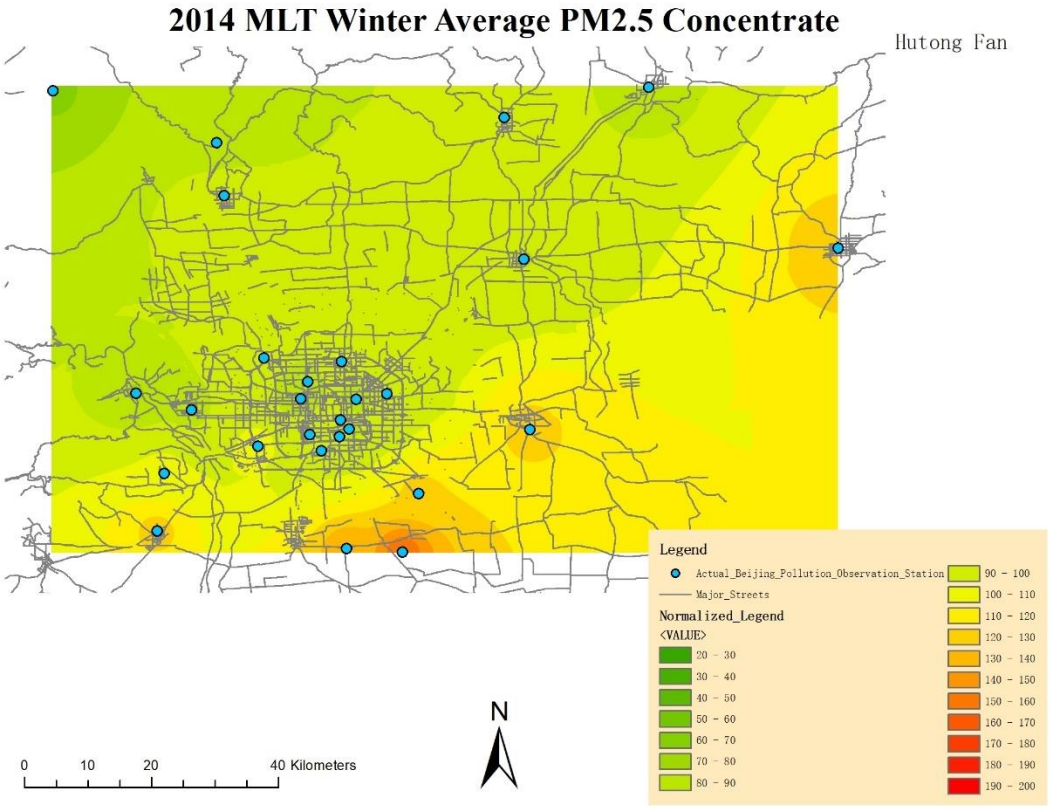
2014 MLT Winter Average PM2.5 Concentrate
Hutong Fan
Legend
Actual_Beijing_Pollution_Observation_Station
Major_Streets
Normalized_Legend
<VALUE>
20 - 30
30 - 40
40 - 50
50 - 60
60 - 70
70 - 80
80 - 90
90 - 100
100 - 110
110 - 120
120 - 130
130 - 140
140 - 150
150 - 160
160 - 170
170 - 180
180 - 190
190 - 200
N
0
10
20
40 Kilometers

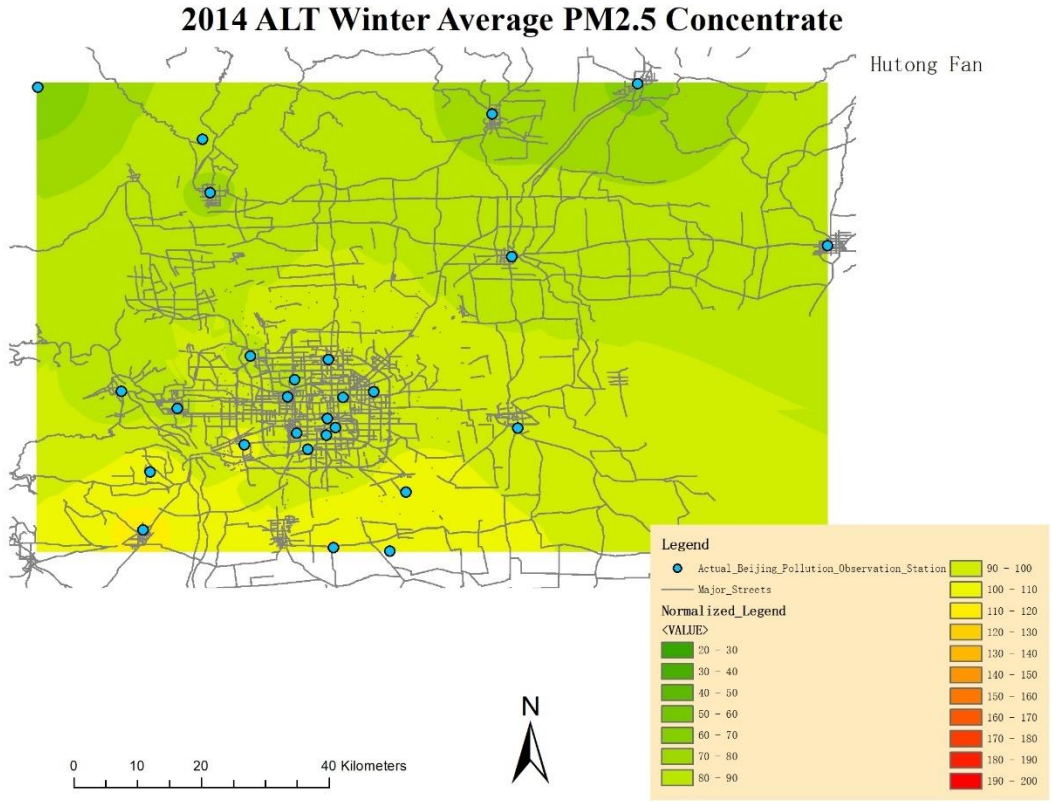
2014 ALT Winter Average PM2.5 Concentrate
Hutong Fan
Legend
Actual_Beijing_Pollution_Observation_Station
Major_Streets
Normalized_Legend
<VALUE>
20 - 30
30 - 40
40 - 50
50 - 60
60 - 70
70 - 80
80 - 90
90 - 100
100 - 110
110 - 120
120 - 130
130 - 140
140 - 150
150 - 160
160 - 170
170 - 180
180 - 190
190 - 200
N
0 10 20 40 Kilometers

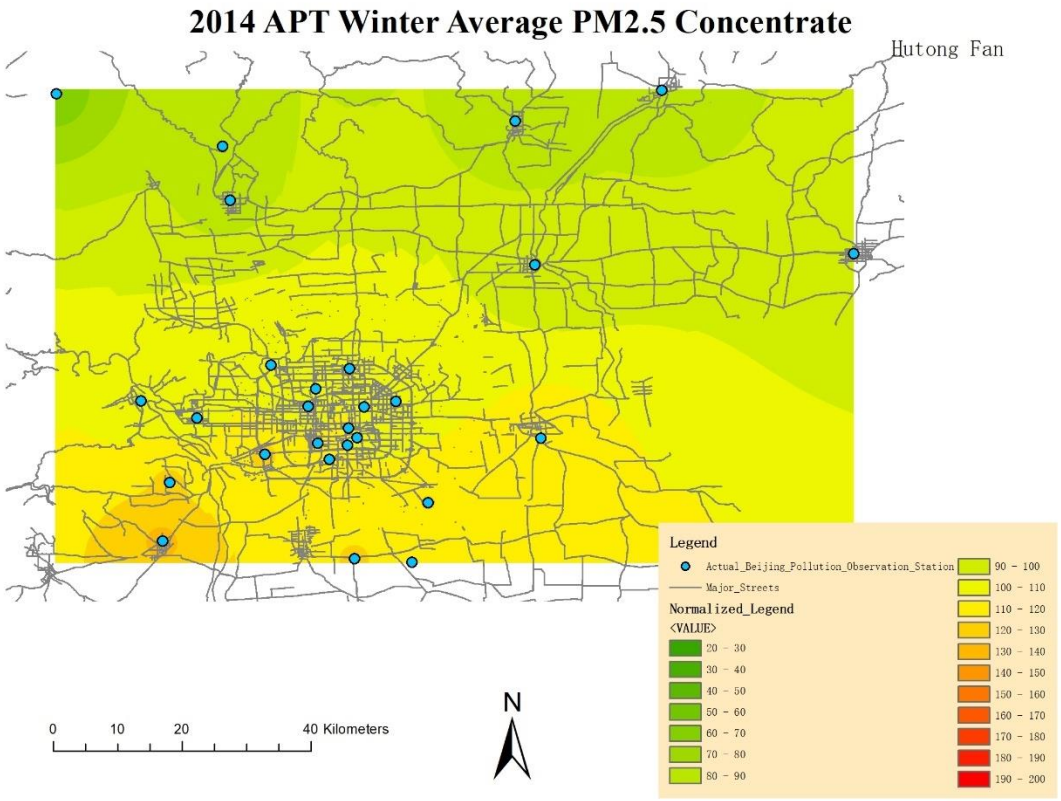
2014 APT Winter Average PM2.5 Concentrate
Hutong Fan
Legend
Actual_Beijing_Pollution_Observation_Station
Major_Streets
Normalized_Legend
<VALUE>
20 - 30
30 - 40
40 - 50
50 - 60
60 - 70
70 - 80
80 - 90
90 - 100
100 - 110
110 - 120
120 - 130
130 - 140
140 - 150
150 - 160
160 - 170
170 - 180
180 - 190
190 - 200
N
0 10 20 40 Kilometers

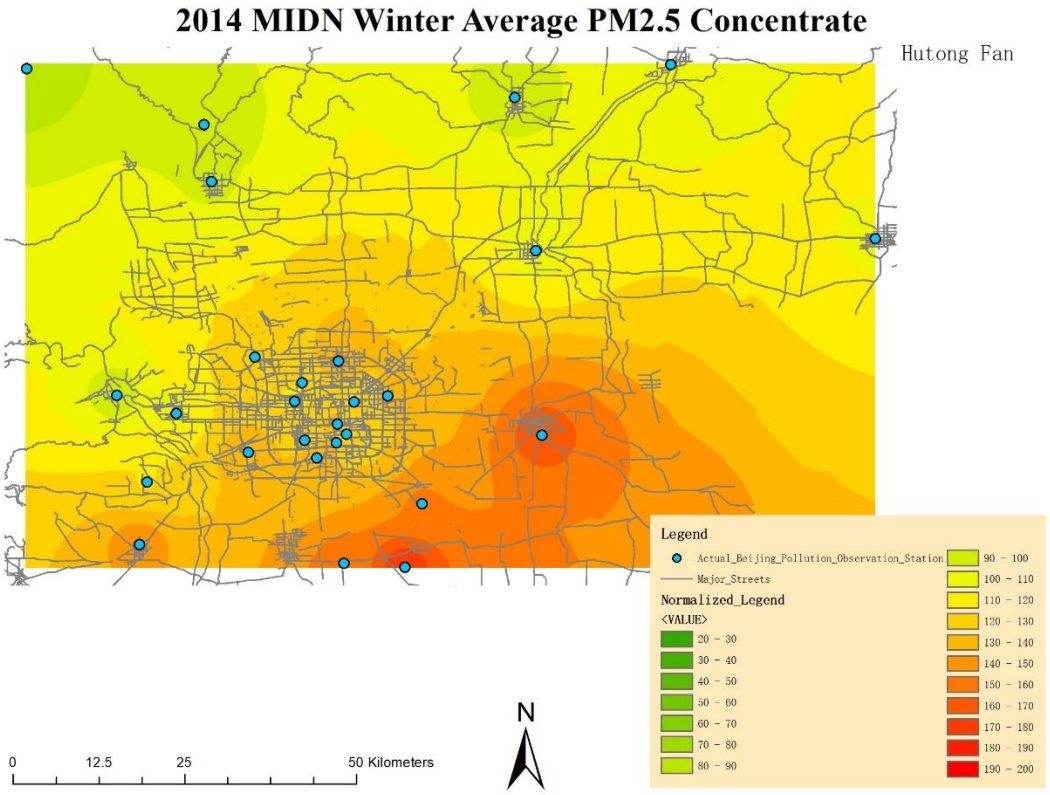
2014 MIDN Winter Average PM2.5 Concentrate
Hutong Fan
Legend
Actual_Beijing_Pollution_Observation_Station
Major_Streets
Normalized_Legend
<VALUE>
20 - 30
30 - 40
40 - 50
50 - 60
60 - 70
70 - 80
80 - 90
90 - 100
100 - 110
110 - 120
120 - 130
130 - 140
140 - 150
150 - 160
160 - 170
170 - 180
180 - 190
190 - 200
N
0
12.5
25
50 Kilometers

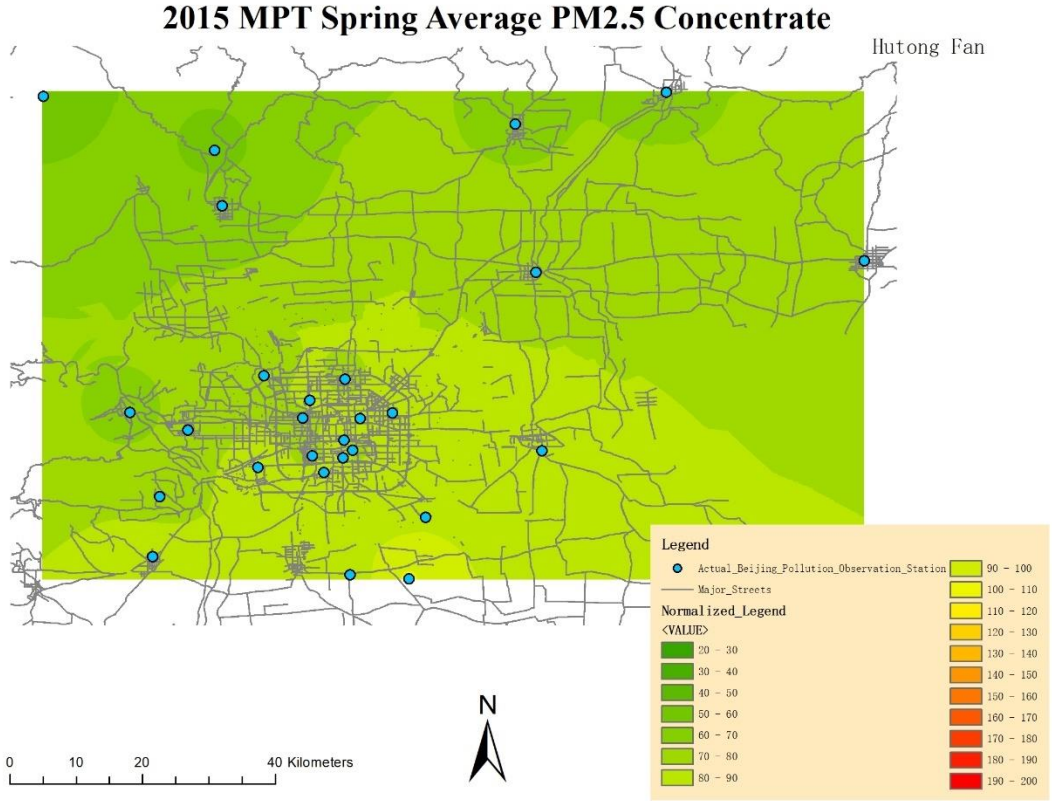
2015 MPT Spring Average PM2.5 Concentrate
Hutong Fan
Legend
Actual_Beijing_Pollution_Observation_Station
Major_Streets
Normalized_Legend
<VALUE>
20 - 30
30 - 40
40 - 50
50 - 60
60 - 70
70 - 80
80 - 90
90 - 100
100 - 110
110 - 120
120 - 130
130 - 140
140 - 150
150 - 160
160 - 170
170 - 180
180 - 190
190 - 200
N
0
10
20
40 Kilometers

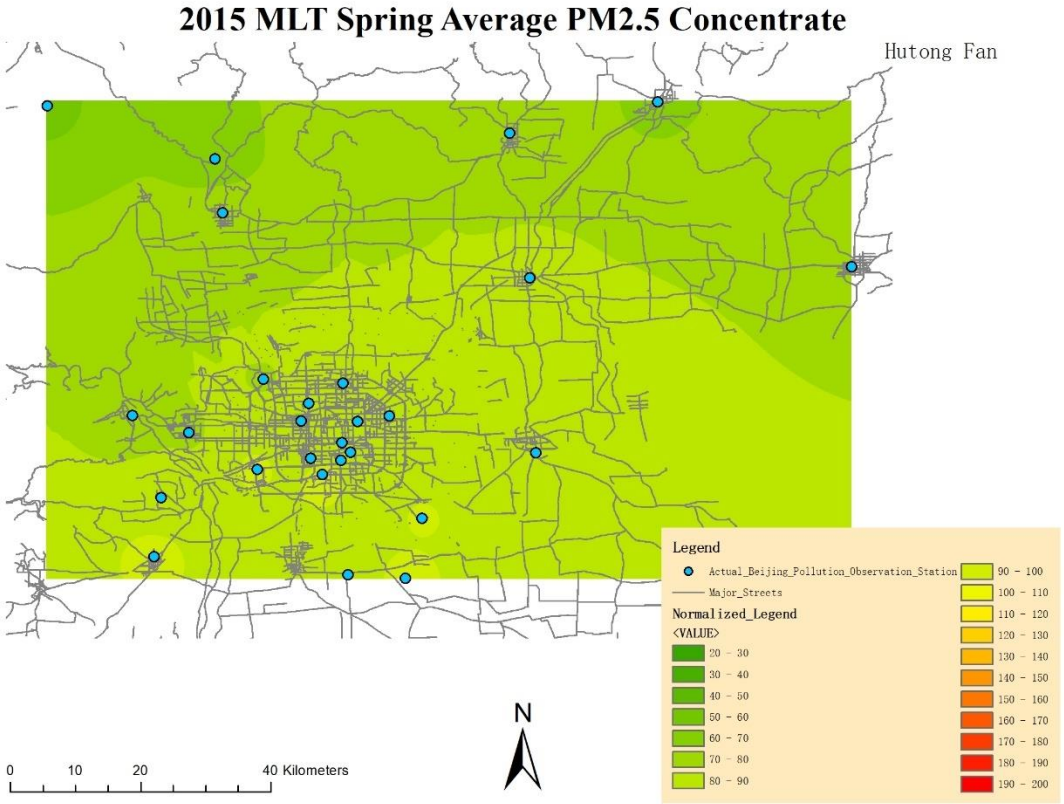
2015 MLT Spring Average PM2.5 Concentrate
Hutong Fan
Legend
Actual_Beijing_Pollution_Observation_Station
Major_Streets
Normalized_Legend
<VALUE>
20 - 30
30 - 40
40 - 50
50 - 60
60 - 70
70 - 80
80 - 90
90 - 100
100 - 110
110 - 120
120 - 130
130 - 140
140 - 150
150 - 160
160 - 170
170 - 180
180 - 190
190 - 200
N
0
10
20
40 Kilometers

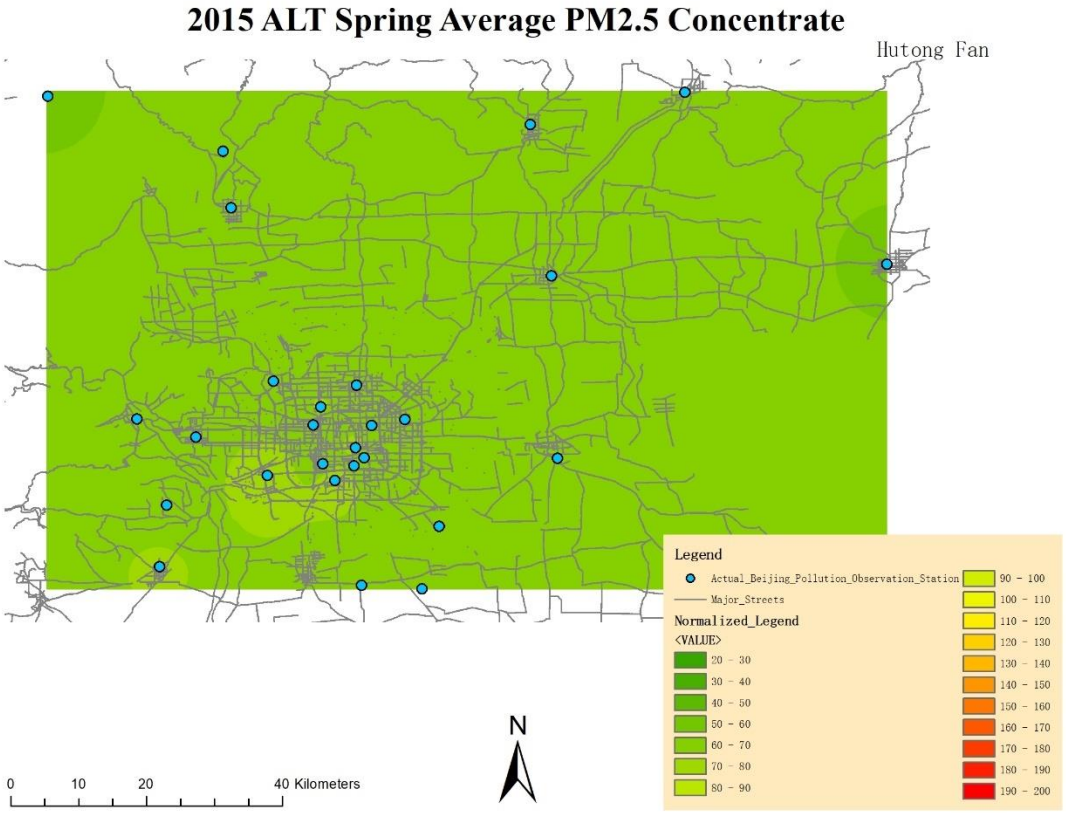
2015 ALT Spring Average PM2.5 Concentrate
Hutong Fan
Legend
Actual_Beijing_Pollution_Observation_Station
Major_Streets
Normalized_Legend
<VALUE>
20 - 30
30 - 40
40 - 50
50 - 60
60 - 70
70 - 80
80 - 90
90 - 100
100 - 110
110 - 120
120 - 130
130 - 140
140 - 150
150 - 160
160 - 170
170 - 180
180 - 190
190 - 200
N
0
10
20
40 Kilometers

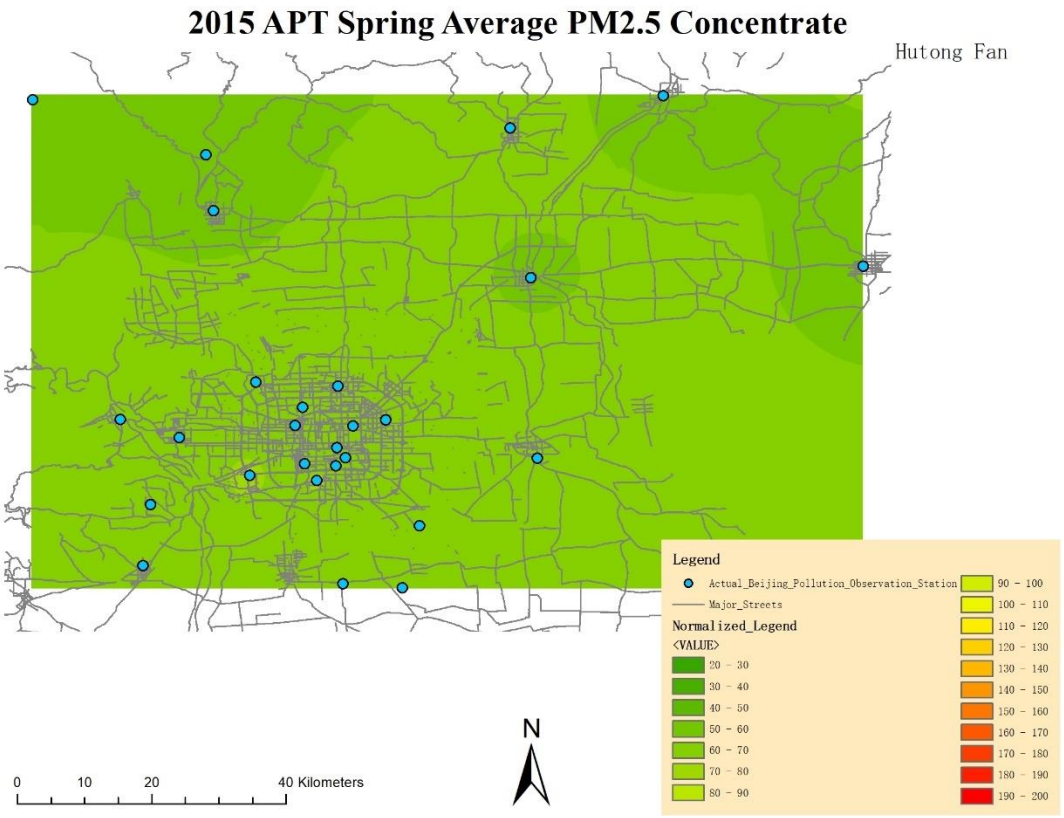
2015 APT Spring Average PM2.5 Concentrate
Hutong Fan
Legend
Actual_Beijing_Pollution_Observation_Station
Major_Streets
Normalized_Legend
<VALUE>
20 - 30
30 - 40
40 - 50
50 - 60
60 - 70
70 - 80
80 - 90
90 - 100
100 - 110
110 - 120
120 - 130
130 - 140
140 - 150
150 - 160
160 - 170
170 - 180
180 - 190
190 - 200
N
0 10 20 40 Kilometers

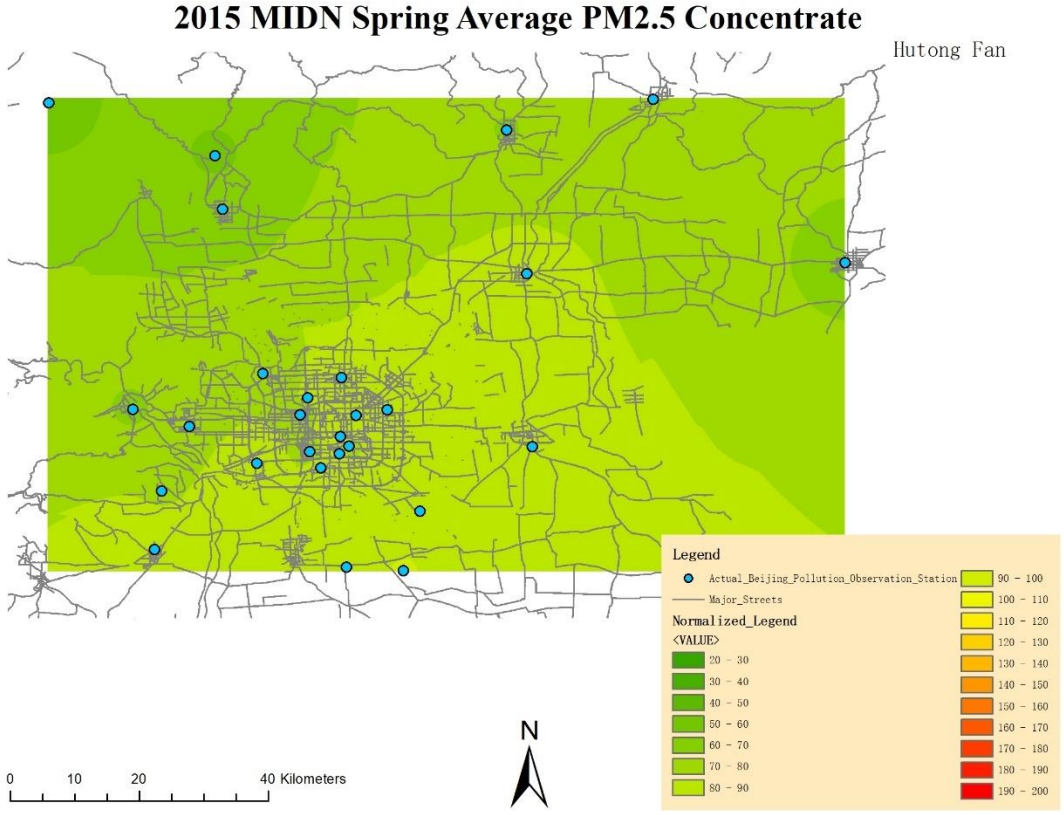
2015 MIDN Spring Average PM2.5 Concentrate
Hutong Fan
Legend
Actual_Beijing_Pollution_Observation_Station
Major_Streets
Normalized_Legend
<VALUE>
20 - 30
30 - 40
40 - 50
50 - 60
60 - 70
70 - 80
80 - 90
90 - 100
100 - 110
110 - 120
120 - 130
130 - 140
140 - 150
150 - 160
160 - 170
170 - 180
180 - 190
190 - 200
N
0 10 20 40 Kilometers

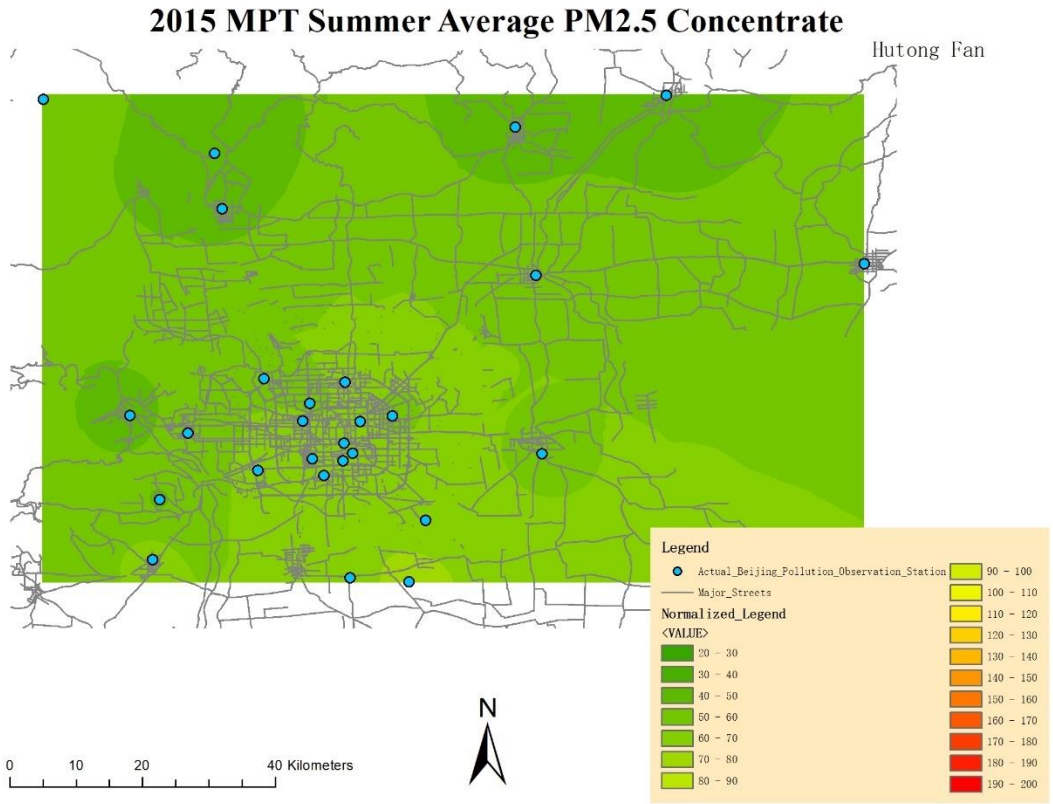
2015 MPT Summer Average PM2.5 Concentrate
Hutong Fan
Legend
Actual_Beijing_Pollution_Observation_Station
Major_Streets
Normalized_Legend
<VALUE>
20 - 30
30 - 40
40 - 50
50 - 60
60 - 70
70 - 80
80 - 90
90 - 100
100 - 110
110 - 120
120 - 130
130 - 140
140 - 150
150 - 160
160 - 170
170 - 180
180 - 190
190 - 200
N
0
10
20
40 Kilometers

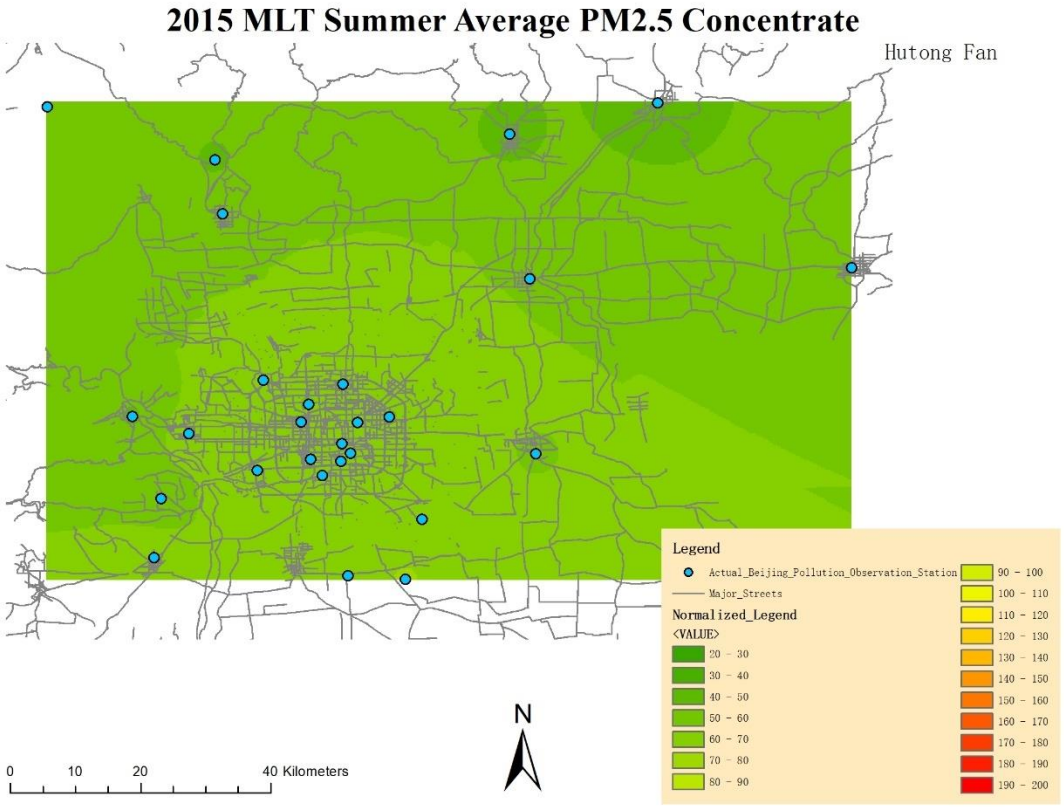
2015 MLT Summer Average PM2.5 Concentrate
Hutong Fan
Legend
Actual_Beijing_Pollution_Observation_Station
Major_Streets
Normalized_Legend
<VALUE>
20 - 30
30 - 40
40 - 50
50 - 60
60 - 70
70 - 80
80 - 90
90 - 100
100 - 110
110 - 120
120 - 130
130 - 140
140 - 150
150 - 160
160 - 170
170 - 180
180 - 190
190 - 200
N
0
10
20
40 Kilometers

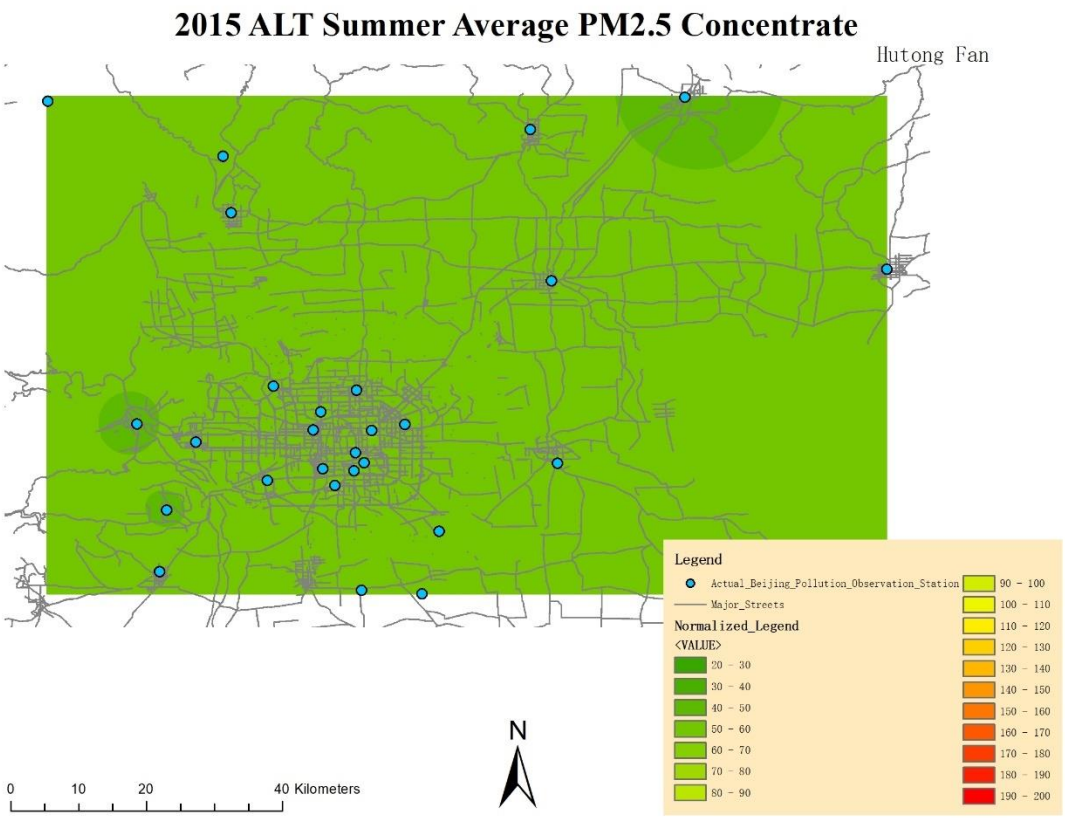
2015 ALT Summer Average PM2.5 Concentrate
Hutong Fan
Legend
Actual_Beijing_Pollution_Observation_Station
Major_Streets
Normalized_Legend
<VALUE>
20 - 30
30 - 40
40 - 50
50 - 60
60 - 70
70 - 80
80 - 90
90 - 100
100 - 110
110 - 120
120 - 130
130 - 140
140 - 150
150 - 160
160 - 170
170 - 180
180 - 190
190 - 200
N
0
10
20
40 Kilometers

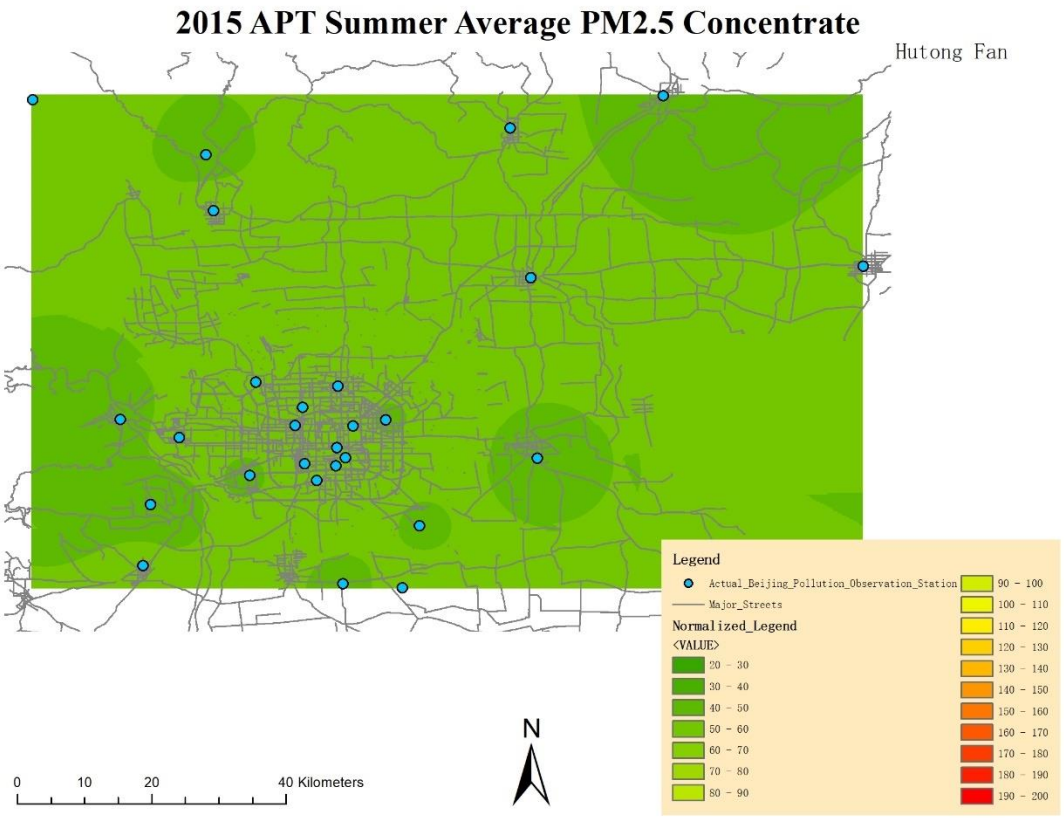
2015 APT Summer Average PM2.5 Concentrate
Hutong Fan
Legend
Actual_Beijing_Pollution_Observation_Station
Major_Streets
Normalized_Legend
<VALUE>
20 - 30
30 - 40
40 - 50
50 - 60
60 - 70
70 - 80
80 - 90
90 - 100
100 - 110
110 - 120
120 - 130
130 - 140
140 - 150
150 - 160
160 - 170
170 - 180
180 - 190
190 - 200
N
0
10
20
40 Kilometers

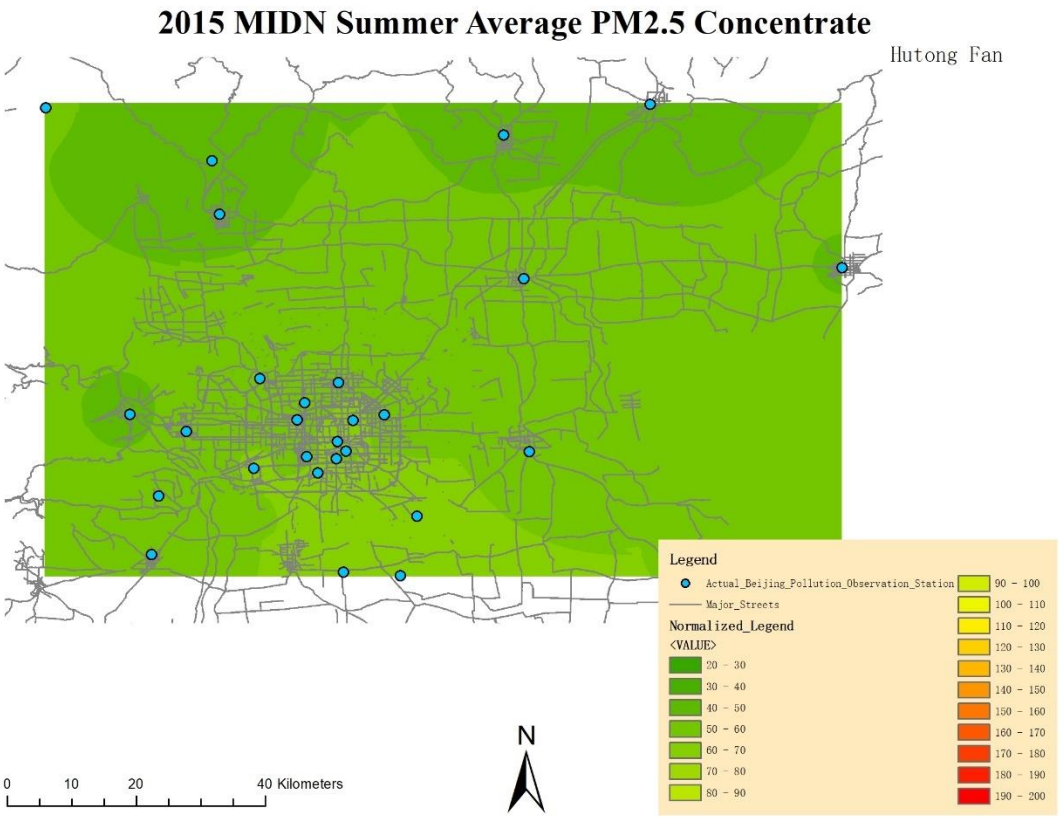
2015 MIDN Summer Average PM2.5 Concentrate
Hutong Fan
Legend
Actual_Beijing_Pollution_Observation_Station
Major_Streets
Normalized_Legend
<VALUE>
20 - 30
30 - 40
40 - 50
50 - 60
60 - 70
70 - 80
80 - 90
90 - 100
100 - 110
110 - 120
120 - 130
130 - 140
140 - 150
150 - 160
160 - 170
170 - 180
180 - 190
190 - 200
N
0
10
20
40 Kilometers

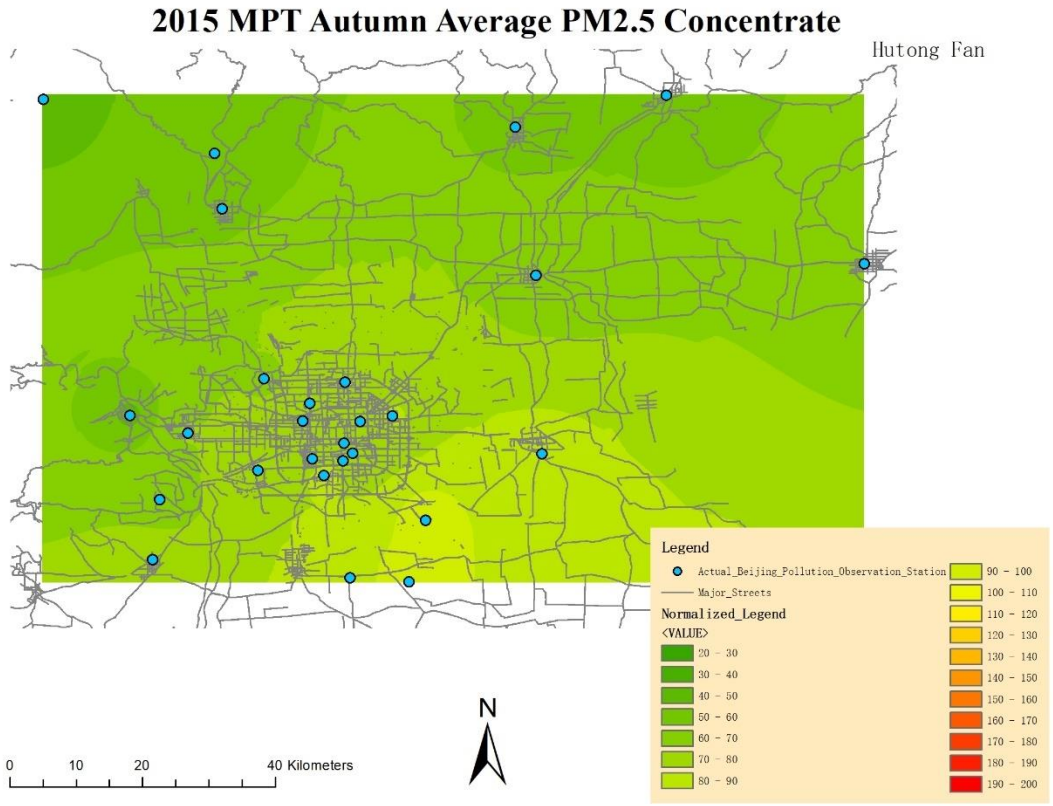
2015 MPT Autumn Average PM2.5 Concentrate
Hutong Fan
Legend
Actual_Beijing_Pollution_Observation_Station
Major_Streets
Normalized_Legend
<VALUE>
20 - 30
30 - 40
40 - 50
50 - 60
60 - 70
70 - 80
80 - 90
90 - 100
100 - 110
110 - 120
120 - 130
130 - 140
140 - 150
150 - 160
160 - 170
170 - 180
180 - 190
190 - 200
N
0
10
20
40 Kilometers

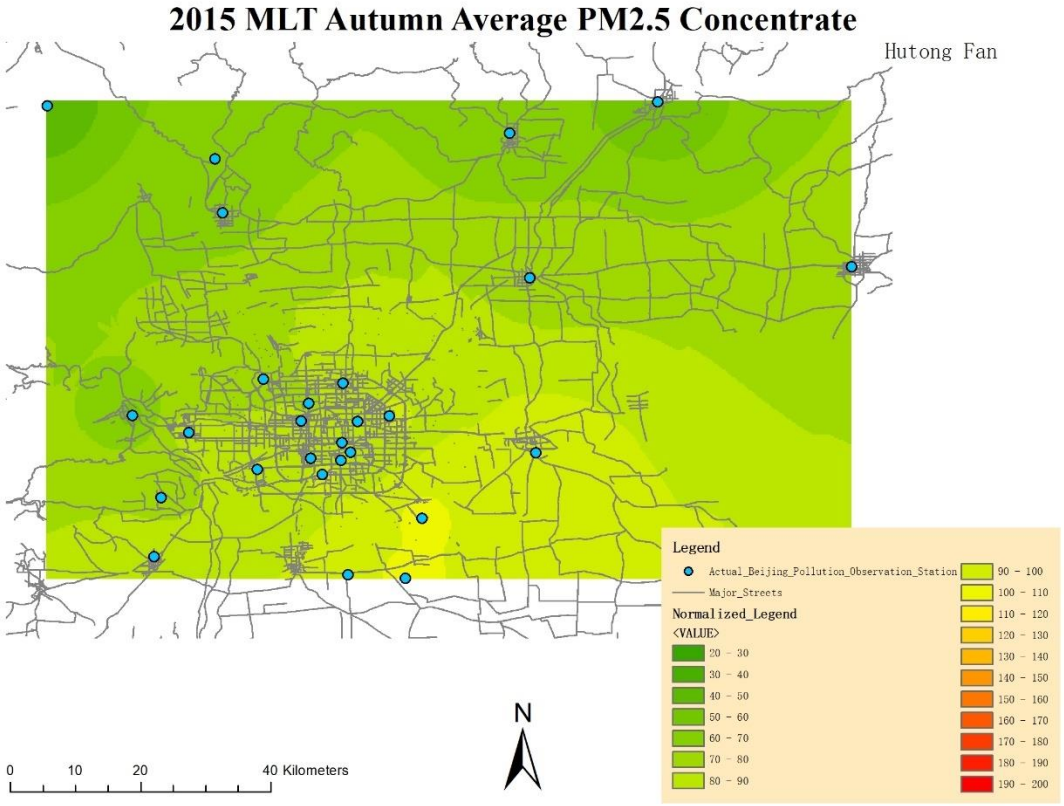
2015 MLT Autumn Average PM2.5 Concentrate
Hutong Fan
Legend
Actual_Beijing_Pollution_Observation_Station
Major_Streets
Normalized_Legend
<VALUE>
20 - 30
30 - 40
40 - 50
50 - 60
60 - 70
70 - 80
80 - 90
90 - 100
100 - 110
110 - 120
120 - 130
130 - 140
140 - 150
150 - 160
160 - 170
170 - 180
180 - 190
190 - 200
N
0
10
20
40 Kilometers

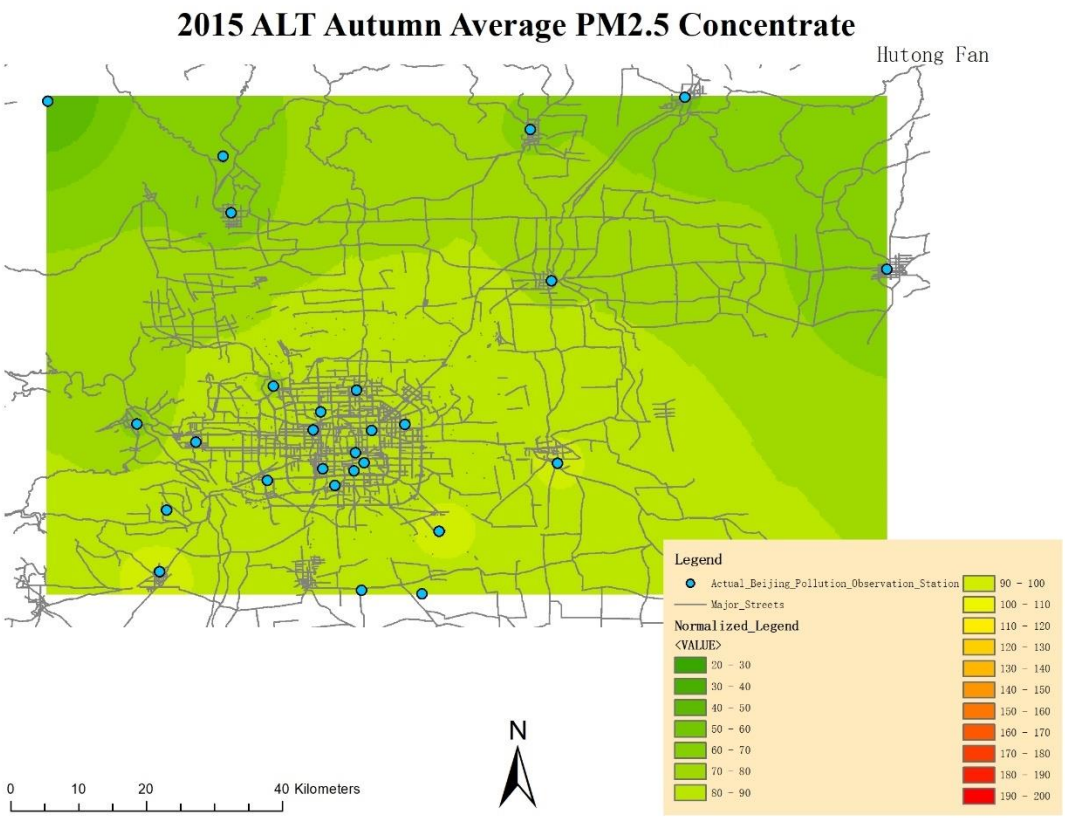
2015 ALT Autumn Average PM2.5 Concentrate
Hutong Fan
Legend
Actual_Beijing_Pollution_Observation_Station
Major_Streets
Normalized_Legend
<VALUE>
20 - 30
30 - 40
40 - 50
50 - 60
60 - 70
70 - 80
80 - 90
90 - 100
100 - 110
110 - 120
120 - 130
130 - 140
140 - 150
150 - 160
160 - 170
170 - 180
180 - 190
190 - 200
N
0
10
20
40 Kilometers

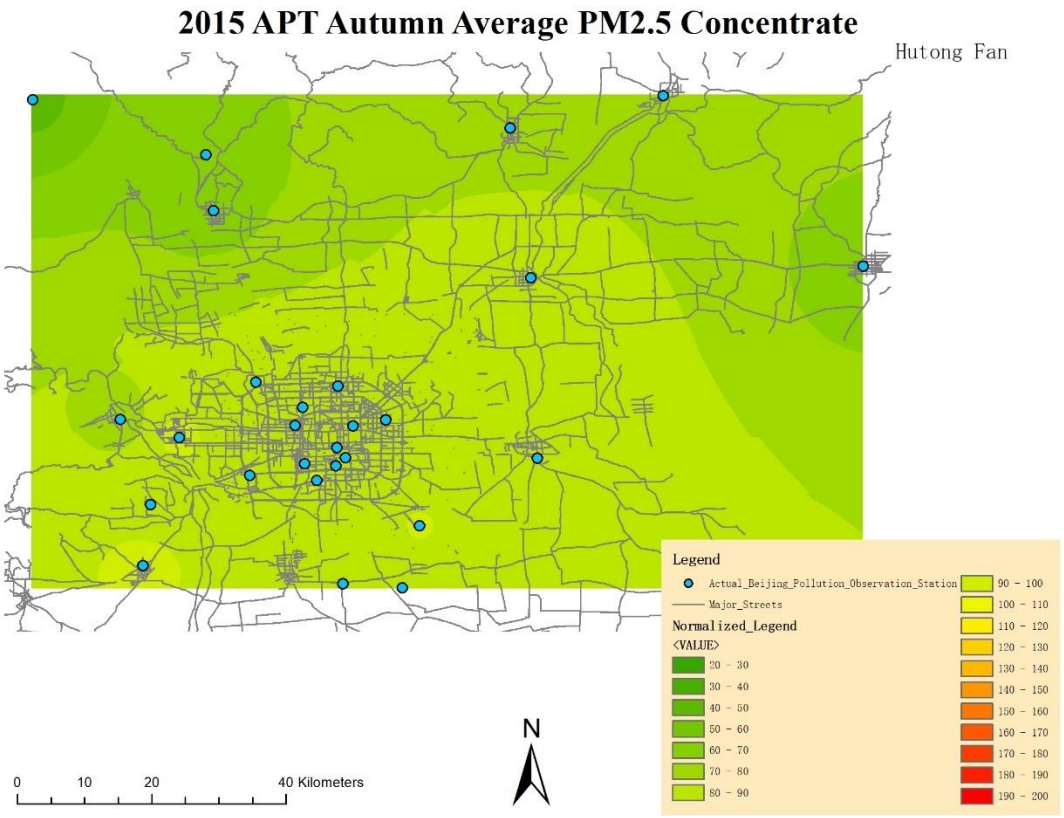
2015 APT Autumn Average PM2.5 Concentrate
Hutong Fan
Legend
Actual_Beijing_Pollution_Observation_Station
Major_Streets
Normalized_Legend
<VALUE>
20 - 30
30 - 40
40 - 50
50 - 60
60 - 70
70 - 80
80 - 90
90 - 100
100 - 110
110 - 120
120 - 130
130 - 140
140 - 150
150 - 160
160 - 170
170 - 180
180 - 190
190 - 200
N
0
10
20
40 Kilometers

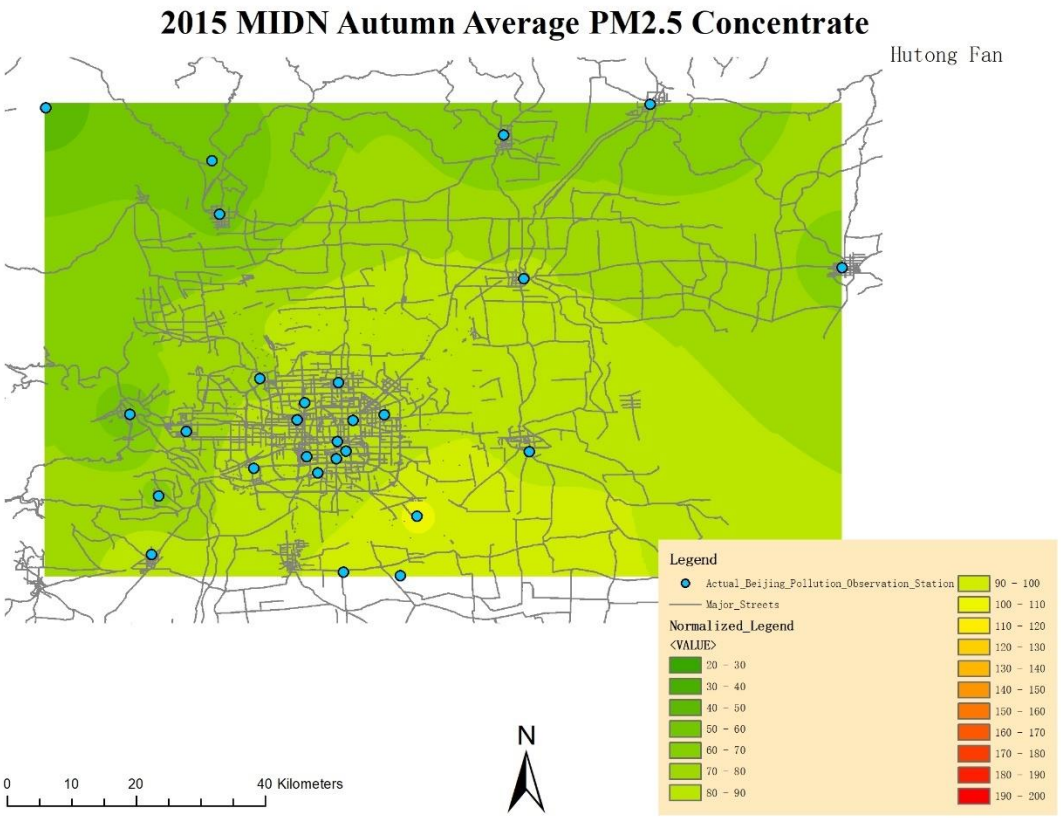
2015 MIDN Autumn Average PM2.5 Concentrate
Hutong Fan
Legend
Actual_Beijing_Pollution_Observation_Station
Major_Streets
Normalized_Legend
<VALUE>
20 - 30
30 - 40
40 - 50
50 - 60
60 - 70
70 - 80
80 - 90
90 - 100
100 - 110
110 - 120
120 - 130
130 - 140
140 - 150
150 - 160
160 - 170
170 - 180
180 - 190
190 - 200
N
0
10
20
40 Kilometers

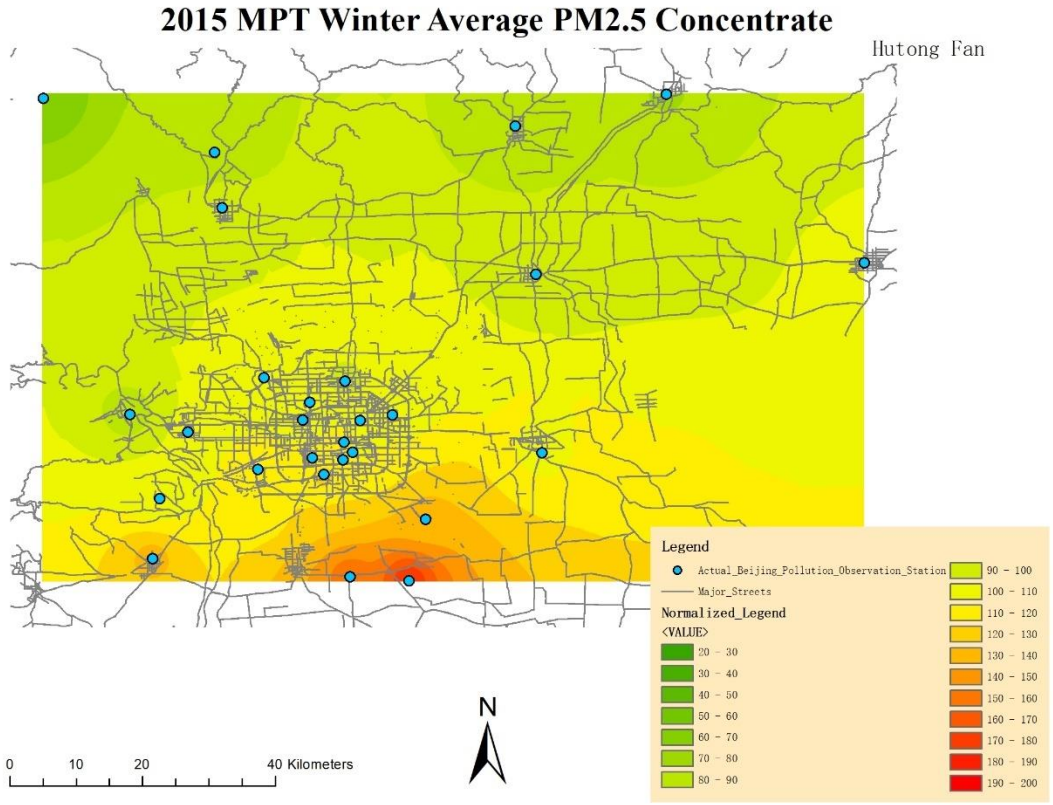
2015 MPT Winter Average PM2.5 Concentrate
Hutong Fan
Legend
Actual_Beijing_Pollution_Observation_Station
Major_Streets
Normalized_Legend
<VALUE>
20 - 30
30 - 40
40 - 50
50 - 60
60 - 70
70 - 80
80 - 90
90 - 100
100 - 110
110 - 120
120 - 130
130 - 140
140 - 150
150 - 160
160 - 170
170 - 180
180 - 190
190 - 200
N
0
10
20
40 Kilometers

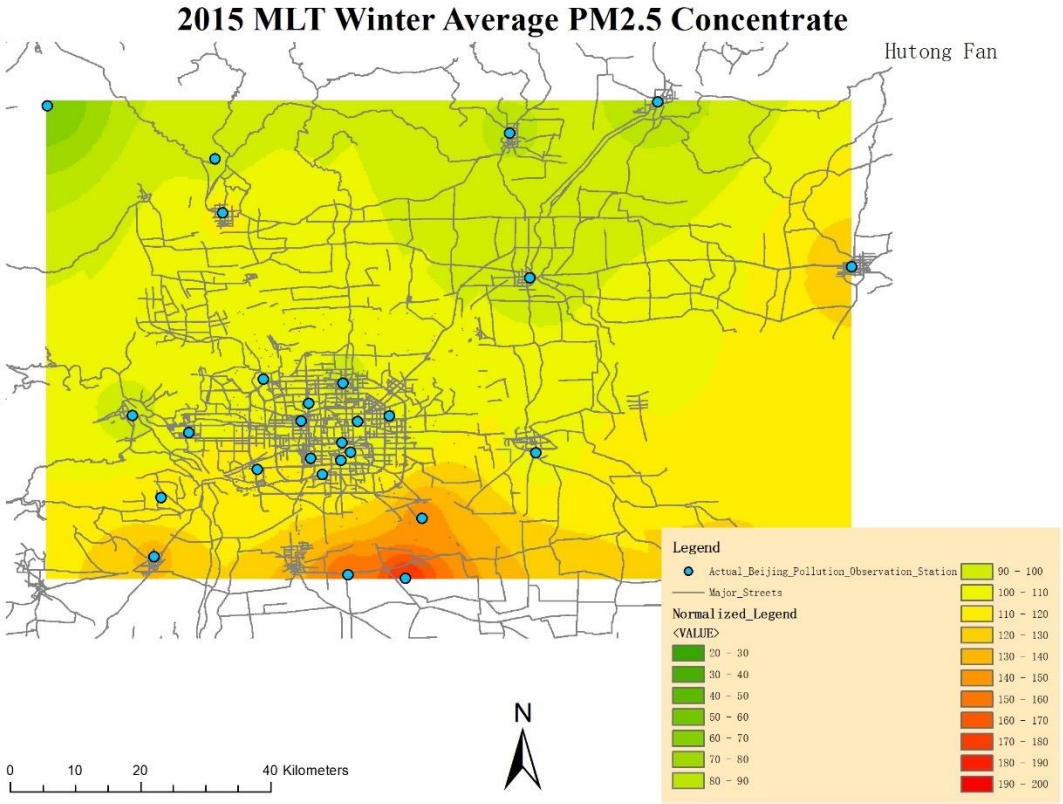
2015 MLT Winter Average PM2.5 Concentrate
Hutong Fan
Legend
Actual_Beijing_Pollution_Observation_Station
Major_Streets
Normalized_Legend
<VALUE>
20 - 30
30 - 40
40 - 50
50 - 60
60 - 70
70 - 80
80 - 90
90 - 100
100 - 110
110 - 120
120 - 130
130 - 140
140 - 150
150 - 160
160 - 170
170 - 180
180 - 190
190 - 200
N
0
10
20
40 Kilometers

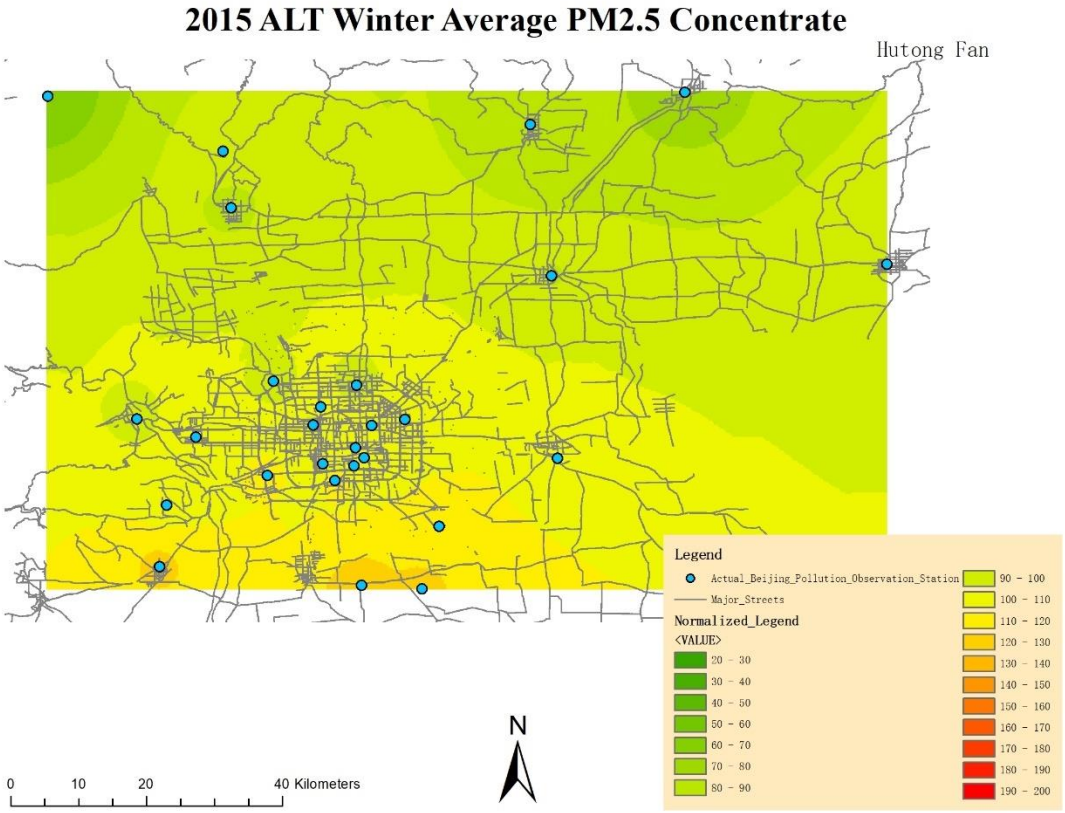
2015 ALT Winter Average PM2.5 Concentrate
Hutong Fan
Legend
Actual_Beijing_Pollution_Observation_Station
Major_Streets
Normalized_Legend
<VALUE>
20 - 30
30 - 40
40 - 50
50 - 60
60 - 70
70 - 80
80 - 90
90 - 100
100 - 110
110 - 120
120 - 130
130 - 140
140 - 150
150 - 160
160 - 170
170 - 180
180 - 190
190 - 200
N
0
10
20
40 Kilometers

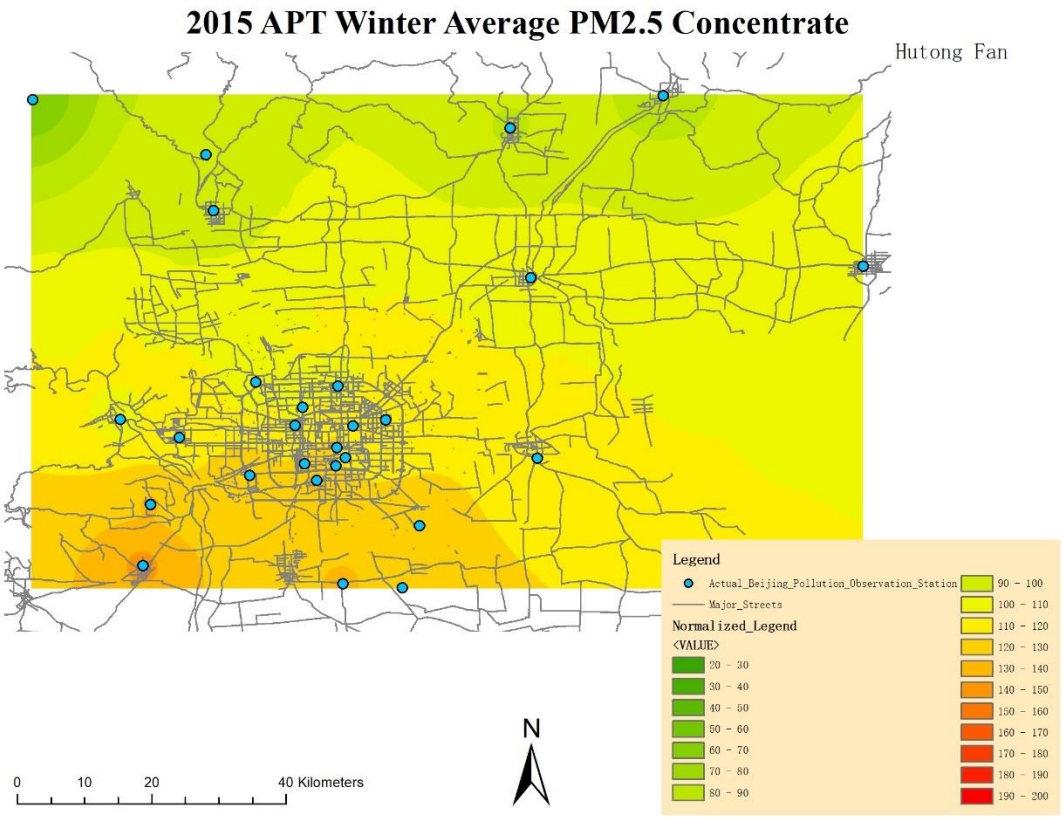
2015 APT Winter Average PM2.5 Concentrate
Hutong Fan
Legend
Actual_Beijing_Pollution_Observation_Station
Major_Streets
Normalized_Legend
<VALUE>
20 - 30
30 - 40
40 - 50
50 - 60
60 - 70
70 - 80
80 - 90
90 - 100
100 - 110
110 - 120
120 - 130
130 - 140
140 - 150
150 - 160
160 - 170
170 - 180
180 - 190
190 - 200
N
0
10
20
40 Kilometers

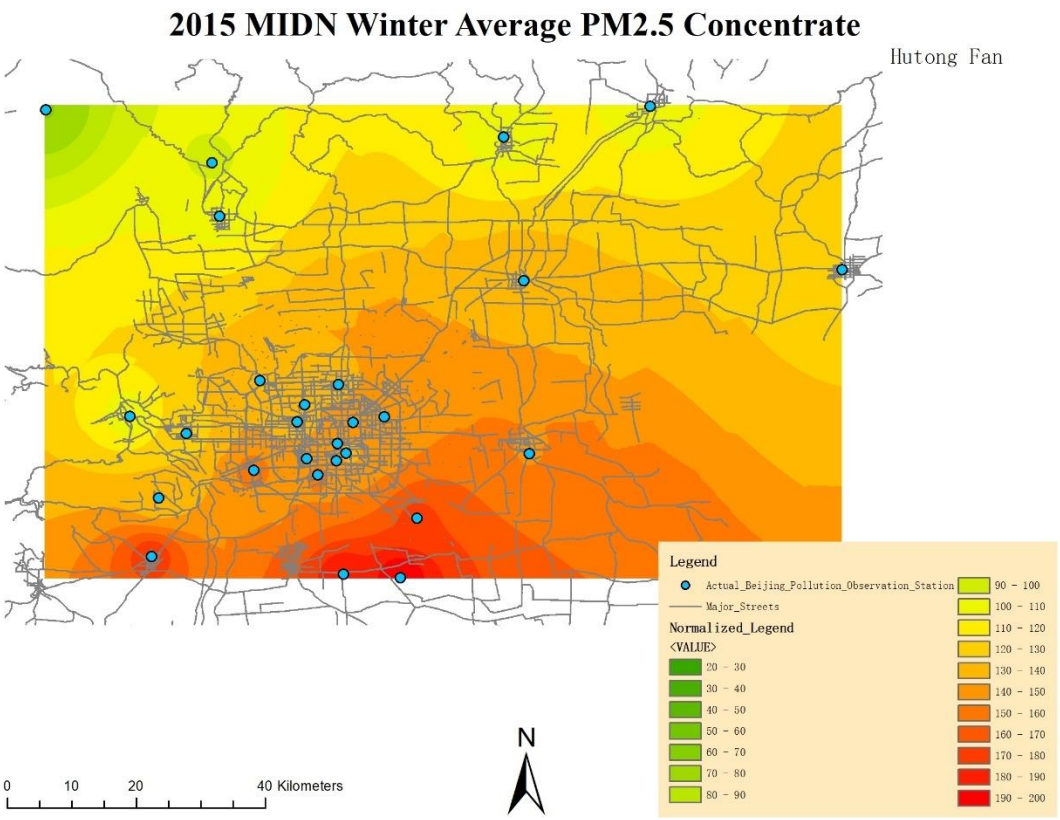
2015 MIDN Winter Average PM2.5 Concentrate
Hutong Fan
Legend
Actual_Beijing_Pollution_Observation_Station
Major_Streets
Normalized_Legend
<VALUE>
20 - 30
30 - 40
40 - 50
50 - 60
60 - 70
70 - 80
80 - 90
90 - 100
100 - 110
110 - 120
120 - 130
130 - 140
140 - 150
150 - 160
160 - 170
170 - 180
180 - 190
190 - 200
N
0
10
20
40 Kilometers

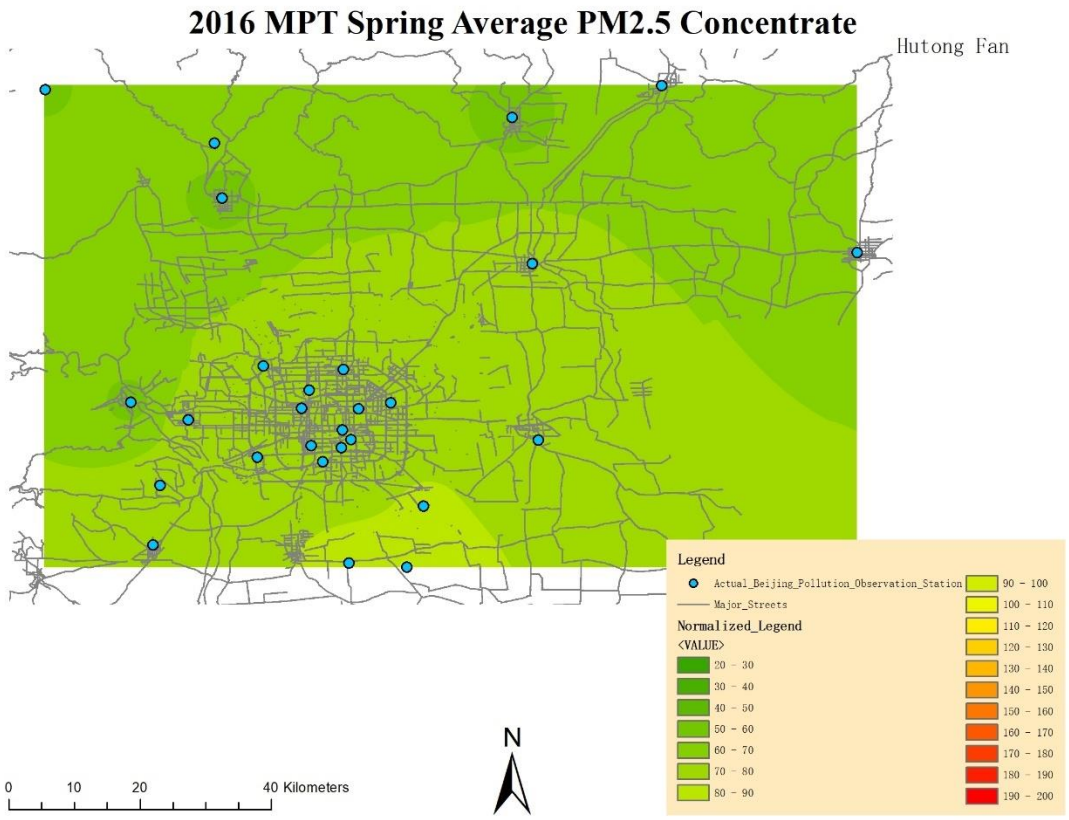
2016 MPT Spring Average PM2.5 Concentrate
Hutong Fan
Legend
Actual_Beijing_Pollution_Observation_Station
Major_Streets
Normalized_Legend
<VALUE>
20 - 30
30 - 40
40 - 50
50 - 60
60 - 70
70 - 80
80 - 90
90 - 100
100 - 110
110 - 120
120 - 130
130 - 140
140 - 150
150 - 160
160 - 170
170 - 180
180 - 190
190 - 200
N
0
10
20
40 Kilometers

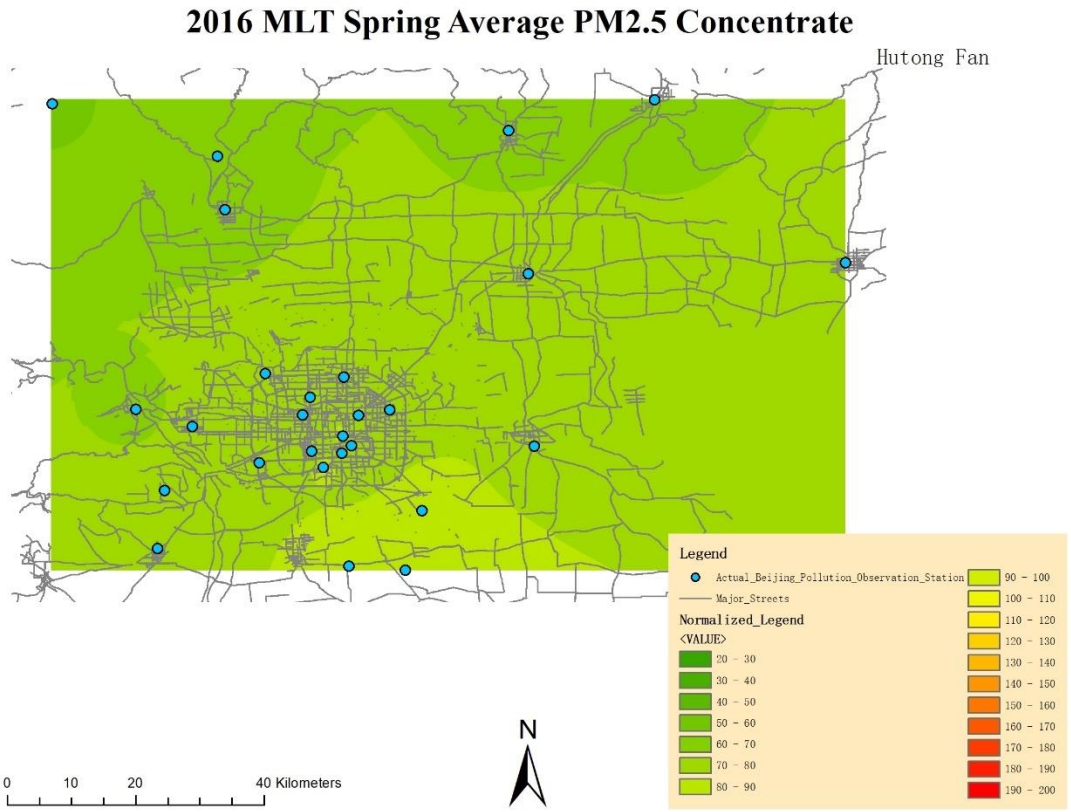
2016 MLT Spring Average PM2.5 Concentrate
Hutong Fan
Legend
Actual_Beijing_Pollution_Observation_Station
Major_Streets
Normalized_Legend
<VALUE>
20 - 30
30 - 40
40 - 50
50 - 60
60 - 70
70 - 80
80 - 90
90 - 100
100 - 110
110 - 120
120 - 130
130 - 140
140 - 150
150 - 160
160 - 170
170 - 180
180 - 190
190 - 200
N
0
10
20
40 Kilometers

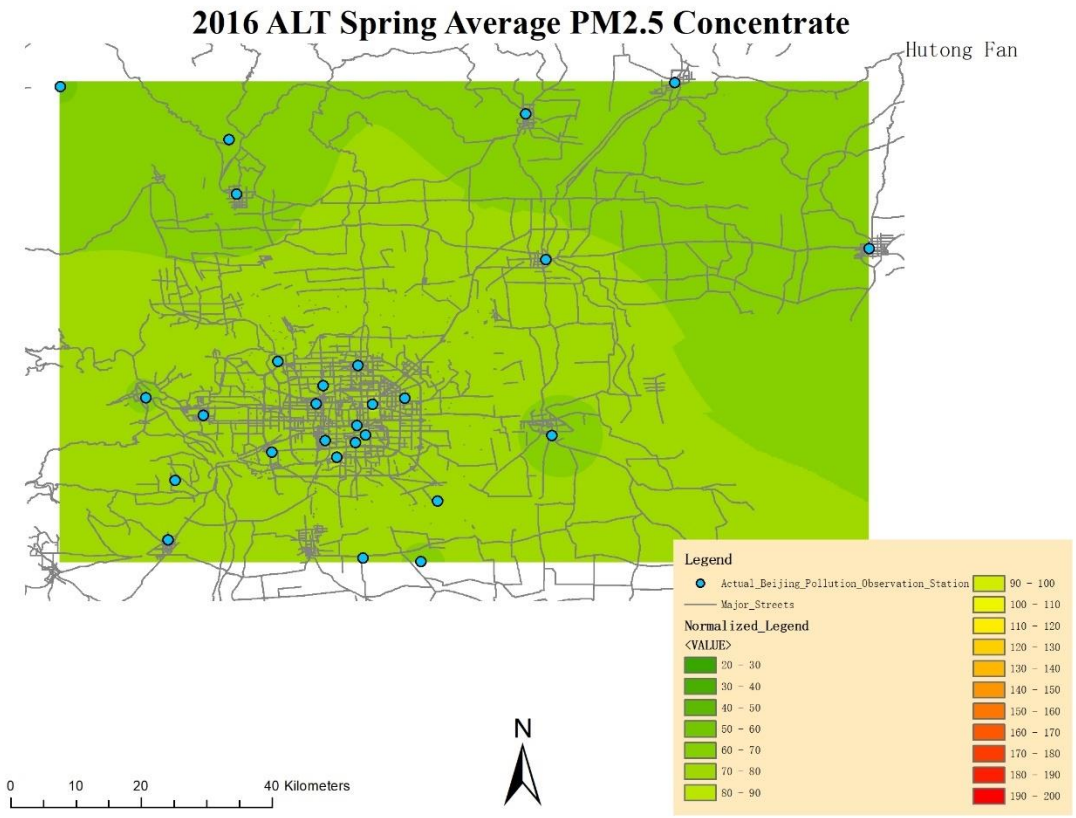
2016 ALT Spring Average PM2.5 Concentrate
Hutong Fan
Legend
Actual_Beijing_Pollution_Observation_Station
Major_Streets
Normalized_Legend
<VALUE>
20 - 30
30 - 40
40 - 50
50 - 60
60 - 70
70 - 80
80 - 90
90 - 100
100 - 110
110 - 120
120 - 130
130 - 140
140 - 150
150 - 160
160 - 170
170 - 180
180 - 190
190 - 200
N
0
10
20
40 Kilometers

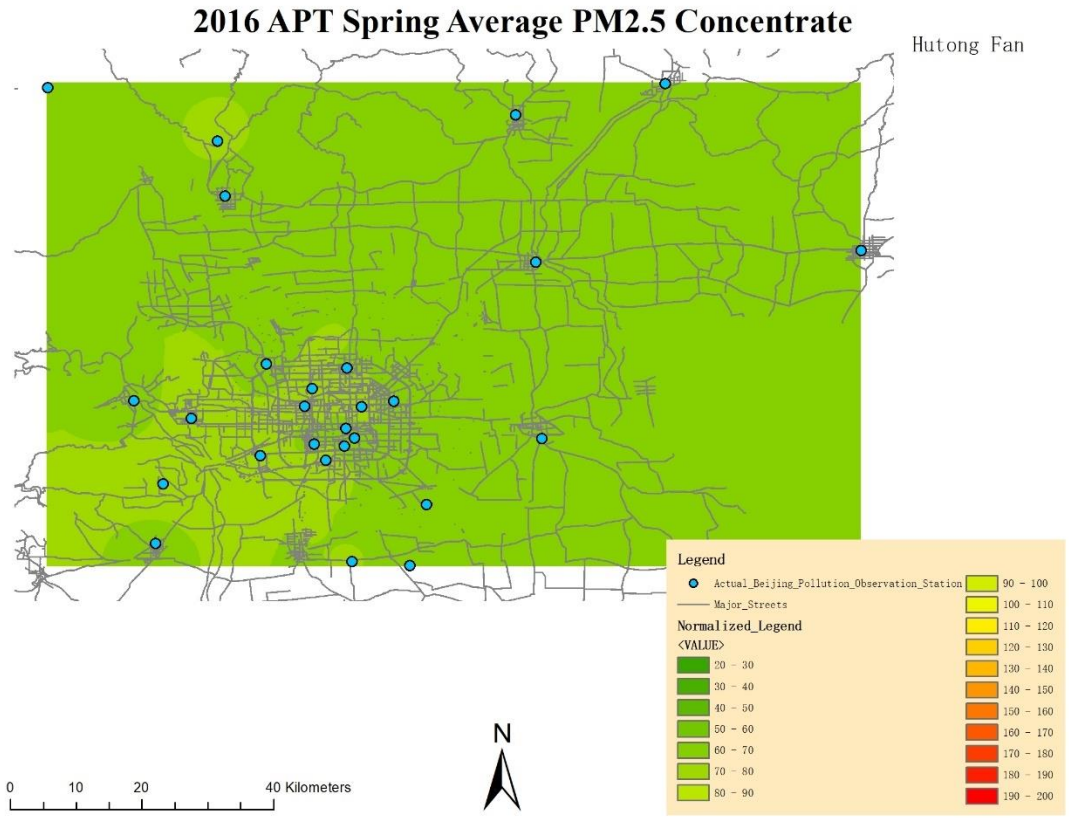
2016 APT Spring Average PM2.5 Concentrate
Hutong Fan
Legend
Actual_Beijing_Pollution_Observation_Station
Major_Streets
Normalized_Legend
<VALUE>
20 - 30
30 - 40
40 - 50
50 - 60
60 - 70
70 - 80
80 - 90
90 - 100
100 - 110
110 - 120
120 - 130
130 - 140
140 - 150
150 - 160
160 - 170
170 - 180
180 - 190
190 - 200
N
0 10 20 40 Kilometers

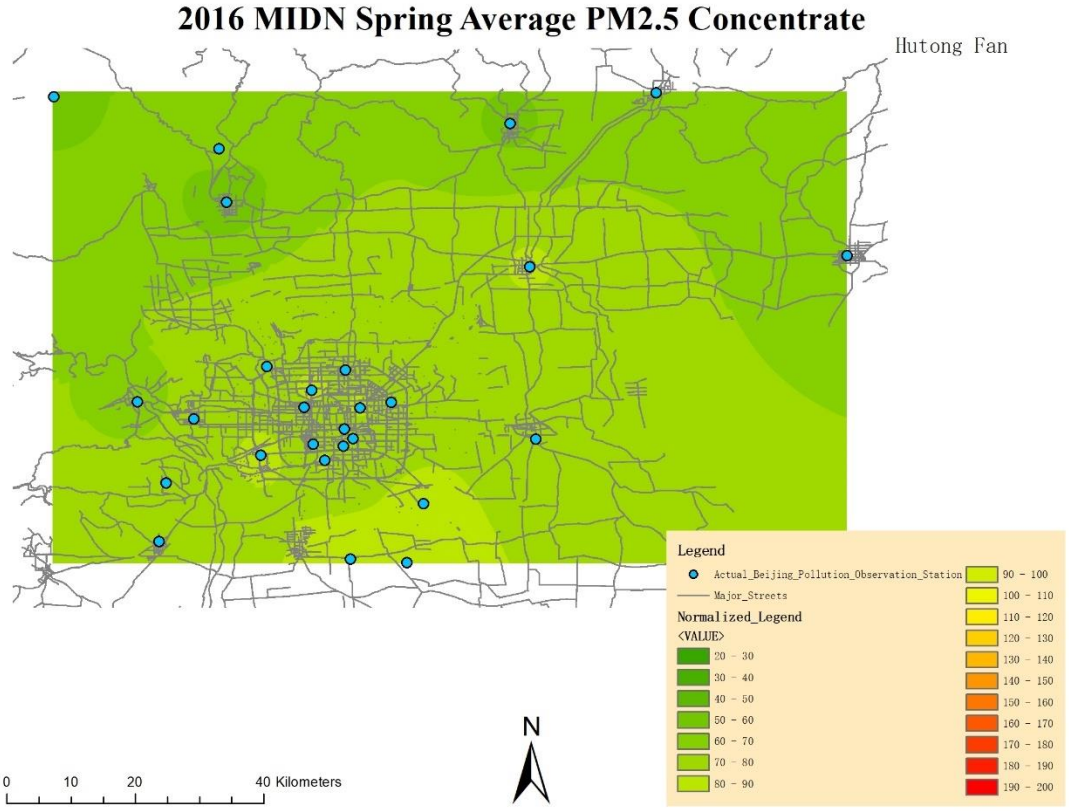
2016 MIDN Spring Average PM2.5 Concentrate
Hutong Fan
Legend
Actual_Beijing_Pollution_Observation_Station
Major_Streets
Normalized_Legend
<VALUE>
20 - 30
30 - 40
40 - 50
50 - 60
60 - 70
70 - 80
80 - 90
90 - 100
100 - 110
110 - 120
120 - 130
130 - 140
140 - 150
150 - 160
160 - 170
170 - 180
180 - 190
190 - 200
N
0 10 20 40 Kilometers

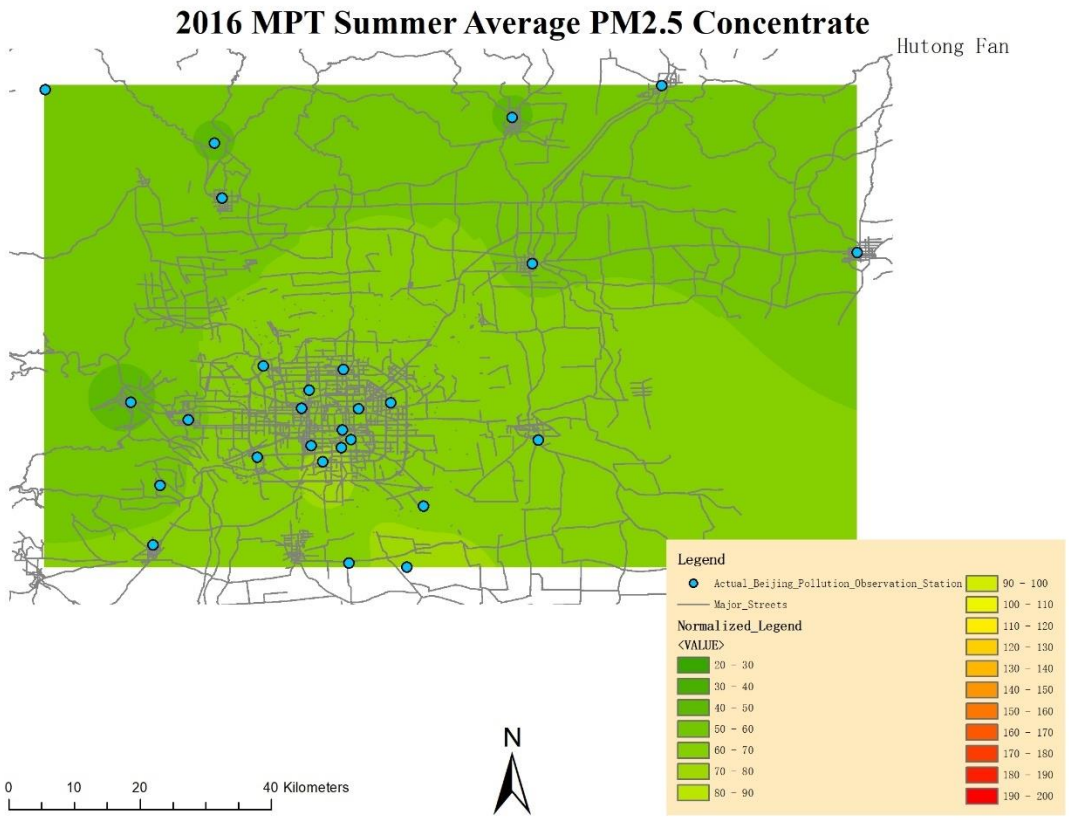
2016 MPT Summer Average PM2.5 Concentrate
Hutong Fan
Legend
Actual_Beijing_Pollution_Observation_Station
Major_Streets
Normalized_Legend
<VALUE>
20 - 30
30 - 40
40 - 50
50 - 60
60 - 70
70 - 80
80 - 90
90 - 100
100 - 110
110 - 120
120 - 130
130 - 140
140 - 150
150 - 160
160 - 170
170 - 180
180 - 190
190 - 200
N
0
10
20
40 Kilometers

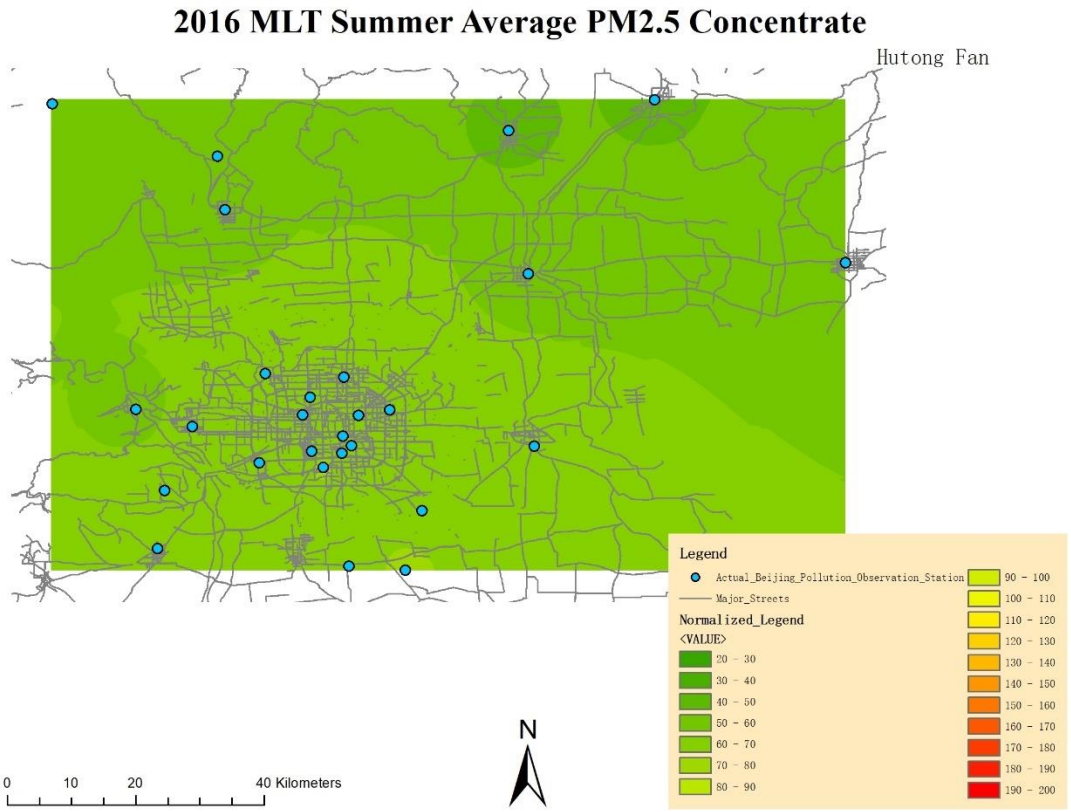
2016 MLT Summer Average PM2.5 Concentrate
Hutong Fan
Legend
Actual_Beijing_Pollution_Observation_Station
Major_Streets
Normalized_Legend
<VALUE>
20 - 30
30 - 40
40 - 50
50 - 60
60 - 70
70 - 80
80 - 90
90 - 100
100 - 110
110 - 120
120 - 130
130 - 140
140 - 150
150 - 160
160 - 170
170 - 180
180 - 190
190 - 200
N
0 10 20 40 Kilometers

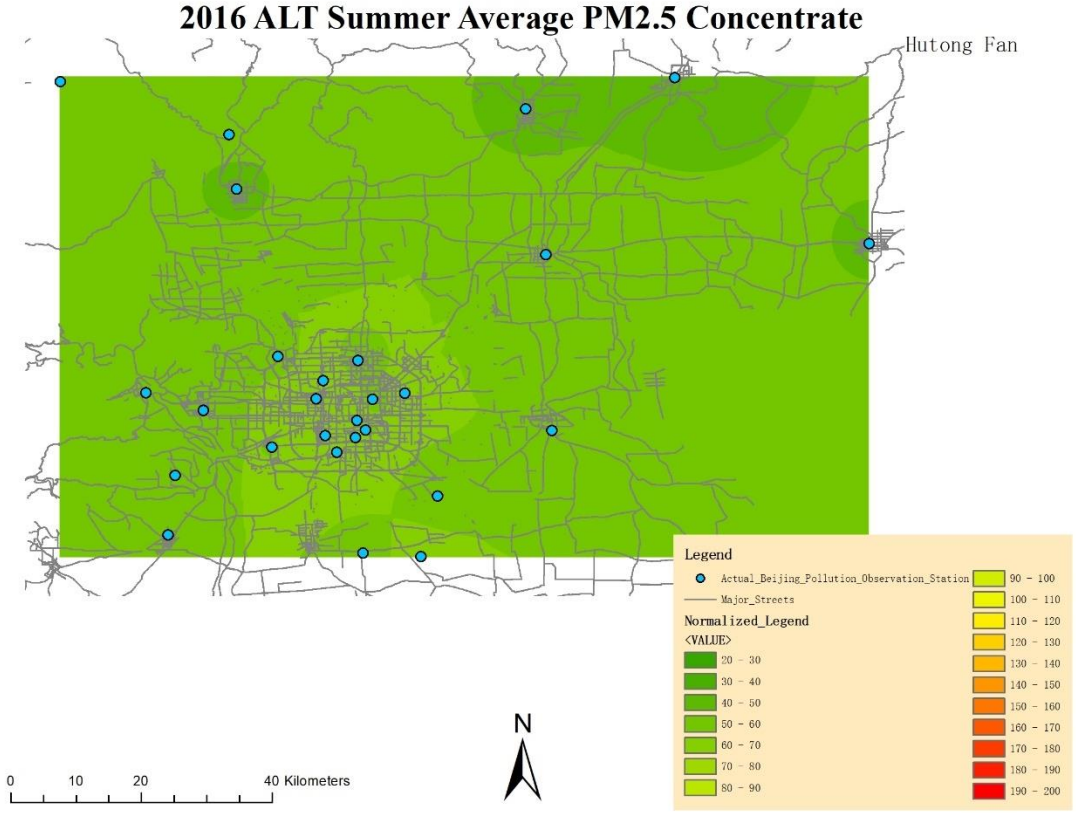
2016 ALT Summer Average PM2.5 Concentrate
Hutong Fan
Legend
Actual_Beijing_Pollution_Observation_Station
Major_Streets
Normalized_Legend
<VALUE>
20 - 30
30 - 40
40 - 50
50 - 60
60 - 70
70 - 80
80 - 90
90 - 100
100 - 110
110 - 120
120 - 130
130 - 140
140 - 150
150 - 160
160 - 170
170 - 180
180 - 190
190 - 200
N
0 10 20 40 Kilometers

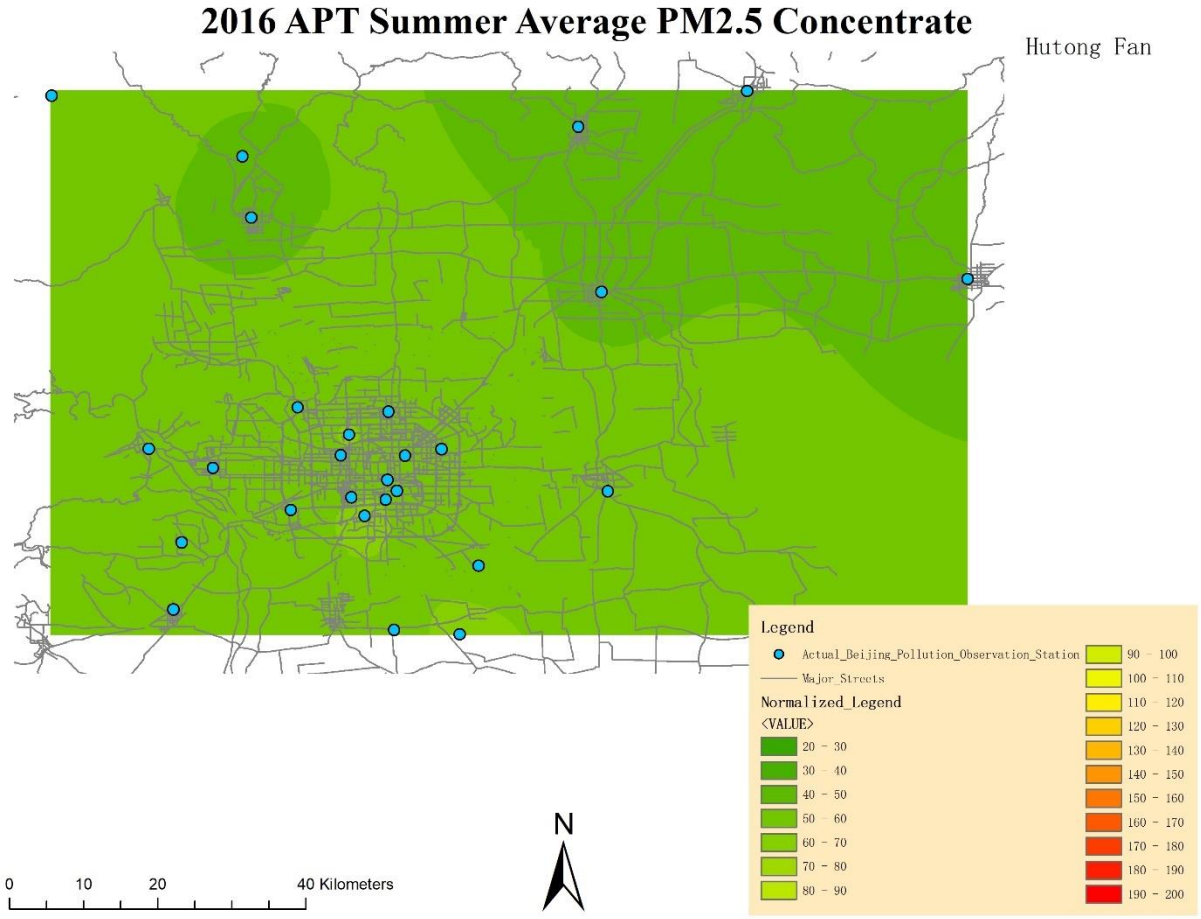
2016 APT Summer Average PM2.5 Concentrate
Hutong Fan
Legend
Actual_Beijing_Pollution_Observation_Station
Major_Streets
Normalized_Legend
<VALUE>
20 - 30
30 - 40
40 - 50
50 - 60
60 - 70
70 - 80
80 - 90
90 - 100
100 - 110
110 - 120
120 - 130
130 - 140
140 - 150
150 - 160
160 - 170
170 - 180
180 - 190
190 - 200
N
0
10
20
40 Kilometers

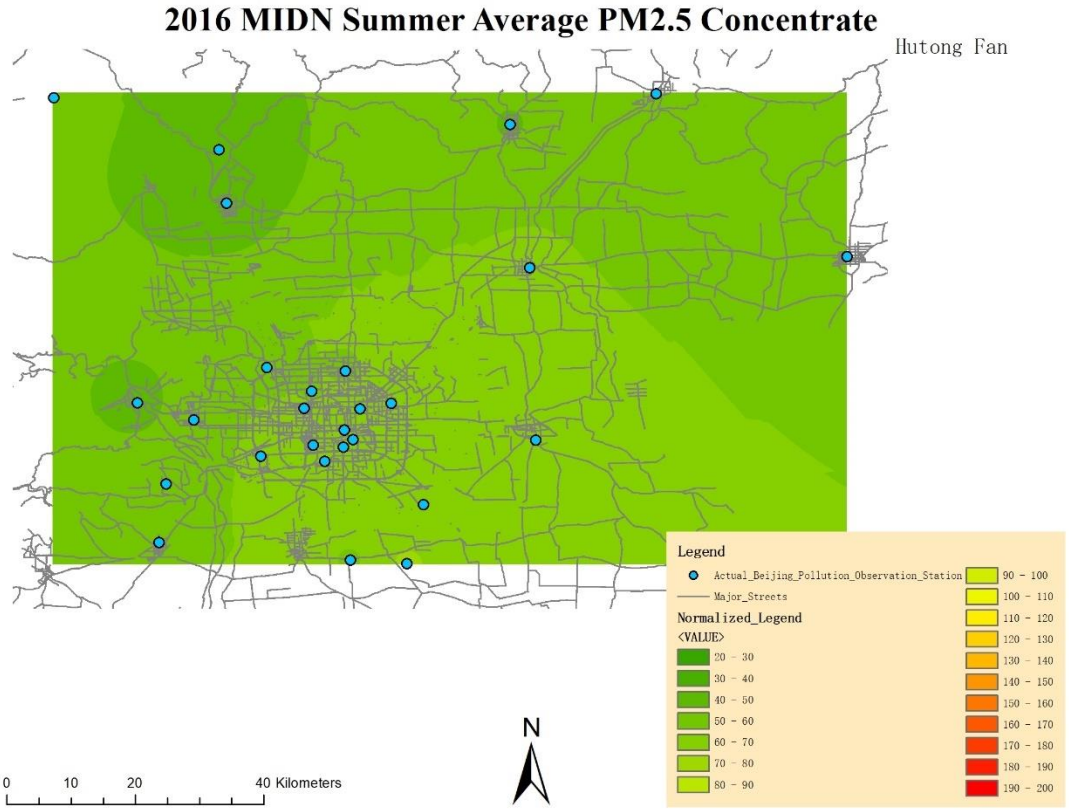
2016 MIDN Summer Average PM2.5 Concentrate
Hutong Fan
Legend
Actual_Beijing_Pollution_Observation_Station
Major_Streets
Normalized_Legend
<VALUE>
20 - 30
30 - 40
40 - 50
50 - 60
60 - 70
70 - 80
80 - 90
90 - 100
100 - 110
110 - 120
120 - 130
130 - 140
140 - 150
150 - 160
160 - 170
170 - 180
180 - 190
190 - 200
N
0
10
20
40 Kilometers

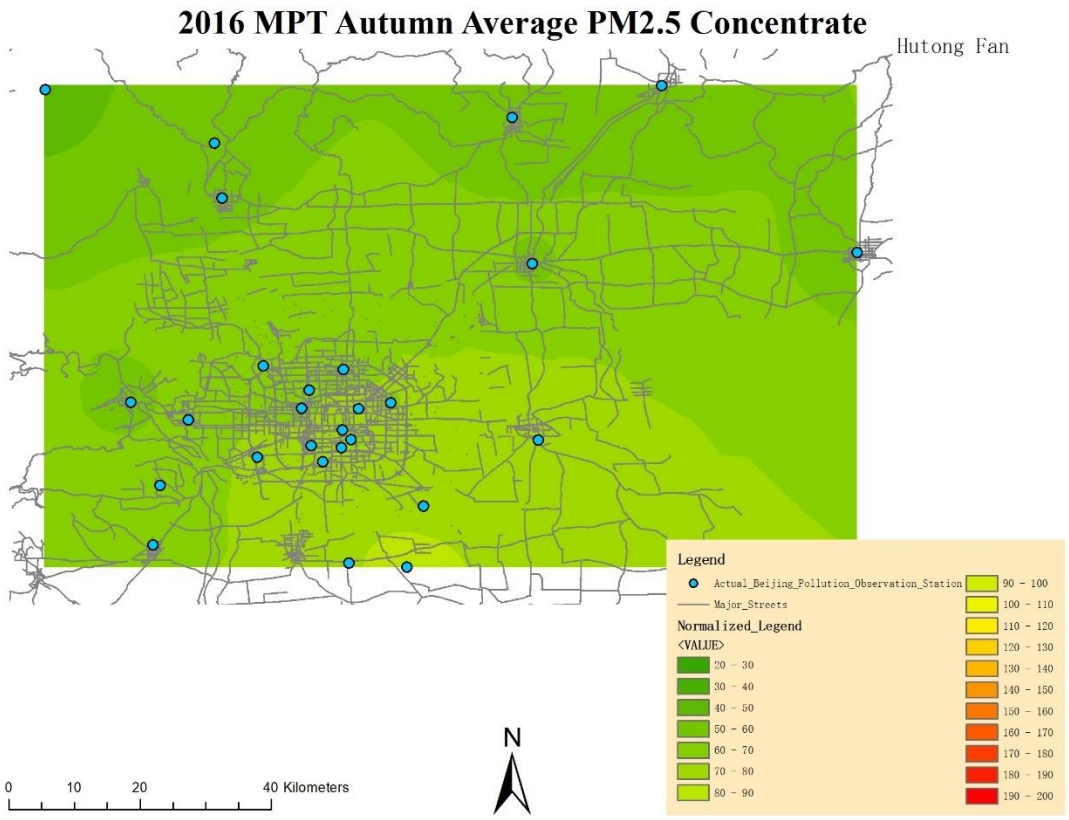
2016 MPT Autumn Average PM2.5 Concentrate
Hutong Fan
Legend
Actual_Beijing_Pollution_Observation_Station
Major_Streets
Normalized_Legend
<VALUE>
20 - 30
30 - 40
40 - 50
50 - 60
60 - 70
70 - 80
80 - 90
90 - 100
100 - 110
110 - 120
120 - 130
130 - 140
140 - 150
150 - 160
160 - 170
170 - 180
180 - 190
190 - 200
N
0
10
20
40 Kilometers

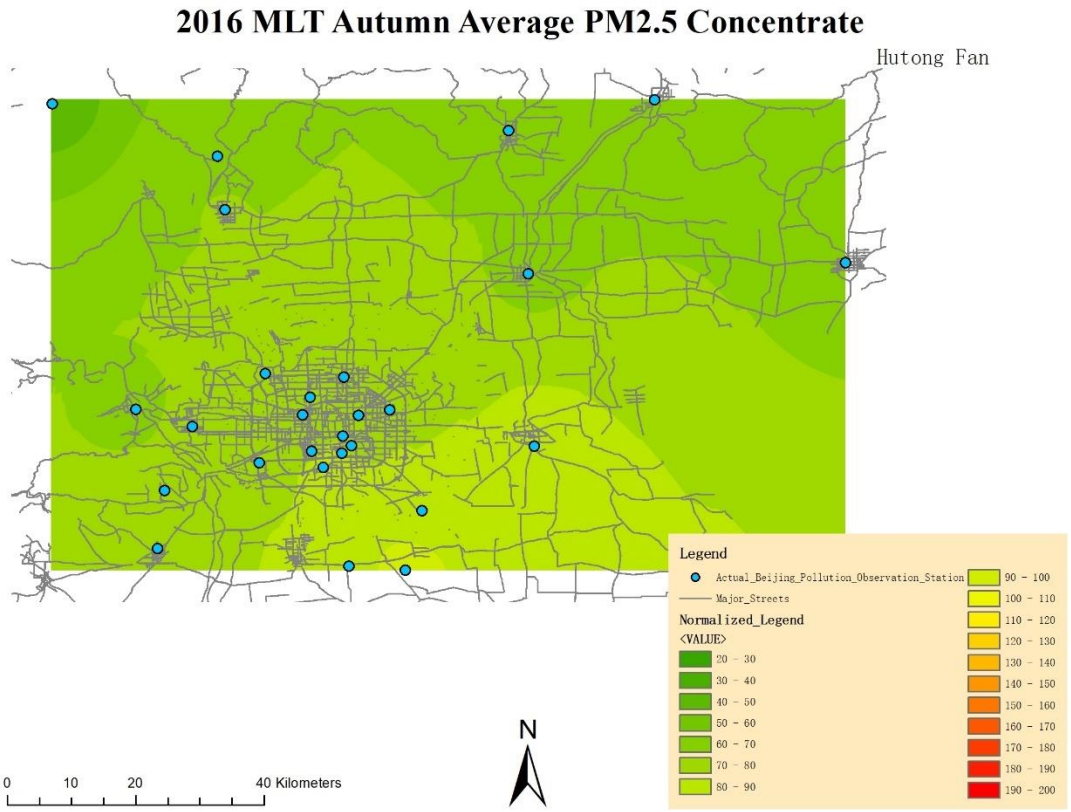
2016 MLT Autumn Average PM2.5 Concentrate
Hutong Fan
Legend
Actual_Beijing_Pollution_Observation_Station
Major_Streets
Normalized_Legend
<VALUE>
20 - 30
30 - 40
40 - 50
50 - 60
60 - 70
70 - 80
80 - 90
90 - 100
100 - 110
110 - 120
120 - 130
130 - 140
140 - 150
150 - 160
160 - 170
170 - 180
180 - 190
190 - 200
N
0
10
20
40 Kilometers

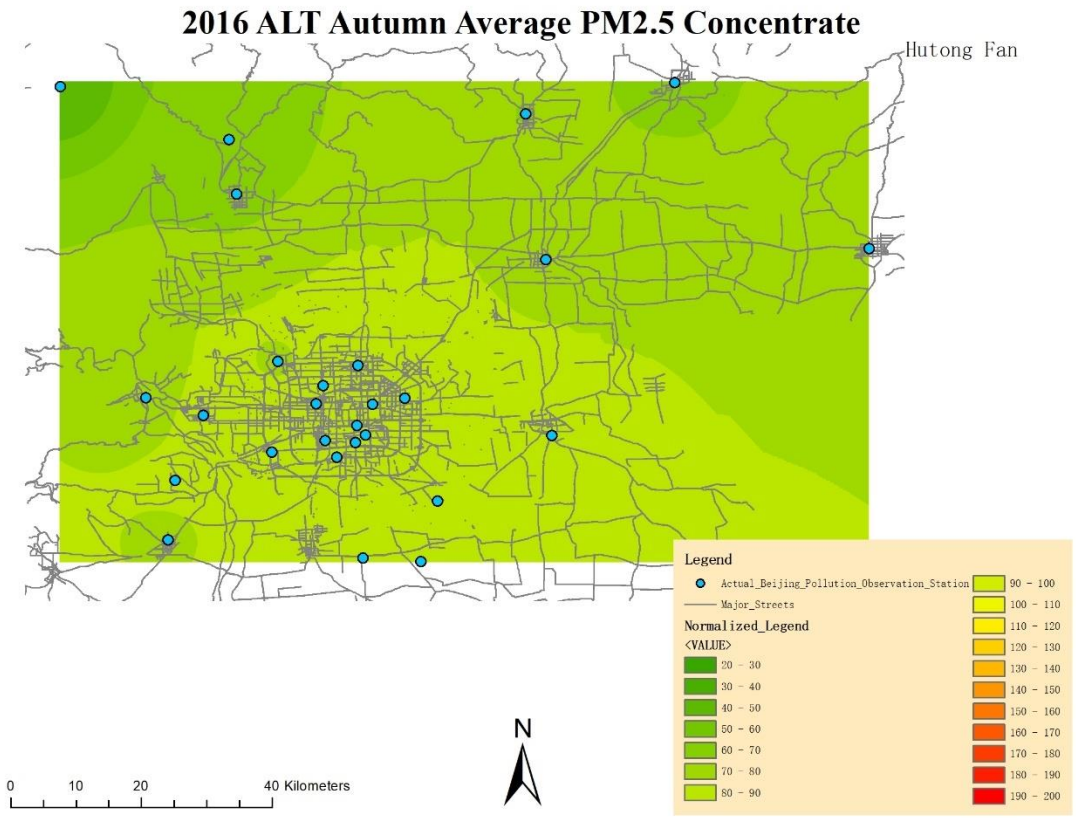
2016 ALT Autumn Average PM2.5 Concentrate
Hutong Fan
Legend
Actual_Beijing_Pollution_Observation_Station
Major_Streets
Normalized_Legend
<VALUE>
20 - 30
30 - 40
40 - 50
50 - 60
60 - 70
70 - 80
80 - 90
90 - 100
100 - 110
110 - 120
120 - 130
130 - 140
140 - 150
150 - 160
160 - 170
170 - 180
180 - 190
190 - 200
N
0
10
20
40 Kilometers

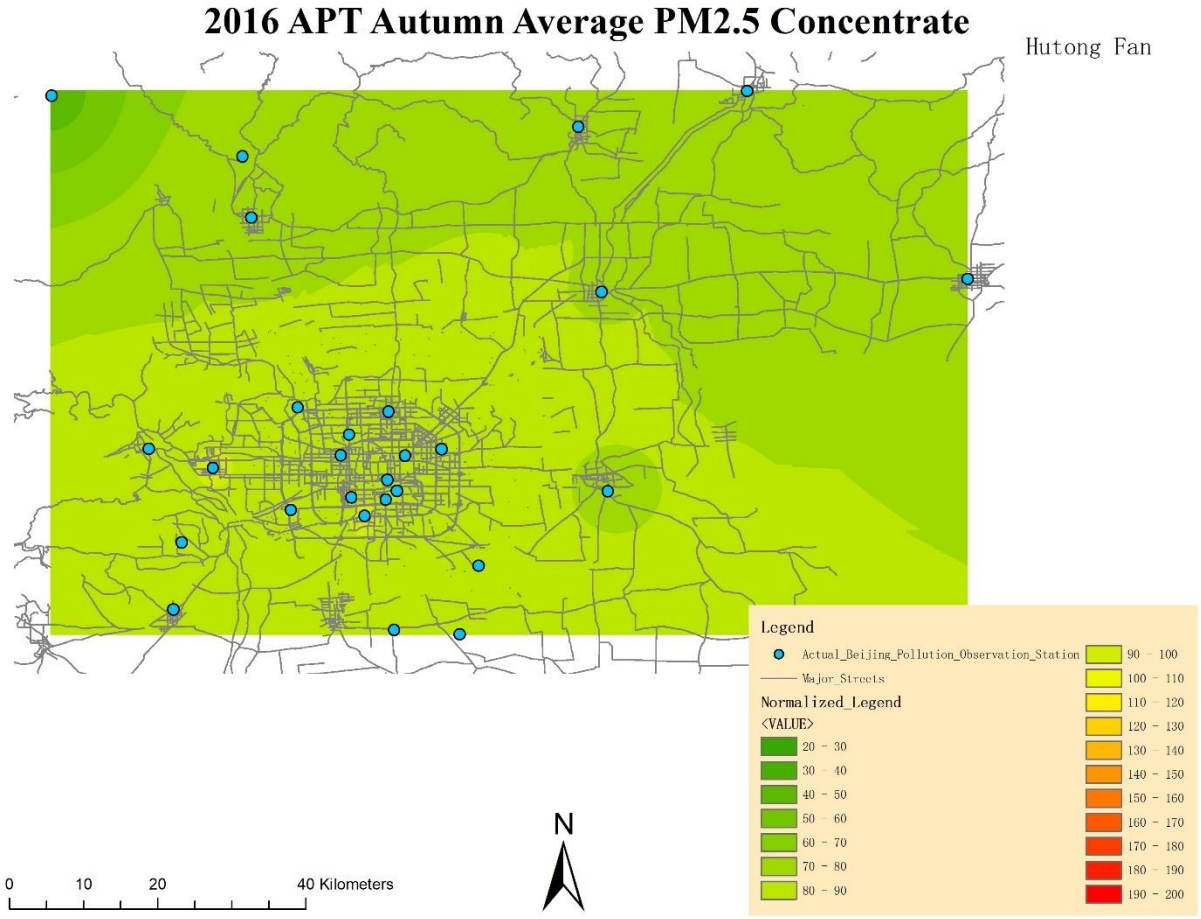
2016 APT Autumn Average PM2.5 Concentrate
Hutong Fan
Legend
Actual_Beijing_Pollution_Observation_Station
Major_Streets
Normalized_Legend
<VALUE>
20 - 30
30 - 40
40 - 50
50 - 60
60 - 70
70 - 80
80 - 90
90 - 100
100 - 110
110 - 120
120 - 130
130 - 140
140 - 150
150 - 160
160 - 170
170 - 180
180 - 190
190 - 200
N
0
10
20
40 Kilometers

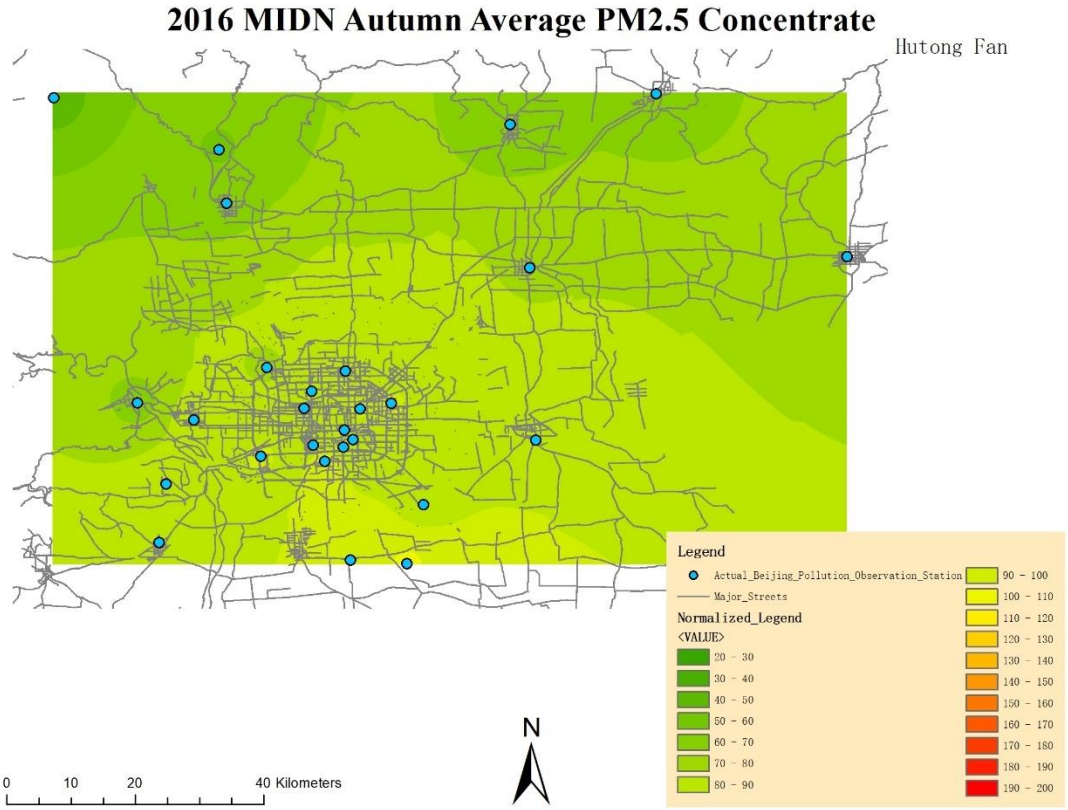
2016 MIDN Autumn Average PM2.5 Concentrate
Hutong Fan
Legend
Actual_Beijing_Pollution_Observation_Station
Major_Streets
Normalized_Legend
<VALUE>
20 - 30
30 - 40
40 - 50
50 - 60
60 - 70
70 - 80
80 - 90
90 - 100
100 - 110
110 - 120
120 - 130
130 - 140
140 - 150
150 - 160
160 - 170
170 - 180
180 - 190
190 - 200
N
0
10
20
40 Kilometers

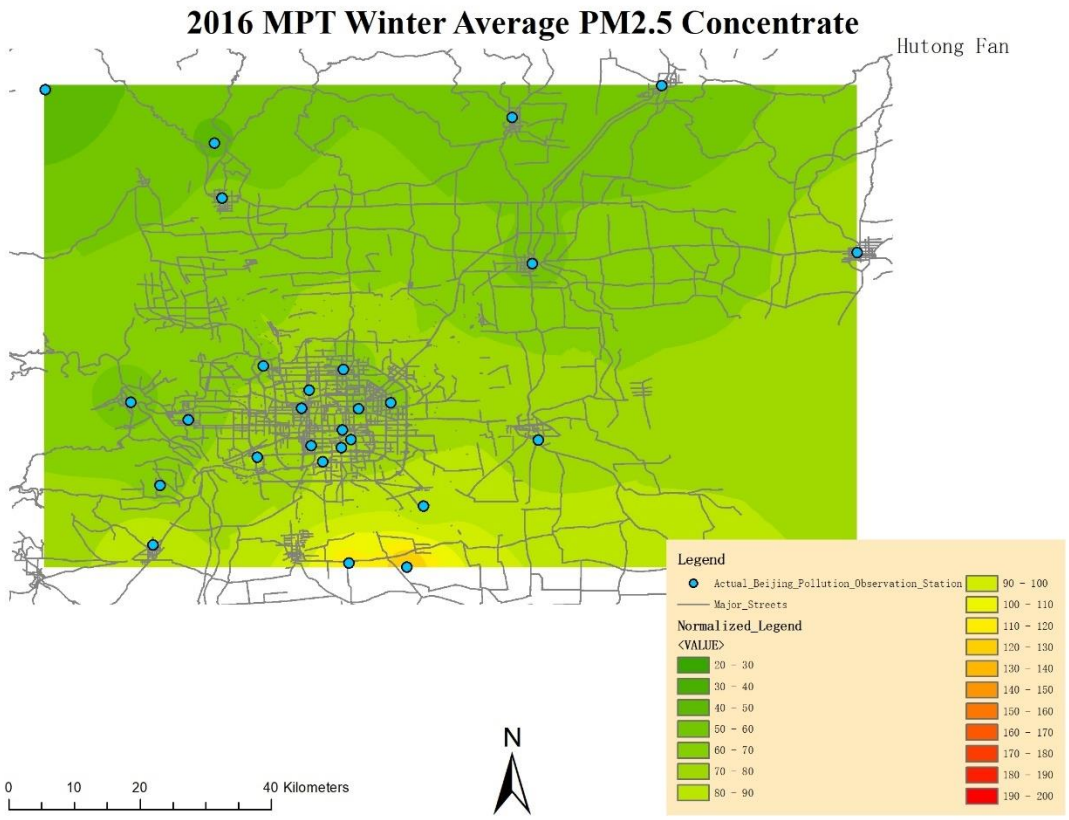
2016 MPT Winter Average PM2.5 Concentrate
Hutong Fan
Legend
Actual_Beijing_Pollution_Observation_Station
Major_Streets
Normalized_Legend
<VALUE>
20 - 30
30 - 40
40 - 50
50 - 60
60 - 70
70 - 80
80 - 90
90 - 100
100 - 110
110 - 120
120 - 130
130 - 140
140 - 150
150 - 160
160 - 170
170 - 180
180 - 190
190 - 200
N
0
10
20
40 Kilometers

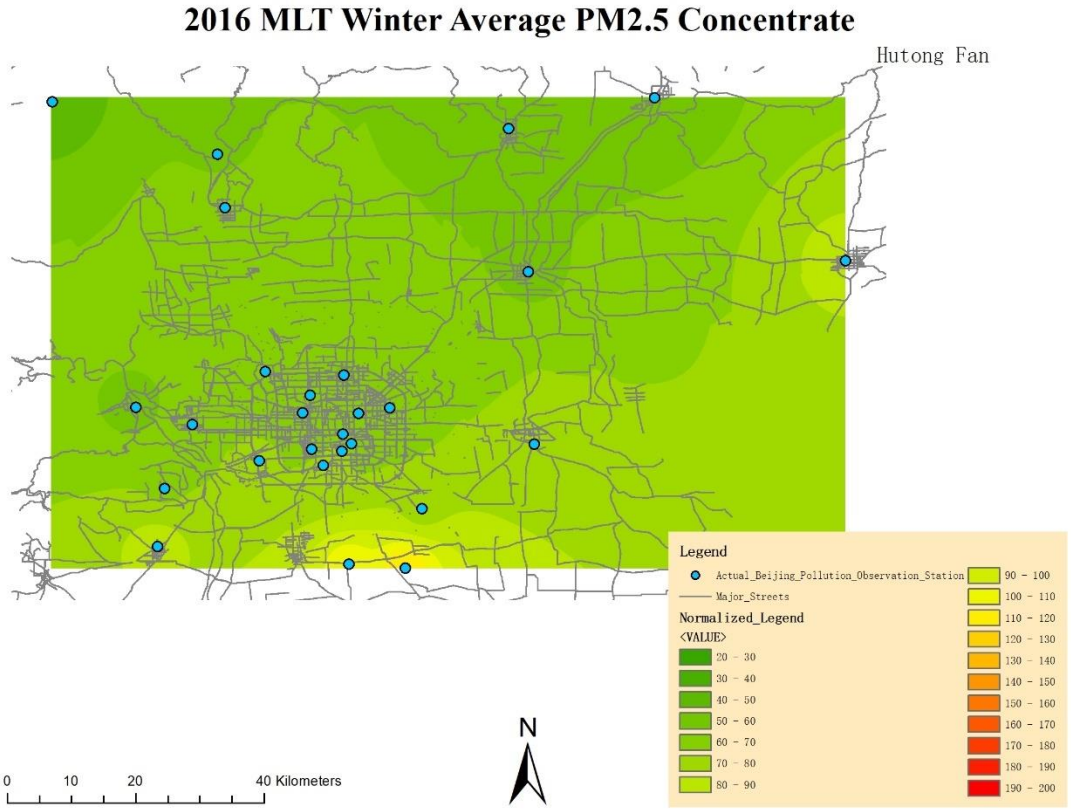
2016 MLT Winter Average PM2.5 Concentrate
Hutong Fan
Legend
Actual_Beijing_Pollution_Observation_Station
Major_Streets
Normalized_Legend
<VALUE>
20 - 30
30 - 40
40 - 50
50 - 60
60 - 70
70 - 80
80 - 90
90 - 100
100 - 110
110 - 120
120 - 130
130 - 140
140 - 150
150 - 160
160 - 170
170 - 180
180 - 190
190 - 200
N
0
10
20
40 Kilometers

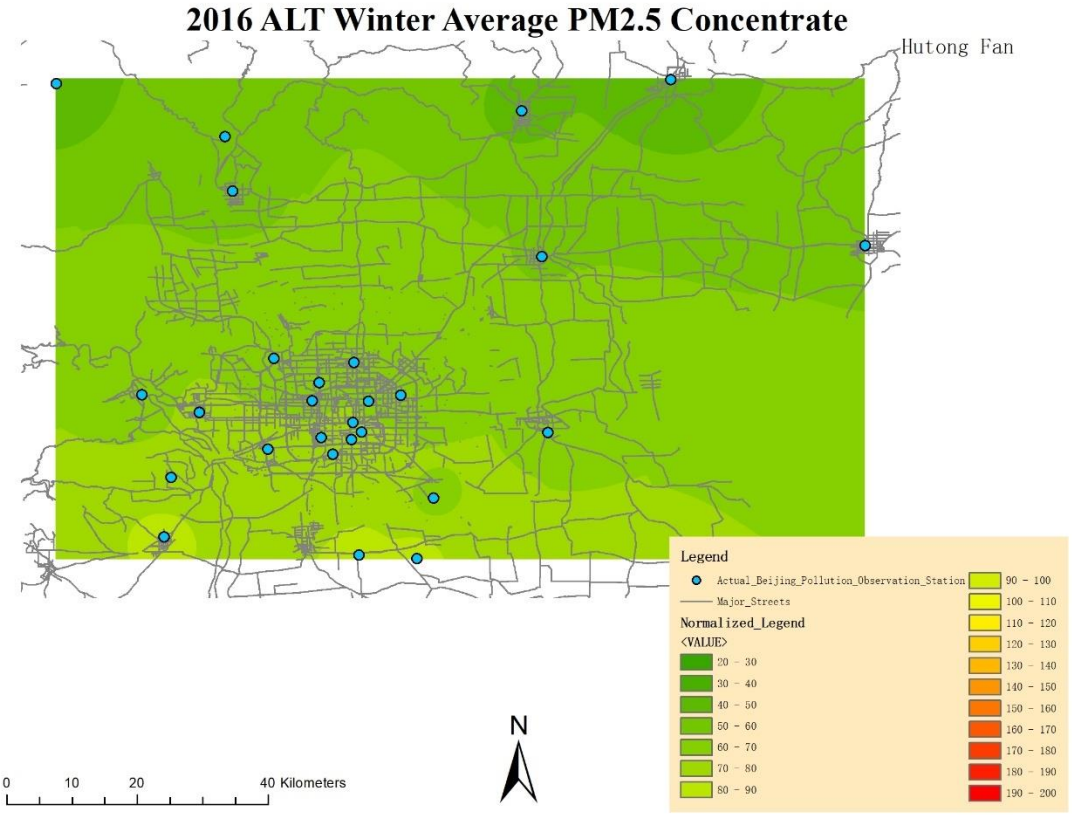
2016 ALT Winter Average PM2.5 Concentrate
Hutong Fan
Legend
Actual_Beijing_Pollution_Observation_Station
Major_Streets
Normalized_Legend
<VALUE>
20 - 30
30 - 40
40 - 50
50 - 60
60 - 70
70 - 80
80 - 90
90 - 100
100 - 110
110 - 120
120 - 130
130 - 140
140 - 150
150 - 160
160 - 170
170 - 180
180 - 190
190 - 200
N
0
10
20
40 Kilometers

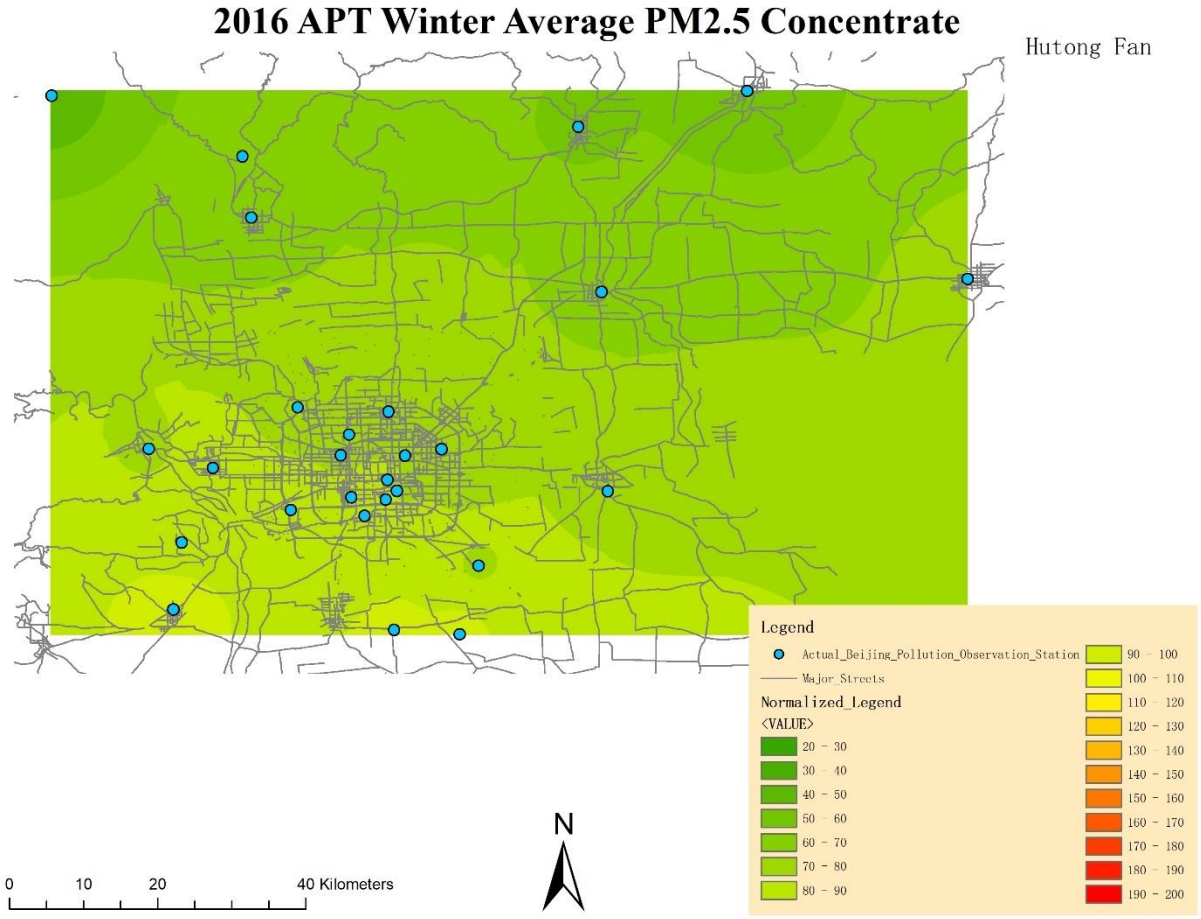
2016 APT Winter Average PM2.5 Concentrate
Hutong Fan
Legend
Actual_Beijing_Pollution_Observation_Station
Major_Streets
Normalized_Legend
<VALUE>
20 - 30
30 - 40
40 - 50
50 - 60
60 - 70
70 - 80
80 - 90
90 - 100
100 - 110
110 - 120
120 - 130
130 - 140
140 - 150
150 - 160
160 - 170
170 - 180
180 - 190
190 - 200
N
0
10
20
40 Kilometers

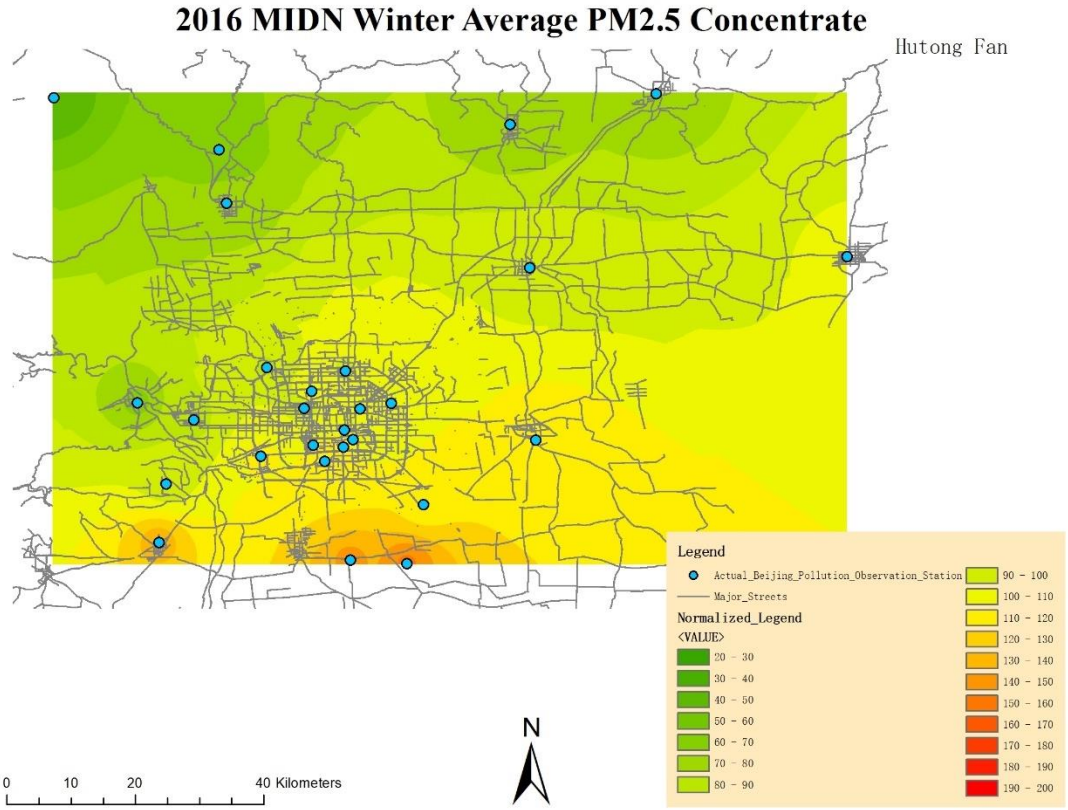
2016 MIDN Winter Average PM2.5 Concentrate
Hutong Fan
Legend
Actual_Beijing_Pollution_Observation_Station
Major_Streets
Normalized_Legend
<VALUE>
20 - 30
30 - 40
40 - 50
50 - 60
60 - 70
70 - 80
80 - 90
90 - 100
100 - 110
110 - 120
120 - 130
130 - 140
140 - 150
150 - 160
160 - 170
170 - 180
180 - 190
190 - 200
N
0
10
20
40 Kilometers

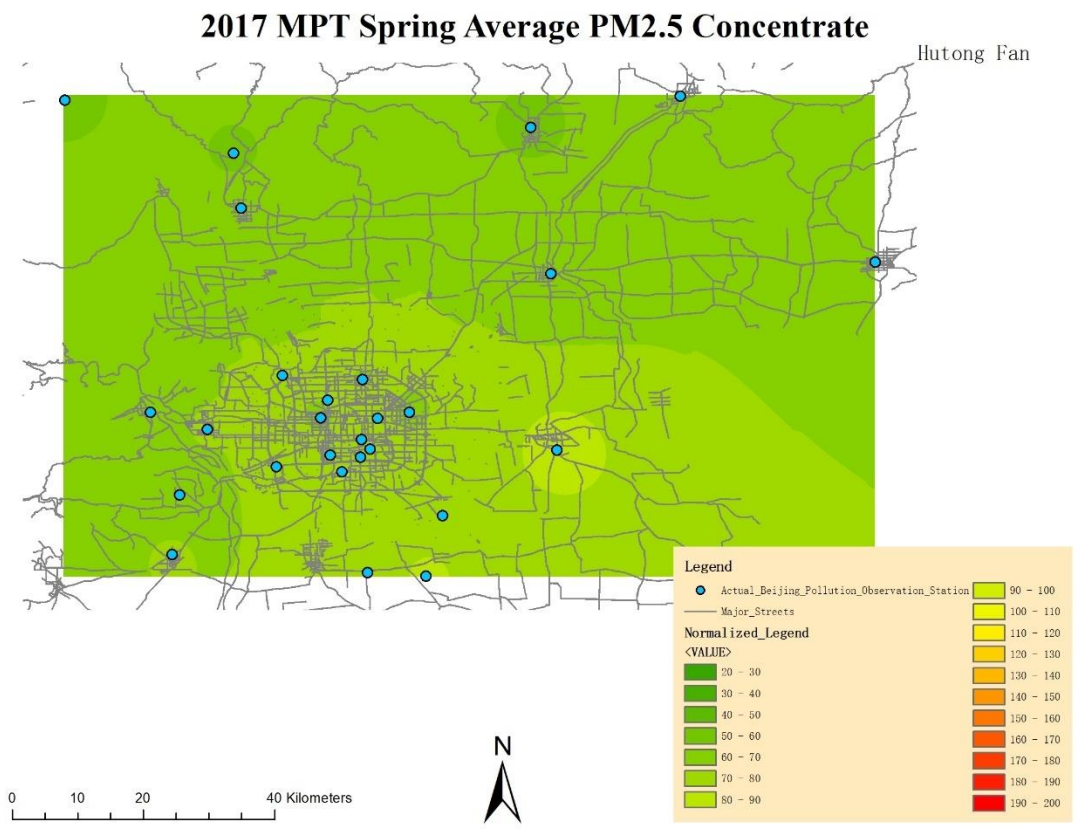
2017 MPT Spring Average PM2.5 Concentrate
Hutong Fan
Legend
Actual_Beijing_Pollution_Observation_Station
Major_Streets
Normalized_Legend
<VALUE>
20 - 30
30 - 40
40 - 50
50 - 60
60 - 70
70 - 80
80 - 90
90 - 100
100 - 110
110 - 120
120 - 130
130 - 140
140 - 150
150 - 160
160 - 170
170 - 180
180 - 190
190 - 200
N
0
10
20
40 Kilometers

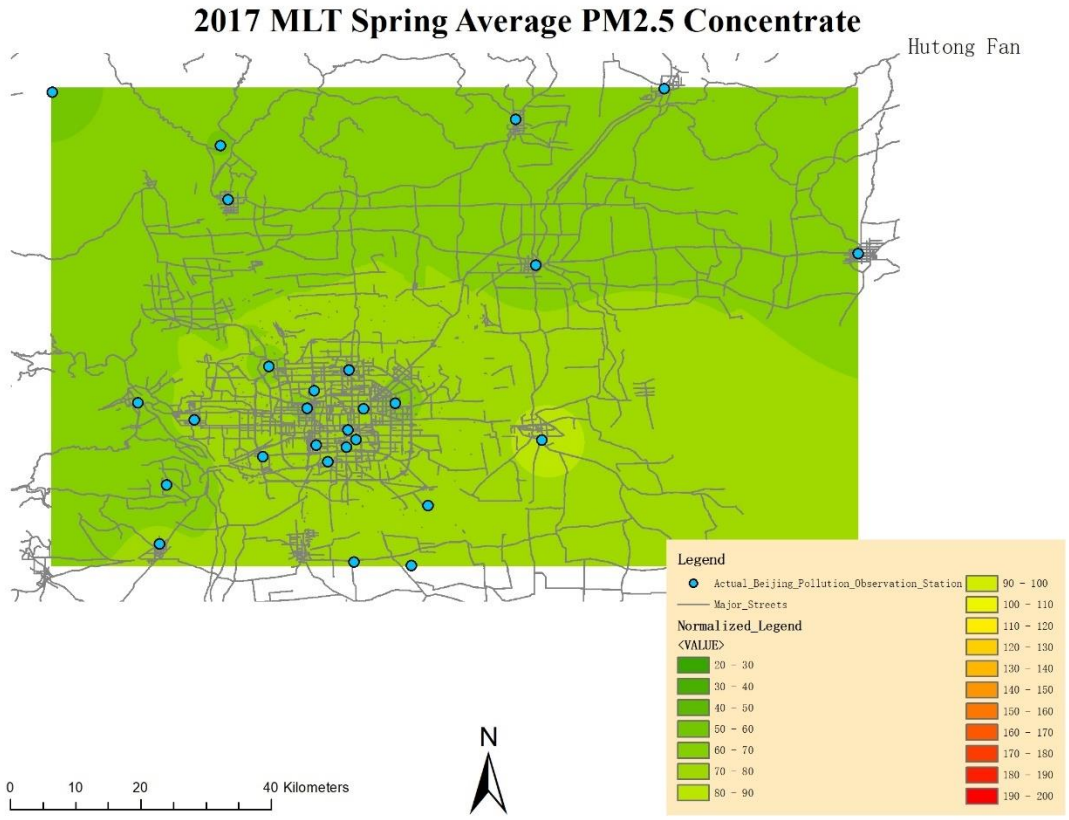
2017 MLT Spring Average PM2.5 Concentrate
Hutong Fan
Legend
Actual_Beijing_Pollution_Observation_Station
Major_Streets
Normalized_Legend
<VALUE>
20 - 30
30 - 40
40 - 50
50 - 60
60 - 70
70 - 80
80 - 90
90 - 100
100 - 110
110 - 120
120 - 130
130 - 140
140 - 150
150 - 160
160 - 170
170 - 180
180 - 190
190 - 200
N
0
10
20
40 Kilometers

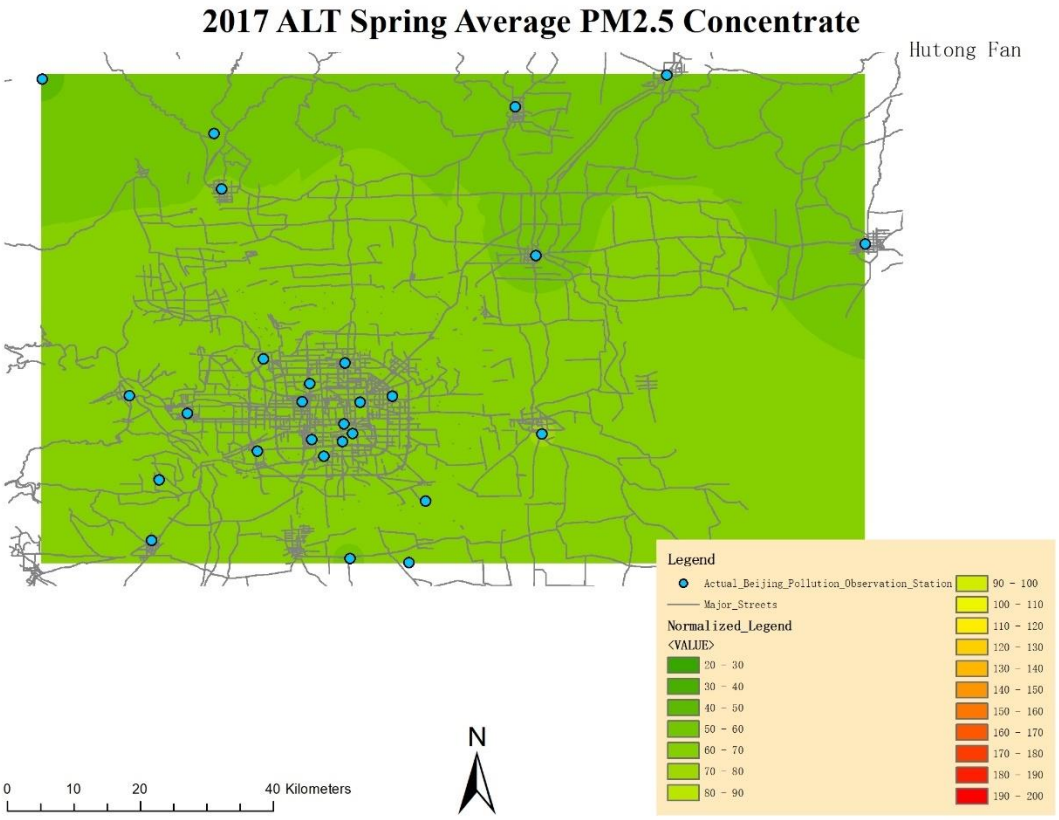
2017 ALT Spring Average PM2.5 Concentrate
Hutong Fan
Legend
Actual_Beijing_Pollution_Observation_Station
Major_Streets
Normalized_Legend
<VALUE>
20 - 30
30 - 40
40 - 50
50 - 60
60 - 70
70 - 80
80 - 90
90 - 100
100 - 110
110 - 120
120 - 130
130 - 140
140 - 150
150 - 160
160 - 170
170 - 180
180 - 190
190 - 200
N
0
10
20
40 Kilometers

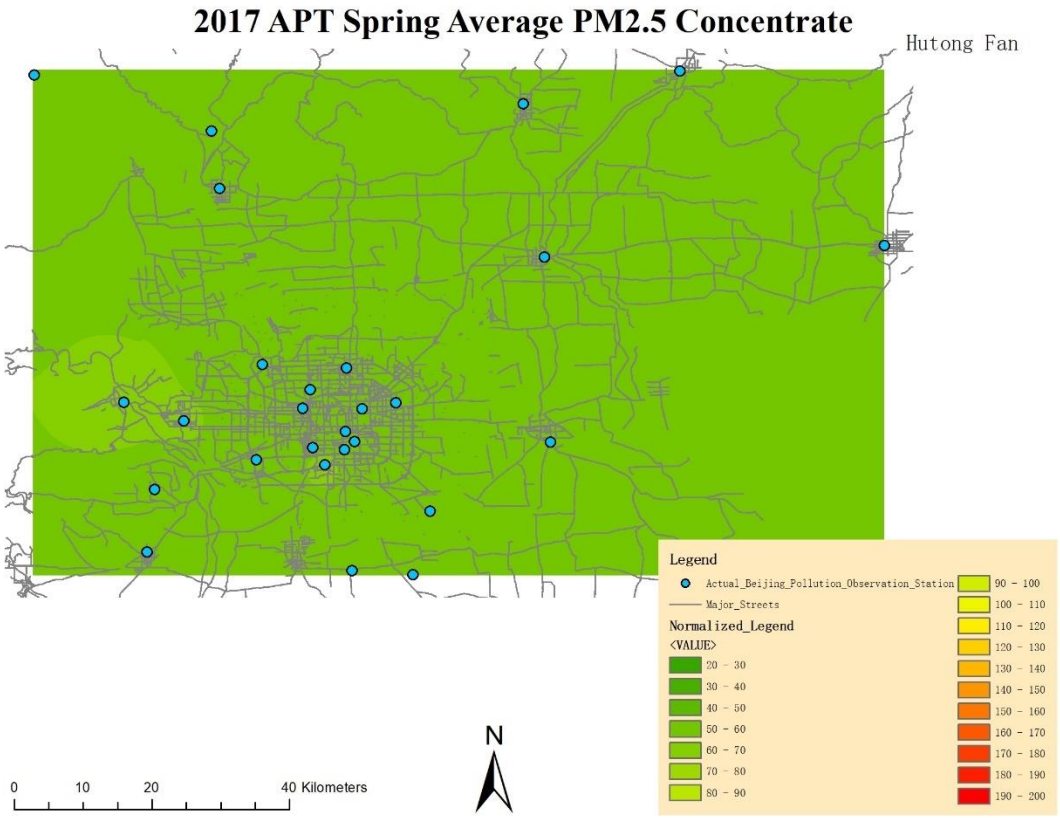
2017 APT Spring Average PM2.5 Concentrate
Hutong Fan
Legend
Actual_Beijing_Pollution_Observation_Station
Major_Streets
Normalized_Legend
<VALUE>
20 - 30
30 - 40
40 - 50
50 - 60
60 - 70
70 - 80
80 - 90
90 - 100
100 - 110
110 - 120
120 - 130
130 - 140
140 - 150
150 - 160
160 - 170
170 - 180
180 - 190
190 - 200
N
0
10
20
40 Kilometers

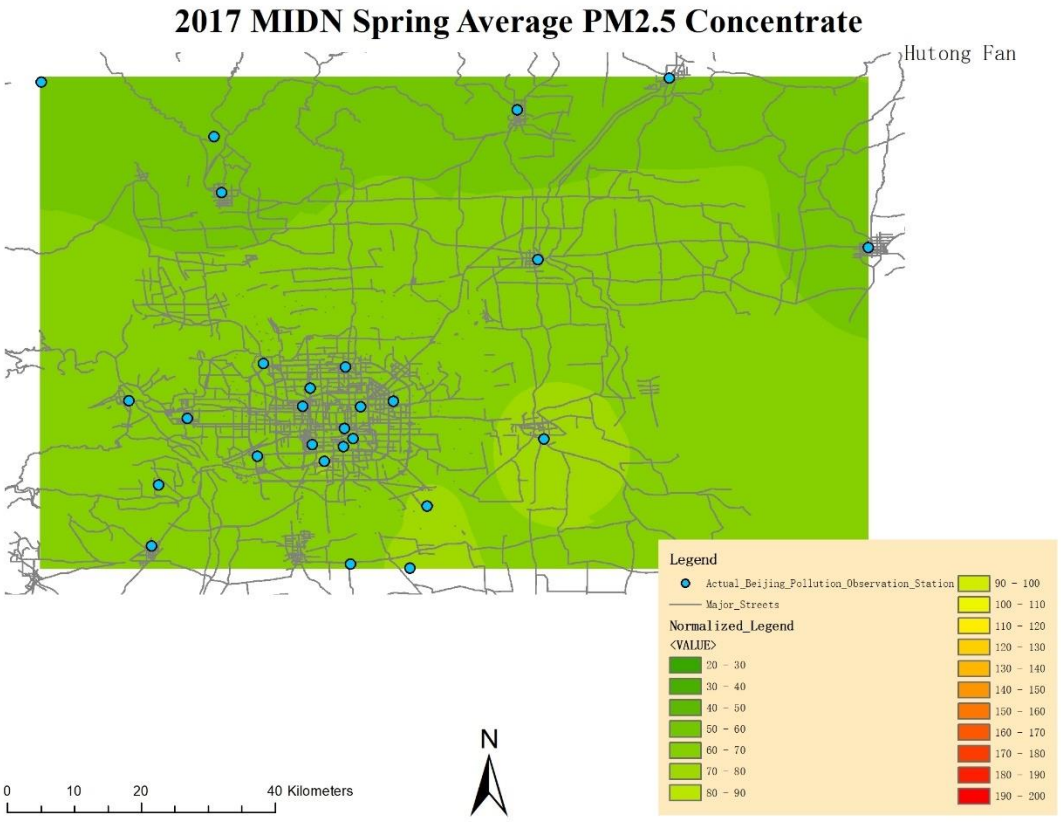
2017 MIDN Spring Average PM2.5 Concentrate
Hutong Fan
Legend
Actual_Beijing_Pollution_Observation_Station
Major_Streets
Normalized_Legend
<VALUE>
20 - 30
30 - 40
40 - 50
50 - 60
60 - 70
70 - 80
80 - 90
90 - 100
100 - 110
110 - 120
120 - 130
130 - 140
140 - 150
150 - 160
160 - 170
170 - 180
180 - 190
190 - 200
N
0
10
20
40 Kilometers

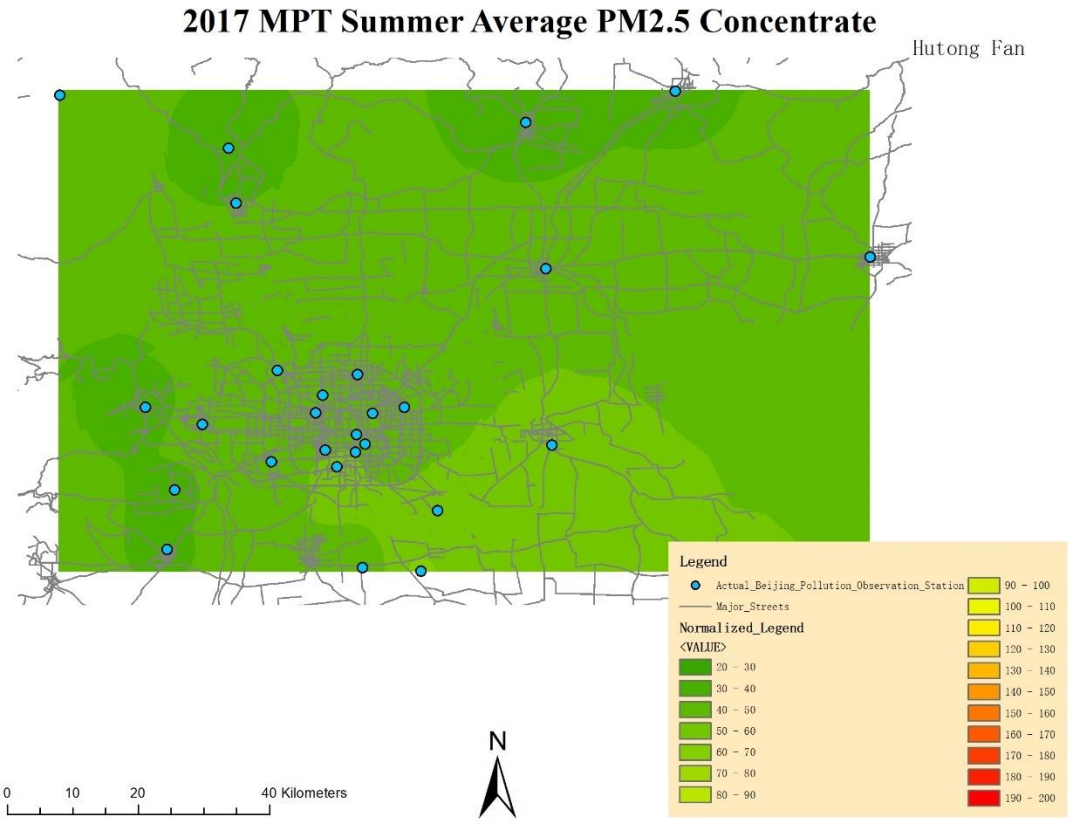
2017 MPT Summer Average PM2.5 Concentrate
Hutong Fan
Legend
Actual_Beijing_Pollution_Observation_Station
Major_Streets
Normalized_Legend
<VALUE>
20 - 30
30 - 40
40 - 50
50 - 60
60 - 70
70 - 80
80 - 90
90 - 100
100 - 110
110 - 120
120 - 130
130 - 140
140 - 150
150 - 160
160 - 170
170 - 180
180 - 190
190 - 200
N
0
10
20
40 Kilometers

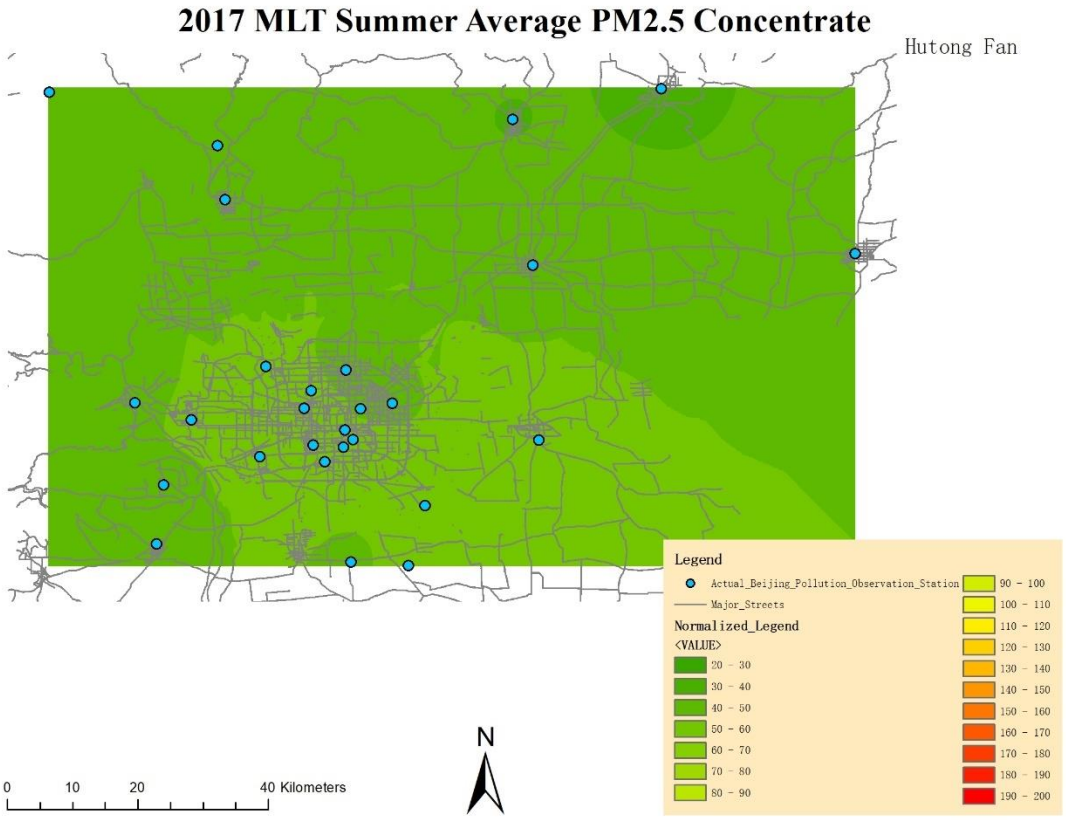
2017 MLT Summer Average PM2.5 Concentrate
Hutong Fan
Legend
Actual_Beijing_Pollution_Observation_Station
Major_Streets
Normalized_Legend
<VALUE>
20 - 30
30 - 40
40 - 50
50 - 60
60 - 70
70 - 80
80 - 90
90 - 100
100 - 110
110 - 120
120 - 130
130 - 140
140 - 150
150 - 160
160 - 170
170 - 180
180 - 190
190 - 200
N
0
10
20
40 Kilometers

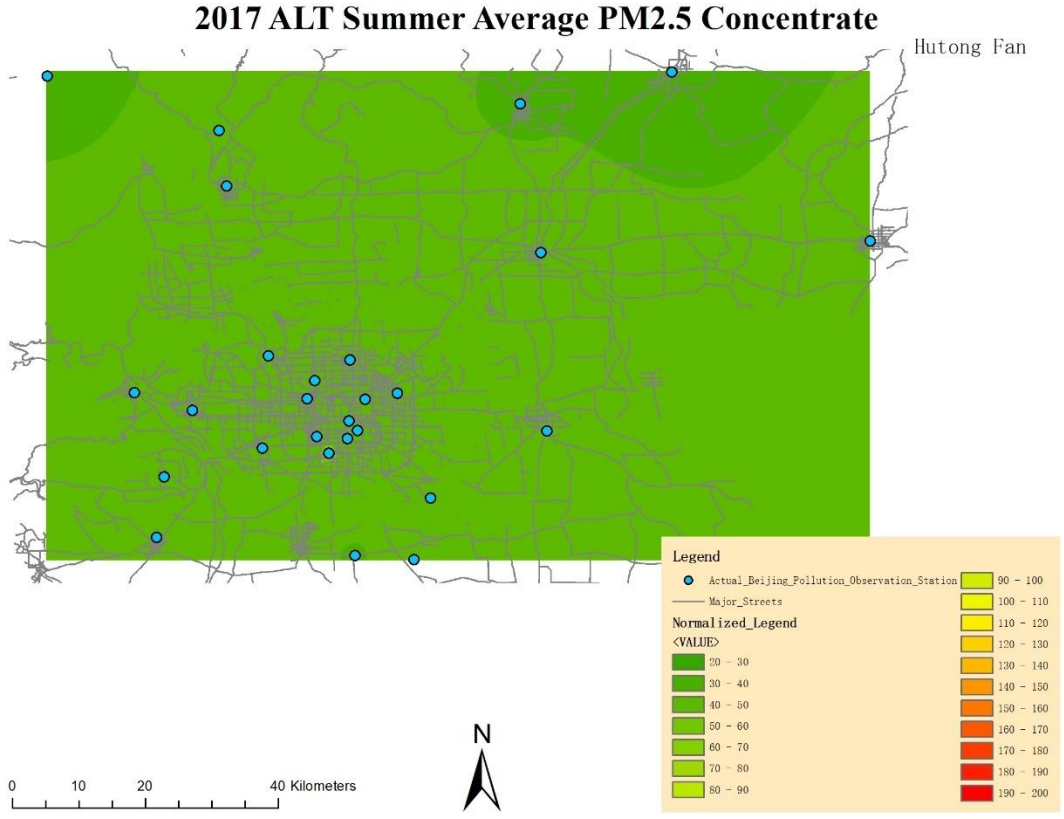
2017 ALT Summer Average PM2.5 Concentrate
Hutong Fan
Legend
Actual_Beijing_Pollution_Observation_Station
Major_Streets
Normalized_Legend
<VALUE>
20 - 30
30 - 40
40 - 50
50 - 60
60 - 70
70 - 80
80 - 90
90 - 100
100 - 110
110 - 120
120 - 130
130 - 140
140 - 150
150 - 160
160 - 170
170 - 180
180 - 190
190 - 200
N
0
10
20
40 Kilometers

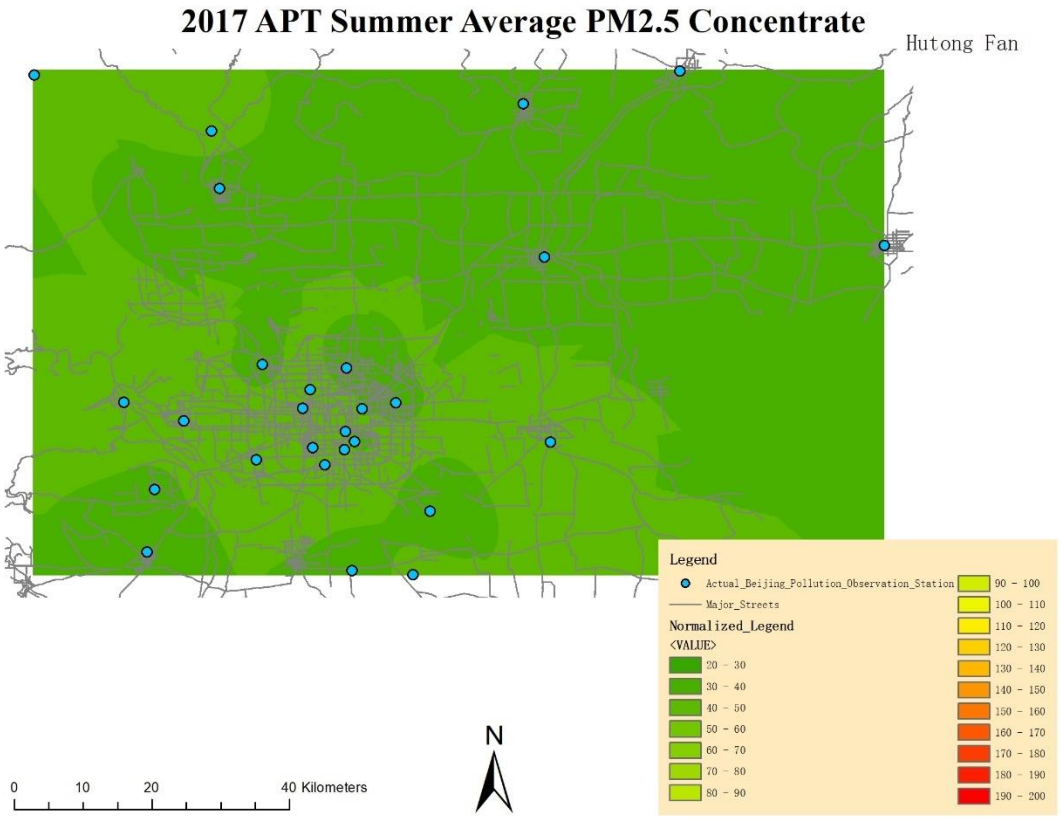
2017 APT Summer Average PM2.5 Concentrate
Hutong Fan
Legend
Actual_Beijing_Pollution_Observation_Station
Major_Streets
Normalized_Legend
<VALUE>
20 - 30
30 - 40
40 - 50
50 - 60
60 - 70
70 - 80
80 - 90
90 - 100
100 - 110
110 - 120
120 - 130
130 - 140
140 - 150
150 - 160
160 - 170
170 - 180
180 - 190
190 - 200
N
0
10
20
40 Kilometers

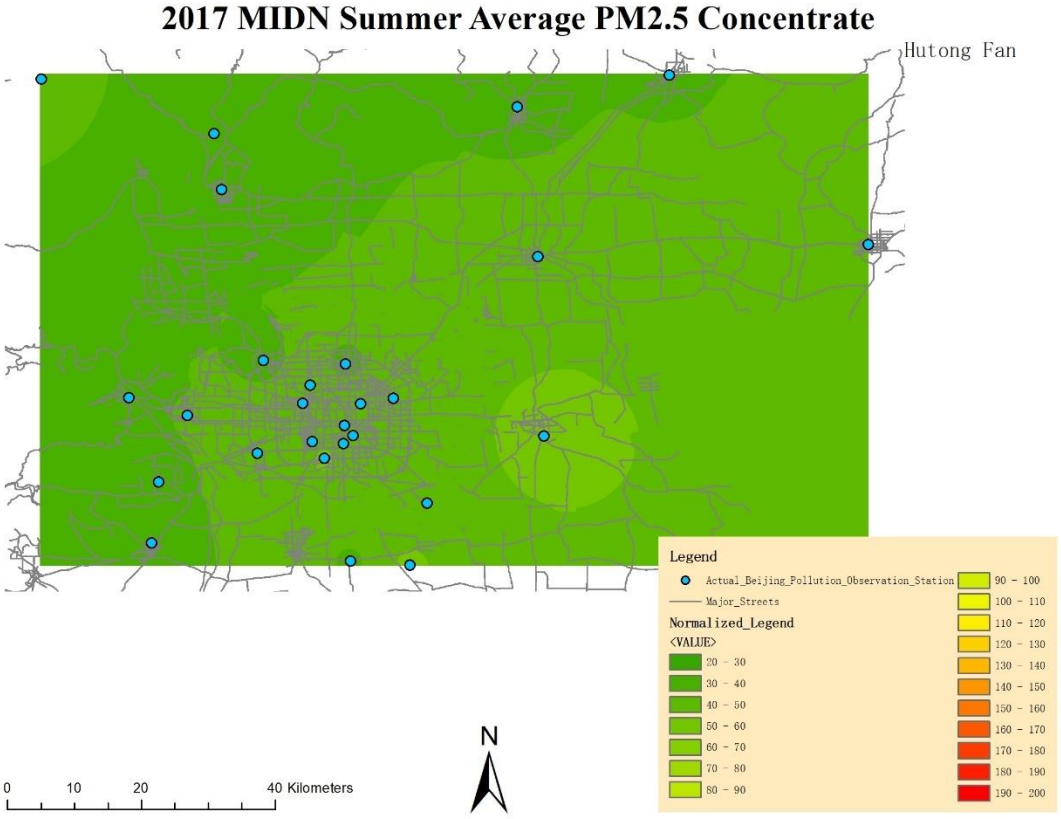
2017 MIDN Summer Average PM2.5 Concentrate
Hutong Fan
Legend
Actual_Beijing_Pollution_Observation_Station
Major_Streets
Normalized_Legend
<VALUE>
20 - 30
30 - 40
40 - 50
50 - 60
60 - 70
70 - 80
80 - 90
90 - 100
100 - 110
110 - 120
120 - 130
130 - 140
140 - 150
150 - 160
160 - 170
170 - 180
180 - 190
190 - 200
N
0
10
20
40 Kilometers

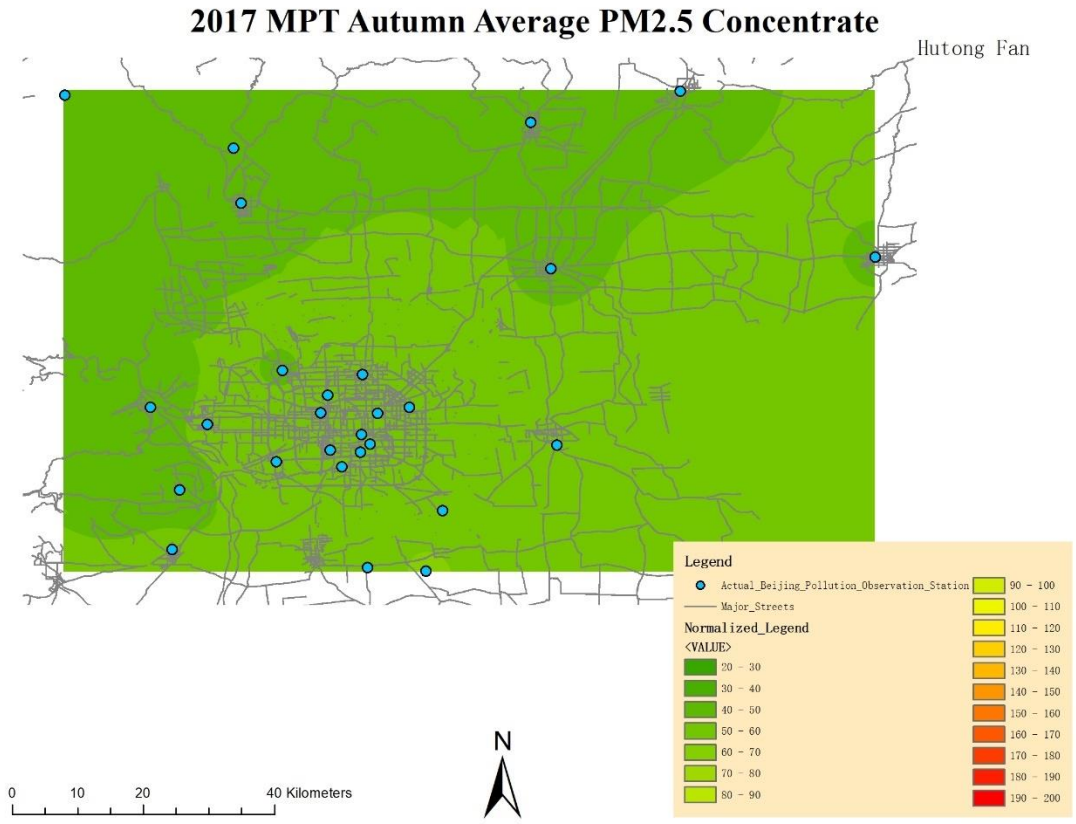
2017 MPT Autumn Average PM2.5 Concentrate
Hutong Fan
Legend
Actual_Beijing_Pollution_Observation_Station
Major_Streets
Normalized_Legend
<VALUE>
20 - 30
30 - 40
40 - 50
50 - 60
60 - 70
70 - 80
80 - 90
90 - 100
100 - 110
110 - 120
120 - 130
130 - 140
140 - 150
150 - 160
160 - 170
170 - 180
180 - 190
190 - 200
N
0
10
20
40 Kilometers

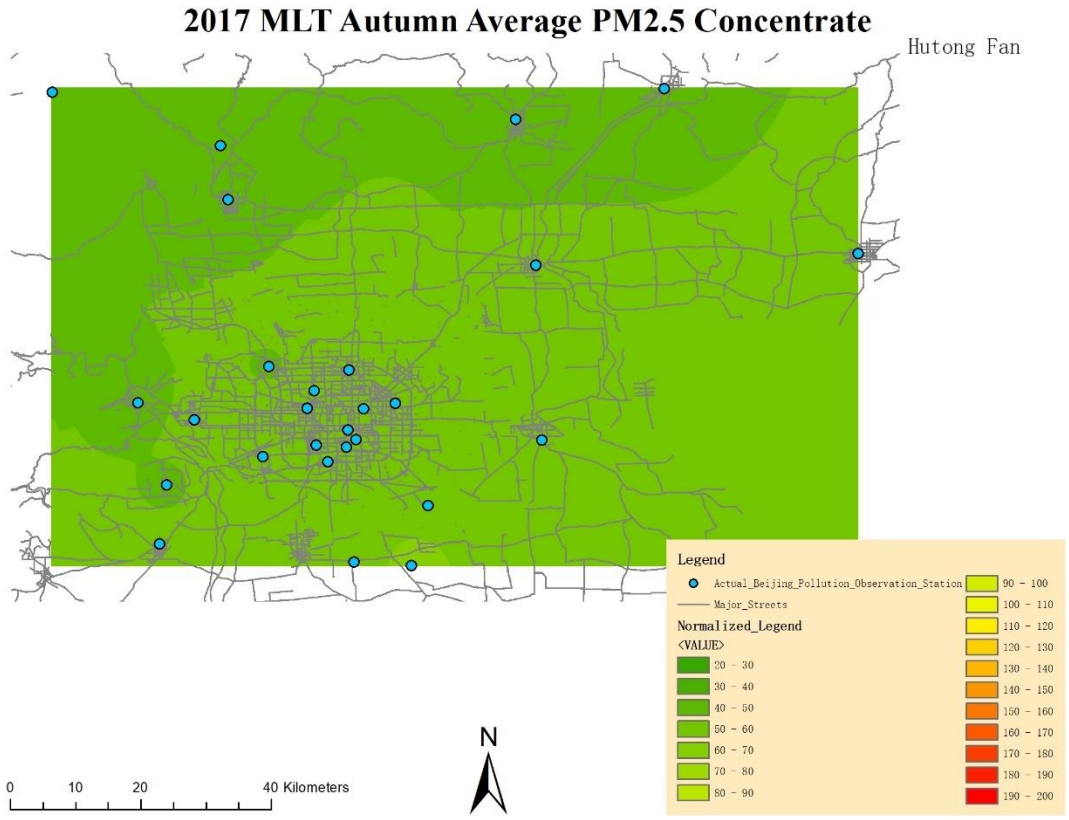
2017 MLT Autumn Average PM2.5 Concentrate
Hutong Fan
Legend
Actual_Beijing_Pollution_Observation_Station
Major_Streets
Normalized_Legend
<VALUE>
20 - 30
30 - 40
40 - 50
50 - 60
60 - 70
70 - 80
80 - 90
90 - 100
100 - 110
110 - 120
120 - 130
130 - 140
140 - 150
150 - 160
160 - 170
170 - 180
180 - 190
190 - 200
N
0
10
20
40 Kilometers

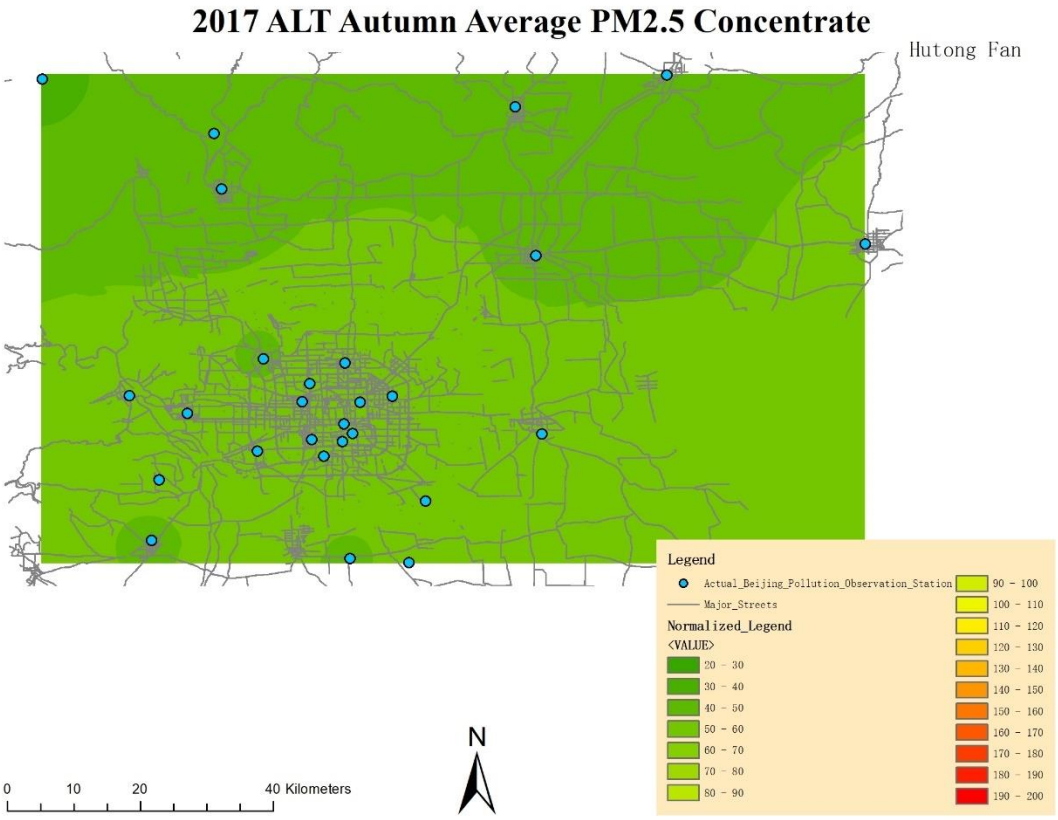
2017 ALT Autumn Average PM2.5 Concentrate
Hutong Fan
Legend
Actual_Beijing_Pollution_Observation_Station
Major_Streets
Normalized_Legend
<VALUE>
20 - 30
30 - 40
40 - 50
50 - 60
60 - 70
70 - 80
80 - 90
90 - 100
100 - 110
110 - 120
120 - 130
130 - 140
140 - 150
150 - 160
160 - 170
170 - 180
180 - 190
190 - 200
N
0
10
20
40 Kilometers

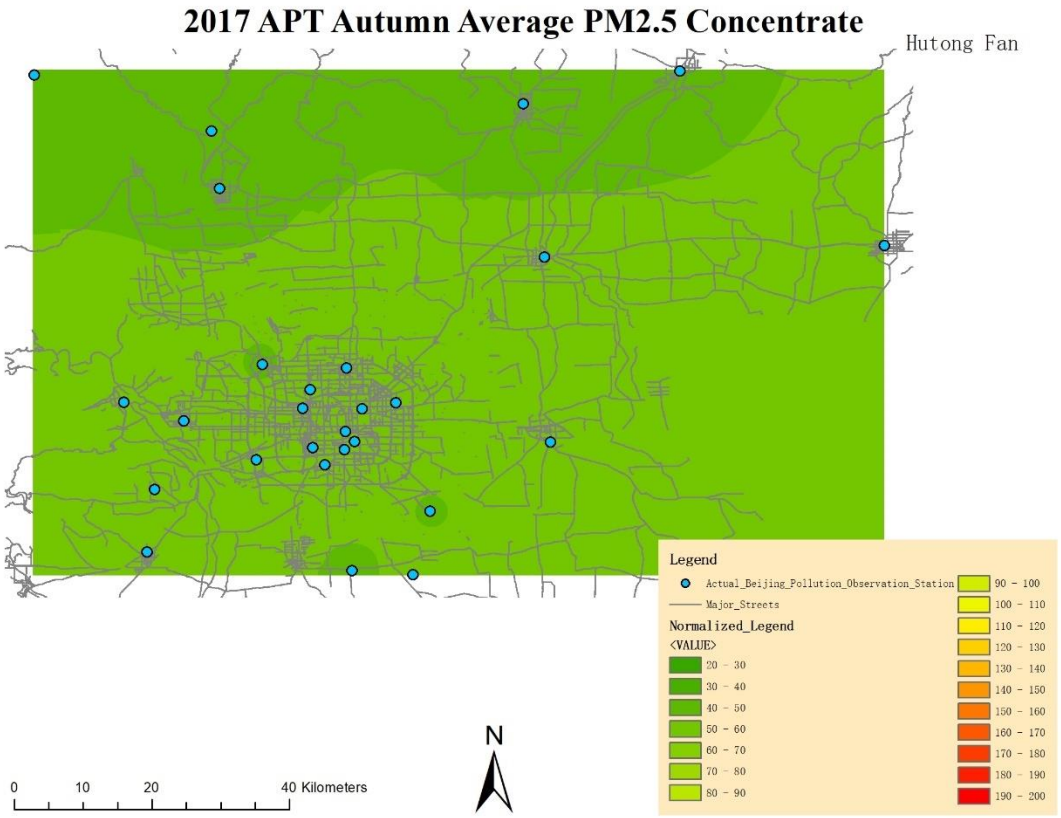
2017 APT Autumn Average PM2.5 Concentrate
Hutong Fan
Legend
Actual_Beijing_Pollution_Observation_Station
Major_Streets
Normalized_Legend
<VALUE>
20 - 30
30 - 40
40 - 50
50 - 60
60 - 70
70 - 80
80 - 90
90 - 100
100 - 110
110 - 120
120 - 130
130 - 140
140 - 150
150 - 160
160 - 170
170 - 180
180 - 190
190 - 200
N
0
10
20
40 Kilometers

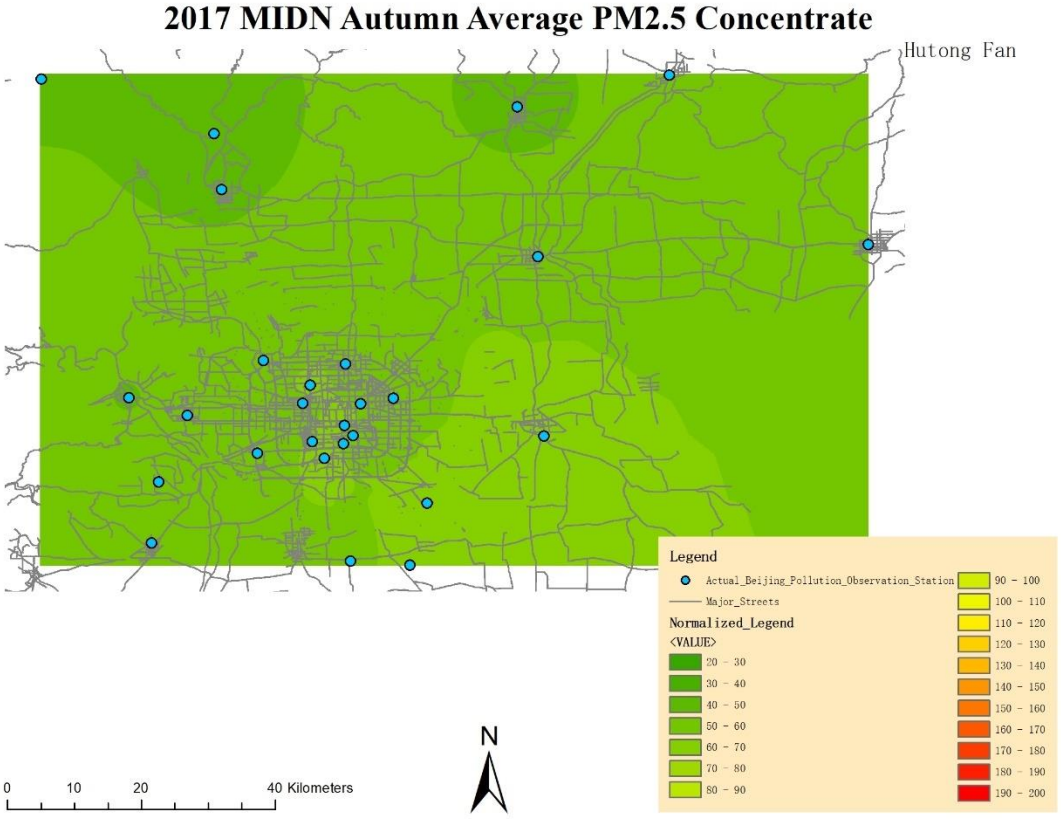
2017 MIDN Autumn Average PM2.5 Concentrate
Hutong Fan
Legend
Actual_Beijing_Pollution_Observation_Station
Major_Streets
Normalized_Legend
<VALUE>
20 - 30
30 - 40
40 - 50
50 - 60
60 - 70
70 - 80
80 - 90
90 - 100
100 - 110
110 - 120
120 - 130
130 - 140
140 - 150
150 - 160
160 - 170
170 - 180
180 - 190
190 - 200
N
0
10
20
40 Kilometers

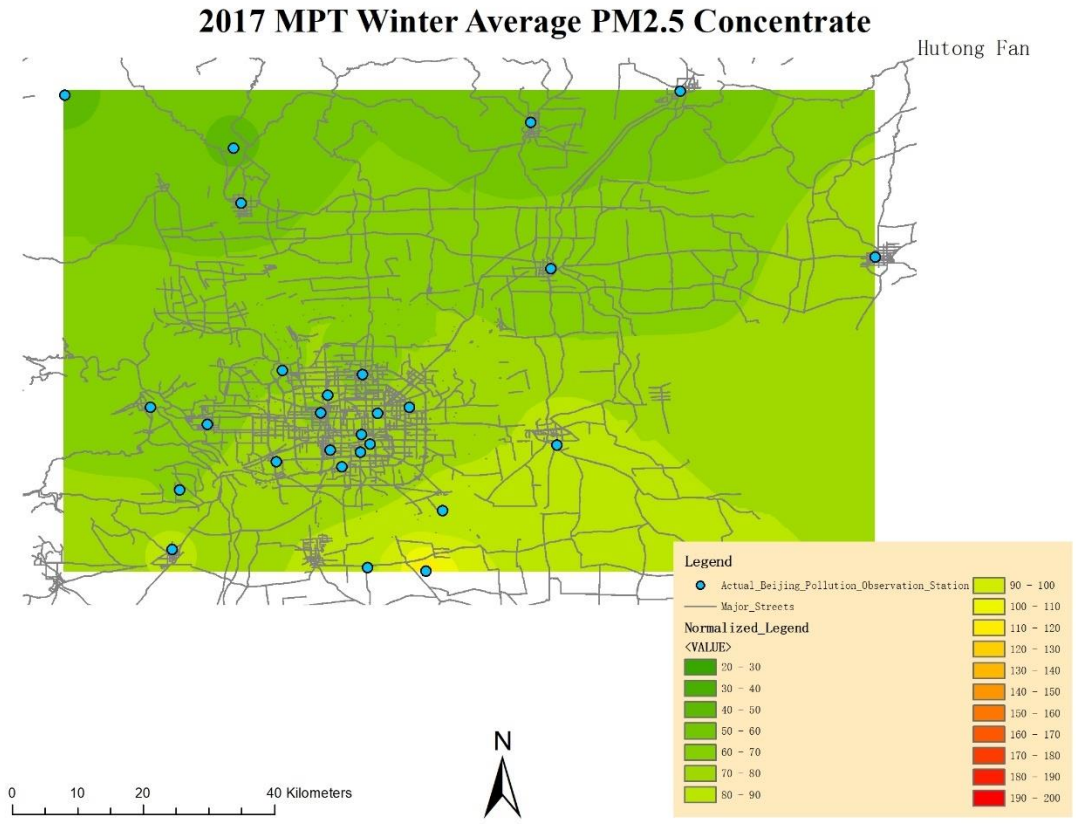
2017 MPT Winter Average PM2.5 Concentrate
Hutong Fan
Legend
Actual_Beijing_Pollution_Observation_Station
Major_Streets
Normalized_Legend
<VALUE>
20 - 30
30 - 40
40 - 50
50 - 60
60 - 70
70 - 80
80 - 90
90 - 100
100 - 110
110 - 120
120 - 130
130 - 140
140 - 150
150 - 160
160 - 170
170 - 180
180 - 190
190 - 200
N
0
10
20
40 Kilometers

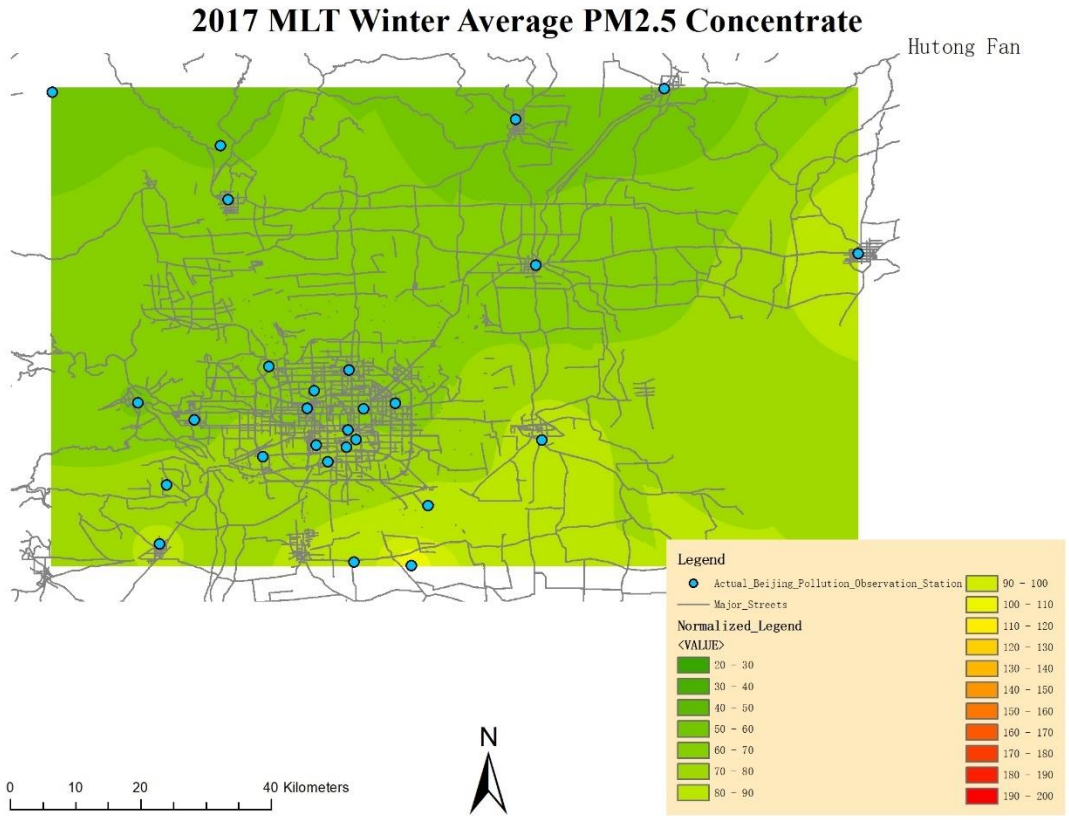
2017 MLT Winter Average PM2.5 Concentrate
Hutong Fan
Legend
Actual_Beijing_Pollution_Observation_Station
Major_Streets
Normalized_Legend
<VALUE>
20 - 30
30 - 40
40 - 50
50 - 60
60 - 70
70 - 80
80 - 90
90 - 100
100 - 110
110 - 120
120 - 130
130 - 140
140 - 150
150 - 160
160 - 170
170 - 180
180 - 190
190 - 200
N
0
10
20
40 Kilometers

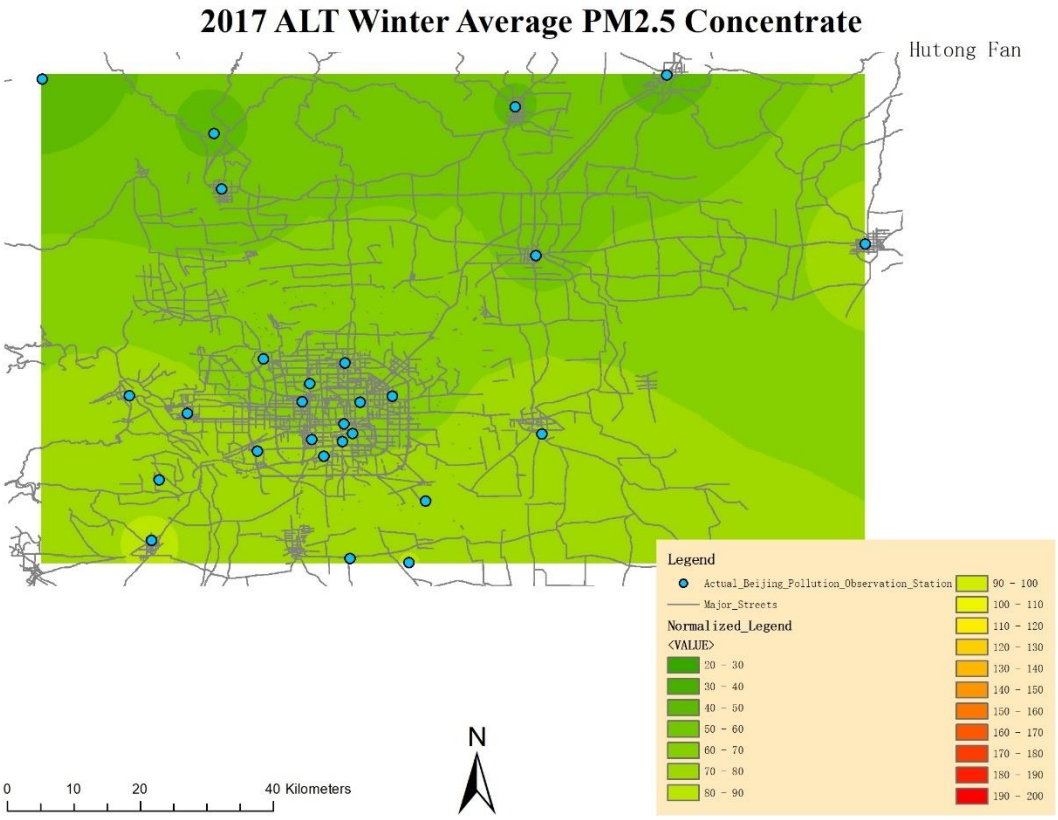
2017 ALT Winter Average PM2.5 Concentrate
Hutong Fan
Legend
Actual_Beijing_Pollution_Observation_Station
Major_Streets
Normalized_Legend
<VALUE>
20 - 30
30 - 40
40 - 50
50 - 60
60 - 70
70 - 80
80 - 90
90 - 100
100 - 110
110 - 120
120 - 130
130 - 140
140 - 150
150 - 160
160 - 170
170 - 180
180 - 190
190 - 200
N
0
10
20
40 Kilometers

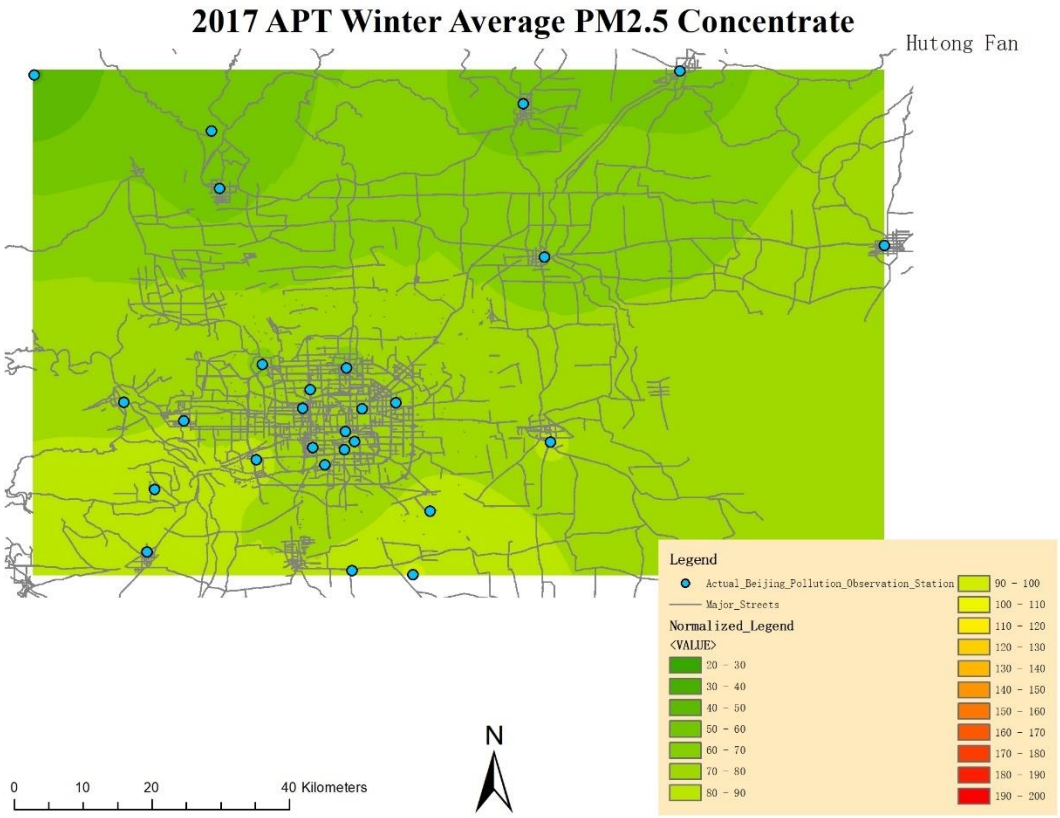
2017 APT Winter Average PM2.5 Concentrate
Hutong Fan
Legend
Actual_Beijing_Pollution_Observation_Station
Major_Streets
Normalized_Legend
<VALUE>
20 - 30
30 - 40
40 - 50
50 - 60
60 - 70
70 - 80
80 - 90
90 - 100
100 - 110
110 - 120
120 - 130
130 - 140
140 - 150
150 - 160
160 - 170
170 - 180
180 - 190
190 - 200
N
0
10
20
40 Kilometers

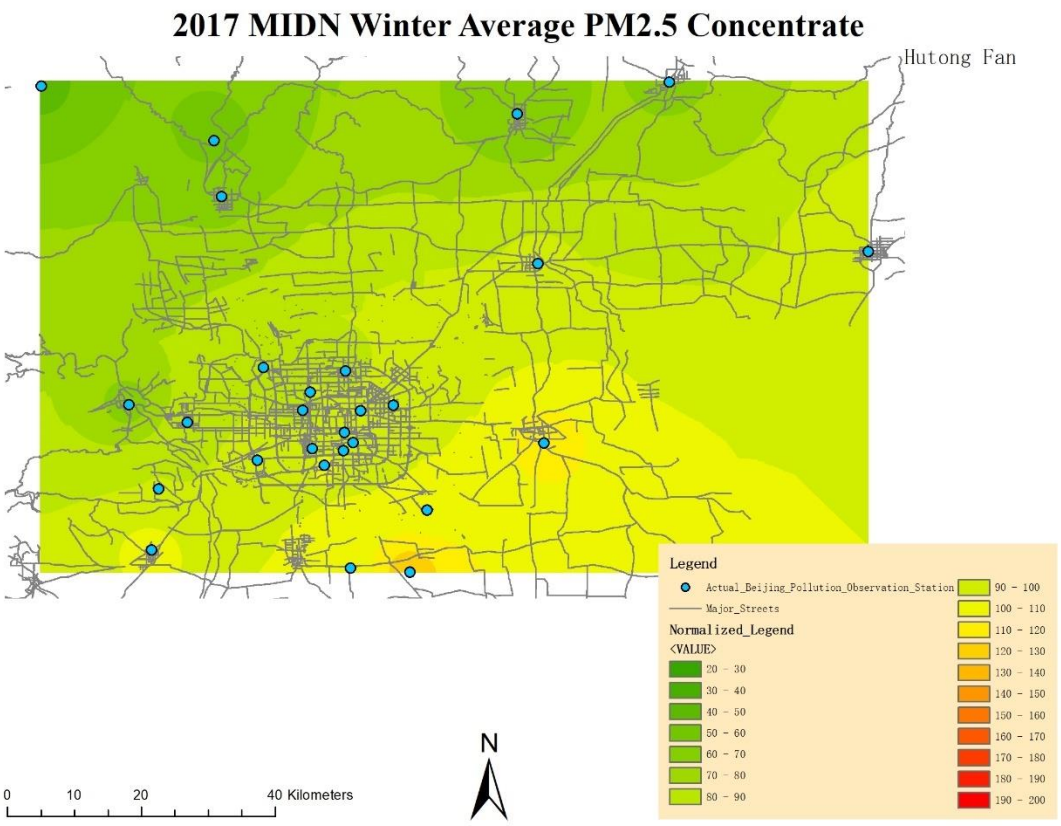
2017 MIDN Winter Average PM2.5 Concentrate
Hutong Fan
Legend
Actual_Beijing_Pollution_Observation_Station
Major_Streets
Normalized_Legend
<VALUE>
20 - 30
30 - 40
40 - 50
50 - 60
60 - 70
70 - 80
80 - 90
90 - 100
100 - 110
110 - 120
120 - 130
130 - 140
140 - 150
150 - 160
160 - 170
170 - 180
180 - 190
190 - 200
N
0
10
20
40 Kilometers

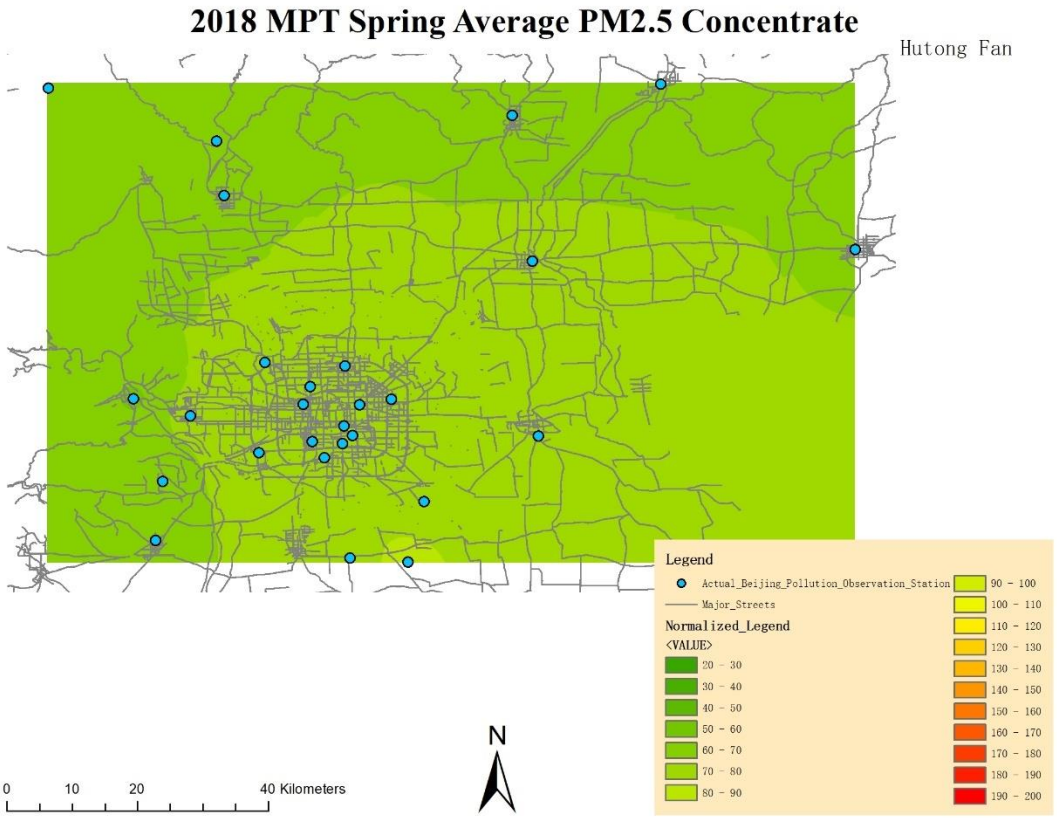
2018 MPT Spring Average PM2.5 Concentrate
Hutong Fan
Legend
Actual_Beijing_Pollution_Observation_Station
Major_Streets
Normalized_Legend
<VALUE>
20 - 30
30 - 40
40 - 50
50 - 60
60 - 70
70 - 80
80 - 90
90 - 100
100 - 110
110 - 120
120 - 130
130 - 140
140 - 150
150 - 160
160 - 170
170 - 180
180 - 190
190 - 200
N
0
10
20
40 Kilometers

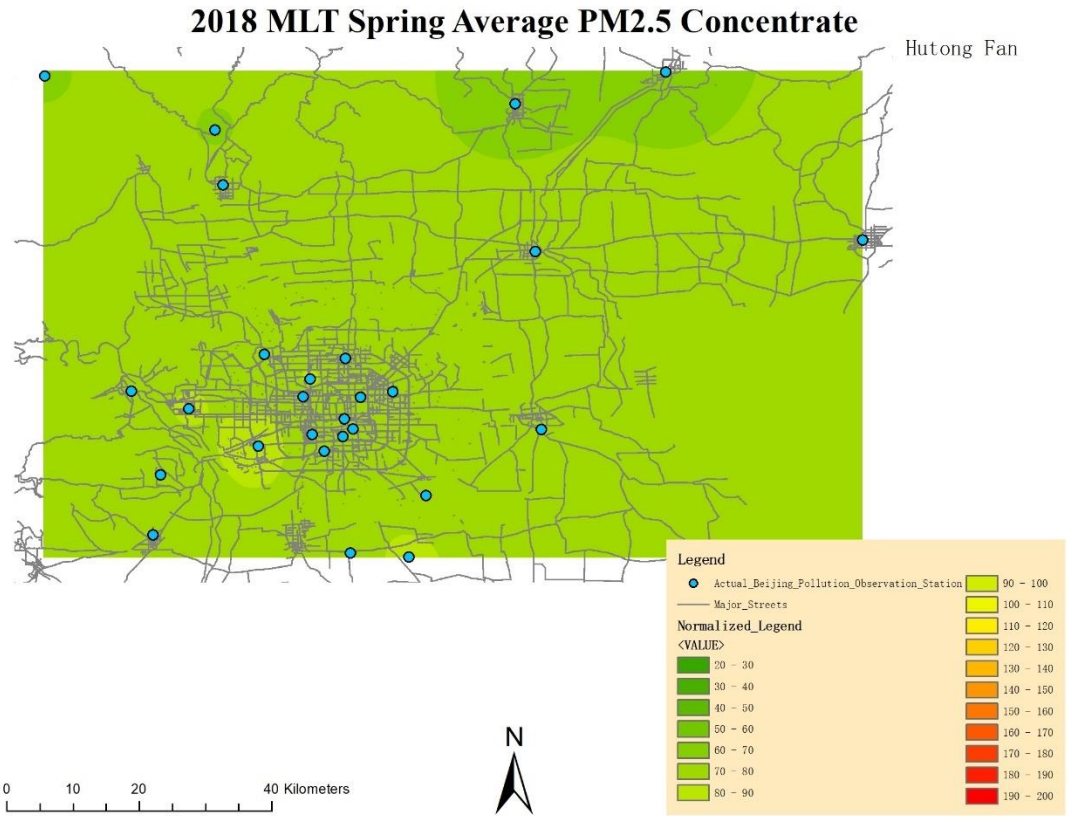
2018 MLT Spring Average PM2.5 Concentrate
Hutong Fan
Legend
Actual_Beijing_Pollution_Observation_Station
Major_Streets
Normalized_Legend
<VALUE>
20 - 30
30 - 40
40 - 50
50 - 60
60 - 70
70 - 80
80 - 90
90 - 100
100 - 110
110 - 120
120 - 130
130 - 140
140 - 150
150 - 160
160 - 170
170 - 180
180 - 190
190 - 200
N
0
10
20
40 Kilometers

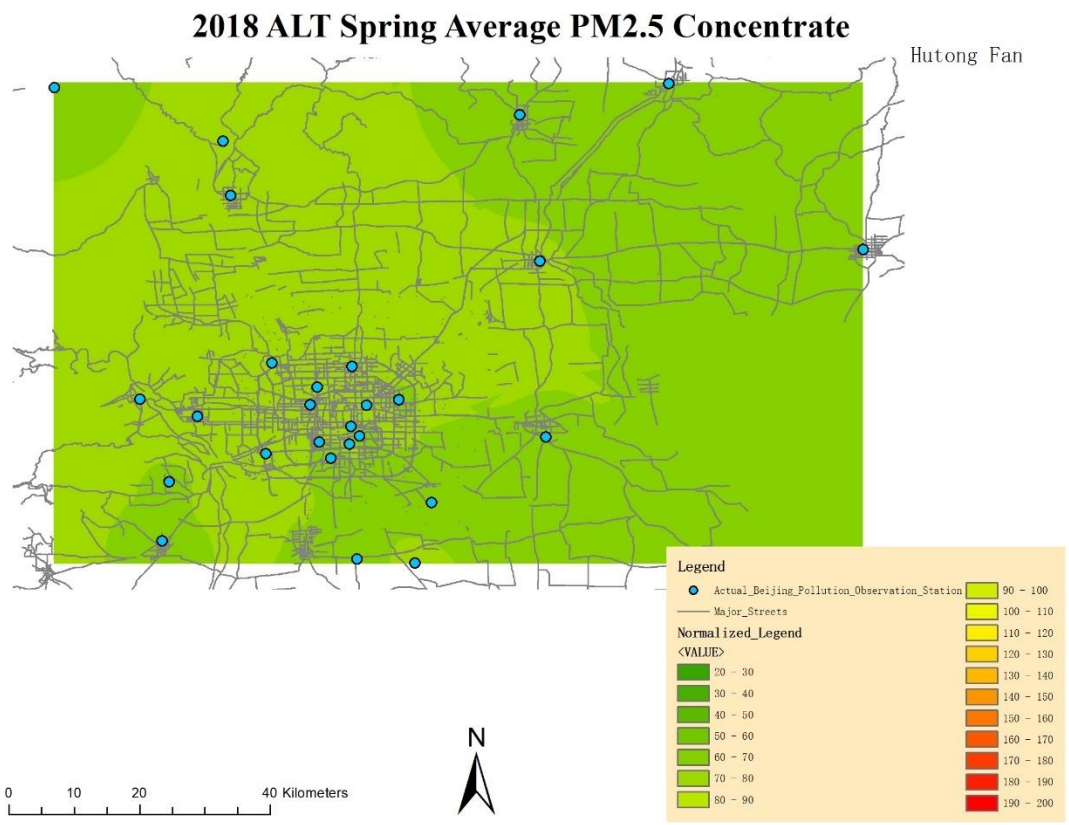
2018 ALT Spring Average PM2.5 Concentrate
Hutong Fan
Legend
Actual_Beijing_Pollution_Observation_Station
Major_Streets
Normalized_Legend
<VALUE>
20 - 30
30 - 40
40 - 50
50 - 60
60 - 70
70 - 80
80 - 90
90 - 100
100 - 110
110 - 120
120 - 130
130 - 140
140 - 150
150 - 160
160 - 170
170 - 180
180 - 190
190 - 200
N
0
10
20
40 Kilometers

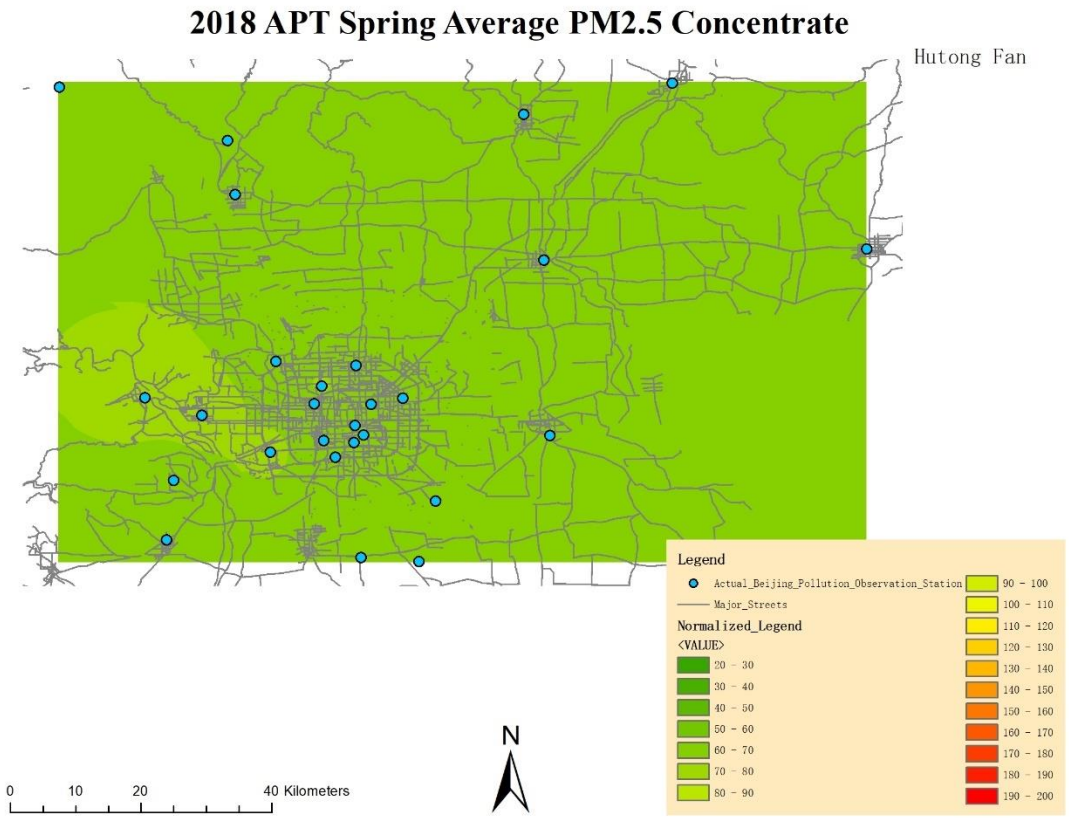
2018 APT Spring Average PM2.5 Concentrate
Hutong Fan
Legend
Actual_Beijing_Pollution_Observation_Station
Major_Streets
Normalized_Legend
<VALUE>
20 - 30
30 - 40
40 - 50
50 - 60
60 - 70
70 - 80
80 - 90
90 - 100
100 - 110
110 - 120
120 - 130
130 - 140
140 - 150
150 - 160
160 - 170
170 - 180
180 - 190
190 - 200
N
0
10
20
40 Kilometers

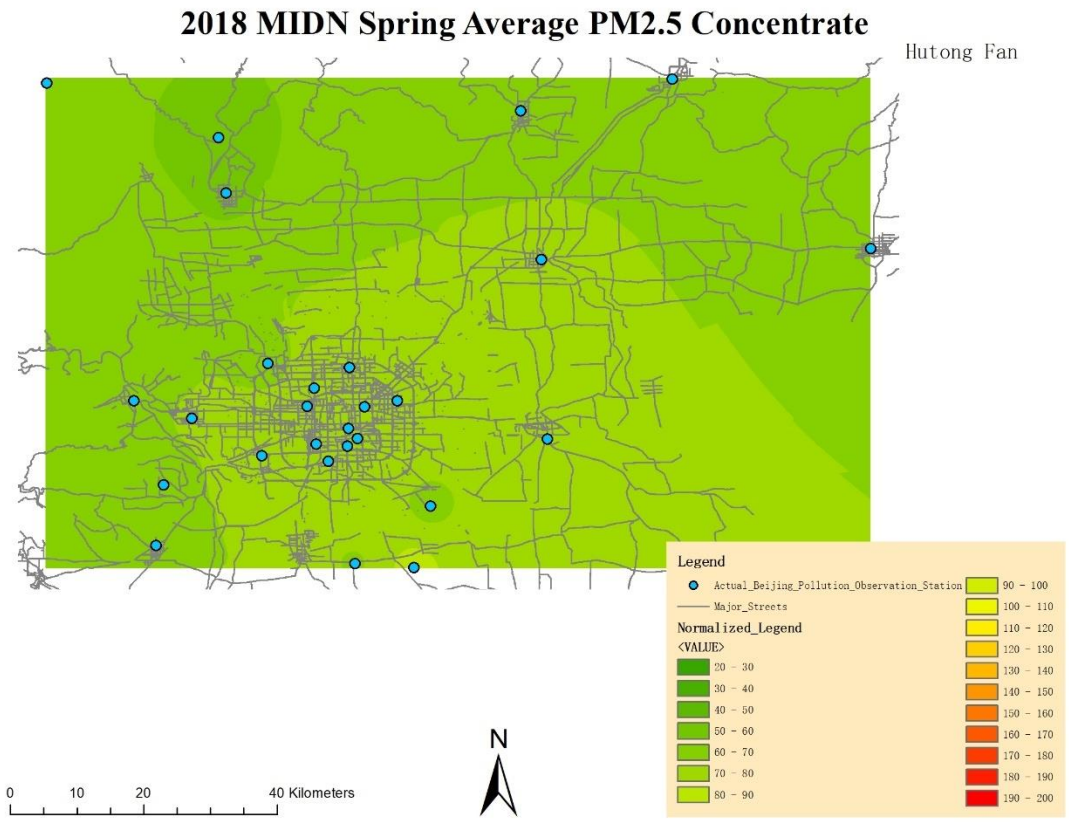
2018 MIDN Spring Average PM2.5 Concentrate
Hutong Fan
Legend
Actual_Beijing_Pollution_Observation_Station
Major_Streets
Normalized_Legend
<VALUE>
20 - 30
30 - 40
40 - 50
50 - 60
60 - 70
70 - 80
80 - 90
90 - 100
100 - 110
110 - 120
120 - 130
130 - 140
140 - 150
150 - 160
160 - 170
170 - 180
180 - 190
190 - 200
N
0
10
20
40 Kilometers

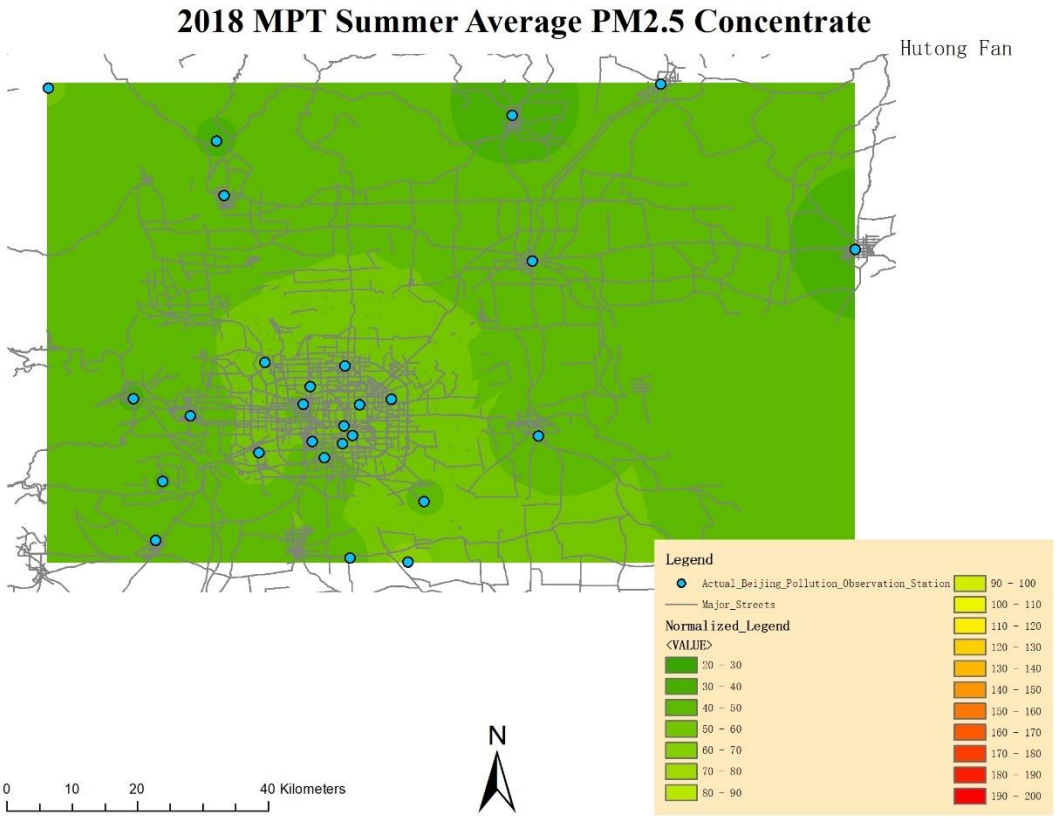
2018 MPT Summer Average PM2.5 Concentrate
Hutong Fan
Legend
Actual_Beijing_Pollution_Observation_Station
Major_Streets
Normalized_Legend
<VALUE>
20 - 30
30 - 40
40 - 50
50 - 60
60 - 70
70 - 80
80 - 90
90 - 100
100 - 110
110 - 120
120 - 130
130 - 140
140 - 150
150 - 160
160 - 170
170 - 180
180 - 190
190 - 200
N
0
10
20
40 Kilometers

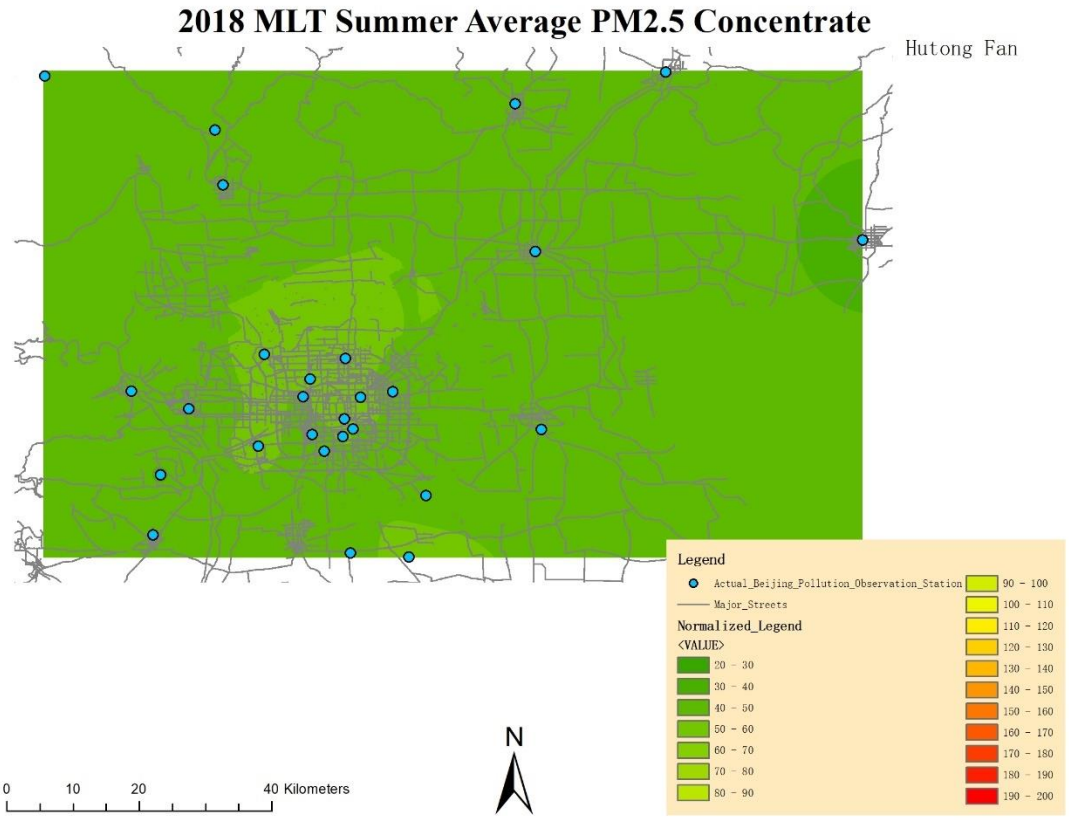
2018 MLT Summer Average PM2.5 Concentrate
Hutong Fan
Legend
Actual_Beijing_Pollution_Observation_Station
Major_Streets
Normalized_Legend
<VALUE>
20 - 30
30 - 40
40 - 50
50 - 60
60 - 70
70 - 80
80 - 90
90 - 100
100 - 110
110 - 120
120 - 130
130 - 140
140 - 150
150 - 160
160 - 170
170 - 180
180 - 190
190 - 200
N
0
10
20
40 Kilometers

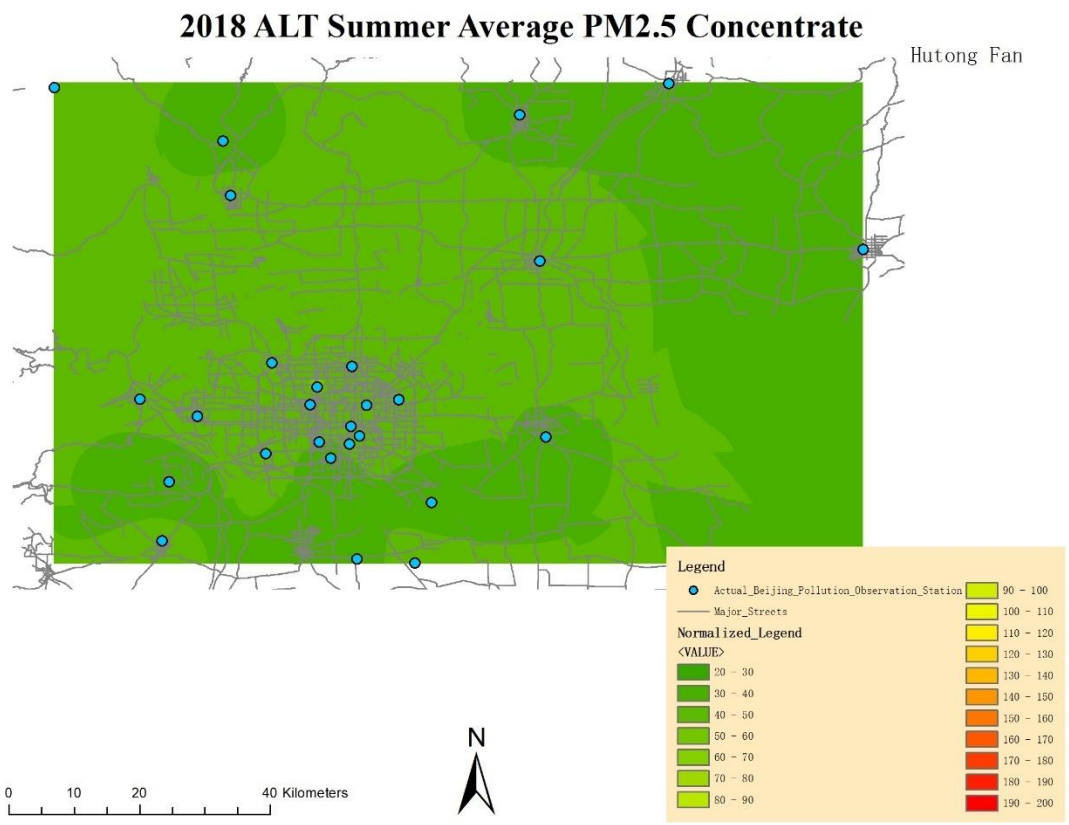
2018 ALT Summer Average PM2.5 Concentrate
Hutong Fan
Legend
Actual_Beijing_Pollution_Observation_Station
Major_Streets
Normalized_Legend
<VALUE>
20 - 30
30 - 40
40 - 50
50 - 60
60 - 70
70 - 80
80 - 90
90 - 100
100 - 110
110 - 120
120 - 130
130 - 140
140 - 150
150 - 160
160 - 170
170 - 180
180 - 190
190 - 200
N
0
10
20
40 Kilometers

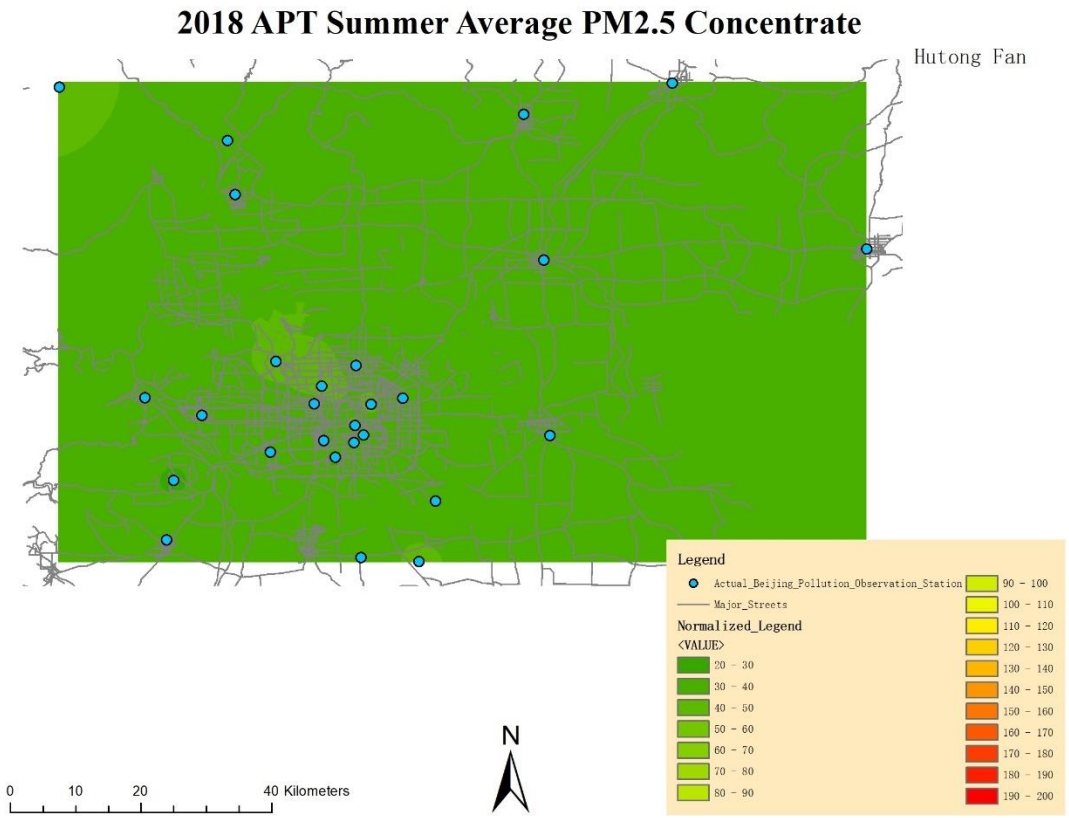
2018 APT Summer Average PM2.5 Concentrate
Hutong Fan
Legend
Actual_Beijing_Pollution_Observation_Station
Major_Streets
Normalized_Legend
<VALUE>
20 - 30
30 - 40
40 - 50
50 - 60
60 - 70
70 - 80
80 - 90
90 - 100
100 - 110
110 - 120
120 - 130
130 - 140
140 - 150
150 - 160
160 - 170
170 - 180
180 - 190
190 - 200
N
0
10
20
40 Kilometers

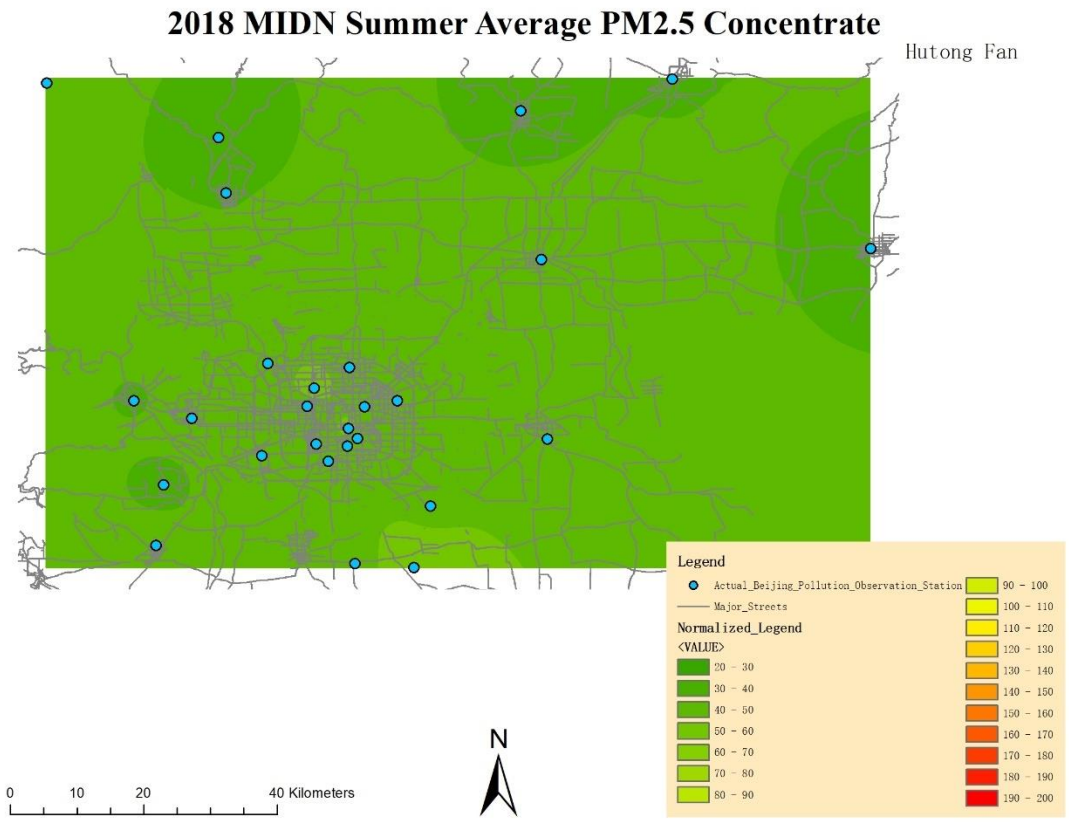
2018 MIDN Summer Average PM2.5 Concentrate
Hutong Fan
Legend
Actual_Beijing_Pollution_Observation_Station
Major_Streets
Normalized_Legend
<VALUE>
20 - 30
30 - 40
40 - 50
50 - 60
60 - 70
70 - 80
80 - 90
90 - 100
100 - 110
110 - 120
120 - 130
130 - 140
140 - 150
150 - 160
160 - 170
170 - 180
180 - 190
190 - 200
N
0
10
20
40 Kilometers

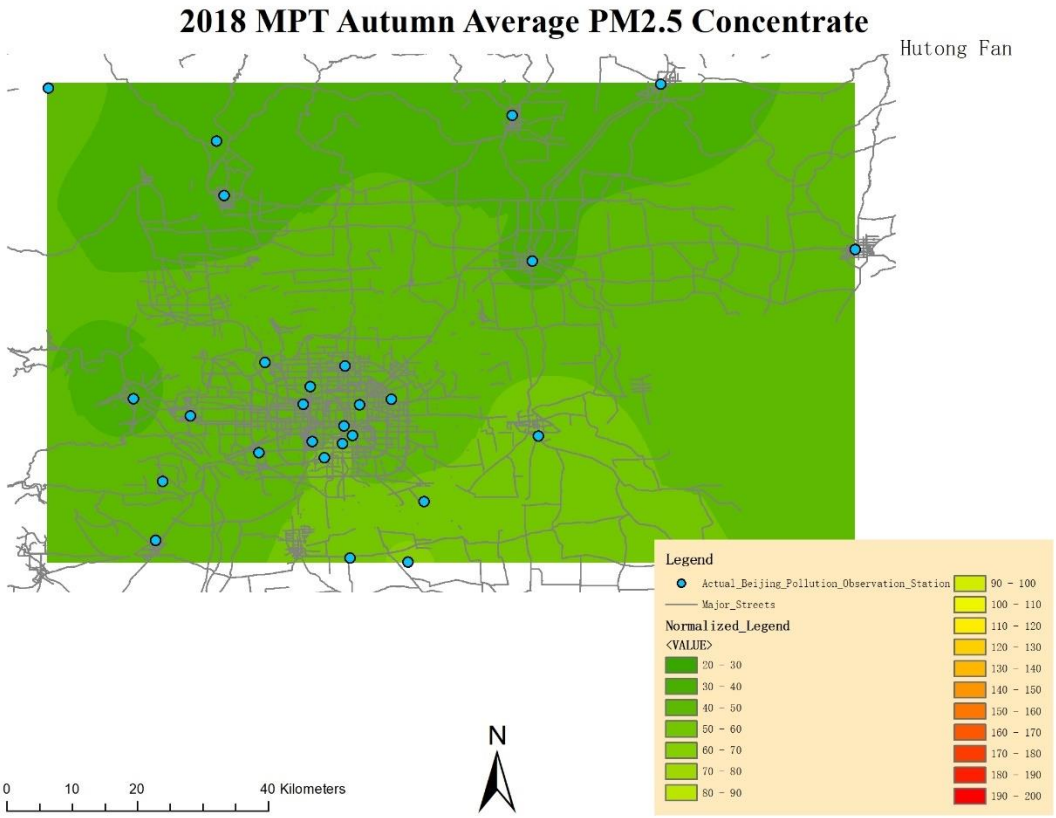
2018 MPT Autumn Average PM2.5 Concentrate
Hutong Fan
Legend
Actual_Beijing_Pollution_Observation_Station
Major_Streets
Normalized_Legend
<VALUE>
20 - 30
30 - 40
40 - 50
50 - 60
60 - 70
70 - 80
80 - 90
90 - 100
100 - 110
110 - 120
120 - 130
130 - 140
140 - 150
150 - 160
160 - 170
170 - 180
180 - 190
190 - 200
N
0
10
20
40 Kilometers

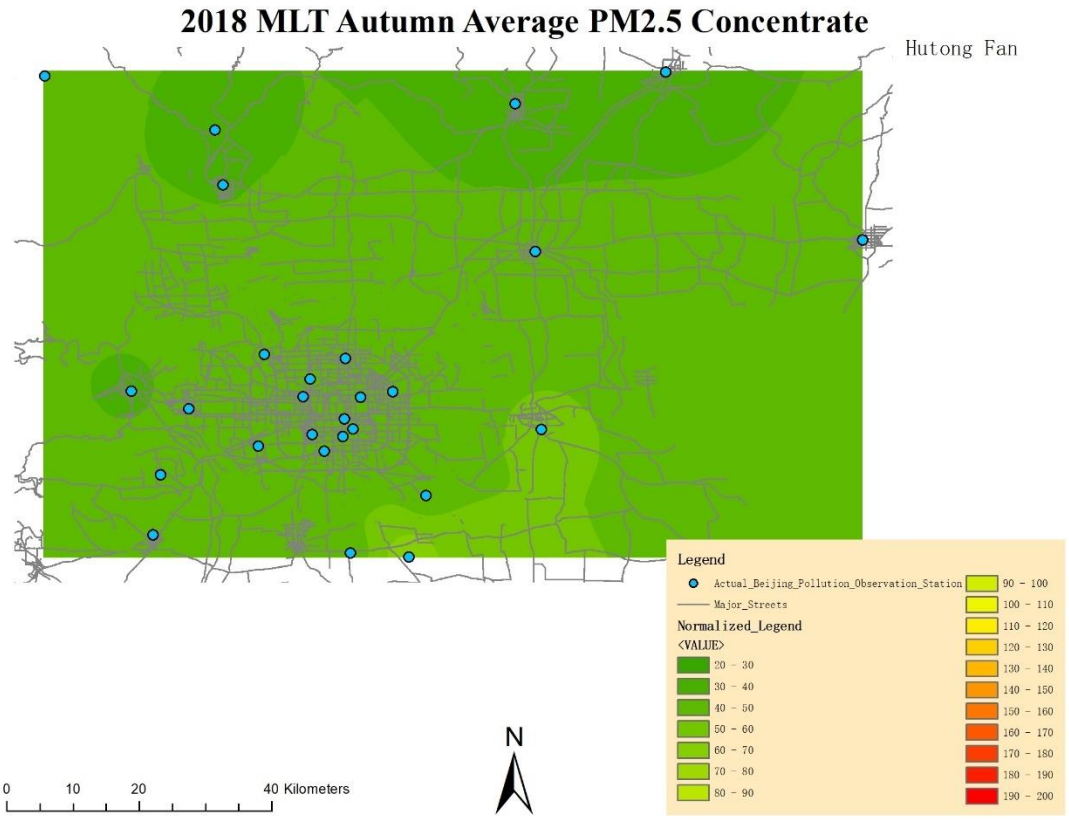
2018 MLT Autumn Average PM2.5 Concentrate
Hutong Fan
Legend
Actual_Beijing_Pollution_Observation_Station
Major_Streets
Normalized_Legend
<VALUE>
20 - 30
30 - 40
40 - 50
50 - 60
60 - 70
70 - 80
80 - 90
90 - 100
100 - 110
110 - 120
120 - 130
130 - 140
140 - 150
150 - 160
160 - 170
170 - 180
180 - 190
190 - 200
N
0
10
20
40 Kilometers

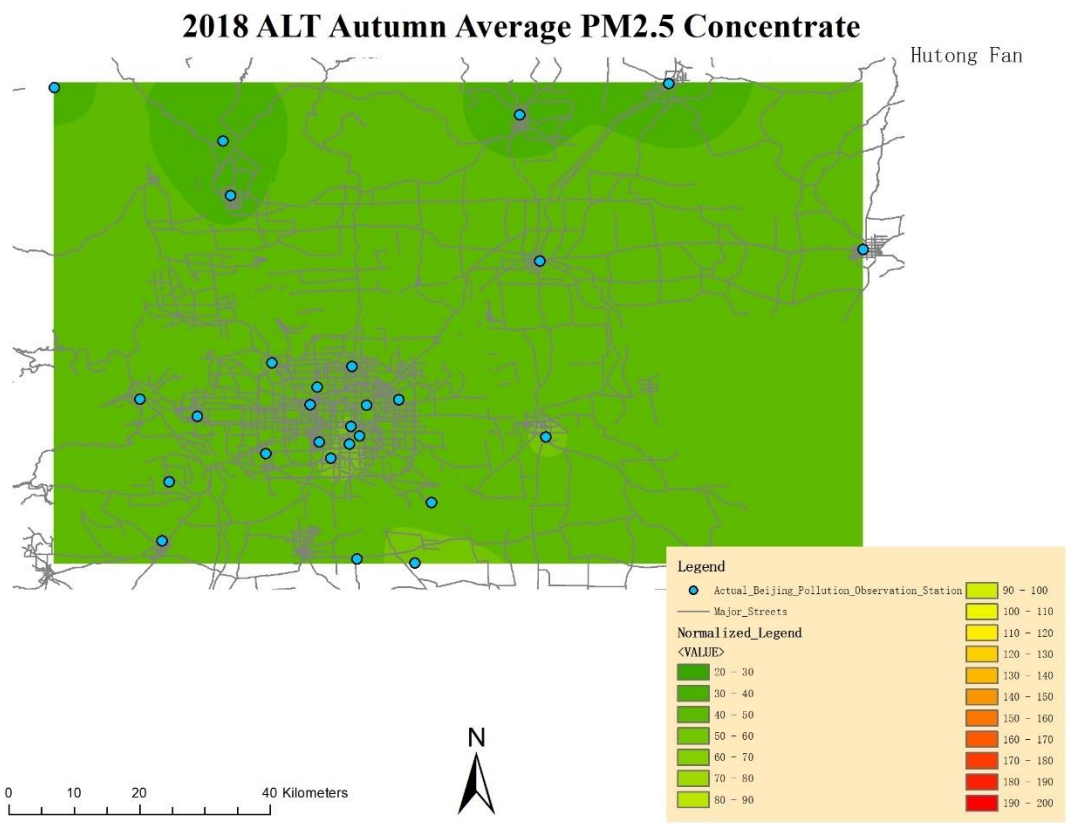
2018 ALT Autumn Average PM2.5 Concentrate
Hutong Fan
Legend
Actual_Beijing_Pollution_Observation_Station
Major_Streets
Normalized_Legend
<VALUE>
20 - 30
30 - 40
40 - 50
50 - 60
60 - 70
70 - 80
80 - 90
90 - 100
100 - 110
110 - 120
120 - 130
130 - 140
140 - 150
150 - 160
160 - 170
170 - 180
180 - 190
190 - 200
N
0
10
20
40 Kilometers

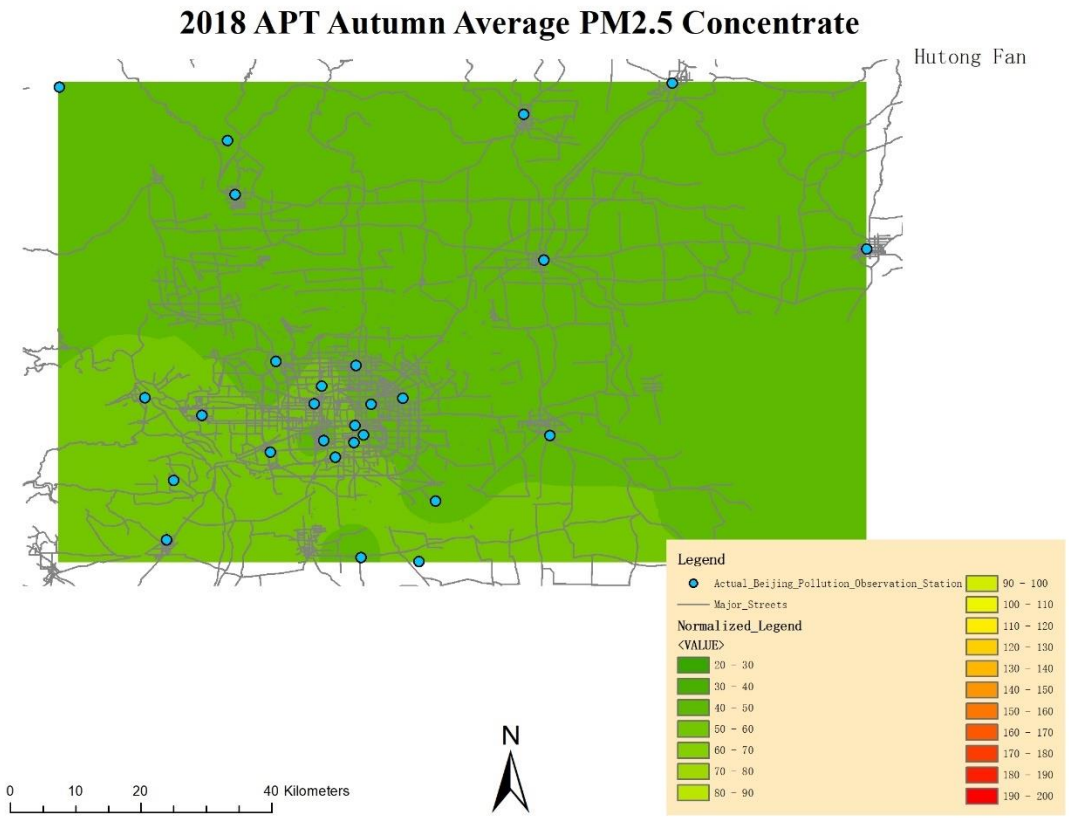
2018 APT Autumn Average PM2.5 Concentrate
Hutong Fan
Legend
Actual_Beijing_Pollution_Observation_Station
Major_Streets
Normalized_Legend
<VALUE>
20 - 30
30 - 40
40 - 50
50 - 60
60 - 70
70 - 80
80 - 90
90 - 100
100 - 110
110 - 120
120 - 130
130 - 140
140 - 150
150 - 160
160 - 170
170 - 180
180 - 190
190 - 200
N
0
10
20
40 Kilometers

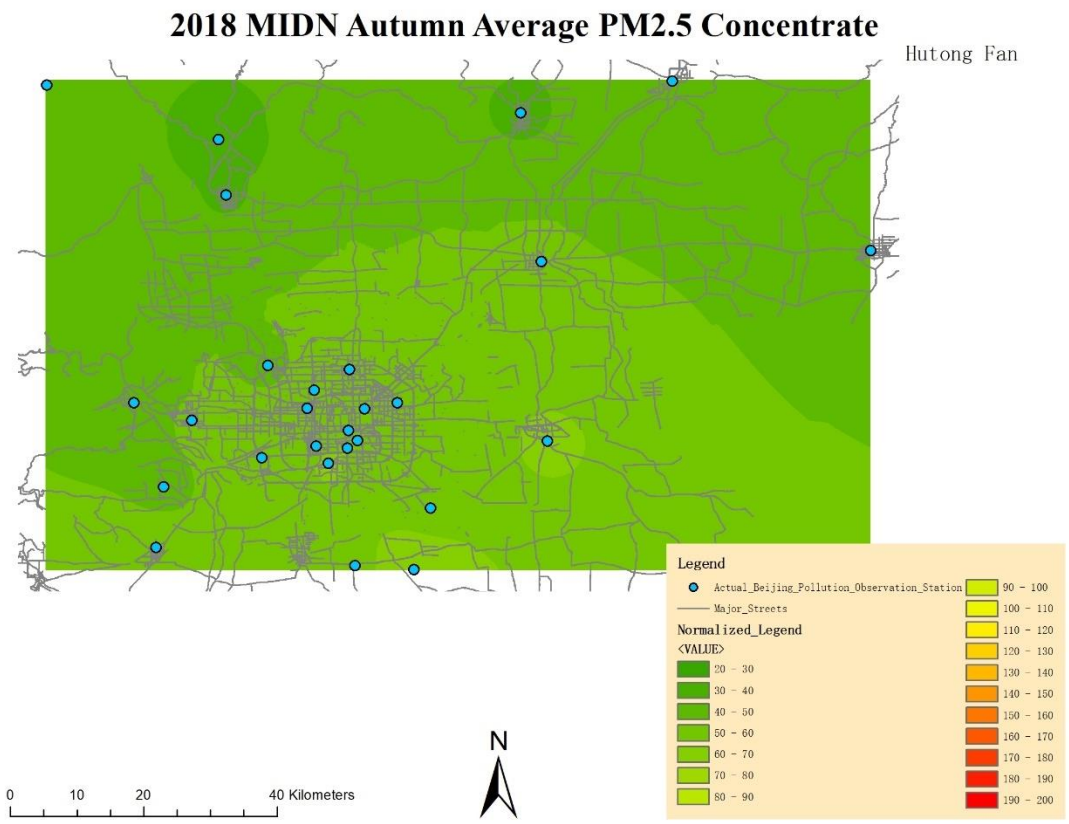
2018 MIDN Autumn Average PM2.5 Concentrate
Hutong Fan
Legend
Actual_Beijing_Pollution_Observation_Station
Major_Streets
Normalized_Legend
<VALUE>
20 - 30
30 - 40
40 - 50
50 - 60
60 - 70
70 - 80
80 - 90
90 - 100
100 - 110
110 - 120
120 - 130
130 - 140
140 - 150
150 - 160
160 - 170
170 - 180
180 - 190
190 - 200
N
0
10
20
40 Kilometers

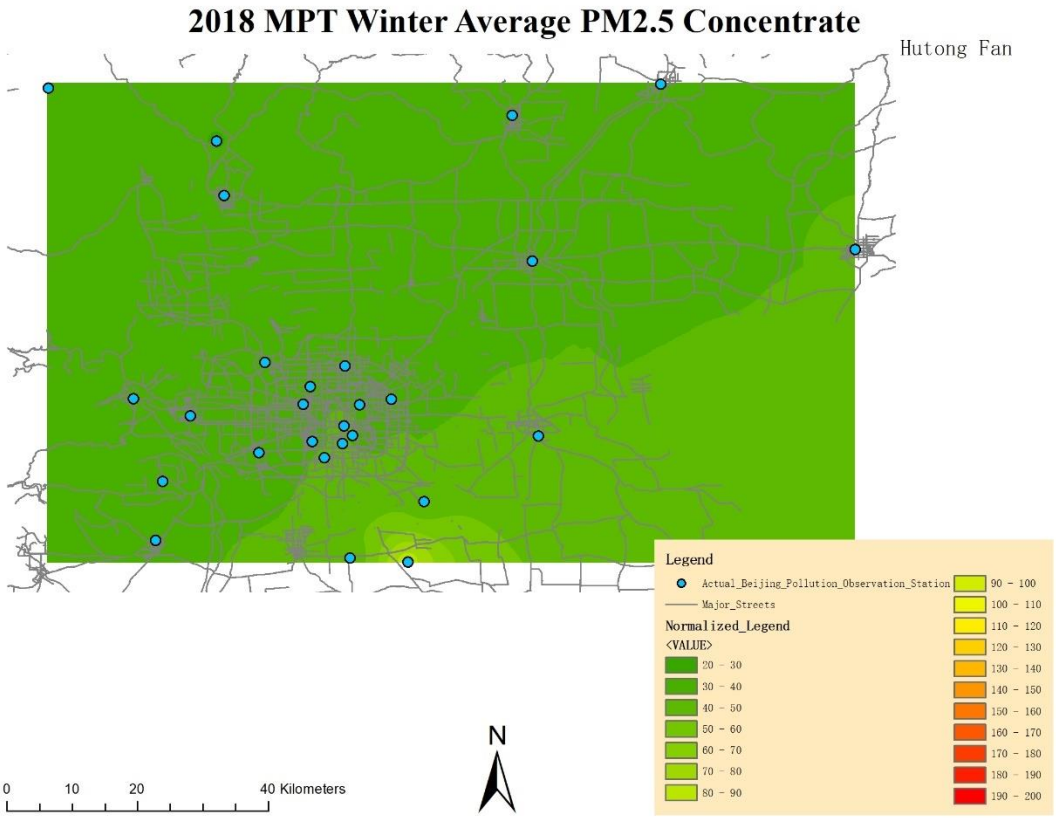
2018 MPT Winter Average PM2.5 Concentrate
Hutong Fan
Legend
Actual_Beijing_Pollution_Observation_Station
Major_Streets
Normalized_Legend
<VALUE>
20 - 30
30 - 40
40 - 50
50 - 60
60 - 70
70 - 80
80 - 90
90 - 100
100 - 110
110 - 120
120 - 130
130 - 140
140 - 150
150 - 160
160 - 170
170 - 180
180 - 190
190 - 200
N
0
10
20
40 Kilometers

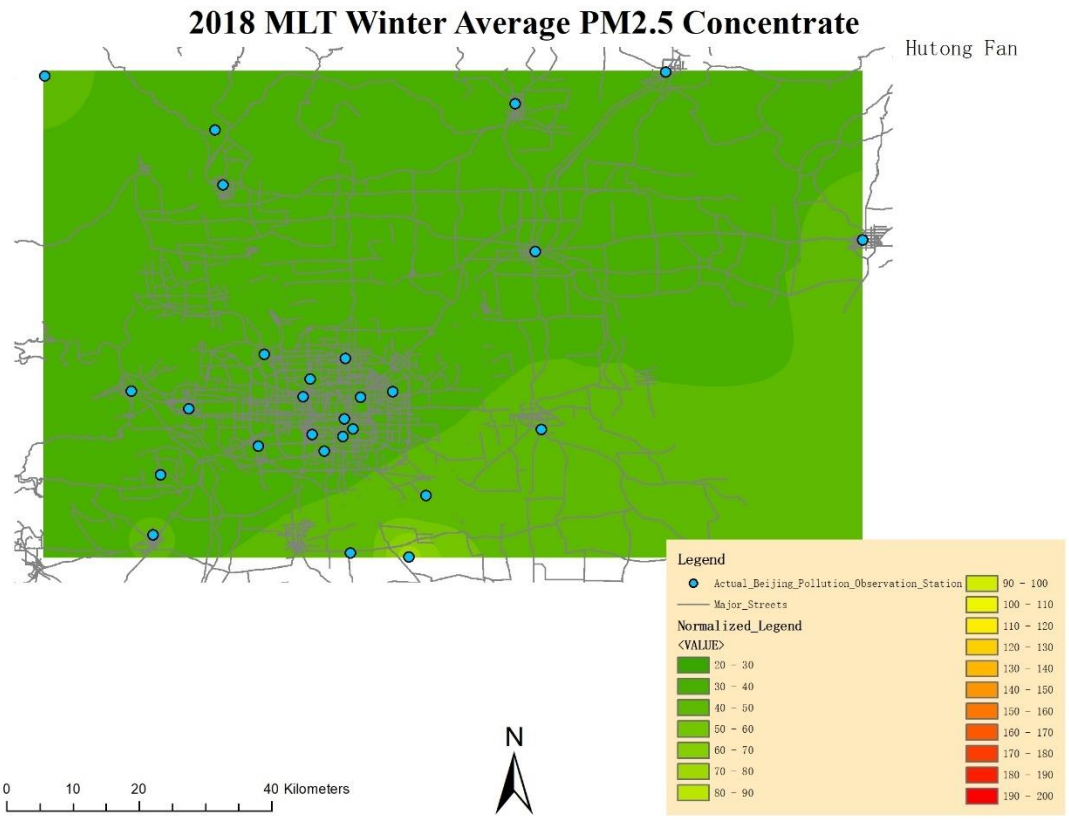
2018 MLT Winter Average PM2.5 Concentrate
Hutong Fan
Legend
Actual_Beijing_Pollution_Observation_Station
Major_Streets
Normalized_Legend
<VALUE>
20 - 30
30 - 40
40 - 50
50 - 60
60 - 70
70 - 80
80 - 90
90 - 100
100 - 110
110 - 120
120 - 130
130 - 140
140 - 150
150 - 160
160 - 170
170 - 180
180 - 190
190 - 200
N
0
10
20
40 Kilometers

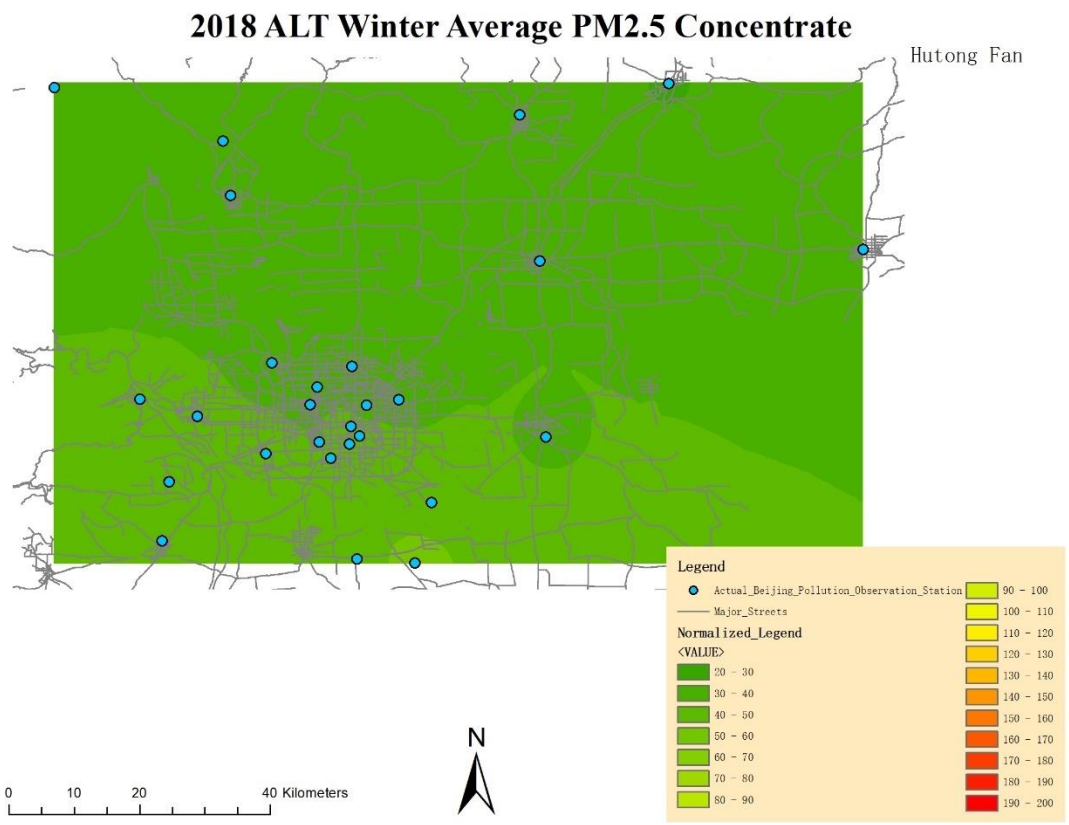
2018 ALT Winter Average PM2.5 Concentrate
Hutong Fan
Legend
Actual_Beijing_Pollution_Observation_Station
Major_Streets
Normalized_Legend
<VALUE>
20 - 30
30 - 40
40 - 50
50 - 60
60 - 70
70 - 80
80 - 90
90 - 100
100 - 110
110 - 120
120 - 130
130 - 140
140 - 150
150 - 160
160 - 170
170 - 180
180 - 190
190 - 200
N
0
10
20
40 Kilometers

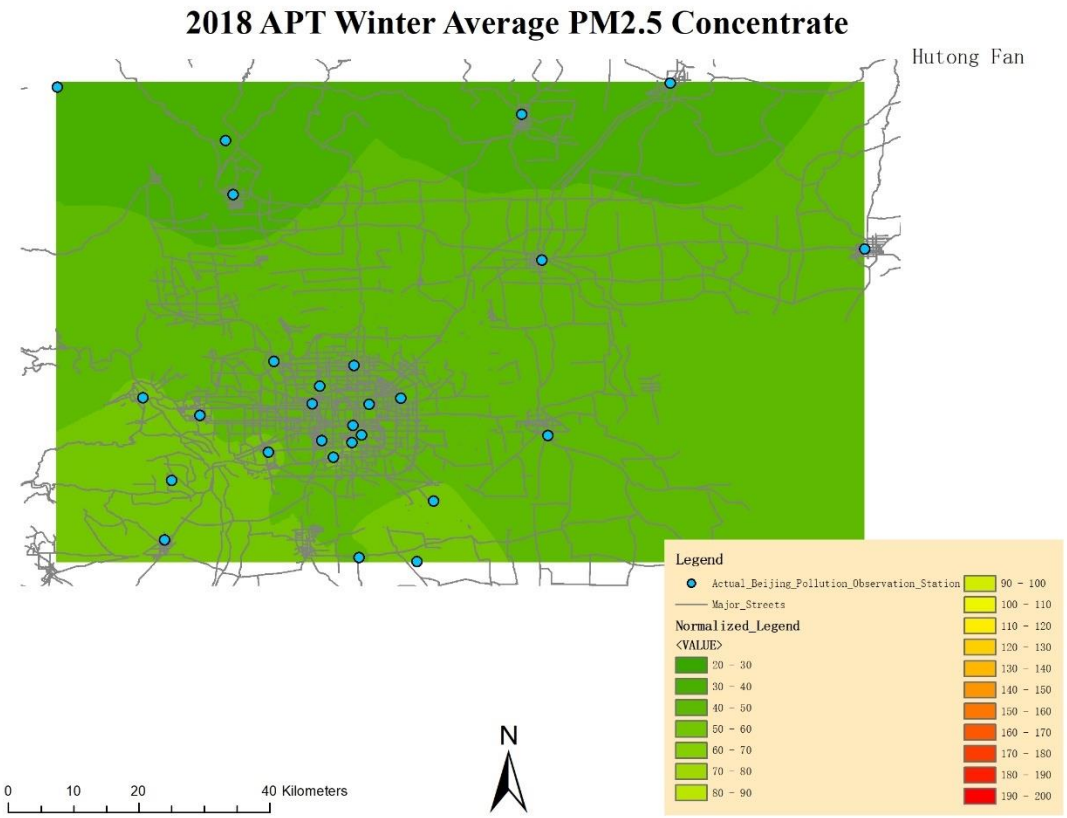
2018 APT Winter Average PM2.5 Concentrate
Hutong Fan
Legend
Actual_Beijing_Pollution_Observation_Station
Major_Streets
Normalized_Legend
<VALUE>
20 - 30
30 - 40
40 - 50
50 - 60
60 - 70
70 - 80
80 - 90
90 - 100
100 - 110
110 - 120
120 - 130
130 - 140
140 - 150
150 - 160
160 - 170
170 - 180
180 - 190
190 - 200
N
0
10
20
40 Kilometers

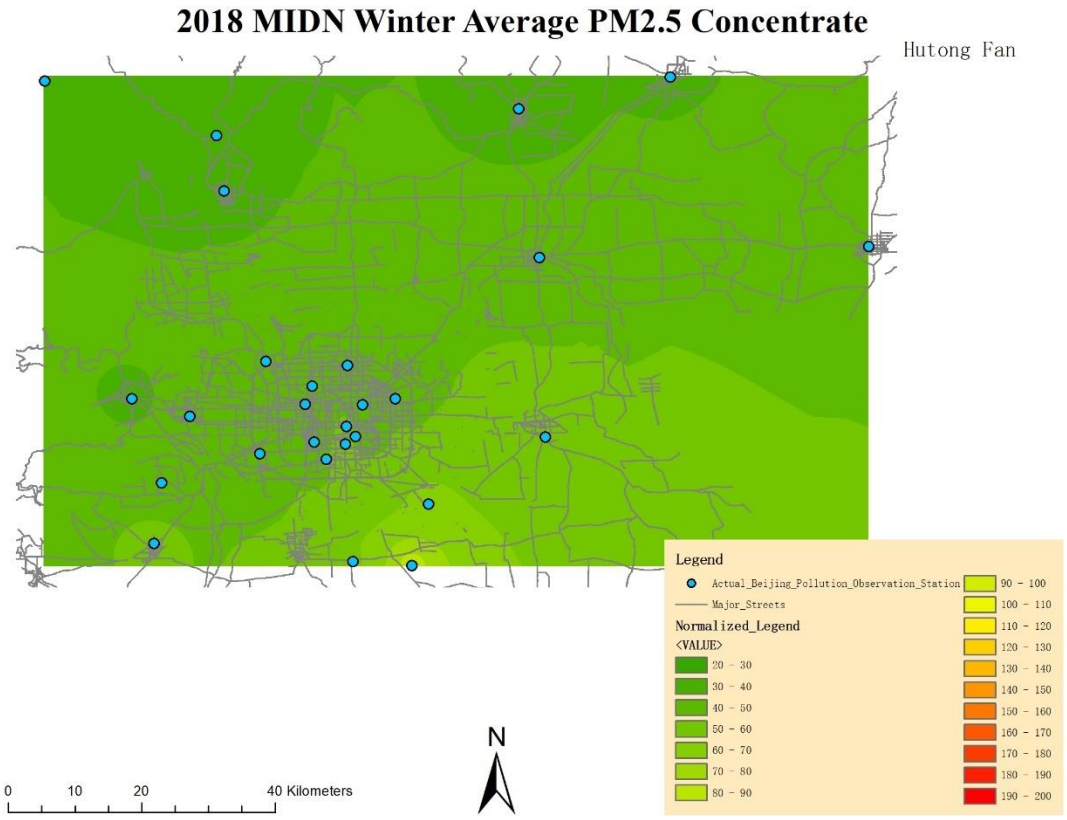
2018 MIDN Winter Average PM2.5 Concentrate
Hutong Fan
Legend
Actual_Beijing_Pollution_Observation_Station
Major_Streets
Normalized_Legend
<VALUE>
20 - 30
30 - 40
40 - 50
50 - 60
60 - 70
70 - 80
80 - 90
90 - 100
100 - 110
110 - 120
120 - 130
130 - 140
140 - 150
150 - 160
160 - 170
170 - 180
180 - 190
190 - 200
N
0
10
20
40 Kilometers